

Aus dem Institut für Lungenforschung  
Geschäftsführender Direktor: Prof. Dr. Bernd Schmeck  
des Fachbereichs Medizin der Philipps-Universität Marburg

---

# Long non-coding RNAs involved in myeloid cell differentiation and macrophage activation

---

Dissertation  
zur Erlangung des Doktorgrades der Naturwissenschaften  
am Fachbereich Medizin  
der Philipps-Universität Marburg

vorgelegt von:

**MARINA AZNAOUROVA**  
aus Tiflis

MARBURG 2019

Angenommen vom Fachbereich Medizin der Philipps-Universität Marburg am: 20. Dezember  
2019

Gedruckt mit Genehmigung des Fachbereichs

Dekan: Prof. Dr. H. Schäfer

Referent: Prof. Dr. L. Schulte

Korreferent: PD Dr. T. Adihary

# TABLE OF CONTENTS

---

<b>Zusammenfassung</b> .....	1
<b>Summary</b> .....	3
<b>List of abbreviations</b> .....	5
<b>1. Introduction</b> .....	13
<b>1.1 The Immune System</b> .....	13
1.1.1 Generation of the immune cell lineages.....	13
1.1.2 Cells of the immune system .....	17
1.1.3 The innate immune system.....	23
1.1.4 Pathogen Recognition by Pattern Recognition Receptors .....	24
<b>1.2 The Non-Coding Genome</b> .....	28
1.2.1 Non-coding RNA species.....	28
1.2.2 Small regulatory RNAs .....	29
1.2.3 Long non-coding RNAs .....	31
1.2.4 Functions of long non-coding RNAs .....	34
1.2.5 Long non-coding RNAs in immunity .....	36
1.2.6 Long non-coding RNAs in inflammatory responses .....	38
<b>1.3 Infection model organisms</b> .....	41
1.3.1 <i>Legionella pneumophila</i> .....	41
1.3.2 <i>Salmonella enterica</i> serovar Typhimurium.....	44
<b>1.4 Aim of this study</b> .....	46
<b>2. Materials and Methods</b> .....	47
<b>2.1 Materials</b> .....	47
2.1.1 Instruments and equipment .....	47
2.1.2 Consumables and plastic ware .....	50
2.1.3 Chemicals .....	53
2.1.4 Stimulants and cytokines.....	56

2.1.5 Kits .....	57
2.1.6 Antibodies .....	58
2.1.7 Primers.....	59
2.1.8 siRNAs .....	63
2.1.9 Plasmids.....	64
2.1.10 Buffers and Solutions .....	64
2.1.11 Software.....	67
2.1.12 Websites .....	67
2.1.13 Vector maps.....	68
<b>2.2 Methods .....</b>	<b>71</b>
2.2.1 Cell culture .....	71
2.2.1.1 Isolation of primary human monocytes .....	71
2.2.1.2 Macrophage differentiation and culture .....	72
2.2.1.3 Dendritic cell differentiation and culture .....	72
2.2.1.4 Isolation of other immune cell populations .....	72
2.2.1.5 Liver and Brain RNA .....	72
2.2.1.6 THP1 and U937 cell culture and differentiation .....	73
2.2.1.7 HEK-293T cell culture .....	73
2.2.2 Transcriptome Analysis.....	73
2.2.2.1 RNA extraction by TRIZOL® .....	73
2.2.2.2 RNA extraction by mirVana™ miRNA kit.....	74
2.2.2.3 DNaseI digestion.....	74
2.2.2.4 RNA quantification and quality check .....	75
2.2.2.5 cDNA synthesis.....	75
2.2.2.6 Quantitative Real Time PCR.....	76
2.2.3 Subcellular fractionation .....	77
2.2.4 Rapid Amplification of cDNA Ends (RACE) .....	78
2.2.5 PCR amplification of the full length MaIL1 .....	82
2.2.6 Lentiviral transduction .....	83

2.2.6.1 Lentiviral production- Small scale .....	83
2.2.6.2 Lentiviral production- Large scale .....	84
<b>2.2.7 Genome editing by CRISPR/Cas9 .....</b>	<b>85</b>
<b>2.2.8 RNA antisense purification coupled with mass spectrometry (RAP-MS) .....</b>	<b>89</b>
2.2.8.1 Cell preparation .....	89
2.2.8.2 Probe preparation .....	89
2.2.8.3 Cell lysis .....	90
2.2.8.4 Pre-clearing of lysates .....	91
2.2.8.5 Hybridization, capture and protein elution .....	92
<b>2.2.9 RNA Immunoprecipitation (RIP) .....</b>	<b>93</b>
2.2.9.1 Preparation of cell lysate .....	93
2.2.9.2 Preparation of magnetic beads .....	94
2.2.9.3 Immunoprecipitation .....	94
<b>2.2.10. Glycerol gradient .....</b>	<b>95</b>
<b>2.2.11 Protein analysis.....</b>	<b>97</b>
2.2.11.1 Western blot .....	97
2.2.11.2 Enzyme Linked Immunosorbent Assay (ELISA) .....	97
2.2.11.3 Quantification of expression levels by flow cytometry .....	98
<b>2.2.12 Transfection of BDMs with siRNAs.....</b>	<b>98</b>
<b>2.2.13 Stimulations of BDMs.....</b>	<b>99</b>
2.2.13.1 Treatments with pro-inflammatory stimuli .....	99
2.2.13.2 Treatments with inhibitors .....	99
<b>2.2.14 Infection of BDMs with <i>Legionella pneumophila</i> .....</b>	<b>99</b>
<b>2.2.15 Determination of infection efficiency by flow cytometry .....</b>	<b>100</b>
<b>2.2.16 MTT assay .....</b>	<b>100</b>
<b>2.2.17 RNA sequencing .....</b>	<b>100</b>
<b>2.2.18 Proteomics .....</b>	<b>101</b>
<b>2.2.19 Conservation analysis.....</b>	<b>102</b>
<b>2.2.20 Bronchoalveolar lavage (BAL) and patient selection .....</b>	<b>102</b>
<b>2.2.21 Statistical Analysis .....</b>	<b>104</b>

<b>3. Results .....</b>	<b>105</b>
<b>3.1 Results- LncRNAs in myeloid cell differentiation .....</b>	<b>105</b>
3.1.1 Differentially expressed lncRNAs in distinct immune cell lineages .....	105
3.1.2 Validation of the expression levels of leukocyte specific lncRNAs. ....	106
3.1.3 Characterisation of LINC00211 .....	108
3.1.4 Functional characterisation of LINC00211 .....	109
3.1.5 LINC00211 is involved in monocyte terminal differentiation .....	112
3.1.6 LINC0211 is regulated by PU.1 transcription factor .....	114
3.1.7 LINC00211 is a biomarker of inflamed lung.....	115
<b>3.2 Results- LncRNAs in macrophage activation .....</b>	<b>117</b>
3.2.1 Resting and activated BDMs deferentially express lncRNAs .....	117
3.2.2 LncRNAs are predominantly localised in the cytosol .....	119
3.2.3 Distinct sedimentation profiles of RNA classes and protein machineries .....	119
3.2.4 MaIL1 lincRNA is a novel TLR-responsive gene .....	121
3.2.5 Functional characterisation of MaIL1 by CRISR/Cas 9 .....	124
3.2.6 MaIL1 controls TLR-induced type I interferon production.....	127
3.2.7 MaIL1 promotes TLR4 induced IRF3 phosphorylation through interaction with optineurin .....	129
3.2.8 MaIL1 is an infection biomarker promoting antimicrobial defence .....	131
<b>4. Discussion .....</b>	<b>134</b>
<b>3.2 Discussion- LncRNAs in myeloid cell differentiation .....</b>	<b>134</b>
<b>3.2 Discussion- LncRNAs in macrophage activation .....</b>	<b>136</b>
<b>4. References.....</b>	<b>140</b>
<b>Curriculum Vitae .....</b>	<b>181</b>
<b>Verzeichnis der akademischen Lehrer.....</b>	<b>182</b>
<b>Acknowledgements.....</b>	<b>183</b>
<b>Ehrenwörtliche Erklärung .....</b>	<b>185</b>

# Zusammenfassung

Das menschliche Genom kodiert für ~ 20.000 lange nicht-kodierende RNAs (lncRNAs), ihre molekularen Funktionen, insbesondere im Immunsystem, sind jedoch weitgehend unbekannt. In dieser Studie wurden zwei Hauptaspekte untersucht: die Beteiligung von lncRNAs an der Differenzierung myeloischer Immunzellen und deren Beteiligung an der entzündungsfördernden Aktivierung menschlicher Makrophagen. In Bezug auf den ersten Aspekt dieser Studie wurden RNA-Sequenzierdaten von verschiedenen Immunzellpopulationen analysiert. Diese Daten zeigten, dass lncRNAs und Protein-kodierende Transkripte die Identität von Immunzellen gleichermaßen spezifizieren. Klassischerweise werden die Leukozyten-Populationen anhand von Oberflächenrezeptoren unterschieden, welche als spezifische Marker dienen. In dieser Studie wurde die nicht-kodierende RNA LINC00211 als spezifischer Marker für die myeloide Abstammung von Immunzellen identifiziert. Die funktionelle Charakterisierung zeigte, dass diese lncRNA die Expression mehrerer Gene reguliert, einschließlich CHI3L1 und S100A9, welche eine Rolle in der Differenzierung myeloider Zellen spielen. Außerdem konnte gezeigt werden, dass LINC00211 durch PU.1, einen Transkriptionsfaktor mit essentiellen Funktionen in der Immunzellentwicklung, reguliert wird. Darüber hinaus konnte LINC00211 als Biomarker für Lungenentzündungen charakterisiert werden, da in bronchoalveolarer Spülflüssigkeit von infizierten Personen und in Lungenextrakten von IPF-Patienten eine hohe Expression beobachtet wurde, die mit dem Grad der Neutrophileninfiltration korreliert.

Um die Beteiligung von lncRNAs an der entzündungsfördernden Aktivierung menschlicher Makrophagen zu untersuchen, wurden RNA-Sequenzierungen durchgeführt und mehrere differentiell exprimierte lncRNAs in ruhenden und immunaktivierten menschlichen Makrophagen identifiziert. Darüber hinaus wurde ein mehrdimensionaler Ansatz entwickelt, um humane lncRNAs nach ihrer subzellulären Lokalisation und Co-Sedimentation mit zellulären Proteinkomplexen in Makrophagen zu kategorisieren. Diese Daten zeigten, dass lncRNAs eine sehr heterogene Klasse von RNAs darstellen, die mit verschiedenen zellulären Komponenten, einschließlich Ribosomen, co-sedimentiert. Anhand dieser Daten wurde lncRNA MaLL1 als hoch immunreaktive, zytosolische und nicht Ribosomen-gebundene intergenische lncRNA (lincRNA) identifiziert. Die funktionellen Analysen assoziierten MaLL1 mit der Typ I Interferonproduktion nach Toll-like-Receptor (TLR) Aktivierung. RNA-

Antisense-Aufreinigung und Massenspektrometrie (RAP-MS) zeigten, dass MaIL1 mit Optineurin interagiert, einem Protein, das bekanntermaßen für die Signalübertragung innerhalb des TBK1-IRF3-Signalweges erforderlich ist, und dadurch die Typ I Interferonproduktion steuert. Insbesondere reguliert MaIL1 die Optineurin-Ubiquitinierung, eine Modifikation, die für die Optineurin-Funktion wesentlich ist. Ein Knockdown von MaIL1 beeinträchtigte die durch den Optineurin-TBK1 Komplex vermittelte IRF3-Phosphorylierung und somit die Typ I Interferonproduktion. Darüber hinaus erwies sich MaIL1 als essentiell für die Abwehr von *Legionella pneumophila*, einem gramnegativen Bakterium, das sich im menschlichen Wirt vorwiegend in Alveolarmakrophagen repliziert und Lungenentzündung verursacht. Darüber hinaus waren die MaIL1-Spiegel während Lungeninfektionen erhöht und korrelierten linear mit den IFN $\beta$ -mRNA-Spiegeln in humaner bronchoalveolarer Lavage. In der vorliegenden Arbeit wird MaIL1 daher als kritischer Regulator von TLR-induzierten IFN-Reaktionen auf Infektionen identifiziert. Zusammenfassend liefern beide Studien detaillierte neue Informationen über die Funktion von lncRNAs in myeloischen Immunzellen und etablieren eine umfangreiche Ressource, sowie Leitfäden für zukünftige Untersuchungen zu lncRNAs im humanen Immunsystem.



## Summary

The human genome encodes for ~ 20.000 long non-coding RNAs (lncRNAs), yet their molecular functions, especially in the immune system, remain largely unknown. In this study, two main aspects were addressed: the participation of lncRNAs in the differentiation of myeloid immune cells and their involvement in pro-inflammatory activation of human macrophages. In order to address the first aspect, RNA sequencing results from distinct immune cell subsets were analysed. These data showed that lncRNAs define immune-cell identity equally well as protein-coding genes, such as surface receptors considered as precise markers of leukocyte subsets. In the present work, non-coding RNA LINC00211 was identified as a specific myeloid cell lineage marker. Functional characterisation demonstrated that this lncRNA regulates the expression of several genes, including CHI3L1 and S100A9, which participate in myeloid cell differentiation. Furthermore, LINC00211 was regulated by PU.1, a transcription factor with fundamental roles in immune cell lineage commitment. Additionally, LINC00211 could be characterised as a biomarker of pulmonary inflammation, since high expression was observed in bronchoalveolar lavage fluid from infected individuals and in lung extracts from IPF patients, correlating with the degree of neutrophil infiltration.

In order to investigate the involvement of lncRNAs in pro-inflammatory activation of human macrophages, RNA sequencing experiments were performed and unveiled several differentially expressed lncRNAs in resting and immune-activated human macrophages. Furthermore, a multidimensional approach was established to categorize human lncRNAs according to their subcellular localization and co-sedimentation with cellular protein complexes in macrophages. The resulting data revealed that lncRNAs constitute a highly heterogeneous class of RNA co-sedimenting with various cellular machineries, including ribosomes. Using these data, lncRNA MaIL1 was identified as a highly immune-responsive, cytosolic and non-ribosome associated intergenic lncRNA (lincRNA). Functional analysis associated MaIL1 with type I interferon production after Toll-like Receptor (TLR) activation. RNA antisense purification and mass spectrometry (RAP-MS) showed that MaIL1 interacts with Optineurin, a protein known to be required for signal transduction within the TBK1-IRF3 axis, thus facilitating type I interferon production. More specifically, MaIL1 regulates Optineurin ubiquitination, a modification essential for Optineurin function. When MaIL1 was knocked down, IRF3 phosphorylation and subsequently type I interferon production was impaired. Moreover, MaIL1 was found to be

essential for defence against *Legionella pneumophila*, a Gram-negative bacterium that predominantly replicates inside alveolar macrophages and causes pneumonia. In addition, MaLL1 levels were increased during pulmonary infections and correlated linearly with IFN $\beta$  mRNA levels in human bronchoalveolar lavage fluid. Thus, the present work identifies MaLL1 as a critical regulator of TLR-induced IFN responses to infection. In summary, both studies revealed detailed information about the function of lncRNAs in myeloid immune cells and provide a rich resource and blueprint for future investigations of lncRNA functions in the immune system.

## List of abbreviations

°C	Grad Celsius
µm	micrometre
ADAR	Adenosine Deaminase
AGM	Aorta gonad mesonephros
Ago2	Argonaute 2
AML	Acute Myeloid Leukaemia
AMPs	Antimicrobial Peptides
ATCC	American Type Culture Collection
BAK1	BCL2-antagonist/killer 1
BAL	Bronchoalveolar Lavage
BCR	B Cell Receptor
BDM	Blood Derived Macrophage
bp	base pairs
BSA	Bovine Serum Albumin
CARD	Caspase Activation and Recruitment Domains
CCL4	C-C Motif Chemokine Ligand 4
CD	Cluster of Differentiation
cDCs	classical Dendritic Cells
cDNA	Complementary DNA
CFU	Colony Forming Unit
circRNA	circular RNA
CLP	Common Lymphoid Progenitor
CLR	C-type Lectin Receptor
CMP	Common Myeloid Progenitor
cNK	conventional Natural killer
CO <sub>2</sub>	Carbon Dioxide
CPC	Coding Potential Calculator
CRISPR	Clustered Regularly Interspaced Short Palindromic Repeats

CSF1	Colony Stimulation Factor 1
Ct	Threshold Cycle
CTD	C-terminal domain
CTLD	C-type Lectin like Domain
CTLs	Cytotoxic T-lymphocytes
CXCL10	C-X-C Motif Chemokine Ligand 10
CXCR4	Chemokine receptor type 4
Da	Dalton
DAMPs	Damage Associated Molecular Patterns
DCs	Dendritic Cells
DMSO	Dimethyl Sulfoxide
DNA	Deoxyribonucleic Acid
DNase	Deoxyribonuclease
dNTP	Deoxyribonucleoside Triphosphate
dot	defective in organelle trafficking
ds	double stranded
ECL	Enhanced Chemoluminescence
EDTA	Ethylenediaminetetraacetic Acid
ELISA	Enzyme Linked Immunosorbent Assay
EMPs	Erythroid myeloid progenitor
ENCODE	Encyclopaedia of DNA Elements
ERK	Extracellular signal Regulated Kinase
eRNA	enhancer RNA
et al.	et alii
EZH2	Enhancer of Zeste Homolog 2
FACS	Fluorescence Activated Cell Sorting
FcR $\gamma$	Fc receptor $\gamma$ chain
FCS	Fetal Calf Serum
g	Acceleration of gravity
g	gram
GAPDH	Glyceraldehyde 3-phosphate dehydrogenase

GFP	Green Fluorescent Protein
GM-CSF	Granulocyte Macrophage Colony Stimulating Factor
h	hour
H <sub>2</sub> O	water
HEPES	4-(2-hydroxyethyl)-1-piperazineethanesulfonic acid
HEXIM1	Hexamethylene Bisacetamide Inducible 1
hnRNPL	heterogeneous nuclear Ribonucleoprotein L
HOTAIR	HOX Transcript Antisense RNA
HRP	Horseradish Peroxidase
HSCs	Haematopoietic Stem Cells
HSCT	Haematopoietic Stem Cells Transplantation
icm	intracellular multiplication
iE-DAP	$\gamma$ -D-glutamyl-meso-diaminopimelic acid
IFN	Interferon
Ig	Immunoglobulin
IKKs	I-kappa-B kinases
IL	Interleukin
IPA	Ingenuity Pathway Analysis
IPF	Idiopathic Pulmonary Fibrosis
IQGAP1	IQ Motif Containing GTPase Activating Protein 1
IRAK	Interleukin 1 Receptor Associated Kinase
IRF	Interferon Regulatory Factor
IRG1	Immune-Responsive Gene 1 Protein
ITAM	Immunoreceptor Tyrosine-based Activation Motif
ITIM	Immunoreceptor Tyrosine-based Inhibition Motif
JNK	c-Jun N terminal Kinase
kDa	kilo Dalton
KEGG	Kyoto Encyclopaedia of Genes and Genomes
KIRs	Killer Immunoglobulin-like Receptors
ko	knock out
L	litter

<i>L.p.</i>	<i>Legionella pneumophila</i>
LB	Lysogeny Broth
LC3	Microtubule-associated protein 1A/1B-light chain
LCV	<i>Legionella</i> Containing Vacuole
lincRNA	long intergenic noncoding RNA
lncRNA	long non coding RNA
LPG2	Laboratory of Genetics and Physiology 2
LPS	Lipopolysaccharide
LRRK2	Leucine Rich Repeat Kinase 2
LSC	Lymphoid Stem Cell
LUCAT1	Lung Cancer Associated Transcript 1
M	Molar
m	milli
MACS	Magnetic Activated Cell Sorting
MAF	Avian Musculoaponeurotic Fibrosarcoma Protooncogene
MaIL1	Macrophage Interferon-regulatory LincRNA 1
MALAT1	Metastasis Associated Lung Adenocarcinoma Transcript 1
MAPK	Mitogen Activated Protein Kinase
MAVS	Mitochondrial Antiviral Signalling Protein
M-CSF	Macrophage Colony Stimulating Factor
MDA5	Melanoma Differentiation-Associated protein 5
MDP	Muramyl Dipeptide
mg	milligram
MHC	Major Histocompatibility Complex
min	Minutes
miRNA	microRNA
ml	Milliliter
mM	Millimolar
MOI	Multiplicity of Infection
mRNA	messenger RNA
MSC	Myeloid Stem Cell

MyD88	Myeloid Differentiation primary response protein 88
NaCl	sodium chloride
ncRNAs	non coding Ribonucleic Acids
NeST	Nettoie Salmonella pas Theiler's
NETs	Neutrophil Extracellular Traps
NFAT	Nuclear Factor of Activated T-cells
NF- $\kappa$ B	Nuclear Factor kappa-light-chain-enhancer of activated B cells
NGS	Next Generation Sequencing
NK	Natural Killer
NLR	NOD-like receptor
NLRs	NOD Like Receptors
nm	Nanometre
NOD	Nucleotide biding Oligomerisation Domain
NP40	Nonidet P-40
NRIR	Negative Regulator of Interferon Response
NRON	Non-coding Repressor of NFAT
nt	nucleotides
O <sub>2</sub>	oxygen
OD	optical density
OE	Overexpression
OPTN	Optineurin
PAA	polyacrylamide
PACER	p50-associated COX-2 extragenic RNA
PAMPs	Pathogen Associated Molecular Patterns
Pax5	Paired box protein 5
PBMC	peripheral blood mononuclear cell
PBS	Phosphate Buffered Saline
PCA	Principal Component Analysis
PCI	Phenol/Chloroform/Isoamyl alcohol
PCR	Polymerase Chain Reaction
pDCs	plasmacytoid Dendritic Cells

pH	potentia hydrogenii
piRNA	piwi-interacting RNA
PMA	Phorbol-12-myristat-13-acetat
PRC2	polycomb repressive complex 2
PRRs	Pathogen Recognition Receptors
PTGS2	Prostaglandin-Endoperoxide Synthase 2
qRT-PCR	quantitative Real Time PCR
RACE	Rapid Amplification of cDNA Ends
RAP-MS	RNA antisense purification coupled with mass spectrometry
RIG-I	Retinoic Acid-Inducible Gene
RIN	RNA integrity number
RIP	RNA Immunoprecipitation
RIP2	Receptor Interacting Protein-2
RIPK2	receptor- interacting serine/threonine-protein kinase 2
RISC	RNA-Induced Silencing Complex
RNA	Ribonucleic Acid
RNAs	Ribonucleic Acids
RNase	Ribonuclease
RPMI	Rosswell Park Memorial Institute
rRNA	ribosomal RNA
RT	Room Temperature
SDF-1	Stromal cell Derived Factor1
SDS	Sodium Dodecyl Sulphate
SDS-PAGE s	Sodium Dodecyl Sulphate Polyacrylamide Gel Electrophoresis
sec	Second
SFPQ	Splicing Factor Proline and Glutamine Rich
SHIP1	Src Homology 2 domain-containing Inositol-5'-Phosphatase 1
siRNA	small interfering RNA
snoRNA	small nucleolar RNA
SNPs	Single Nucleotide Polymorphisms
snRNA	small nuclear RNA



SOCS1	Suppressor of Cytokine Signalling 1
ss	single stranded
STAT3	Signal transducer and activator of transcription 3
STING	Stimulator of Interferon Genes
T2SS	type II secretion system
T4BSS	type IV B secretion system
T4SS	type IV secretion system
TAK1	TGFbeta Activated Kinase 1
Taq	<i>Thermus aquaticus</i>
TBK1	TANK Binding Kinase 1
TCR	T Cell Receptor
TEMED	tetramethylethyldiamine
TF	Transcription Factor
TGFβ	Tumour Growth Factor β
Th	T Helper
THRIL	TNF and HNRNPL Related Immunoregulatory LncRNA
TIR	Toll/IL-1 receptor
TIRAP	TIR domain containing Adapter Protein
TLRs	Toll Like Receptors
TNF	Tumour Necrosis Factor
TNFα	Tumour Necrosis Factor α
TRAF	TNF Receptor Associated Factor
TRAM	TRIF-related adapter molecule
Tregs	T-regulatory cells
TRIF	TIR domain containing adapter inducing Interferon-β
tRNA	transfer RNA
trNK	tissue resident Natural Killer
U	Unit
Ubi	Ubiquitination
UCHL1	Ubiquitin C-terminal hydrolase L1
UV	ultraviolet

V	Volt
vtRNA	vault RNA
WB	western blot
WT	wildtype
μ	micro
μg	microgram
μl	microliter

# 1. Introduction

## 1.1 The immune system

### 1.1.1 Generation of the immune cell lineages

During a life-span, the human organism is faced by countless attempts of microorganisms to colonize and breach the skin and mucosal surfaces. In order to survive attacks from different microorganisms vertebrates have evolved a sophisticated innate and adaptive immune system. While central components of the innate immune system are found in many life forms, ranging from plants to molluscs and primates, the adaptive immune-system evolved late in the chordate lineage of organisms. Professional cells of the innate and adaptive immune system are generated continuously or during embryonic development in a process referred to as haematopoiesis. In primates, during early development, there is the primitive wave of haematopoiesis, which entails an erythroid progenitor that arises from the yolk sack and gives rise to erythrocytes and macrophages (Palis et al., 2001, Galloway and Zon, 2003, Jagannathan-Bogdan and Zon, 2013). The main function of the primitive wave of haematopoiesis is to produce erythrocytes, in order to allow the embryo to receive oxygen (Orkin and Zon, 2008). After the primitive wave, there is a second wave, also referred to as the “permanent” or “definitive wave” (Orkin and Zon, 2008). This wave may be divided into two arms. The first arm consists of a transient wave that produces erythroid-myeloid progenitors (EMPs) (Bertrand et al., 2007 McGrath et al., 2011). The second arm, which is initiated later and maintained during adulthood, starts from Haematopoietic Stem Cells (HSCs), which are characterised by pluripotency and self-renewal and give rise to all professional immune cell types generated during adult lifespan (Keller et al., 1990, Cumano and Codin, 2007). During embryogenesis haematopoiesis starts after the gastrulation when specific mesodermal cells are committed to become blood cells. Later in embryogenesis, the Pre-HSCs emerge in the aorta-gonad mesonephros (AGM) region in humans, whereas in mice Pre-HSC are also found in placenta and in yolk sac (Mikolla and Orkin, 2006). The permanent definitive wave of haematopoiesis starts at the AGM and then continues in the fetal liver and finally the bone marrow. Upon expansion in the fetal liver HSCs form a stable, self-renewing population in the bone marrow (Figure 1.1), which constitutes the primary source of immune cells during adulthood.

In the bone marrow, HSCs, depending on the signals that they receive, differentiate into two distinct progenitors: the Lymphoid Stem Cell (LSC) or Common Lymphoid Progenitor (CLP)

and the Myeloid Stem Cell (MSC) or Common Myeloid Progenitor (CMP) (Figure 1.2) (Iwasaki and Akashi, 2007).

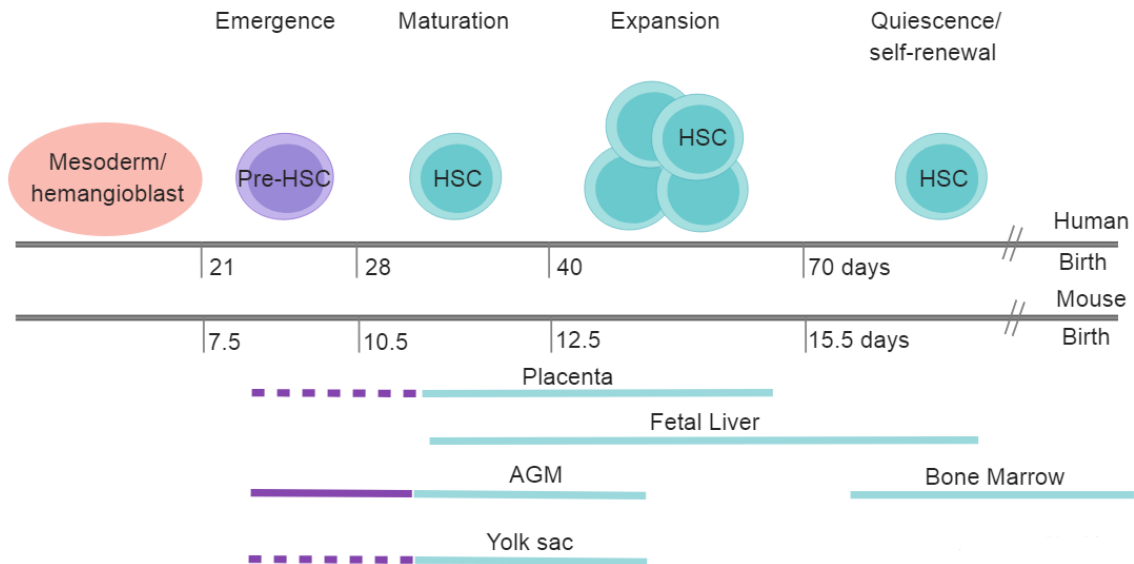


**Figure 1.1: Schematic representation of the HSC development during embryogenesis.** After gastrulation, specialised cells of mesoderm create the hemangioblasts, which are multipotent precursor cells that can differentiate both into hematopoietic and endothelial cells. On day 21 of human and on day 7.5 of mouse embryonic development the first Pre-HSC appear. In human, pre-HSC come from the AGM whereas in mice they are present both in the placenta and yolk sac. After day 26 in human and day 10.5 in mouse embryonic development the first mature HSC appear in AGM, yolk sac, placenta and fetal liver. On day 40 (or day 12.5 in mice) the HSC start to proliferate in fetal liver. Later, on day 70 (or 15.5 in mice), the cells migrate to the bone marrow where they remain in a quiescent state and have the ability for self-renewal.

The CLP can generate the different T-lymphocyte subsets (T-cells), B-lymphocytes (B-cells), and Natural Killer cells (NK cells). Its counterpart, the CMP, can generate the different granulocytic populations (Basophils, Eosinophils, and Neutrophils), the monocytes (that may later differentiate to macrophages and dendritic cells), platelets and erythrocytes (Iwasaki and Akashi, 2007). The differentiation processes may be triggered by extrinsic signals (Kondo et al., 2000) or intrinsic signals (Fairbairn et al., 1993, Maraskovsky et al., 1997), which are controlled by transcription factors essential for lineage-specific differentiation (Dahl et al., 2003, Laslo et al., 2006). Well-studied examples for those transcription factors are PU.1, C/EBP $\alpha$ , and C/EBP $\beta$ . Mice lacking PU.1 and C/EBP $\alpha$  show a severe dysregulation of myeloid cell development. PU.1 knock out mice die during the late stage of embryonic development or immediately after birth and show impaired formation of granulocytes, monocytes, B-cells and NK cells, but not megakaryocytes and erythrocytes (McKercher et al., 1996, Scott et al., 1994,

Colucci et al., 2001). On the other hand, mice lacking *C/EBP $\alpha$*  do not develop neutrophils or eosinophils (Zhang et al., 1997), indicating an important function in myoblast differentiation. *C/EBP $\beta$*  knock out mice display normal haematopoiesis and *C/EBP $\beta$*  expression in the *C/EBP $\alpha$*  gene locus also confers normal haematopoiesis, and thus it can rescue *C/EBP $\alpha$*  function (Jones et al., 2002). A possible explanation for this is the differential expression of the two genes during the development. *C/EBP $\alpha$*  is upregulated gradually upon HSC to CMP differentiation but *C/EBP $\beta$*  is downregulated (Hirai et al., 2006). Furthermore, mice lacking *C/EBP $\alpha$*  can produce neutrophils in presence of high concentrations of cytokines and *C/EBP $\beta$*  overexpression. Thus, *C/EBP $\beta$*  is important for stress induced neutrophil production, which can be important during the course of an infection (Hirai et al., 2006). PU.1 and *C/EBP $\alpha$*  also regulate maintenance of the HSC population. Disrupting PU.1 expression at birth can lead to loss of the HSC population (Iwasaka et al., 2005), whereas loss of *C/EBP $\alpha$*  may cause expansion of HSCs (Zhang et al., 2004).

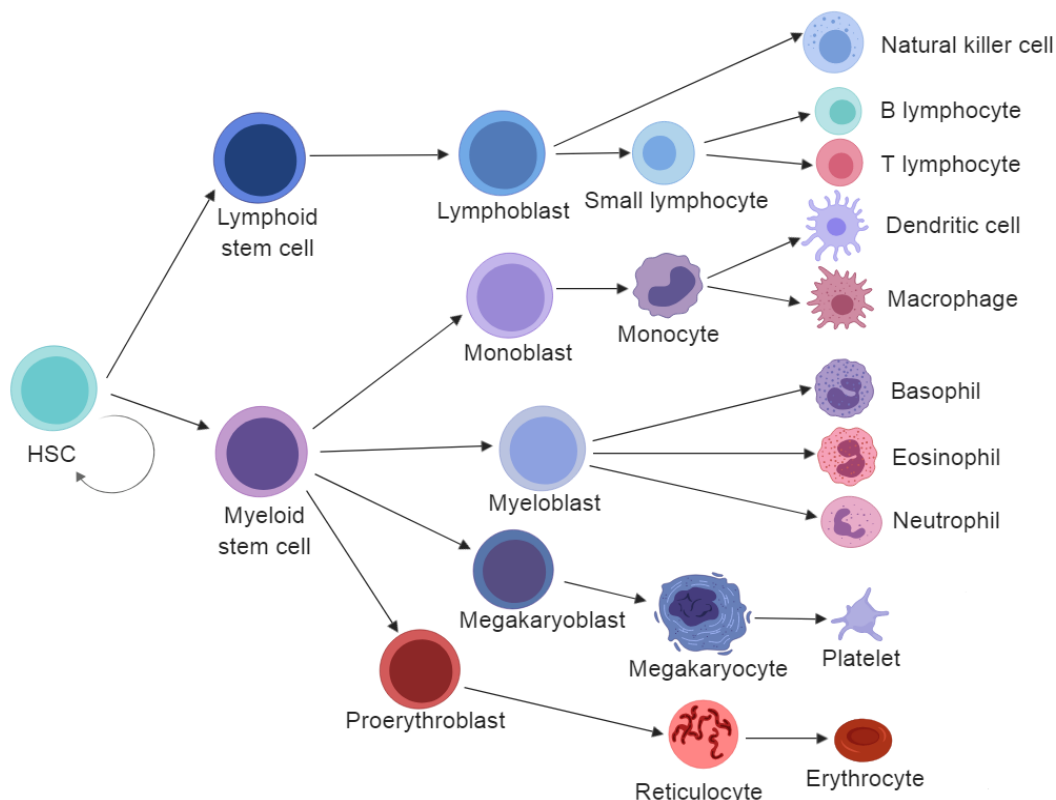


**Figure 1.2 Schematic representation of immune cell populations.** Early during differentiation, a common progenitor, termed Hematopoietic Stem Cell (HSC), can divide to create another HSC or differentiate either into a Lymphoid Stem Cell (LSC) or a Myeloid Stem Cell (MSC) depending on incoming signals. LSCs and MSCs are responsible for the generation of the lymphoid and myeloid cell lineage, respectively. After undergoing several cycles of differentiation and depending on external signals, they create the different cell types of the immune system.

In the bone marrow the different immune cell populations during their differentiation receive divert signals from the stromal cells that are located in the bone marrow medullary cavity. Stromal cells are comprised of osteoblasts, endothelial cells, reticular cells, fibroblasts and adipocytes. These stromal cells provide the signals for leucocyte differentiation and migration from the bone marrow to the blood stream (Zhao et al., 2012). A very well- studied example of a signal from stromal cells that controls haematopoiesis is the stromal cell-derived factor 1 (SDF-1, also known as CXCL12) (Nagasawa et al., 1996, Bleul et al., 1996). SDF-1 is a chemoattractant for CD34+ haematopoietic precursors, mature B-cells and T-cells, and monocytes (Aluti et al 1997, D'Apuzzo et al., 1997). All these cell types express C-X-C chemokine receptor type 4 (CXCR-4) and the interaction between the receptor and SDF-1 is responsible for chemoattraction and retention of B-cells and granulocytic precursors within the bone marrow microenvironment (Ma et al., 1998, Ma et al., 1999). Whereas B-cells, NK cells, and the cells from the CMP lineage initially mature in the bone marrow until they receive the appropriate signals to migrate to the blood stream, T-cell precursors first migrate to the thymus for their maturation (Donskoy et al., 1992, James et al., 2018). The precursors of T-cells in the thymus are called thymocytes. During the prenatal period,  $\gamma\delta$ T-cells and  $\alpha\beta$ T-cells mostly migrate from the fetal liver, and during adulthood the main source of T-cells is the bone marrow, from where  $\alpha\beta$ T-cells enter the thymus. In the thymus,  $\alpha\beta$ T Cells undergo positive and negative selection. Negative selection is the process were thymocytes undergo apoptosis when they recognize a peptide of the Major Histocompatibility Complex (MHC) with high affinity. Negative selection is very important for elimination of self-reactive thymocytes. On the other hand, positive selection occurs if the T-cell receptor (TCR) binds to a peptide–MHC ligand with low affinity. This engagement is a signal for survival and differentiation. If the thymocytes bind to a peptide MHC class I ligand they become CD8+ T-cells, whereas if they bind to peptide-MHC class II ligand CD4+ T-cells are generated (Palmer, 2003). Only the mature T-cells can leave the thymus and enter the blood stream.

Generally, the major immune-cell populations after maturation can be found in the blood stream and from there may reach different tissues and the secondary lymphatic organs. Specific signals from the tissues may initiate terminal differentiation programs. For example, monocytes from the blood stream can migrate through the endothelium in a process referred to as diapedesis and differentiate into macrophages within the tissue environment. (Ebert and Florey, 1939). Research over the past few years indicates however, that the bone marrow derived immune cells cannot be the only source of immune cells found in the tissues (Davies et al., 2013). For example, cells with unclear origin until recently, are the tissue resident alveolar macrophages.

In 1968, Ralph van Furth and Zanvil Cohn, proposed that macrophages generally derive from monocytes which infiltrate the tissues and differentiate into macrophages (Mononuclear Phagocyte System, MPS). This model was in dispute though, because as mentioned earlier, macrophages do exist in the yolk sac before primitive haematopoiesis. Furthermore, evidence existed that macrophages can proliferate within tissues (Sawyer et al., 1982, Czernielewski et al. 1987) and gain self-renewal capacity (Merad et al., 2002). A clear evidence for the existence of tissue resident macrophages, originating from a precursor different from HSCs, came from Myb-deficient mice, which lack HSCs (Schulz et al., 2012). In this model, yolk sac macrophages gave rise to a distinct macrophage population expressing F4/80<sup>hi</sup>, and found in many adult tissues, including skin (Langerhans cells), brain (microglia), spleen (red pulp macrophages), lung (Alveolar macrophages), pancreas and kidney. This F4/80<sup>hi</sup> population had a gene expression signature found in yolk sac macrophages, but not in F4/80<sup>low</sup> (blood-derived) macrophages. Thus, the model of macrophage origin is presently being revised in order to include prenatal lineages of resident macrophages, which arise from a distinct embryonic macrophage lineage during embryonic development.

It is evident that the generation of immune cells is a highly complex process with many underlying layers of positive and negative control. The diversity of signals that control all stages of haematopoiesis predict sophisticated genetic control mechanisms ensuring proper immune cell development and activation to prevent from e.g. auto-immunity or over-shooting inflammatory reactions. In the next chapters, some of the most important features of the distinct leukocyte populations and the molecular circuitries underlying their proper activation are explained.

### **1.1.2 Cells of the immune system**

As mentioned in the previous chapter, several different immune cell types exist. Each major cell type however can be further sub-classified depending on distinct surface marker expression (e.g. CD4<sup>+</sup> Th1 and Th2 cells). Some subtypes share some common characteristics depending on either their origin or the way they respond to danger signals. In the following, the major immune cell types and their most important characteristics are described.

T cells can be divided into two main subpopulations, the CD4<sup>+</sup> T-cells or T helper cells (Th cells) and the CD8<sup>+</sup> T-cells or cytotoxic T-cells. Mossman and Coffman in 1986 showed that CD4<sup>+</sup> T-cells can be subdivided into two groups. The first group produces IFN $\gamma$  as signature cytokine and is referred to as Th1 cells, while the second group produces IL-4 and is referred

to as Th2 cells. Later it became evident that T-cells are even more diverse. Naïve CD4 T-cells receive signals during development to differentiate into Th1, Th2, Th17 and T regulatory cells (Tregs). These four populations express different cytokines and are involved in different pathological conditions. Th1 cells produce mainly IFN $\gamma$  and IL-2, are involved in autoimmune diseases and are critical for defence against intracellular microorganisms. Th2 cells produce IL-4, IL-5, IL-13, IL-25, IL-10 and amphiregulin and play role in asthma and allergies, but also in defence against extracellular parasites. Th17 cells express mainly IL-23, IL17a, IL-17f, and IL-22, are also involved in autoimmunity and play a critical innate function in protection against extracellular bacteria and fungi (Weaver et al., 2006). Lastly, Tregs have an immunomodulatory role and are involved in lymphocyte homeostasis and immune tolerance. These cells express TGF $\beta$ , IL 35, IL10 and are distinguished from the other CD4+ populations by expression of the forkhead box P3 (Foxp3) gene (Chen et al., 2003).

CD8+ T-cells, on the other hand, are a more homogenous population. Naïve CD8+ T cells recirculate through secondary lymphoid organs and are activated via interaction of their T cell receptor (TCR) with an antigen that is presented to them by dendritic cells. Once activated, CD8+ T cells start to proliferate and differentiate into effector cells named cytotoxic T lymphocytes (CTLs). These cells are able to kill infected or malignant cells and thus provide protection against infections or cancer (Zhang et al., 2011). Most CTLs generated during primary infection are short-lived and are contracting, leaving behind a smaller population of ‘memory’ CD8 T cells that can respond rapidly during a secondary infection. Memory CD8+ T cells can be subdivided into ‘central memory’, ‘effector memory’ and ‘resident memory’ CD8+ T cells. ‘Central memory’ and ‘effector memory’ cells express different receptors and are located in different tissues (Obar et al., 2010). ‘Resident memory’ CD8+ T cells are found permanently in non-lymphoid tissues after specific infections (Mueller et al., 2013). CTLs undergo rapid expansion after activation and they migrate to the inflamed or infected tissues. To find their targets chemokines and chemokine receptors, like CXCL10, CXCR3 and CXCR5, are thought to be involved (Harris et al., 2012, Hickman et al., 2015). CTL-mediated killing requires direct contact between the TCR on the CTL and the peptide–MHC class I complex on the target cell. After the contact is established, the CTL realises several biochemical mediators, such as perforin and granzyme in order to induce the cell death. Except the mediators, it is believed that CTLs can also activate specific cell inducing signals in the target cell (Halle et al., 2017).



The main cell population responsible for adaptive humoral immune responses are B-cells. This type of cells is also generated from CLPs and is a population of cells that express clonally diverse cell surface immunoglobulin (Ig) receptors recognizing specific antigenic epitopes. During development, the CLP becomes committed to differentiate into B-cells by the expression of paired box protein 5 (Pax5) (Cobaleda et al., 2007). B-cell development occurs through sequential maturation steps within the bone marrow before release of immature B cells into the circulation that travel to the spleen for maturation. Developing B cells progress through rearrangement of immunoglobulin heavy- and light-chain gene segments (variable V, diversity D, joining J) from pro-B to pre-B to immature B cells, leading to the expression of IgM mature B cell receptor BCR. The contact between B-cells and bone marrow stromal cells is important for maturation of B-cells, since these cells are the suppliers of integrins, growth factors, chemokines, and cytokines (Hoffman et al., 2016). The random rearrangement process of immunoglobulin genes during B-cell development is responsible for the diversity of BCR receptors that can recognise a large number of epitopes. B-cells are also going through positive and negative selection. BCR receptors with high affinity to own epitopes undergo negative selection whereas BCRs with low affinity undergo positive selection. The negative selection process is important for elimination of autoreactive BCRs that can potentially lead to autoimmune diseases. The humoral immunity provided by B-cells is due to production of antibodies that develop through recombination events of V, D, and J gene segments in the H (Heavy) chain locus and the V and J gene segments in the L (Light) chain loci (Brack et al., 1978). Five classes, of antibodies exist, the IgM, IgD, IgG, IgA, and IgE class. They may be distinguished according to the C-terminal regions of the heavy chains, which are constant and do not participate in antigen binding, but are important e.g. for activation of other immune cells like macrophages. Furthermore, there are four subclasses or isotypes of IgG antibodies (IgG1, IgG2, IgG3, and IgG4). Antibodies can neutralize their targets (e.g., they bind to a virus and prevent it from entering a cell), they can activate macrophages and other immune cells or activate the classic pathway of the complement system (Laßien and Tedder, 2008).

Another member of the lymphoid lineage is the NK population. NK cells account for approximately 10-15% of circulating lymphocytes in healthy adults and even though they share many common features with T-cells, especially CD8<sup>+</sup> T cells, they follow a different path during development and have distinct genetic background. The maturation of NK cells takes place outside the thymus and they do not express a rearranged TCR (Ritz et al., 1985). Major functions of NK cells are to produce IFN $\gamma$  and mediate cellular cytotoxicity. To facilitate their functions, NK cells express two major types of MHC class I-binding receptors: the C-type

lectin-like receptors formed primarily by the combination of CD94 with either NKG2A (inhibitory) or NKG2C (activating); and the large and highly diverse family of killer immunoglobulin-like receptors (KIRs) (Colonna et al., 1999). NK cells act based on the hypothesis of ‘missing self’, which refers to the ability to recognise and destroy cells that have downregulated MHC class I molecules (Ljunggren and Kärre, 1990). Because of this ability, they are of high importance to the elimination of cancer cells. In 2002, Ruggeri and his colleagues showed that NK cells are critical to successful outcomes following T cell-depleted, MHC haploidentical, allogeneic, hematopoietic stem cell transplantation (allo-HSCT) in acute myeloid leukaemia (AML) therapy. Patients who received donor-differentiated NK cells that demonstrate alloreactivity in the graft-versus-leukaemia direction had a better survival rate compared to the ones that received NK cells without alloreactivity. In the last few years, it became evident that NK cells are a very heterogeneous population with different phenotype, function and developmental path (Freud et al., 2017). The population can be divided into conventional NK cells (cNK), and tissue-resident NK cell (trNK). The first identified were the cNK cells in the circulation and were divided into two populations the CD56<sup>bright</sup>CD16<sup>lo/-</sup> and CD56<sup>dim</sup>CD16<sup>+</sup> (Lanier et al., 1983, 1986). The two populations show differential expression of receptors and cytokines with CD56<sup>bright</sup> cNK cells being more immunomodulatory and CD56<sup>dim</sup> cNK cells serving more of a cytotoxic effector role (Cooper et al., 2001). More recently, trNK cell populations have been described in human secondary lymphoid tissues, bone marrow, spleen, lung, and liver (Cuff et al., 2016, Lugthart et al., 2016, Lunemann et al., 2013, Marquardt et al., 2015, 2017, Stegmann et al., 2016). These cells share some features with each other but they are different from cNK cells, especially with CD56<sup>bright</sup> cNK cells.

Granulocytes are cells of the myeloid cell lineage and are comprised of three distinct morphologically and functionally populations, the neutrophils, eosinophils and basophils. They are responsible for clearing pathogens and have immunomodulatory functions (Geering et al., 2013). The cells mature in the bone marrow and fully differentiate in the blood circulation. In the blood, they do not proliferate since they are arrested in G<sub>0</sub> phase of the cell cycle and their lifespan is between 1-5 days. Granulocytes migrate from the blood circulation into tissues in response to chemoattractants, such as interleukin (IL)-8 (neutrophils) or eotaxin (eosinophils and basophils). At the site of inflammation, they secrete a variety of toxic molecules against pathogens, which can also harm the host tissue and thus the balance between antimicrobial defence and host damage is important. Lifespan of granulocyte is important during the course of infection. Several cytokines and proinflammatory mediators can regulate the survival of granulocytes. The classical granulocyte-regulating cytokines are IL-3, IL-5, and granulocyte

macrophage colony stimulating factor (GM-CSF) (Simon, 2001). All three cytokines can increase the lifespan of eosinophils but only GM-CSF is important for neutrophil survival. In Basophils, by contrast, only IL-3 seems to have a significant effect on survival (Didichenco et al., 2008). Granulocytes express pathogen recognition receptors (PRRs) and can recognise pathogen-associated molecular patterns (PAMPs) and damage-associated molecular patterns (DAMPs). Another important characteristic of neutrophils and eosinophils, which it is essential for the fight against microorganisms is the formation of extracellular DNA traps, which are called neutrophil extracellular traps (NETs) (Brinkmann et al., 2004, Yousefi et al., 2008). This phenomenon is described as a special form of neutrophil death that is different from apoptosis and necrosis and it is called NETosis. NETs are a form of innate response were microorganisms are trapped inside the released DNA, which prevents microorganisms from spreading, and facilitates to their death because of high local concentration of antimicrobial agents.

Blood monocytes also belong to the myeloid cell lineage and they are considered precursors of some populations of macrophages and dendritic cells (Sprangers et al., 2016). In human peripheral blood, three different subsets of monocytes have been identified and characterized based on their expression of surface markers CD14 and CD16. The main monocytes, the classical monocytes, expresses high levels of CD14 and no CD16 (CD14<sup>++</sup>CD16<sup>-</sup>). The intermediate monocytes express relatively high levels of CD14 and some CD16 (CD14<sup>+(+)</sup>CD16<sup>+</sup>) and the nonclassical monocytes are characterised by low levels of CD14 and high levels of CD16 (CD14<sup>+</sup>CD16<sup>++</sup>) (Ingersoll et al., 2010, Wong et al., 2012). During inflammation or injury, first the classical monocytes are recruited to the inflamed tissue and induce immunological responses. Intermediate monocytes are recruited later, and they are mainly responsible for antigen presentation, high secretion of proinflammatory cytokines and chemokines and wound healing. Nonclassical monocytes constantly survey the endothelium for any threat in order to induce the rapid recruitment of other immune cells. During inflammation, monocytes differentiate into macrophages and dendritic cells in response to several stimuli such as INF $\gamma$ , produced from NK cells, and collaborate with the existing tissue resident macrophages. The recruitment of monocytes is controlled by the chemokine receptor CCR2 and its ligands CCL2 and upon recruitment they produce high levels of proinflammatory cytokines, such as interleukin IL-1 and TNF- $\alpha$ . In addition, they phagocytose dead cells and produce IL-18 to activate NK cells (Serti et al., 2014). When the acute inflammation resolves, the number of classical monocytes is reduced and they are subsequently replaced by intermediate and nonclassical monocytes. The migration of these monocytes is controlled by CX3CR1 and its

ligand CX3CL1. The non-classical monocytes secrete IL-10 and transforming growth factor TGF- $\beta$  and induce tissue repair (Sprangers et al., 2016).

Monocyte-derived Dendritic Cells (DCs) are professional antigen-presenting cells and link the innate and adaptive immune system. DCs are separated into at least two populations, the classical and plasmacytoid DCs (cDCs and pDCs respectively) (Colin et al., 2013). The plasmacytoid DCs are not derived from monocytes but originate from precursor cells in the bone marrow (Christiakov et al., 2014). cDCs can arise from monocytes during inflammation and are different from the DCs that are produced in steady state. *In vivo* experiments have shown that injected monocytes migrate to inflammatory sites and differentiate into DCs in various models of inflammation (Hou et al., 2012). As part of the innate immune system, monocyte-derived DCs during inflammation secrete high amounts of the anti-inflammatory cytokine IL-10 and engulf apoptotic erythroid cells. Accordingly, blocking differentiation of monocytes into DCs leads to tissue damage, increased cytotoxic T cell activity, and reduced life expectancy (Ohyagi et al., 2013). The different subtypes of monocytes give rise to different types of DCs. Classical monocytes are differentiated into more immune responsive DCs and non-classical monocytes generate DCs with better immune tolerance (Jakubzik et al., 2008).

Monocyte-Derived Macrophages are a population of macrophages that is distinct from tissue resident macrophages. Monocyte derived macrophages are constantly recruited to the tissues when required and together with their resident counterparts contribute to tissue homeostasis and fight against threats. In some tissues, classical monocytes can differentiate into macrophages also in steady state, but in most cases, the differentiation occurs during inflammation (Sprangers et al., 2016). Macrophages derived from classical monocytes express higher levels of CD14 compared to macrophages derived from nonclassical monocytes when cultured *in vitro* (Frankenbergen et al., 2012). Furthermore, macrophages from classical monocytes exhibit phagocytic, proteolytic, and inflammatory functions, whereas macrophages derived from CD16- expressing monocytes promote tissue repair (Nahrendorf et al., 2010). The heterogeneity of macrophages is important in pathological conditions. For example, infection with parasites, such as *Schistosoma mansoni* and *Heligmosomoides polygyrus* induce invasion of classical monocytes into the adult murine heart, where they differentiate into macrophages and drive inflammation and tissue damage (Lavine et al., 2014). These macrophages have limited capacity to promote tissue repair (Mylonas et al., 2015). On the other hand, in the concept of different pathological condition such as cardiac pressure overload, nonclassical monocytes are recruited and differentiate into macrophages (Weisheit et al., 2014). Thus,

macrophages derived from the different monocyte subsets have been shown to maintain some of the properties of their progenitors.

All different types of immune cells interact in order to provide a complete immune response. This interaction is mediated through cytokines, chemokines and receptors that are expressed on the surface of the cells. The synergy between the different cell types and the timing of their respective responses is tightly regulated, in order not only to defeat foreign invaders but also to avoid self-destruction.

### **1.1.3 The innate immune system**

The immune system may be divided into two parts: the innate and the adaptive immune system. These two systems are composed of different cell types and are activated at different time points in response to distinct signals. The innate immune system provides the first line of defence, whereas adaptive immunity is usually fully induced later on. Furthermore, adaptive immunity is much more specific than innate immunity, recognizing a virtually infinite number of different epitopes, whereas the innate immune system recognises primarily conserved features of pathogens and cellular stress. Ilya Mechnikov was the first who described the innate immune system in 1908, but for many years it was neglected due to the impressive discoveries made in the field of adaptive immunity. The innate immune system is evolutionary ancient and conserved core concepts of innate immunity are found in all eukaryotic species, whereas the adaptive immune system is restricted to vertebrates (Janeway and Medzhitov, 2002, Turvey et al., 2010).

The innate immune system comprises not only cells derived from haematopoietic stem cells but also other cell types, such as epithelial cells. Physical barriers like the skin, but also mucociliary clearance, low stomach pH, lysozymes in tears and saliva and other non-cellular components are also part of the innate immune system. Leukocytes primarily involved in innate immune responses are macrophages, dendritic cells, mast cells, neutrophils eosinophils, basophils, NK cells and Natural Killer T-cells (NKT cells). As mentioned above, cells of the innate immune system can recognise a variety of conserved features on the surface of pathogens, which are called pathogen-associated molecular patterns (PAMPs). PAMPs can be recognised by specific receptors on the surface of the cells that are called pattern recognition receptors (PRRs). Downstream immunity is either cell-mediated, for example through phagocytosis and cytotoxicity, or involves extracellular factors like antimicrobial peptides (AMPs) (Dubos, 1939), alarmins or damage-associated molecular patterns (DAMPs) (Matzinger et al., 2004),

chitinases/chitinase-like receptors (Suzuki et al., 1984), complement factors, proteases, cytokines/ chemokines and other molecules (Gasteiger et al., 2016).

#### **1.1.4 Pathogen recognition by Pattern Recognition Receptors**

Several cell types, including epithelial cells, and many cells of the haematopoietic cell lineage express PRRs. The signalling cascades downstream of these receptors are highly important for host defence. PRR signalling is not only important for the activation of the innate immune system but also for the adaptive, since it induces e.g. maturation of dendritic cells, which can trigger the secondary line of defence, or activation of T- and B-cells. Different types of PRRs exist. Toll-like receptors (TLRs) were the first to be identified (Lemaitre et al., 1996). To date several types of TLRs have been characterised (10 in humans and 12 in mice). The different types of TLRs can recognise a variety of different PAMPs. TLR1, 2 and 6 can recognise lipoproteins, TLR3 double stranded (ds) DNA, TLR5 flagellin, TLR7 and 4 lipopolysaccharide (LPS), TLR7 and 8 single stranded (ss) RNA and TLR9 can recognise DNA (Kawai and Akira, 2011). TLR2 recognises many PAMPs both in Gram-positive and Gram-negative bacteria, such as lipoproteins and peptidoglycans (present in both Gram-positive and negative), as well as lipoteichoic acid (present only in Gram-positive). In order to distinguish between the different PAMPs, TLR2 forms heterodimers. For example, TLR2-TLR1 heterodimer can recognise triacylated lipopeptides from Gram-negative bacteria, whereas TLR2-TLR6 heterodimer recognises diacylated lipopeptides from Gram-positive bacteria (Akira et al., 2006).

Some of the TLRs are localised on the surface of the cells, like TLR1, 2, 4, 5 and 6, whereas others, like TLR3, 7, 8 and 9 are expressed within intracellular vehicles, such as the endoplasmic reticulum (ER), endosomes, lysosomes and endolysosomes (Kawai and Akira, 2011). The intracellular localisation of these receptors is of high importance, since the intracellular recognition of nucleic acids provides the cell with a means to sense and eliminate infectious agents within phago/endosomal cargo. These receptors are sequestered in the ER and are transferred to endosomes via the Golgi apparatus. After entering the endosome, the receptors are being further modified in the N-terminal region by different proteases, such as cathepsins and asparagine endopeptidase to generate functional receptors that can induce signalling (Ewald et al., 2011). When TLRs recognize their respective PAMPs, a signalling cascade is activated and leads to induction of mediators of host defence. The TLR response is initially activated by recruitment of adaptor proteins that have TIR-domains, such as myeloid differentiation primary response 88 (MyD88), Toll/interleukin-1 receptor domain-containing adapter protein (TIRAP), TIR-domain-containing adapter-inducing interferon- $\beta$  (TRIF) and

TRIF-related adaptor molecule (TRAM). MyD88 is essential for the signalling of all TLRs, except TLR3, and leads to nuclear factor kappa beta (NF- $\kappa$ B) and mitogen activated protein (MAP) kinase activation. TLR3 and TLR4 can use TRIF as an adaptor protein and activate IRF3 to induce the production of type I interferons (IFNs) (Kawai and Akira, 2011). TIRAP is used as an adaptor protein by TLR2 and TLR4 to recruit MyD88 and TIRAM connects TLR4 and TRIF. TLR4 is the only member of the TLR family that can activate both the TRIF-dependent and the MyD88 dependant pathway (Figure 1.3). The two pathways have different kinetics. First, MyD88 is activated and recruits the IRAKs, TRAF6 and TAK1 complex and leads to NF- $\kappa$ B and MAP kinase activation. In the second phase, TLR4 gets endocytosed and forms a complex with TRAM and TRIF, which leads to recruitment of TRAF3 and subsequently the kinases TBK1 and IKK $\epsilon$ , which phosphorylate IRF3 and lead to expression of type I IFNs (Kawai and Akira, 2011). TRAM-TRIF also recruit TRAF6 in order to induce a late-phase NF- $\kappa$ B and MAP kinase activation. In the second phase, TLR4 is delivered from endosomes to phagosomes with the help of RaB11a GTP-ase and this delivery is important for type I interferon induction (Husebye et al., 2010). A splice variant of TRIF, TAG can disrupt the TRAM-TRIF interaction, which leads to inhibition of the TRIF-Dependent pathway and subsequently type I IFN production (Palson-McDermott et al., 2009).

The Heterodimers TLR2-TLR1 and TLR2-TLR6 signal through TIRAP and MyD88 to induce inflammatory cytokines. However, TLR2 alone can induce type I IFNs in inflammatory monocytes (Barbalat et al., 2009). TLR2 is internalised and induces activation of IRF3 and IRF7 through MyD88. TLR7 and TLR9 signal also through MyD88, which forms a complex with TRAF3, TRAF6, IRAK1 and IKK $\alpha$  and leads to IRF3 phosphorylation and Induction of type I IFNs. TLR9 can actually activate two pathways in two different cellular compartments. In the early endosomes, after CpG DNA stimulation, TLR9 triggers MyD88-TRAF6 dependent NF- $\kappa$ B activation and IL12p40 production. Later, TLR9 travels to lysosome-related organelles (LRO), where it utilises TRAF3 to activate IRF7 and subsequently induce type I IFNs (Sasai et al., 2010). TLR5 induces inflammatory cytokines through MyD88-TRAF6 dependent NF- $\kappa$ B activation but in intestinal epithelial cells can also recruit TRIF, which leads to NF- $\kappa$ B activation rather than IRF3 (Choi et al., 2010).

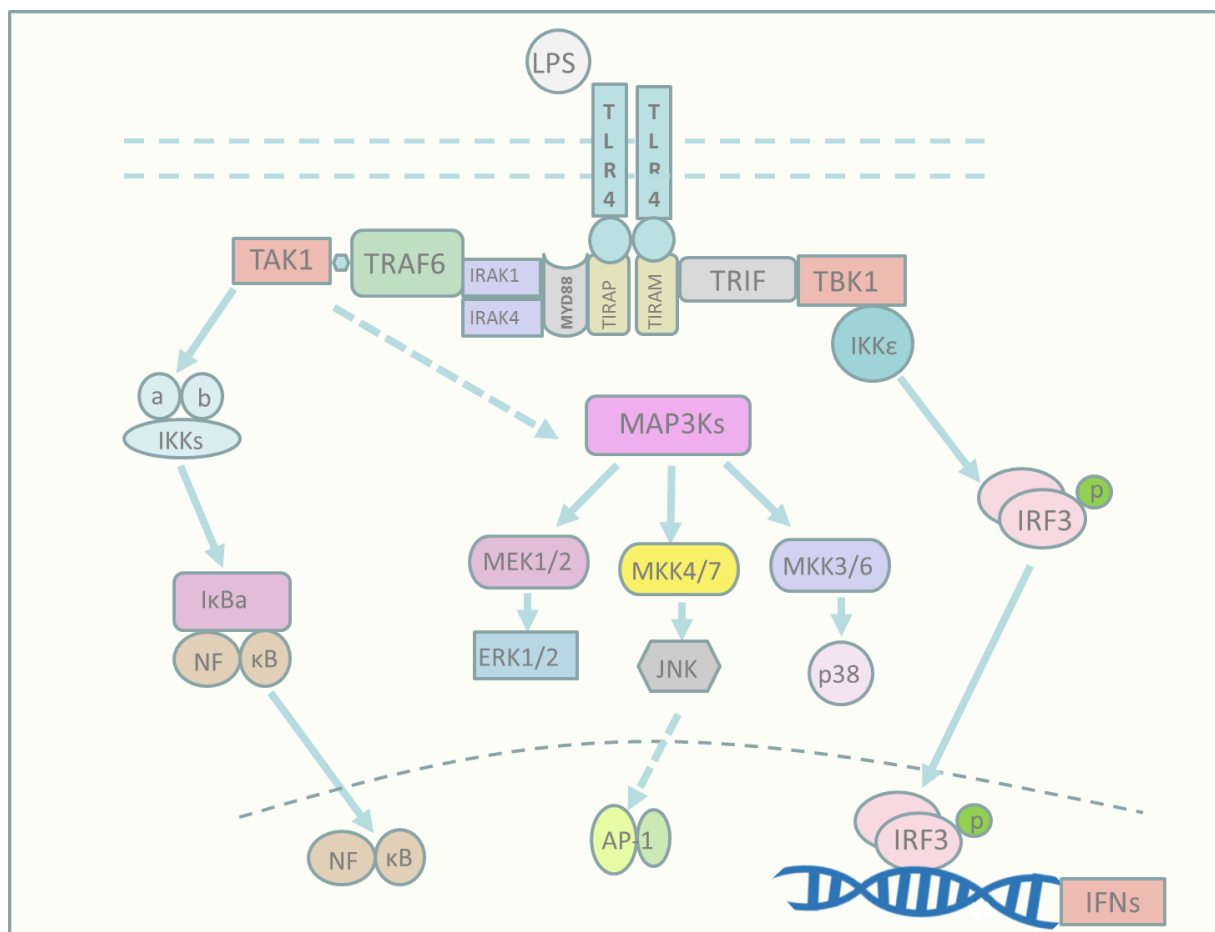


**Figure 1.3: Simplified schematic representation of the TLR4 signalling pathway.** Upon LPS stimulation, TLR4 can induce in early phase MyD88-TRAF6 dependent NF- $\kappa$ B activation and MAP kinase activation. After TLR4 gets endocytosed, it forms a complex with TRAM and TRIF, which leads to IRF3 phosphorylation and type I IFN induction.

Other PRR types are the nucleotide-binding oligomerisation domain (NOD) proteins that belong to the NOD-like receptor (NLR) family. NOD1 and NOD2 are the best-studied members of this family (Bertin et al., 1999, Inohara et al., 1999, Ogura et al., 2001). Both receptors have a caspase activation and recruitment domain (CARD), a nucleotide binding domain (NOD) and multiple leucine-rich repeats (LRRS) (Caruso et al., 2014). These two receptors can activate NF- $\kappa$ B in response to peptidoglycans (Inohara et al., 2001). NOD1 can recognise  $\gamma$ -D-glutamyl-meso-diaminopimelic acid (iE-DAP), a motif present in many Gram negative and some Gram positive bacteria (Chamaillard et al., 2003, Girard et al., 2003), and NOD2 can recognise muramyl dipeptide (MDP) which is present in both Gram negative and Gram positive bacteria (Inohara et al., 2003). The two receptors are oligomerised upon PAMP sensing and recruit receptor-interacting serine/threonine-protein kinase 2 (RIPK2). RIPK2 then leads to activation of TAK1, which eventually leads to activation of NF- $\kappa$ B and MAP kinases and inflammatory genes.



C-type lectin receptors (CLRs) are another class of PRRs. These proteins were first identified as a family of calcium-dependant carbohydrate-binding proteins (Drickamer et al., 1999). Later, because of sequence homology the term got more general and is now used for any protein that contains one or more C-type-lectin-like domain (CTLD) (Zelensky and Gready, 2005). CLRs are a diverse group of receptors that can recognise various PAMPs on the surface of pathogens. For example, Mannose-binding lectin (CD206) binds to various sugars (such as N-acetyl-D-glucosamine, mannose, N-acetyl-mannosamine, fucose and glucose) found on the surface of some viruses, bacteria, fungi and protozoa (Robinson et al., 2006). The signal transduction downstream of CLRs is not shared upon the members of the family, but rather depends on the type of the receptor. Some lectins, like Dectin-1, can induce Spleen tyrosine kinase (SyK)-dependant cytokine production (Rogers et al., 2005). SyK activation can recruit adaptors, like Fc receptor  $\gamma$  chain (FcR $\gamma$ ), which have an immunoreceptor tyrosine-based activation motif (ITAM) or can act via a single tyrosine based motif found in the cytoplasmic domains of some lectins (hemITAM). Other lectins bind to immunoreceptor tyrosine-based inhibitory motif (ITIM) and recruit phosphatases, such as Src homology 2 (SH2) domain containing inositol polyphosphate 5-phosphatase 1 and 2 (SHIP1 and SHIP2) and negatively regulate the inflammatory signals and some others act directly without a clear evidence of binding to a motif (Sancho and Reis e Sousa, 2012).

The RIG-I-like receptors Retinoic inducible gene I (RIG-I), melanoma differentiation association gene 5 (MDA5) and laboratory of genetics and physiology 2 (LPG2) are important PRRs for recognition of viruses. These proteins belong to DExD/H box helicase subfamily and can sense viral RNA (Loo and Gale, 2011). The receptors of this family have three distinct domains: an N-terminal region consisting of caspase activation and recruitment domains (CARD), a central DExD/H box RNA helicase domain and a C-terminal repressor domain (RD) within the C-terminal domain (CTD). RIG-I was originally characterised in stimulation experiments with synthetic dsRNA poly I:C (Yoneyama et al., 2004). This PRR preferentially recognises 5' triphosphorylated (5'ppp) RNA (Hornung et al., 2006), but it can also recognise monophosphate and diphosphate RNAs, although these modifications are not able to induce its full signalling potential (Pichlmair et al., 2006). RIG-I can also bind to single stranded (ss) RNA (Kato et al., 2006). MDA5 can interact with synthetic dsRNA poly I:C but preferentially recognises high molecular weight poly I:C fragments and does not bind to (ss) RNA. For LPG2 little is known about its RNA ligands, but it seems to bind a variety of RNA species (Murati et al., 2008, Pippig et al., 2009, Takehata et al., 2009). The signalling of RIG-I, which is better characterised than to the other two members of this family, involves interactions between

CARDs and RD (Saito et al., 2007). At steady state RIG-I is held in closed conformation and upon RNA binding, its conformation opens and it interacts with its adaptor protein MAVS and induces type I IFN production (Scott, 2010).

## **1.2 The Non-coding genome**

### **1.2.1 Non-coding RNA species**

In recent years the central dogma of genetics, stating that DNA is transcribed into RNAs, which are translated into protein or participate in protein-synthesis, was significantly challenged. It is now evident, that only 4% of the human genome is actually protein coding. At least 90 % of the remaining non-protein-coding genome, large parts of which were previously thought to constitute ‘junk’ DNA, is transcribed (Barbagallo et al., 2018). This ‘non-coding genome’ gives rise to a variety of RNA species that are functionally and morphologically different and are called the non-coding RNAs (ncRNAs). It is thus reasonable to believe that important clues to understand several pathophysiological phenomena are hidden within this region. NcRNAs are found in all domains of life, which further underlines the importance of these molecules (Barbagallo et al., 2018). The first non-protein-coding RNA species to be discovered were the transfer RNAs (tRNAs) and the ribosomal RNAs (rRNAs), back in the 1950s (Zamecnik et al., 1954, Scherrer and Durnell, 1962). Later in the 1980s, Yang and his colleagues discovered small nuclear RNAs (snRNAs) (Yang et al., 1981). Until the early 2000s, very few other non-protein-coding RNAs were discovered. One of the most important findings in this research field was the discovery of Xist, an RNA that is responsible for X chromosome inactivation in mammals (Brockdorff et al., 1992, Brown et al., 1992). After the development of next generation sequencing (NGS), the identification of non-coding RNAs expanded dramatically. To date several classes of non-coding RNAs have been identified, such as micro (miRNAs), small nucleolar RNAs (snoRNAs), small Cajal body-specific RNAs (scaRNAs), enhancer RNAs (eRNAs), small interfering RNAs (siRNAs), piwi-interacting RNAs (piRNAs), vault RNAs (vtRNAs) and long non-coding RNAs (lncRNAs). The snoRNAs and scaRNAs together with tRNAs, rRNAs and snRNAs belong to the group of housekeeping RNAs, which are constitutively expressed and play critical roles in the production of proteins. On the other hand, miRNAs, siRNAs, piRNAs and lncRNAs belong to the family of regulatory RNAs (Wu et al., 2016).

## 1.2.2 Small regulatory RNAs

The family of small regulatory RNAs comprises the subfamilies of miRNAs, siRNAs and piRNAs. The first miRNA, *lin-4*, was first discovered in *C. elegans* in 1993 (Lee et al., 1993) and since then the field has expanded dramatically. MiRNAs are endogenous, non-coding, single-stranded RNA molecules with a length of 20-24 nucleotides that negatively regulate mRNA levels. MiRNAs are conserved among species and are expressed in a tissue-specific or developmental-stage-specific manner. In humans, over 2,500 matured miRNAs (based on miRBase.org, released August 2010, Last Update: November 2010) have been identified so far and it is estimated that about 60% of the human proteome is regulated by them (Friedman et al., 2009). MiRNAs can be transcribed either from independent miRNA genes or are found within introns, and occasionally exons of other genes (Carthew and Sontheimer, 2009). Several genes can be targeted by a specific miRNA, and several miRNAs can target one gene (Krek et al., 2005). Most of the times, miRNAs reduce protein expression but their binding can also favour enhanced translation (Lytle et al., 2007, Vasudevan et al., 2007, Lin et al., 2011). MiRNAs are also important regulators of adaptive and innate immunity. They are considered as fine tuners of the immune responses against pathogens but also involved in the differentiation and polarisation of leukocytes. Well-studied examples of such miRNAs are miR-155 and miR-146a (Taganov et al., 2006, O'Connell et al., 2007). Both miRNAs are upregulated downstream TLR4 activation but may control the inflammatory responses in opposite directions. MiR-146a is a negative regulator of the NF- $\kappa$ B signalling through targeting multiple proteins of the pathway like TLR4, MyD88, IRAK-1, and TRAF6 (Curtale et al., 2013). MiR-155, on the other hand, may promote the inflammatory responses via targeting suppressor of cytokine signalling 1 (SOCS1) and Src homology 2 domain-containing inositol-5'-phosphatase 1 (SHIP1) (Wang et al., 2010, McCoy et al., 2010). Other reports however suggest that miR-155 has a negative feedback function as well, similar to miR-146 (Janga et al., 2018, Schulte et al., 2013). Other miRNAs, like miR-125, are involved in the control of haematopoiesis. For example, miR-125 is able to control stem cell numbers by negatively regulating BCL2-antagonist/killer 1 (BAK1), a gene regulating apoptosis (Guo et al., 2010).

While miRNAs are regulators of endogenous gene expression, siRNAs and piRNAs are defenders of genome integrity in response to foreign or invasive nucleic acids such as viruses, transposons, and transgenes. The discovery of siRNAs came five years after the discovery of

miRNAs (Fire et al., 1998). The size of siRNAs is 21-25 nucleotides. The mechanism of action of siRNAs is called RNA interference (RNAi). SiRNA biogenesis and their mode of action have many similarities with miRNAs. In both cases the RNA target is recognised by Watson-Crick base pairing and similar proteins participate in their biogenesis.

The last type of small regulatory RNAs are piRNAs, which are 21–35 nucleotides long and in contrast to miRNAs and siRNAs, they are animal specific. piRNAs bear 2'-O-methyl-modified 3' termini and guide PIWI-clade Argonautes (PIWI proteins) rather than the AGO-clade proteins, which function in the miRNA and siRNA pathways (Aravin et al., 2001, Aravin et al., 2006, Girard et al., 2006, Vagin et al., 2006, Ozata et al., 2019). Whereas miRNAs and siRNAs derive from double-stranded RNA precursors, piRNAs are processed from long single-stranded precursor transcripts, except the piRNAs in *C. elegans*, which are made one at a time from single-stranded precursors of 25–27 nucleotides in length, each of which is transcribed from its own gene (Gu et al., 2012). The main function of piRNAs is to silence transposon elements in the germline. Transposons are dangerous for the integrity of the genome since they can induce DNA breaks, disruption of expression of open-reading frames or dysregulation of gene expression and thus animals rely of piRNAs in order to silence them (Davis et al., 2017). In the past few years it has become evident that piRNAs also have other functions such as gene regulation. In mice, piRNAs can induce both DNA and H3K9me3 histone methylation, which leads to gene silencing (Aravin et al., 2008). In some species, like mosquitos, piRNAs have been implicated in antiviral defence were two mosquito PIWI proteins - Piwi5 and Ago3 - participate in a heterotypic ping-pong and consume viral (+) and (-) strand RNAs to produce piRNAs (Miesen et al., 2015, Lewis et al., 2018).

Generally, small regulatory RNAs have been implicated in many pathophysiological conditions and for more than two decades, researchers try to unravel the mechanisms of their regulation and function. The discovery of small regulatory RNAs made the scenery of genome regulation more complex. To this big family of ncRNAs another member was added: the long non-coding RNAs. This class of RNA molecules is the most recently discovered (even though founding-members of the family, such as XIST, have been known for almost 30 years), and adds an entirely new level of genome complexity.

### 1.2.3 Long non-coding RNAs

The development of NGS technologies made it possible to identify novel regulatory RNAs at a genome scale. Some of the discovered RNAs were called long non-coding RNAs (lncRNAs), defined as regulatory RNAs that are longer than 200 nucleotides and have no coding potential. As mentioned above, prior to the development of NGS technologies only few members of this family were known, such as Xist (Brockdorff et al., 1992, Brown et al., 1992) and H19 (Brannan et al., 1990), but even after the existence of lncRNAs as an abundant class of cellular transcripts was verified their functions remained under debate. The ability of RNA polymerase to (Pol II) to transcribe most of the genome and the low copy numbers of some lncRNAs rise questions regarding their functionality (Struhl, 2007). Today it is believed that numerous lncRNAs are functional and to distinguish them from transcriptional noise several parameters should be taken into account. For example, if the expression of an lncRNA is evidently regulated by transcription factors (TF) or if there are chromatin signatures, such as DNaseI hypersensitivity or characteristic histone modifications like H3K9ac, H3K4me3, and H3K36me3 with the gene body, the chances of the transcript to be functional increase (Struhl, 2007, Guttman et al., 2009, Kung et al., 2013). Depending on their functionality lncRNAs are divided in three categories: non-functional lncRNAs which are the result of transcriptional noise, lncRNAs for which the act of transcription alone is sufficient for their function but the transcript itself does not fulfil a further function and lncRNAs that can act in *cis* and/or in *trans* as regulatory cellular biomolecules (Quinn and Chang, 2016).

The biogenesis of lncRNAs is similar to messenger RNAs (mRNAs), as their transcription is largely mediated by Pol II. Furthermore, lncRNAs can be polyadenylated, 5'-capped and alternative cleaved and spliced, leading to different isoforms. In most instances, they lack any biochemical distinction from mRNAs besides the absence of a translated open reading frame (Quinn and Chang, 2016). Despite these similarities, lncRNAs and mRNAs exhibit several differences, both in their expression profiles and the chromatin status of their loci. Transcriptome-wide studies showed that lncRNAs in general exhibit more specific expression profiles than mRNAs, in that they are expressed in a more cell type-, tissue-, developmental stage- or disease state-specific manner (Cabili et al., 2011, Quinn and Chang, 2016). Furthermore, lncRNAs are evolutionary less conserved and less abundant than mRNAs (Ulitsky and Bartel, 2013). Recent studies were also able to distinguish lncRNAs from mRNAs on chromatin level. In one study, a comparison of lncRNAs with mRNAs that are expressed at similar levels revealed that in general fewer histone marks and transcription factors are bound

to lncRNA promoters than to mRNA promoters (Mele et al., 2017). However, H3K9me3, a histone modification typically associated with transcriptional repression, is more enriched at the promoters of lncRNA loci than at those of mRNAs. Moreover, lncRNAs have weaker internal splicing signals and thus they are less efficiently spliced than mRNAs. In addition, U2AF65, an important splicing factor binds less in lncRNAs than in mRNAs (Mele et al., 2017). In another study, it was shown that lncRNAs and pre-mRNAs are transcribed by different Pol II phospho-c-terminal domain (CTD) isoforms (Schlaskow et al., 2017). Pol II is associated with the spliceosome through a serine 5 P (S5P) CTD, and mRNA 3' ends are generated cotranscriptionally by cleavage and polyadenylation specificity factor subunit 3 (CPSF73) and this promotes Pol II termination (Schlaskow et al., 2017). In contrast, most lncRNAs are weakly spliced and polyadenylated, and thus they are degraded by the nuclear exosome on chromatin. Interestingly, the termination of transcription of many lncRNAs is independent from CPSF73 and the threonine 4-phosphorylated (T4P) CTD mark, which correlates with protein-coding gene termination, is distributed more evenly across the gene body of lncRNAs (Schlaskow et al., 2017). The functional lncRNAs should overcome these limitations in order to accumulate in high levels in specific cell types (Yang and Chen, 2017).

In recent years there has also been a dispute about how many of the RNAs that are classified as lncRNAs are actually non-coding. Recent studies show that some of the lncRNAs may code for small peptides or proteins (Bazzini et al., 2014, Anderson et al., 2015, Jackson et al., 2018). In these studies ribosomal foot printing unveiled that, some of the putative lncRNAs are associated with ribosomes, and thus there is a high chance for them to be translated to proteins. The misclassification of these transcripts as lncRNAs may be because these proteins have non-canonical open reading frames. It is still not clear how many of the existing annotated lncRNAs are actually protein coding.

Because of the diversity of the lncRNAs when it comes to their function or their structural properties, their classification is based on their genomic loci in association with coding genes. Thus, depending on their location in the genome, lncRNAs have been divided in different subfamilies (Figure 1.4). A lncRNA is typically classified as intergenic when it is expressed as a distinct unit from the 'empty' space between two coding genes and intronic when it is expressed from an intron of a protein coding gene. Furthermore, lncRNAs can be classified as antisense when expressed from the opposite strand of a coding gene and bidirectional when a lncRNA is derived from the same promoter as a coding RNA but is transcribed from the opposite strand. Finally, enhancer RNAs (eRNAs) are transcribed in one or two directions at

genomic transcriptional enhancers, most of the times in close proximity to protein-coding genes (Spurlock et al., 2016).

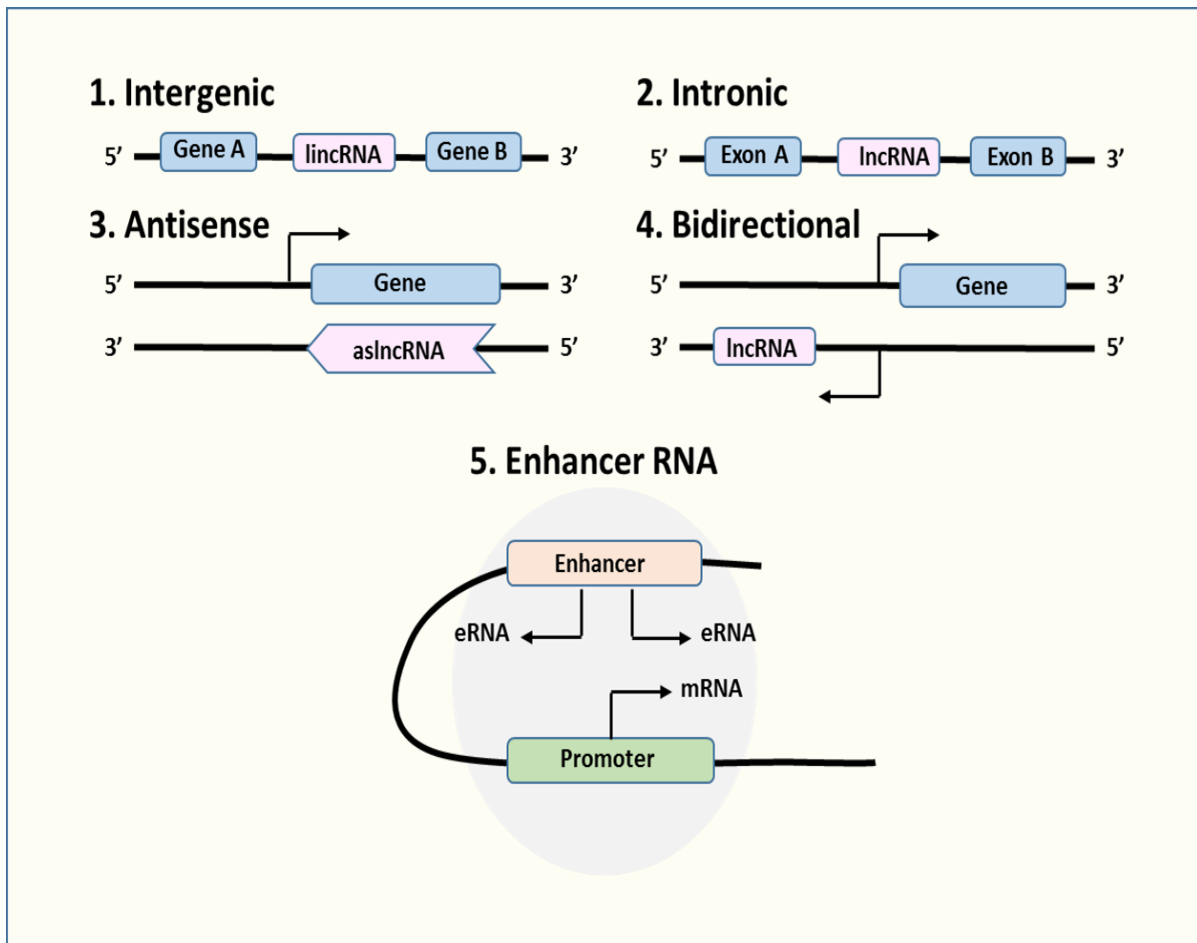


**Figure 1.4: Subtypes of lncRNAs.** The lncRNAs can be divided into five different groups depending on their location in the genome. Long- intergenic non-coding RNAs (lincRNAs) are distinct transcriptional units that do not overlap with coding genes. Intronic lncRNAs are transcribed from an intron of a protein-coding gene. Both antisense and bidirectional lncRNAs are transcribed from the opposite strand of the coding gene: an antisense lncRNA transcript overlaps with the transcript of a coding gene whereas the bidirectional lncRNAs share the promoter with a coding gene on the opposite strand. Finally, enhancer RNAs (eRNAs) are transcribed from an enhancer region, from one or 2 directions, usually in close proximity to an mRNA promoter.

Another important characteristic of lncRNAs is their secondary structures. Several studies have tried to reveal the secondary structures using methods like selective 2'-hydroxyl acylation analysed by primer extension (SHAPE) (Wan et al., 2011, Watts et al., 2009). lncRNAs can generally form stem loops, like Xist, in order to bind to protein binding partners (Maenner et al., 2010). Cloverleaf elements, like the ones found in tRNAs, are also common architectures of lncRNAs. One of the purposes of this secondary structure is the 3'-end maturation of the lncRNAs transcripts, which has been demonstrated in the case of MALAT1 and NEAT1 lncRNAs. Non-canonical end maturation of the MALAT1 ncRNA involves a cloverleaf

secondary element at its 3'-end. This structural element is responsible for recruiting RNase P, which is involved in maturation of tRNA molecules, for cleavage and generation of mature MALAT1 transcripts (Wilusz et al., 2008). Other structures like helical segments, terminal loops, internal loops and junction regions were identified in other lncRNAs like steroid receptor RNA activator (SRA) (Navikova et al., 2012).

In recent years after the development of epitranscriptomics, RNA editing and RNA modifications were recognized as important for the dynamic regulation of RNA activity, depending on the signal-induced cellular changes. Most of the RNA molecules, including lncRNAs, undergo some form of editing or modification during their lifespan, either co-transcriptionally or post-transcriptionally. Specific modifications can alter the function of the RNA because of alterations in the protein binding capability or changes in the secondary structures (Meyer et al., 2012, Dominissini et al., 2012, Squires et al., 2012). The most common type of RNA editing is the deamination of adenosine to inosine in Alu repeat elements found in introns or intergenic regions (Picardi et al., 2014). Due to different preferences in base pairing between the adenosine and inosine the secondary structure of RNA may change (Levanon et al., 2004). This modification is important for preventing the immune response against self-RNAs that can be recognised by cytosolic RNA sensors, like MDA5 (Liddicoat et al., 2015). The adenosine-deaminase (ADAR) family, comprising ADAR1, which is found in both nucleus and cytoplasm and ADAR2, which is found only in the nucleus, is responsible for the adenosine-to-inosine deamination (Pulsen et al., 2001, Desterro et al., 2003). There is evidence that ADAR affects tissue specific expression of lncRNAs (Goldstein et al., 2017). One way of ADAR function is through changing the ability of lncRNA to bind to mRNA and the best example is the intronic lncRNA PCR3 that has been implicated in prostate cancer (Salameh et al., 2015). The lncRNA forms an RNA duplex with the coding gene PRUNE2, which is transcribed from the same genomic locus, and leads to its degradation. Low levels of PRUNE2 are found in prostate tumours. The complex formation is regulated by ADAR, and thus the depletion of ADAR leads to higher levels of PRUNE2 (Salameh et al., 2015). Other modifications have been found in different RNA species like rRNAs and tRNAs but the field is still young.

#### **1.2.4 Functions of Long-non coding RNAs**

Long non-coding RNAs are a highly diverse family, and thus they have several functional repertoires, unlike the classes of small non-coding RNAs, which have a common mechanism of function, like silencing the mRNA target. Despite their diversity, there are some common



features shared by several RNAs. LncRNAs can serve as scaffolds, guides and decoys (Rinn and Chang, 2012). As scaffolds, lncRNAs bring together two or more proteins into RNA–protein complexes. A well-studied lincRNA of this class is HOTAIR, which can bind both the polycomb repressive complex 2 (PRC2) and the LSD1-CoREST complex (Tsai et al., 2010). The binding is facilitated by the structure of the lncRNA and leads to gene silencing via induction of H3K27 methylation and H3K4me2 demethylation (Tsai et al., 2010). To this category belong several other lncRNAs that form complexes with proteins, such as NEAT1 (Clemson et al., 2009) which is essential for paraspeckles formation and interacts with SFPQ and HEXIM1 to form a complex essential for IRF3 phosphorylation (Morchikh et al., 2017). LncRNAs with decoy functions titrate away e.g. DNA-binding proteins from DNA, including transcription factors. Gas5 is a good example of this family since it binds to the glucocorticoid receptor through its harpin structure and inhibits the transcription of metabolic genes during starvation (Kino et al., 2010). Guide lncRNAs are responsible for proper localization of specific protein complexes. This class has two molecular properties: interaction with another protein and a mechanism to interface with selective regions of the genome. These lncRNAs are involved in dosage compensation and imprinting and serve as guides to target gene silencing activity in an allele-specific fashion. Xist for instance functions as a guide lncRNA, which is responsible for X-chromosome inactivation in females (Penny et al., 1996).

Another major classification of lncRNAs is made according to the proximity of their regulated target genes compared to their own transcriptional genomic loci. According to this classification, lncRNAs can act in *cis* or in *trans*. When lncRNAs target neighbouring genes then they are considered to act in *cis*, whereas when they regulate expression of distant genes, they act in *trans*. Despite this separation, it is evident today that a *cis* acting lncRNA may also regulate genes further away from its genomic locus due to chromatin looping, which brings the lncRNA locus and the target gene locus into close proximity (Nagano et al., 2008).

The lncRNA mechanisms of action are highly diverse and thus no classification can include all the unique functional properties. For example, lncRNAs have also the ability to bind to RNA molecules, such as mRNA, miRNAs and other lncRNAs, and control their availability, expression and function. A good example is the antisense lncRNA Uchl1 which binds to UCHL1 gene mRNA and this interaction is essential for the association of the mRNA with active polysomes for translation (Carrieri et al., 2012).

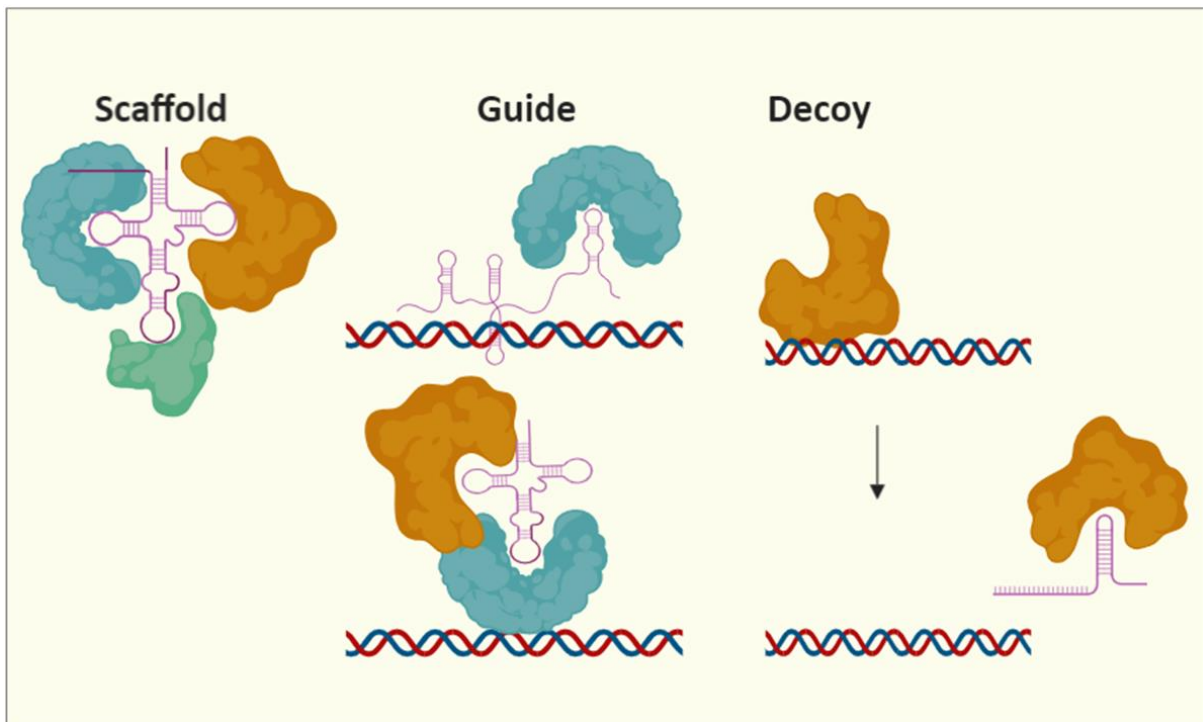


**Figure 1.4: Models of lncRNA mechanisms of action.** lncRNAs can act as scaffolds in order to bring different proteins into close proximity or facilitate a protein complex formation. They can act as guides to bring transcription factors or other molecules to the desired genomic loci in order to activate or inhibit transcription. Finally, lncRNAs can act as decoys binding to transcription factors and driving them away from the genomic loci.

The functional diversity of lncRNAs makes their characterisation more complicated compared to other members of the ncRNA family, like miRNAs and siRNAs that have a specific way of regulating gene expression. Another obstacle for the functional characterisation of lncRNAs is the lack of methodological approaches, even though due to rapid development of new technologies, such as CRISPR/Cas9, this may no longer be a hindrance.

### 1.2.5 Long-non coding RNAs in immunity

Over the last decade, several lncRNAs have been implicated in regulation and function of the immune system. As lncRNAs are often cell-type specific, different lncRNAs have been identified in the distinct immune cell populations. They can have significant functions in the immune responses or be responsible for the cell differentiation fate.

In order to have a productive immunity HSCs differentiate into highly specialised immune cells. This process is tightly controlled through the expression of cell-type-specific genes, and evidence suggests that lncRNAs might also have an important role in this process. For example, the lncRNA H19 has been implicated in the quiescence of adult HSCs (Venkatraman et al., 2013). H19 is highly expressed in long-term HSCs and it is downregulated when they differentiate into short-term HSCs. Deletion of maternal H19 in the hematopoietic compartment

leads to a loss of long-term HSCs and subsequently gain of short-term HSCs. H19-deficient long-term HSCs lose the ability to self-renew and differentiate into downstream cell types (Venkatraman et al., 2013). Two other lncRNAs, lncHSC-1 and lncHSC-2 were implicated in HSC regulation (Luo et al., 2015). Depletion of lncHSC-1 resulted in dysregulation of myeloid lineage differentiation, while depletion of lncHSC-2 lead to impaired self-renewal of HSC and increased T cell differentiation. lncHSC-2 is important for the recruitment of the transcription factor E2A to its targets, which has critical regulatory roles in the HSC and lymphoid-cell development (Luo et al., 2015).

Another lncRNA, lnc-DC is also involved in differentiation of immune cells. It is upregulated during the differentiation of common myeloid progenitor cells or monocytes into DCs and is highly expressed in classical DC subsets (Wang et al., 2014). Knock down of lnc-DC reduces the expression of several DC-specific genes, such as CD40, CD80, CD86 and CCR7. DCs depleted of lnc-DC are unable to efficiently prime CD4<sup>+</sup> T cells or secrete inflammatory cytokines after pathogen stimulation. Its function is mediated through interaction with STAT3. The lncRNA facilitates the STAT3 phosphorylation and its translocation to the nucleus, through inhibiting the SHIP1-STAT3 interaction (Wang et al., 2014). On the other hand, lncRNA Morrbrid, is induced when common myeloid progenitor cells differentiate into terminal cells and is highly expressed in neutrophils, eosinophils and monocytes (Kotzin et al., 2016). Morrbrid knockout leads to a decrease in the number of neutrophils, eosinophils and monocytes due to induction of cell death. Morrbrid is found mainly in the nucleus, and it acts in cis to repress the expression of its neighbouring gene Bcl2l11. Chromosomal looping brings Morrbrid and Bcl2l11 in spatial proximity, where the lncRNA recruits PRC2 to deposit silencing H3K27me3 histone marks on the Bcl2l11 promoter. Morrbrid expression can be induced *in vitro* by cytokines such as interleukin 3 (IL-3), IL-5 and GM-CSF, and thus has been associated with the hypereosinophilic syndrome. Patients with this syndrome have high concentrations of IL-5 in their plasma and eosinophils from these patients express significantly more Morrbrid than do eosinophils from healthy control subjects (Kotzin et al., 2016).

Several lncRNAs have also been implicated in the differentiation of T-cell subsets. For example, lncRNA lincR-Ccr2-5'AS is specifically expressed in the Th2 subset of helper T cells (Hu et al., 2013). GATA-3, which is a signature transcription factor of the Th2 cell population, regulates lincR-Ccr2-5'AS expression. Knockdown of lincR-Ccr2-5'AS led to dysregulation of genes that depend on GATA-3, such as Ccr1, Ccr2, Ccr3 and Ccr5, which are Th2 cell specific. Human homologue of lincR-Ccr2-5'AS, TH2-LCR, has a similar regulatory function

and controls the transcription of its neighbouring genes encoding Th2 cell cytokines, such as IL4, IL5, and IL13 (Spurlock et al., 2015). During differentiation of T-cells towards the Th1 population, the lncRNA linc-MAF-4 seems to play a critical role (Ranzani et al., 2015). Linc-MAF-4 represses the expression of the Th2 cell transcription factor MAF to promote T cell differentiation toward the Th1 cell lineage. The genomic regions of linc-MAF-4 and MAF come into close proximity and linc-MAF-4 recruits EZH2-and LSD1 to place repressive chromatin marks at the MAF promoter and repress transcription. Thus, knockdown of linc-MAF-4 favours T cell differentiation towards the Th2 cell lineage (Ranzani et al., 2015). Together these studies suggest that lncRNAs can serve as critical regulators of cell-type-specific differentiation programs and are important for immune-cell lineage commitment.

### **1.2.6 Long non-coding RNAs in inflammatory responses**

LncRNAs have been involved both in the innate and the adaptive immune system. In adaptive immunity, lncRNAs have been implicated in inflammatory responses of both CD4<sup>+</sup> T-cells and CD8<sup>+</sup> T-cells (Gomez et al., 2013, Willingham et al., 2005, Sharma et al., 2011, Wang et al., 2015). One of the first examples of an lncRNA functioning in the immune response *in vivo* was the lncRNA NeST (Nettoie Salmonella pas Theiler's), which is expressed in a genomic region previously associated with persistence of neurotropic Theiler's virus infection (Gomez et al., 2013). Two strains of mice show a different susceptibility in Theiler's virus infection. B10.S can clear the infection, while SJL/J mice are more susceptible. A known difference between the two mouse strains exists in the genomic region that expresses NeST, IFN- $\gamma$ , and IL-22. Gene-expression analysis revealed that NeST expression is much higher in T cells from mice that retain the locus derived from the SJL strain. NeST regulates the transcription of the *Ifng* gene by binding to WDR5 and recruiting the transcription-activation complex to the *Ifng* promoter sequence in trans. Overexpression of NeST increases IFN- $\gamma$  production in activated CD8<sup>+</sup> T cells. Moreover, NeST also regulates bacterial infection, since it is responsible for reduction of *Salmonella enterica* pathogenesis (Gomez et al., 2013). Another lncRNA, NRON (Non-coding Repressor Of NFAT), functions as a repressor of the calcium-dependent transcription factor NFAT (Nuclear Factor of Activated T-cells) (Willingham et al., 2005, Sharma et al., 2011). NRON belongs to a large RNA–protein complex in resting T cells, which sequesters the phosphorylated form of NFAT in the cytoplasm. The RNA–protein complex also includes the calmodulin-binding protein IQ Motif Containing GTPase Activating Protein 1 (IQGAP1), the Leucine Rich Repeat Kinase 2 (LRRK2), and the nuclear-transport factor karyopherin  $\beta$ 1. After stimulation of T cells, NFAT is released from the NRON complex and is dephosphorylated by

the Ca<sup>2+</sup>-calmodulin-dependent phosphatase calcineurin. Afterwards, NFAT is transported into the nucleus, where it can activate transcription. When NRON is absent, NFAT gets more dephosphorylated and higher copies of the transcription factor are found in the nucleus, which leads to aberrant production of cytokines (Willingham et al., 2005, Sharma et al., 2011). In CD8<sup>+</sup> T cells, expression of lncRNA-CD244 is induced by signalling through the T cell inhibitory receptor CD244 (2B4) and leads to repression of IFN- $\gamma$  and TNF (Wang et al., 2015). Similar to linc-MAF-4, lncRNA-CD244 physically interacts with EZH2 (Enhancer of zeste homolog 2) and recruits it to the IFN $\gamma$  and TNF promoters for the deposition of repressive chromatin marks. Knockdown of lncRNA-CD244 in T-cells of mice, that were infected with *Mycobacterium tuberculosis* led to significantly lower organ bacterial burden in comparison to mice that express normal levels of lncRNA-CD244 in their T-cells (Wang et al., 2015).

In innate immunity, several lncRNAs have been involved in inflammatory responses (Carpenter et al., 2013, Li et al., 2013, Krawczyk et al., 2014, Atianand et al., 2016, Castellanos-Rubio et al., 2016, Rapicavoli et al., 2013, Liu et al., 2015). One example is lincRNA-Cox2 that is highly induced upon TLR1, TLR2, TLR7 and TLR8 activation, but not after activation of TLR3 in bone-marrow-derived DCs and bone-marrow-derived macrophages (Carpenter et al., 2013). Moreover, transcription of lincRNA-Cox2 is MyD88 and NF- $\kappa$ B dependent. LincRNA-Cox2 knock-out during inflammatory stimulation leads to dysregulation of 500 genes encoding inflammatory molecules. LincRNA-Cox2 interacts with the heterogeneous nuclear ribonucleoproteins hnRNP-A/B and hnRNP-A2/B1. Depletion of the two ribonucleoproteins in bone-marrow-derived macrophages results in the dysregulation of the same genes as upon knockdown of lincRNA-Cox2. Furthermore, overexpression of lincRNA-Cox2 in bone-marrow-derived macrophages lacking the ribonucleoproteins was sufficient to restore the expression of Ccl5 (Carpenter et al., 2013). The lncRNA THRIL is a regulator of TLR2 signalling that was identified in a gene-expression screen of the THP-1 human macrophage cell line treated with Pam3CSK4 (Li et al., 2013). Transcriptome-wide analysis of THRIL-depleted THP1 cells identified more than 300 differentially regulated genes downstream of TLR2, including TNF, IL8, CXCL10, CCL1 and CSF1, both upon activation of TLR2 and at steady state. Mass-spectrometry studies have identified hnRNPL as a binding partner of THRIL and knockdown of hnRNPL resulted in a decreased production of TNF by macrophages. Furthermore, THRIL was found to be associated with the TNF genomic locus, and chromatin-immunoprecipitation analysis of hnRNPL resulted in enrichment of a region within the TNF promoter in a THRIL-dependent manner (Li et al., 2013). The lncRNA PACER also acts in the NF- $\kappa$ B signalling pathway (Krawczyk et al., 2014). PACER is induced by lipopolysaccharide

(LPS), and it regulates its neighbouring gene PTGS2, which encodes cyclooxygenase 2 (COX-2) and participates in the inflammatory responses. PACER acts as a decoy and binds to the NF- $\kappa$ B subunit p50, driving it away from the PTGS2 promoter, where p50 homodimers can repress transcription. The reduction of free p50 subunits leads to the formation of p50-p65 heterodimers, which are recruited to the PTGS2 promoter and lead to transcriptional activation (Krawczyk et al., 2014). The lincRNA-EPS is expressed in erythrocytes, macrophages and DCs, and it is downregulated after activation of the innate immune system (Atianand et al., 2016). LincRNA-EPS-deficient mice display no defects in erythroid development but show hyperactivation of immune responses *in vivo*. Bone-marrow-derived macrophages from lincRNA-EPS-deficient mice stimulated with TLR ligands show higher expression pro-inflammatory molecules, such as Il6, Cxcl10, Ccl4 and Irg1 compared to wild-type animals. This was linked to higher chromatin accessibility and nucleosome-free chromatin, as well as a greater content of H3K4me3 marks, associated with transcriptional activation, in the promoters of pro-inflammatory genes. LincRNA-EPS is localized to the nucleus and binds to hnRNPL to exert these regulatory effects. Thus, lincRNA-EPS acts at the chromatin level and controls chromatin accessibility in order to regulate the expression of pro-inflammatory genes in myeloid cells (Atianand et al., 2016). The lncRNA lnc13 functions similar to lincRNA-EPS and represses the transcription of immune genes. Lnc13 is expressed in macrophages and downregulated after activation of the TLR4 pathway (Castellanos-Rubio et al., 2016). In resting cells, lnc13 localizes to the nucleus and interacts with hnRNPD and the histone deacetylase HDAC1 to suppress the transcription of immune related molecules, such as Myd88, Stat1, Stat3 and Tnf. Single-nucleotide polymorphisms (SNPs) in the lnc13 gene that generate a transcript with impaired ability to bind to hnRNPD have been associated with celiac disease. Patients with celiac disease have lower expression of lnc13 and higher expression of lnc13-regulated genes, and thus the polymorphism, which leads to impaired lnc13 function, may be important for the development of the inflammatory disease (Castellanos-Rubio et al., 2016). The pseudogene lncRNA Lethe was induced in mouse embryonic fibroblasts after stimulation with IL-1 $\beta$  and TNF. Lethe is induced through NF- $\kappa$ B but knockdown of the lncRNA results in the upregulation of NF- $\kappa$ B targets and overexpression leads to a decreased NF- $\kappa$ B activity, which suggests a negative feedback loop (Rapicavoli et al., 2013). RNA-immunoprecipitation showed that Lethe interacts with p65 homodimers in the nucleus, preventing their accumulation at target-gene loci, including Nfkb1a, Il6 and Il8. Thus, Lethe acts as a decoy for NF- $\kappa$ B and provides negative feedback to restrict inflammatory responses (Rapicavoli et al., 2013). Similarly, lncRNA NKILA negatively regulates NF- $\kappa$ B signalling by binding to NF- $\kappa$ B and to the inhibitor of NF-

$\kappa$ B (I $\kappa$ B) (Liu et al., 2015). NKILA is induced in breast cancer cells following stimulation with IL-1 $\beta$  or TNF and knockdown of NKILA enhances NF- $\kappa$ B activity whereas its overexpression inhibits NF- $\kappa$ B. Mechanistically, NKILA masks phosphorylation motifs of I $\kappa$ B from the I $\kappa$ B kinase (IKK), which prevents the phosphorylation and degradation of I $\kappa$ B by IKK and results in the retention of NF- $\kappa$ B in the nucleus (Liu et al., 2015).

## 1.3 Infection model organisms

### 1.3.1 *Legionella pneumophila*

In infection biology, several bacteria have been established as model organisms to study host-pathogen interactions. One of the model pathogens to study pneumonia-related inflammatory responses is *Legionella pneumophila* (*L. pneumophila*). *L. pneumophila* was first identified in 1977 during an outbreak in an American Legion convention (Fraser et al., 1977). Legionellosis, the disease caused by the bacteria, is a type of community-acquired pneumonia and it is responsible for approximately, 2%–15% of all community-acquired pneumonias that require hospitalization. The most common source of infection by the bacteria are aerosols and water droplets. *L. pneumophila* also causes Pontiac fever, which is characterised by fever, chills, dry cough, myalgia, malaise, and headache but not pneumonia. *L. pneumophila* is a rod-shaped bacterium with strict growth requirements for iron and cysteine. It is a non-encapsulated, aerobic gram-negative bacillus with a single polar flagellum (Swanson and Hammer, 2000). In the soil and water *L. pneumophila*'s main hosts are amoebae and two species of ciliated protozoa (Rowbotham, 1980). In humans, the main target of *L. pneumophila* are alveolar macrophages and since there is no transmission between humans it is believed that amoebae have equipped the bacteria with the necessary factors allowing their replication within alveolar macrophages (Newsome et al., 1985, Cianciotto and Fields 1992, Franco et al., 2009). During its life cycle, the bacterium can be found in two different forms: the transmissive or virulent and replicative or avirulent form. In the replicative form, *L. pneumophila* replicates within the *Legionella* containing vacuole (LCV) inside the infested host cell or in media and is non-motile and non-cytotoxic. It remains in this form as long as sufficient nutrients and living space are available (Swanson and Hammer, 2000). When nutrients become scarce, *L. pneumophila* changes into the transmissive form and it can infect or re-infect host cells. The first step during the infection cycle is the attachment of the bacterium to the host cell. Assisted by important factors like flagellae, pili and bacterial surface proteins, such as major outer membrane proteins, heat shock proteins, and the mip protein, *L. pneumophila* enters the host cell (Swanson and Hammer, 2000). The mechanism of entry is not well understood, but it seems to depend on the

type of host and the bacterial strain. Macrophages normally take up the bacteria through conventional phagocytosis. Other forms can be coiling phagocytosis, zipper-like conventional phagocytosis, opsonin-dependent phagocytosis and micropinocytosis, which has been observed in bone-marrow derived macrophages (Harwitz et al., 1984, Watarai et al., 2001). After the internalisation, the bacterium uses its Dot/Icm (Dot: defective in organelle trafficking, Icm: intracellular multiplication) type IVB secretion system (T4BSS) in order to form the LCV, where *L. pneumophila* normally replicates. T4BSS together with Lsp type II secretion system (T2SS), are the two secretion systems of *L. pneumophila* and play a major role in bacterial pathogenesis (Kubori and Nagai, 2016). Via the T2SS, proteins translocate across the inner membrane and exit the bacterial cell through a specific outer membrane pore (Nivaskumar and Francetic 2014). The T2SS secretes over 25 proteins, including 18 enzymes and *L. pneumophila* specific proteins. (DebRoy et al., 2006, Tyson et al., 2013). Via the T4BSS the bacteria secrete over 330 effector proteins to promote the formation of the LCV and their own replication. These effector proteins modulate the eukaryotic cell in order to acquire nutrients, block microbial degradation and host defences, and enable pathogen transmission to other hosts (Ensminger, 2016). The Dot/Icm systems are highly conserved among all *Legionella* species (Berger and Isberg, 1993, Brand et al., 1994). About 10% of the genome of *L. pneumophila* encode for these effector proteins (Al-Quadan et al., 2012) and many of them possess eukaryotic-like domains, which allows these proteins to interact with host cell components. (Cazalet et al., 2004, Hubber and Roy 2010). The LCV escapes the host cell defence mechanisms because it is negative for canonical markers of the endocytic pathways such as Rab5 for early endosomes, Rab7 for late endosomes and Lamp-1 for lysosomes (Clemens et al., 2000) and does not undergo acidification, maintaining a pH of ~6.1, which prevents fusion with the lysosome (Horwitz and Maxfield 1984). The escape from phagosome-lysosome fusion is a hallmark of *Legionella* pathogenesis and mutants lacking this feature are not able to multiply within human macrophages (Horwitz, 1987). When the LCV is established inside the host cell it is surrounded by mitochondria, ribosomes and smooth vacuoles derived from the endoplasmic reticulum (ER). This association, allows the LCV to change the thickness of its membrane in order to resemble the ER (Tilney et al., 2001). At four hours post infection ribosomes are recruited to the LCV resulting in a rough ER-like vacuole. In the third step of the infection, *L. pneumophila* inhibits the bactericidal activity of the host and converts the phagosome into a safe intracellular niche for its replication. After replication within the LCV, when nutrients become limited, *L. pneumophila* differentiates into the flagellated transmissive form and is released from the LCV (Garduno et al., 2002). In the cytosol the bacteria cause disintegration of the plasma membrane



and structural and functional disruption of cytoplasmic organelles, which eventually results in osmotic lysis of the host cells. The released bacteria can then infect neighbouring cells and start a new cycle of replication.

*L. pneumophila* can be recognised by the innate immune system through different PAMPs, such as lipopeptides, lipoproteins and LPS, which are expressed on the surface of the bacteria (Massis and Zamboni, 2011). The PAMPs are recognised by a variety of PRRs, such as TLR2, which recognises the unique *L. pneumophila* LPS, TLR5, which can sense flagellin, and NLRs. The bacterial nucleic acids can also activate the STING pathway and induce type I IFN responses (Massis and Zamboni, 2011). As mentioned before, TLR2 is activated by lipopeptides and lipoproteins, which are cell wall components of *Legionella*. Furthermore, lipid A signals via TLR2 to induce the expression of CD14. The LPS of *Legionella* is mainly recognized by TLR2, because of its unique structure, which is different from LPS derived from other bacteria, such as *Salmonella enterica* Typhimurium. (Zahringer et al., 1995, Akamine et al., 2005, Shim et al., 2009). Mice deficient in the *tlr2* gene showed impaired cytokine production and an increased susceptibility to bacterial replication in the lungs (Hawn et al., 2006). TLR5 sensing of flagellin is important for *L. pneumophila* infection in humans, since a stop codon polymorphism in the gene of TLR5 increases the susceptibility to Legionnaires' disease (Hawn et al., 2003). The same was observed in mice lacking TLR9 (Newton et al., 2007). All mentioned TLRs lead to activation of the adapter molecule MyD88, which mediates the downstream NF- $\kappa$ B-dependent production of pro-inflammatory cytokines. NLRs, NOD1 and NOD2, are also activated by *L. pneumophila* (Frutuoso et al., 2010). Knockout studies with mice deficient in both NLRs, NOD1 and NOD2, showed impaired neutrophil recruitment and reduced bacterial clearance during lung infection (Frutuoso et al., 2010). The recognition of nucleic acids of *L. pneumophila* is also important for the inflammatory responses of the host. Sensor cyclic GMP-AMP synthase (cGAS) and the RIG-I-like receptor family, respectively recognise the DNA and RNA of *Legionella*. The binding of the DNA to cGAS induces the production of the second messenger cyclic 2'3'-GMP-AMP (2'3'-cGAMP), which leads to activation of a STING-dependent signalling pathway (Sun et al., 2013, Watson et al., 2015). On the other hand, *L. pneumophila*'s RNA is recognised by RIG-I and MDA5, which leads to activation of MAVS and IRF3 and subsequently to the production of type I IFNs, such as IFN $\alpha$  and IFN $\beta$  (Opitz et al., 2006). The production of Type I IFNs is important for defence against *L. pneumophila*, since when the pathway is blunted the bacteria display higher replication and infection rates (Lippmann et al., 2011, Naujoks et al., 2016). There are indications for ncRNAs to be involved in the regulation of inflammatory responses against *L. pneumophila* as well.

Some miRNAs, like miR146a, are differentially regulated upon *L. pneumophila* infection (Jung et al., 2017), which suggests potential roles in *Legionella*-host interaction.

### **1.3.2 *Salmonella enterica* serovar Typhimurium**

Another popular bacterium used as an infection model in many studies is *Salmonella enterica* serovar Typhimurium. The genus *Salmonella* is a relative of the genus *Escherichia* and its members are Gram-negative, non-spore-forming, rod-shaped bacteria belonging to the Enterobacteriaceae family (Fabrega and Vila, 2013). *Salmonella enterica* serovar Typhimurium (henceforth *Salmonella*) is a primary enteric pathogen infecting both humans and animals and causing gastrointestinal diseases. The usual origin of infection is upon ingestion of contaminated foods or water. The bacteria infect thousands of people every year and cause life-threatening systemic infections in immune-compromised individuals (Kozak et al., 2013, Kariuki et al., 2006). The clinical symptoms after infection include fever, headache, abdominal pain, and transient diarrhoea or constipation, and infection can produce fatal respiratory, hepatic, spleen, and neurological damage (Ohl and Miller, 2001). After entering the host gastric system, the bacteria adjust to the acidic environment by activating the acidic tolerance response (ATR), which allows maintaining an intracellular pH higher than the surrounding environment (Foster and Hall, 1991). The *Salmonellae* then adhere to the intestinal epithelial cells and induce cytoskeletal rearrangements that allow the engulfment of the bacteriae (Takeuchi, 1967, Finlay et al., 1991). When inside the cell, the bacteria form large vesicles called *Salmonella*-containing vacuoles (SCVs). In these vehicles, the bacteria are able to survive and replicate (Francis et al., 1993, Garcia del Portillo et al., 1994). Initially, the SCVs enter the early endocytic pathway, but later they manage to escape the lysosomes (Garcia del Portillo and Finlay, 1995). SCVs are located next to the Golgi apparatus and obtain nutrients through endocytic and exocytic transport vesicles (Deiwick et al., 2006, Salcedo et al., 2003). When *Salmonella* crosses the epithelium, it interacts with immune cells, like neutrophils, macrophages and dendritic cells. In these cells, *Salmonella* behaves the same way as in epithelial cells, forming SCVs and inducing inflammatory responses (Johansson et al., 2006, Rydström and Wick, 2007). When inside the phagocytes *Salmonella* can travel from the blood stream to other tissues and organs.

*Salmonella* is a model pathogen for activation of immune responses. Even inside the SCV, the pathogen is not completely escaping the host inflammatory responses. In phagocytic cells, *Salmonella* can be recognised by most of the PRRs and thus it induces a robust inflammatory response, inducing the release of several cytokines such as IL-1 $\beta$ , IL-8 and TNF $\alpha$  (Broz et al., 2012). Another important defence mechanism against *Salmonella* is the activation of the

inflammasome and induction of pyroptosis. Inflammasomes are molecular complexes that regulate the activation of the proteolytic enzyme caspase-1 (Franchi, 2011). In macrophages, *Salmonella* induces the activation of caspase-1, necessary for the maturation of the proinflammatory cytokines IL-1 $\beta$  and IL-18. Caspase-1 dependent pyroptosis is a form of programmed cell death with characteristics of both apoptosis and necrosis. During pyroptosis, there is formation of pores in the cell membrane, which leads to release of cellular cargo and pro-inflammatory cytokines. This process benefits the host since it amplifies the inflammatory response by triggering recruitment of other mediators of inflammation and exposing the intracellular bacteria to extracellular immune defences (Miao et al., 2010).

Some non-coding RNAs have been also implicated in the immune responses to *Salmonella*. For example, the let-7 family is downregulated upon *Salmonella* infection, which relieves negative regulation of IL-6 and IL-10 cytokines (Schulte et al., 2011). Another miRNA family, which was reported as regulator of *Salmonella* infection is the mir-15 family. Through regulation of the cell cycle, the microRNA family is able to inhibit *Salmonella* infection (Maudet et al., 2014). In mice, lncRNA NeST has been associated with lymphoid cell immunity to *Salmonella* (Gomez et al., 2013). Furthermore, a recent study demonstrated that accumulation of unstable nuclear RNAs, like the long non-coding RNAs NEAT1v2 and eRNA07573, is important for the host defence against *Salmonella* infection (Imamura et al., 2018).

## **1.4 Aim of this study**

During the past decade, several lncRNAs have been characterised as important riboregulators of many pathophysiological processes. More recently, few lncRNAs have also been implicated in the immune system. This study attempts to establish a comprehensive catalogue of lncRNAs regulated during leukocyte terminal differentiation and immune-activation, including information on their subcellular localization and their formation of functional RNA-subclasses. Moreover, a central goal of this project was to determine the precise molecular functions of selected lncRNAs in human immunity. Finally, the current work aims at the establishment of a reproducible methodological workflow for lncRNA mechanistic analysis, to be employed by subsequent lncRNA studies within and beyond the field of leukocyte biology. Together, these objectives are expected to broaden the still rudimentary current knowledge about lncRNA functions in the human innate immune system.

## 2. Materials and methods

### 2.1 Materials

#### 2.1.1 Instruments and equipment

**Table 2.1.1: List of instruments and equipment**

<b>Instrument</b>	<b>Name</b>	<b>Company</b>
Automated cell counter	TC10™	BioRad Laboratories Hercules, USA
Bioanalyzer	2100 Bioanalyzer Instrument	Agilent Technologies Santa Clara, USA
Bioluminescence and Chemoluminescence Imager	ChemoCam Imager 3.2	INTAS Science Imaging Göttingen, Germany
Camera	AxioCam MRm	Zeiss Oberkochen, Germany
Cell Counting Chamber	Neubauer Counting Chamber	Paul Marienfeld GmbH & Co. KG Lauda-Königshofen, Germany
Cell culture bench	SAFE 2020	Thermo Fisher Scientific, Waltham, USA
Centrifuge	HERAEUS Multifuge X3R	Thermo Fisher Scientific, Waltham, USA
Centrifuge	Centrifuge 5424R	Eppendorf Hamburg, Germany
Centrifuge	Sprout® Mini-Centrifuge	Heathrow Scientific® LLC Illinois, USA
Centrifuge	Heraeus Fresco L7	Thermo Fisher scientific Waltham, USA
CO <sub>2</sub> Incubator	HERAcell 240i	Thermo Fisher scientific Waltham, USA
Dispenser	Multipette® plus	Eppendorf Hamburg, Germany
Dispenser	Multipette® Xstream	Eppendorf

		Hamburg, Germany
FACS	Guava easyCyte™	Merck Millipore™ Billerica, USA
FACS-Sorter	FACS Aria III Cell Sorter	Miltenyi Biotec GmbH Bergisch Gladbach, Germany
Fluorometer	Qubit® 2.0 Fluorometer	Thermo Fisher scientific Schwerte, Germany
Gel comb	10 Well, 12 Well, 14 Well	Peqlab Erlangen, Germany
Gel documentation apparatus	Gel-x Imager	INTAS Science Imaging Göttingen, Germany
Gel electrophoresis apparatus	PerfectBlue Gel System	Peqlab Erlangen, Germany
Gel preparation equipment	Multiple Gel Casting	Peqlab Erlangen, Germany
Gel preparation equipment	Gel Trays	Peqlab Erlangen, Germany
Hybridization Oven / UV	HL-2000 HybriLinker	UVP
Incubated/refrigerated stackable Shaker	MaxQ 600	Thermo Fisher scientific Schwerte, Germany
Laboratory roller mixer	SRT6D	Stuart ® Marseille, France
Laboratory shaker	See-Saw rocker SSL4	Stuart ® Marseille, France
Liquid nitrogen storage tanks	Cryo Plus 2	Thermo Fisher Scientific Waltham, USA
Macs multi stand magnet	quadroMacs	Miltenyi Biotec GmbH Bergisch Gladbach, Germany
Magnetic & Heating Stirrer	RCT Standard	IKA Staufen, Germany

Magnetic stand for 1.5 ml tubes	PureProteome™ Magnetic Stand	Merck Millipore™ Billerica, USA
Microscope	AXIO Vert.A1	Zeiss Oberkochen, Germany
Microscope	PrimoVert	Zeiss Oberkochen, Germany
Microwave	Inverter	SHARP Hamburg, Germany
PCR Cycler	PeqSTAR 2x Gradient	Peqlab Erlangen, Germany
Photometer	Ultraspec 10 CeII densitometer	Amersham Biosciences Freiburg, Germany
Pipette (0.1 - 1000 µl)		Gilson Middleton, USA
Plate reader	Tecan Infinite M200 PRO	Thermo Fisher scientific Waltham, USA
Power supplies	PeqpowerE300 200/300V	Peqlab Erlangen, Germany
Precision Scales		Denver Instruments Göttingen, Germany
Real Time PCR System	ViiA7™	Life Technologies™ Darmstadt, Germany
Real Time PCR System	QuantStudio3	Thermo Fisher Scientific Waltham, USA
Spectrophotometer	NanoDrop 2000c	Thermo Fisher Scientific Waltham, USA
Steam sterilizer	Varioklav®	HP Medizintechnik GmbH Oberschleißheim, Germany
Surgical preparation set		Fine Science Tools Heidelberg, Germany
Thermomixer (1.5 ml; 2 ml)	Thermomixer Comfort	Eppendorf Hamburg, Germany

Vacuum pump	AC 04	VACUUBRAND GMBH + CO KG Wertheim, Germany
Vortex	VortexGenie2	Scientific Industries New York, USA
Vortex	IKA®MS3	Agilent Technologies Santa Clara, USA
Vortex	Vortex V-1 plus	Peqlab Erlangen, Germany
Water bath		GFL® Burgwedel, Germany

## 2.1.2 Consumables and plastic ware

**Table 2.1.2: List of consumable and plastic ware**

Type	Name	Company
15 - 50 ml tube	Falcon	SARSTEDT AG & Co. Nümbrecht, Germany
6-well plate, 12-well plate, 24-well plate, 96-well plate	CELLSTAR® Cell culture plate	Greiner Bio-One GmbH Frickenhausen, Germany
96-well plate for ELISA		Thermo Fisher scientific Waltham, USA
Cap tube for cultivation of bacteria	14 ml PP tube	Greiner Bio-One GmbH Frickenhausen, Germany
Cell culture dish		Greiner Bio-One GmbH Frickenhausen, Germany
Cell culture flask (T25; T75)	TC Flask	SARSTEDT AG & Co. Nümbrecht, Germany
Cell scraper (25 - 50 cm)		SARSTEDT AG & Co. Nümbrecht, Germany
Cotton buds	Cotton buds, Rotilabo	Carl Roth GmbH & Co. KG Karlsruhe, Germany



Cryo-tubes		SARSTEDT AG & Co. Nümbrecht, Germany
Cuvette (polystyrene)		SARSTEDT AG & Co. Nümbrecht, Germany
Disposal Bags		Carl Roth GmbH & Co. KG Karlsruhe, Germany
Dissecting set		Fine Science Tools GmbH Heidelberg, Germany
Filter	Cell Strainer 40 - 100 $\mu$ m Nylon	BD Biosciences Heidelberg, Germany
Inoculation spreader		SARSTEDT AG & Co. Nümbrecht, Germany
Inoculation tube	Loop Soft 10 $\mu$ l	VWR International GmbH Darmstadt, Germany
Lab gloves	Examination gloves, latex free	Sempercure® Vienna, Austria
Lintfree tissues	Delicate task wipes	Kimberly-Clark Professional® Roswell, USA
Magnetic columns	MACS LS Columns	Miltenyi Biotec GmbH Bergisch Gladbach, Germany
Nitrocellulose Blotting membrane	Amersham Protran, 0.2 $\mu$ m	GE Healthcare Life Science Hyclone laboratories Logan, USA
Parafilm	PARAFILM® M	VWR International GmbH Darmstadt, Germany
Pasteur pipette		Glaswarenfabrik Karl Hecht GmbH & Co KG Sondheim, Germany
qPCR 96- well plates (0.1 ml)		Life Technologies™

		Darmstadt, Germany
RNA Nano Chip		Agilent Technologies Santa Clara, USA
Serological pipette (5 ml - 25 ml)		SARSTEDT AG & Co. Nümbrecht, Germany
Steril filtration filters (0.2 µm)	Filtropur S	SARSTEDT AG & Co. Nümbrecht, Germany
Surgical disposable scalpel		B. Braun Melsungen AG Melsungen, Germany
Tips (0.5 ml – 25 ml)	Combitips advanced®	Eppendorf Hamburg, Germany
Tips (10 µl - 1000 µl)		Safe Seal-Tips® professional
Tips (10 µl - 1000 µl)		Gilson Middleton, USA
Tips (10 µl - 1000 µl)	Diamond®	Gilson Middelton, USA
Tips (10 µl - 1000 µl)	TOWERPACK™	Gilson Middelton, USA
Tips (5 ml - 50 ml)	Tips for PIPETMAN®	Gilson Middelton, USA
Tubes		Eppendorf Hamburg, Germany
Tubes (0.5 - 2.0 ml)	Safelock Tubes	Eppendorf Hamburg, Germany
Tubes (1.8 ml)	CryoPure Tubes	SARSTEDT AG & Co. Nümbrecht, Germany
ZipTip® Pipette Tips		Merck Millipore TM Billerica, USA

## 2.1.3 Chemicals

**Table 2.1.3: List of chemicals**

Chemical	Name	Company
2-Mercaptoethanol		Carl Roth GmbH & Co. KG Karlsruhe, Germany
ACES		Carl Roth GmbH & Co. KG Karlsruhe, Germany
Acetic acid		Carl Roth GmbH & Co. KG Karlsruhe, Germany
Acetonitrile		Sigma-Aldrich St. Louis, USA
Acid phenol chloroform		Ambion by life technologies Carlsbad, USA
Acrylamide	Acrylamide (Rotiphoresis Gel 30,37.5:1)	Carl Roth GmbH & Co. KG Karlsruhe, Germany
Agar Agar (Kobe I)		Carl Roth GmbH & Co. KG Karlsruhe, Germany
Agarose	Biozym LE Agarose	Biozym Scientific GmbH Hessisch Oldendorf, Germany
Ammonium bicarbonate		Carl Roth GmbH & Co. KG Karlsruhe, Germany
Ammonium persulfate (APS)		Carl Roth GmbH & Co. KG Karlsruhe, Germany
Ammonium sulfate (NH <sub>4</sub> ) <sub>2</sub> SO <sub>4</sub>		Sigma-Aldrich St. Louis, USA
Ampicilin Sodium Salt		Sigma-Aldrich St. Louis, USA
Aqua-PCI	Roti® Aqua- Phenol/Chloroform/Isoam yl alcohol	Carl Roth GmbH & Co. KG Karlsruhe, Germany

BSA	Albumin Fraktion V	Carl Roth GmbH & Co. KG Karlsruhe, Germany
Calcium chloride		Carl Roth GmbH & Co. KG Karlsruhe, Germany
Charcoal activated		Carl Roth GmbH & Co. KG Karlsruhe, Germany
Chloramphenicol		Carl Roth GmbH & Co. KG Karlsruhe, Germany
Chloroform	Trichloromethane	Carl Roth GmbH & Co. KG Karlsruhe, Germany
Complete Mini Protease Inhibitor Cocktail		Roche Mannheim, Germany
DMSO	Dimethyl sulfoxide	Carl Roth GmbH & Co. KG Karlsruhe, Germany
ECL Reagent	ECL Prime Western Blotting Detection Reagent	GE Healthcare Life Science Hyclone laboratories Logan, USA
EDTA		Carl Roth GmbH & Co. KG Karlsruhe, Germany
Ethanol	Ethanol absolute	Sigma-Aldrich St. Louis, USA
Ethylene Diamine Tetra-Acetic Acid (EDTA)		Carl Roth GmbH & Co. KG Karlsruhe, Germany
Fetal Bovine Serum (FBS)	FBS Superior	Biochrom GmbH Berlin, Germany
Ficoll	Lymphoprep™	AXIS-SHIELD Oslo, Norway
GelRed nucleic acid stain	GelRed™	Biotium Scarborough, Canada
Gentamicin		Gibco™ life technologies Thermo Fisher Carlsbad, USA
Glycerol		Carl Roth GmbH & Co. KG

		Karlsruhe, Germany
GlycoBlue	GlycoBlue™	Invitrogen, Thermo Fisher Carlsbad, USA
Isopropanol		Carl Roth GmbH & Co. KG Karlsruhe, Germany
Kanamycin sulphate		Carl Roth GmbH & Co. KG Karlsruhe, Germany
LB Agar	LB Agar (Lennox)	Carl Roth GmbH & Co. KG Karlsruhe, Germany
LB Broth	LB Broth (Lennox)	Carl Roth GmbH & Co. KG Karlsruhe, Germany
Lipofectamine 2000		Invitrogen, Thermo Fisher Carlsbad, USA
Liquid Nitrogen		Linde Düsseldorf, Germany
Loading Dye	6x Mass Ruler	Thermo Fisher Waltham, USA
Methanol		Carl Roth GmbH & Co. KG Karlsruhe, Germany
Normocin™		Invivogen, San Diego, California, United States
PBS (1x)	Phosphate Buffered Saline (1x)	Healthcare Life Science Logan, USA
Pen/Strep	Penicillin/Streptomycin	Biochrom GmbH Berlin, Germany
Powdered milk		Carl Roth GmbH & Co. KG Karlsruhe, Germany
Sodium Acetate		Carl Roth GmbH & Co. KG Karlsruhe, Germany
Sodium Dodecyl Sulfate Pellets	SDS Pellets	Carl Roth GmbH & Co. KG Karlsruhe, Germany
T4 DNA Ligase Buffer		New England Biolabs Ipswich, USA

Tetraethymethylenediamine (TEMED)		Carl Roth GmbH & Co. KG Karlsruhe, Germany
Tri (hydroxymethyl) aminomethane (TRIS)		Carl Roth GmbH & Co. KG Karlsruhe, German
TRIS hydrochloride		Carl Roth GmbH & Co. KG Karlsruhe, Germany
Trizol	TRIzol™ Reagent	Invitrogen™, Carlsbad, California, United States
TWEEN 20		Carl Roth GmbH & Co. KG Karlsruhe, Germany
Ultra-Pure water		Biochrom GmbH Berlin, Germany
X-VIVO™ 15 Serum-free Hematopoietic Cell Medium		Lonza, Basel, Switzerland

## 2.1.4 Stimulants and cytokines

**Table 2.1.4: List of stimulants and cytokines**

Name	Compound	Company
c-di-GMP		Invivogen, San Diego, California, United States
gDNA	Genomic DNA	
GM-CSF (human)	granulocyte macrophage colony-stimulating factor	PeprTech Hamburg, Germany
IFN $\gamma$	Interferon gamma	Peprtech, Rocky Hill, United States
Imiquimod (R837)		Invivogen, San Diego, California, United States

LPS	Lipopolysaccharide from <i>Salmonella enterica</i> serotype typhimurium	Sigma-Aldrich St. Louis, USA
M-TriDAP		Invivogen, San Diego, California, United States
Pam3CSK4		Invivogen, San Diego, California, United States
PMA	Phorbol-12-myristat-13-acetate	Sigma-Aldrich St. Louis, USA
Poly I:C	Polyinosine- polycytidylic acid	Invivogen, San Diego, California, United States
Resiquimod (R848)	Invivogen	Invivogen, San Diego, California, United States

## 2.1.5 Kits

**Table 2.1.5: List of kits**

Kits	Name	Company
PCR purification	Gene JET	Thermo Fisher
Gel Extraction	Gene JET	Thermo Fisher
Genomic DNA Isolation	Nucleospin Tissue	Macherey- Nagel
Plasmid Isolation	Nucleospin Plasmid	Macherey- Nagel
RNA Isolation	mirVana™ miRNA isolation	Ambion
Poly A RNA isolation	Dynabeads® mRNA DIRECT	Ambion
RACE	SMARTer® RACE 5'/3'	Clontech

## 2.1.6 Antibodies

**Table 2.1.6: List of antibodies**

Specificity	Source	Class	Conju- gated	Company	Ordering number	Application
Actin	goat	IgG	-	Santa Cruz Biotechnology	sc-1616	Western Blot
Actin	mouse	IgG	-	Santa Cruz Biotechnology	sc-47778	Western Blot
IgG	rabbit	IgG	-	Cell signalling	7074	IP
Flag	mouse	IgM2	-	Sigma-Aldrich	F1804	IP
Tubulin	mouse	IgG2a	-	Santa Cruz Biotechnology	sc-5286	Western Blot
SND1	rabbit	IgG	-	Sigma-Aldrich	HPA002632	Western Blot, IP
SFPQ	mouse	IgG1	-	Abcam	ab11825	Western Blot, IP
TBK1	rabbit	IgG	-	Cell signalling	3504	Western Blot, IP
p-TBK1 (Ser172)	rabbit	IgG	-	Cell signalling	5483	Western Blot, IP
IRF3	rabbit	IgG	-	Cell signalling	11904	Western Blot, IP
pIRF3 (Ser386)	rabbit	IgG	-	Abcam	ab76493	Western Blot
p-p65	rabbit	IgG	-	Abcam	ab86299	Western Blot
p65	mouse	IgG1	-	Santa Cruz Biotechnology	sc-8008	Western Blot
pERK1/2	rabbit	IgG	-	Abcam	ab214362	Western Blot
ERK1/2	mouse	IgG2a	-	Santa Cruz Biotechnology	sc-514302	Western Blot
OPTN-C1	mouse	IgG1	-	Santa Cruz Biotechnology	sc-271549	Western Blot, IP
OPTN-C2	mouse	IgG2b	-	Santa Cruz	sc-166576	IP



				Biotechnology		
CD4	mouse	IgG2b	PE	eBioscience	12-0048-41	FACS
CD8	mouse	IgG1	FITC	eBioscience	11-0087-42	FACS
CD11b	mouse	IgG1	PE	eBioscience	12-0118-42	FACS
CD11c	mouse	IgG1	APC	eBioscience	17-0116-42	FACS
CD14	mouse	IgG1	FITC	eBioscience	11-0149-42	FACS
CD19	mouse	IgG1	FITC	eBioscience	11-0199-41	FACS
CD33	mouse	IgG2b	APC	Beckman Coulter	6604121	FACS
CD56	mouse	IgG	APC	eBioscience	17-0567-41	FACS
CD66b	mouse	IgM	APC	eBioscience	17-0666-42	FACS
CD169	mouse	IgG1	APC	BioLegend	346008	FACS
HLA-DR	mouse	IgG	PE	eBioscience	12-9952-42	FACS
Anti-mouse	goat	IgG	HRP	Santa Cruz Biotechnology	sc-2005	Western Blot
Anti-rabbit	mouse	IgG	HRP	Cell signalling	5127S	Western Blot

## 2.1.7 Primers

**Table 2.1.7: List of primers**

Gene	List Name	Sequence	Application
hCXCL8 (IL-8)	OBS-0017	Fwd: ACTGAGAGTGATTGAGAGTGGAC	qPCR
	OBS-0018	Rev: AACCTCTGCACCCAGTTTTTC	qPCR
hGAPDH	OBS-0430	Fwd: CCACATCGCTCAGACACCAT	qPCR
	OBS-0431	Rev: CGCAACAATATCCACTTTACCAGAG	qPCR
SparQ MCS	OBS-0659	Fwd: AGGAGGATTTGATATTCACCTG	Sanger sequencing
	OBS-0660	Rev: ACCTTCTCTAGGCACCCG	Sanger sequencing
U6-pX458	OBS-0663	Fwd: ACTATCATATGCTTACCGTAAC	Sanger sequencing

hNEAT1	OBS-0678	Fwd: ACTCTTCTTGTGAGCTCACTCC	qPCR
	OBS-0679	Rev: ACAATACCGACTCCAACAGCC	qPCR
hU6	OBS-0712	Fwd: GCTTCGGCAGCACATATACTAAAAT	qPCR
	OBS-0713	Rev: ATATGGAACGCTTCACGAATTTG	qPCR
hIL1 $\beta$	OBS-0720	Fwd: ATGGAGCAACAAGTGGTGTTC	qPCR
	OBS-0721	Rev: TCAACACGCAGGACAGGTACAG	qPCR
hIFIT1	OBS-0729	Fwd: ATGCAGGAAGAACATGACAACC	qPCR
	OBS-0730	Rev: TCTGGACACTCCATTCTATAGCG	qPCR
hMMP9	OBS-0735	Fwd: ACAAGCTCTTCGGCTTCTGC	qPCR
	OBS-0736	Rev: TCGCTGGTACAGGTCGAGTAC	qPCR
hCD80	OBS-0768	Fwd: AACCGGACCATCTTTGATATCATC	qPCR
	OBS-0769	Rev: TCGTATGTGCCCTCGTCAGA	qPCR
ENSG00000250 274	OBS-0805	Fwd: AACTCCTTGAGATTGGTATTGCC	qPCR
	OBS-0806	Rev: TCTAGAGTGTGTGGCTCATAATGG	qPCR
hLINC00211	OBS-0808	Fwd: TGAGTGTACTGCCTGGACTCATC	qPCR
	OBS-0809	Rev: TAAATGAAGCCTGCCACTTCAG	qPCR
ENSG00000248 323	OBS-0811	Fwd: ACCCAGCTGGAACCTTTATGG	qPCR
	OBS-0812	Rev: TTACCTGTAGCTCAGCATGTAGCC	qPCR
hMALAT1	OBS-0815	Fwd: AGGTGCTACACAGAAGTGGATTTCAG	qPCR
	OBS-0816	Rev: CTTCCCGTACTTCTGTCTTCCAGT	qPCR
pX458 sequencing	OBS-0842	Fwd: CTGGCCTTTTGCTCACATGT	PCR-Sanger sequencing
	OBS-0843	Rev: GTCTGCAGAATTGGCGCAC	PCR-Sanger sequencing
hLUCAT1	OBS-0849	Fwd: ACCATGTGTCAAGCTCGGATTG	qPCR
	OBS-0850	Rev: TTGTGGTCTCTGGTGCCAAG	qPCR
hRP11- 473M20.16	OBS-0851	Fwd: AGCTCAGTCGGTAGAGCATG	qPCR
	OBS-0852	Rev: TGCAAGGTATACGGAGTCACTTCC	qPCR
hMaIL1	OBS-0865	Fwd: AGCTCTGAGGAGTGAATCCAC	qPCR

	OBS-0866	Rev: ACATGGCTTTCATGCTAAATCTGTG	qPCR
hLINC00278	OBS-0873	Fwd: AGCCAGGAGTGAAGACGACAG	qPCR
	OBS-0956	Rev: TAGGTTCTGTTGTGCTGTCAGAG	qPCR
hLINC00346	OBS-0875	Fwd: TCATGGAGTGAGTGCGGAAGAC	qPCR
	OBS-0876	Rev: TGGATCTGATGACACTGCAGC	qPCR
hRP11- 316P17.2 F	OBS-0887	Fwd: AAGATGACACAGCCTCTGCC	qPCR
	OBS-0888	Rev: TGCAGGATCACTCATTGACGTG	qPCR
hRP11- 861A13.4 F	OBS-0889	Fwd: ATTCTCCTGCCTCACAAGTGC	qPCR
	OBS-0890	Rev: TCTGCTCTATGTCTGCACTGG	qPCR
ENSG00000261 222	OBS-0899	Fwd: TAATAAGCAGCAATTGCAGTTCC	qPCR
	OBS-0900	Rev: TATCTGCTCCTGAGGCAGAGG	qPCR
ENSG00000245 164	OBS-0907	Fwd: AACACTGAGCAATCCTGACCTG	qPCR
	OBS-0908	Rev: TATCGGTCCTCCACTCTTGTTTC	qPCR
ENSG00000272 908	OBS-0911	Fwd: TGGACATCTGGAATACAGCATG	qPCR
	OBS-0912	Rev: TTTGTGTGGTGAGAACATAGTTACC	qPCR
ENSG00000258 511	OBS-0935	Fwd: AAGCTGTGGCTGTTGTCAGC	qPCR
	OBS-0936	Rev: ACACTTGTCTCAGTAGGCCTGG	qPCR
ENSG00000256 039	OBS-0937	Fwd: TGTCACCTGTGGACAACTTGC	qPCR
	OBS-0938	Rev: TTATCTTGACCAGGTGCGAGAC	qPCR
Mail1-RACE	OBS-1042	Fwd: AGGCTGAGAAGCTCTGAGGAGTGAAT CC	RACE PCR
	OBS-1043	Rev: TGACAATCTTTCCCCACATTCCAGTGC	RACE PCR
ENSG237803_ RACE	OBS-1058	Fwd: AGAGTGAGTGTACTGCCTGGACTCATC AC	RACE PCR
	OBS-1059	Rev1: ACATAAAGATGTGGACAGTCACCATTG TC	RACE PCR

	OBS-1060	Rev2: TGAAGCCTGCCACTTCAGTGTAGAAAA C	
MaIL1-Full length	OBS-1191	Fwd: ATCGGATTCGAAAGCTCAGAGAAAAG ATGC	PCR
	OBS-1182	Rev: TCCGATGCGGCCGCTTTTTTTTTTCTTT TAAGTAGAG	PCR
hAPOE	OBS-1994	Fwd: TTCCTGGCAGGATGCCAGGC	qPCR
	OBS-1995	Rev: GGTCAGTTGTTCCCTCCAGTTC	qPCR
hIGFBP2	OBS-2075	Fwd: TATGAAGGAGCTGGCCGTGTTC	qPCR
	OBS-2076	Rev: ATGGTGGAGATCCGCTCCAGGA	qPCR
hS100A8	OBS-2077	Fwd: AGACTGTAGCAACTCTGGCAG	qPCR
	OBS-2078	Rev: TCCAGCTCGGTCAACATGATG	qPCR
hKLF4	OBS-2177	Fwd: AGAGTTCCCATCTCAAGGCAC	qPCR
	OBS-2178	Rev: TGCCTCTTCATGTGTAAGGCG	qPCR
hTREM2	OBS-2073	Fwd: TGCTCATCTTACTCTTTGTAC	qPCR
	OBS-2074	Rev: AGTGCTTCATGGAGTCATAGG	qPCR
hCHI3L1 F	OBS-2179	Fwd: AGGGACCCTTGCCTACTATGA	qPCR
	OBS-2180	Rev: TGGAAGTCATCCAGGTCCAGG	qPCR
hS100A9	OBS-2198	Fwd: ACCAATACTCTGTGAAGCTGG	qPCR
	OBS-2199	Rev: TCCTCGAAGCTCAGCTGCTTG	qPCR
hIFNA8	OBS-2200	Fwd: ACTTGACCAGCAGCTGAATG	qPCR
	OBS-2201	Rev: TCATGATTTCTGCTCTGACAACC	qPCR
hIFNA1	OBS-2202	Fwd: CAGGAGGACCTTGATGCTC	qPCR
	OBS-2203	Rev: TCTGCTGGATCAGCTCATGG	qPCR
hIFNB1	OBS-2204	Fwd: AACATGACCAACAAGTGTCTCC	qPCR
	OBS-2205	Rev: TGTCCTTGAGGCAGTATTCAAG	qPCR
hIFNL1	OBS-2206	Fwd; ACTTCCAAGCCCACCACAAC	qPCR
	OBS-2207	Rev: ACAGGAGAGCTGCAACTCCAG	qPCR
hIFNA2	OBS-2259	Fwd: TGAAGGACAGACATGACTTTGG	qPCR
	OBS-2260	Rev: AGATGAGTCCTTTGTGCTGAAG	qPCR

hIFNA13	OBS-2261	Fwd: ATGAGCAGAATCTCTCCTTCCTC	qPCR
	OBS-2262	Rev: TGAAGATCTGCTGGATCAGCTC	qPCR
hIFNA14	OBS-2263	Fwd: ATGAATGAGGACTCCATCCTG	qPCR
	OBS-2264	Rev: ATCTCATGATTTCTGCTCTGAC	qPCR
hNRIR	OBS-2323	Fwd: ACCTTGATCTTGGACTTCCTAG	qPCR
	OBS-2324	Rev: ACTGGATGAGACAGAATGCTG	qPCR
hIL10	OBS-0126	Fwd: GACTTTAAGGGTTACCTGGGTTG	qPCR
	OBS-0127	Rev: TCACATGCGCCTTGATGTCTG	qPCR
IL23A	OBS-1580	Fwd: CTCTGCTCCCTGATAGCCCT	qPCR
	OBS-1581	Rev: GGGACTGAGGCTTGGAAATCT	qPCR
hIFNL1	OBS-2206	Fwd; ACTTCCAAGCCCACCACAAC	qPCR
	OBS-2207	Rev: ACAGGAGAGCTGCAACTCCAG	qPCR
hCD70	OBS-2208	Fwd: TAGCTGAGCTGCAGCTGAATC	qPCR
	OBS-2209	Rev: CCTGGATGTGTACCATGTAGA	qPCR
hPU.1	OBS-2399	Fwd: AGAGCCATAGCGACCATTACTG	qPCR
	OBS-2400	Rev: ATCTGCTCCAGCTCCATGTG	qPCR

## 2.1.8 siRNAs

**Table 2.1.8: List of siRNAs**

Name	Sequence	Company
Silencer™ Select Negative Control No. 1 siRNA		Thermo Fisher
MaIL1-1	UCUUUGAACUGUAUUGUGGAU (guide) CCACAAUACAGUUCAAAGAGA (passenger)	Thermo Fisher (custom designed)
MaIL1-2	AAAUACAUGGCUUUCAUGCUA (guide) GCAUGAAAGCCAUGUAUUUAA (passenger)	Thermo Fisher (custom designed)

MaIL1-3	UUUACAUUUCUAUUAUGUGUG (guide) CACAUAAUAGAAAUGUAAAAG (passenger)	Thermo Fisher (custom designed)
---------	--	---------------------------------

## 2.1.9 Plasmids

**Table 2.1.9: List of Plasmids**

Name	Company
pSpCas9(BB)-2A-GFP (PX458)	Addgene
pLV hU6-sgRNA hUbc-dCas9-KRAB-T2a-GFP	Addgene
SparQ™	System Bioscience
psPAX2	Addgene
pCMV-VSVG	Addgene
pSC-A-amp/kan	Agilent

## 2.1.10 Buffers and Solutions

**Table 2.1.10: List of prepared buffers and solutions**

Name	Composition
ELISA coating buffer	7.13 g Natriumhydrogencarbonat 1.59 g Natriumcarbonat ad 1 L H <sub>2</sub> O to pH 9.5 with 10 N NaOH
ELISA dilution buffer	10% v/v FCS in 1x PBS
ELISA wash buffer	0.05% v/v Tween in 1x PBS
FACS blocking buffer	10% v/v FCS 0.5% v/v Tween in PBS
FACS Fixation buffer	4% v/v PFA

	in PBS
FACS Permeabilisation buffer	
FACS Wash Buffer	0.5% v/v FCS in PBS
Laemmli Buffer	13.15 % v/v Stacking Buffer 21.05 % v/v 10 % SDS 10.5 % v/v Glycerol 5.75 % v/v 1 % Bromophenol Blue
LB Agar	3.5 % w/v LB Agar in H <sub>2</sub> O
LB Medium	2 % w/v LB Broth in H <sub>2</sub> O.
MACS Buffer	0.5% v/v FCS 0.2 mM EDTA in PBS
RIPA Buffer	10 mM Tris, pH 7.5 150 mM NaCl 1% v/v NP-40 1% v/v Desoxycholat 1 mM EDTA
TAE buffer (50X)	242 g Tris-Base 57.1 ml Ethanoic acid 100 ml EDTA (0.5 M) ad 1 L in H <sub>2</sub> O
TBS buffer (10x)	10 mM Tris 0.9% (w/v) 90 g NaCl ad 1 L H <sub>2</sub> O to pH 7.4 with 37% (v/v) HCl
TBST-T	100 ml 10X TBS buffer 0.1% (v/v) Tween-20 ad 1 L in H <sub>2</sub> O
Western Blot Blocking Solution	10% (w/v) milk

	5% (w/v) BSA in 1X TBS-T
Western Blot Resolving Gel 10 %	4.94 ml ddH <sub>2</sub> O 7.56 ml Tris-HCl pH 8.8 6.68 ml Acrylamide/Bisacrylamide 500 µl 10% (v/v) Glycerol 200 µl 10% (w/v) SDS 100 µl 10% (w/v) APS 20 µl TEMED
Western Blot Running Buffer for SDS-PAGE (10X)	250 mM Tris 1.92 M Glycin in H <sub>2</sub> O
Western Blot Running Buffer for SDS-PAGE (1X)	100 ml Western Blot Running Buffer for SDS-PAGE 0.1% SDS ad 1 L H <sub>2</sub> O
Western Blot Stacking Gel 5 %	5.68 ml ddH <sub>2</sub> O 2.5 ml Tris-HCl pH 6,8 1.66 ml Acrylamid/Bisacrylamid 100 µl 10% (w/v) SDS 50 µl 10% (w/v) APS 10 µl TEMED
Western Blot Wet Blot Buffer (10X) pH 8.3	250 mM Tris 1.92 M Glycin ad 1 L H <sub>2</sub> O to pH 7.4 with 37% (v/v) HCl
Western Blot Wet blot running buffer (1X)	200 ml 10X Wet-Blot Puffer 20% (v/v) Methanol 0.1% (w/v) SDS ad 2 L H <sub>2</sub> O



## 2.1.11 Software

**Table 2.1.11: List of software**

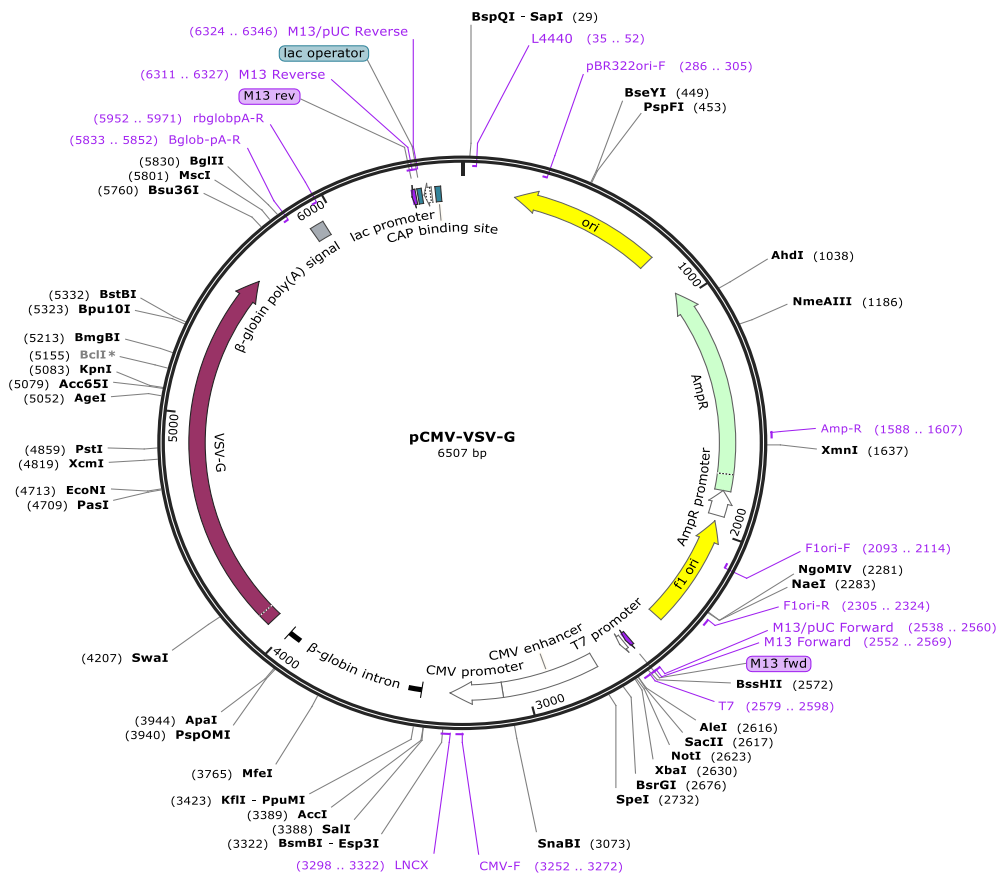
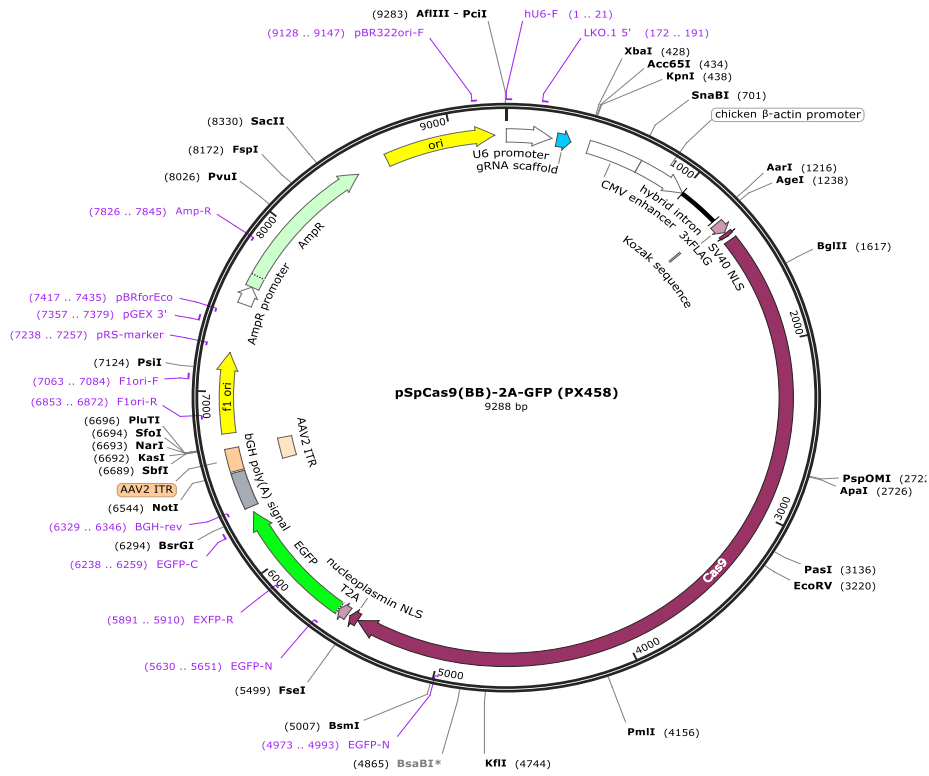
Software	Version
Adobe Photoshop CS	5.1
Agilent 2100 Expert Software	B.02.08.SI648 (SR1)
Clone manager	9
SnapGene	5.0.6
FlowJo v. 7.6.5	2.0
GraphPad Prism	6
Microsoft Office 2010	
ViiA7 RUO	1.2
Windows	7 Professional

## 2.1.12 Websites

**Table 2.12: List of websites.**

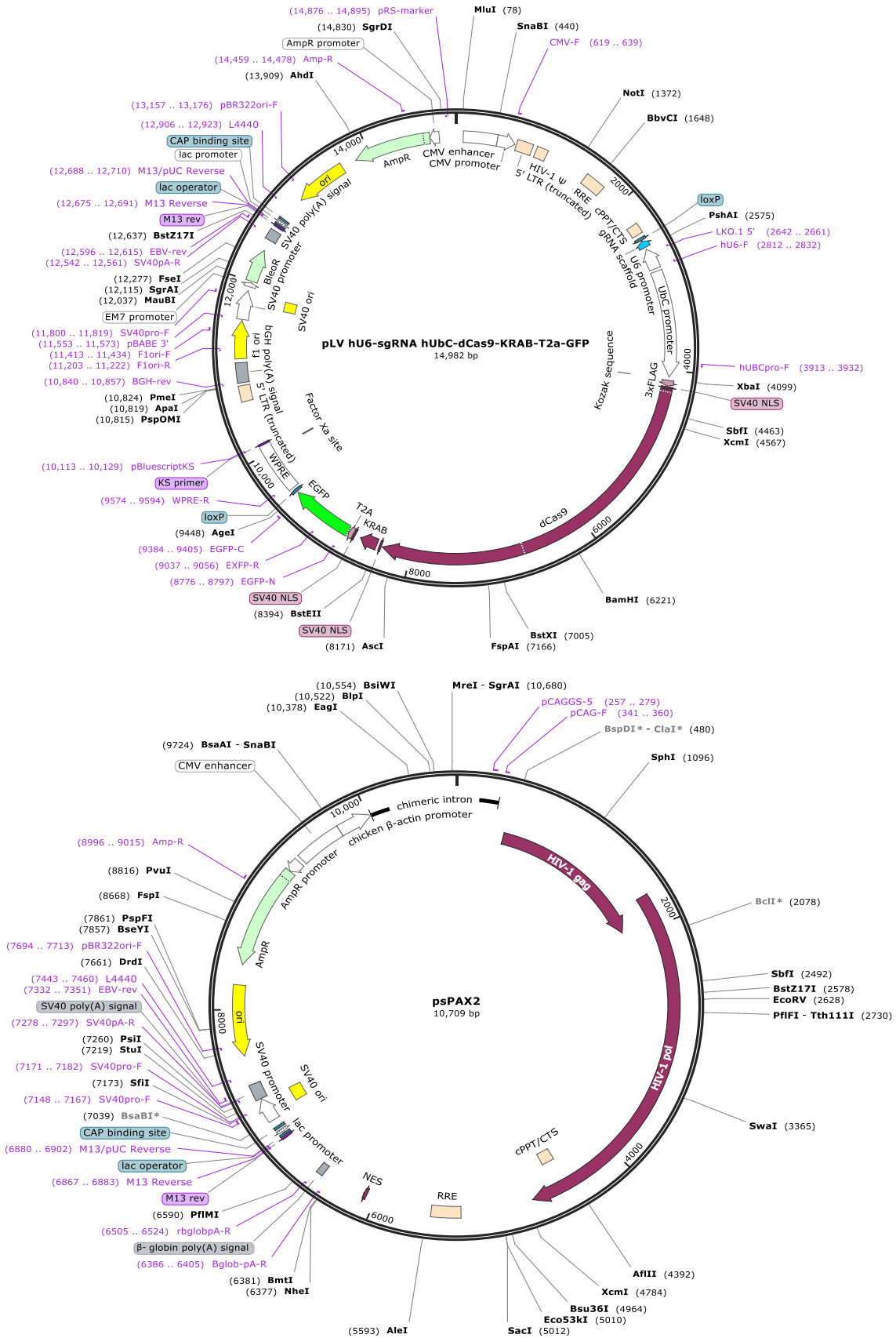
Homepage	Link
Ensembl	<a href="http://www.ensembl.org/index.html">http://www.ensembl.org/index.html</a>
NCBI	<a href="https://www.ncbi.nlm.nih.gov/">https://www.ncbi.nlm.nih.gov/</a>
Reverse complement	<a href="https://www.bioinformatics.org/sms/rev_comp.html">https://www.bioinformatics.org/sms/rev_comp.html</a>
Tm Calculator- Thermo Fisher Scientific	<a href="https://www.thermofisher.com/de/en/home/brands/thermo-scientific/molecular-biology/molecular-biology-learning-center/molecular-biology-resource-library/thermo-scientific-web-tools/tm-calculator.html">https://www.thermofisher.com/de/en/home/brands/thermo-scientific/molecular-biology/molecular-biology-learning-center/molecular-biology-resource-library/thermo-scientific-web-tools/tm-calculator.html</a>
Biorender	<a href="http://www.biorender.com">www.biorender.com</a>
CPC calculator	<a href="http://cpc2.cbi.pku.edu.cn/">(http://cpc2.cbi.pku.edu.cn/)</a>
gRNA design tool	<a href="http://crispr.mit.edu/">(http://crispr.mit.edu/)</a>
siRNA design tool	<a href="http://design.RNAi.jp/">(http://design.RNAi.jp/)</a>

## 2.1.13 Vector maps



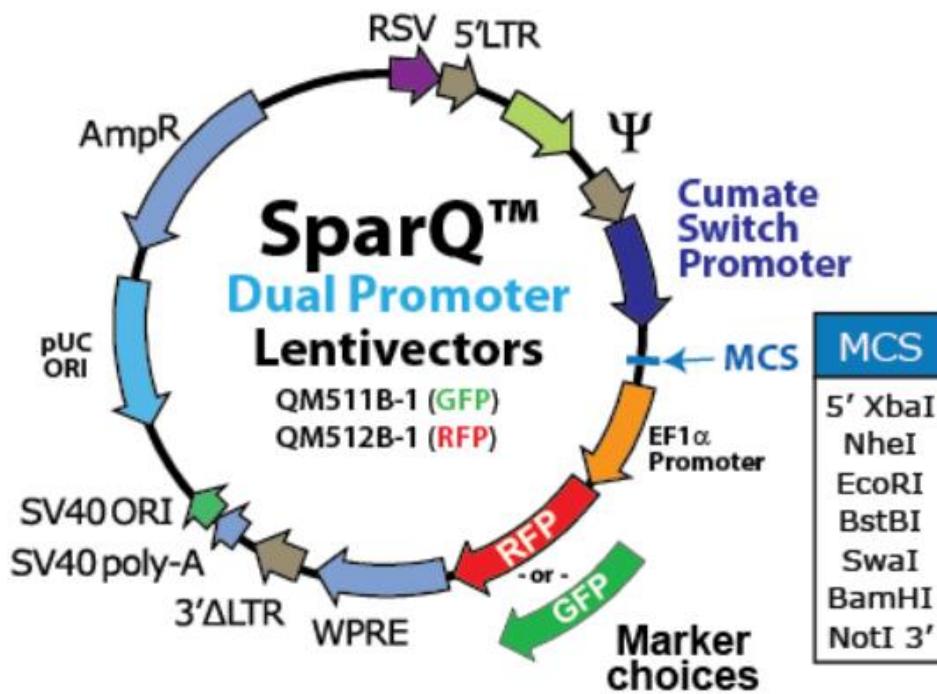
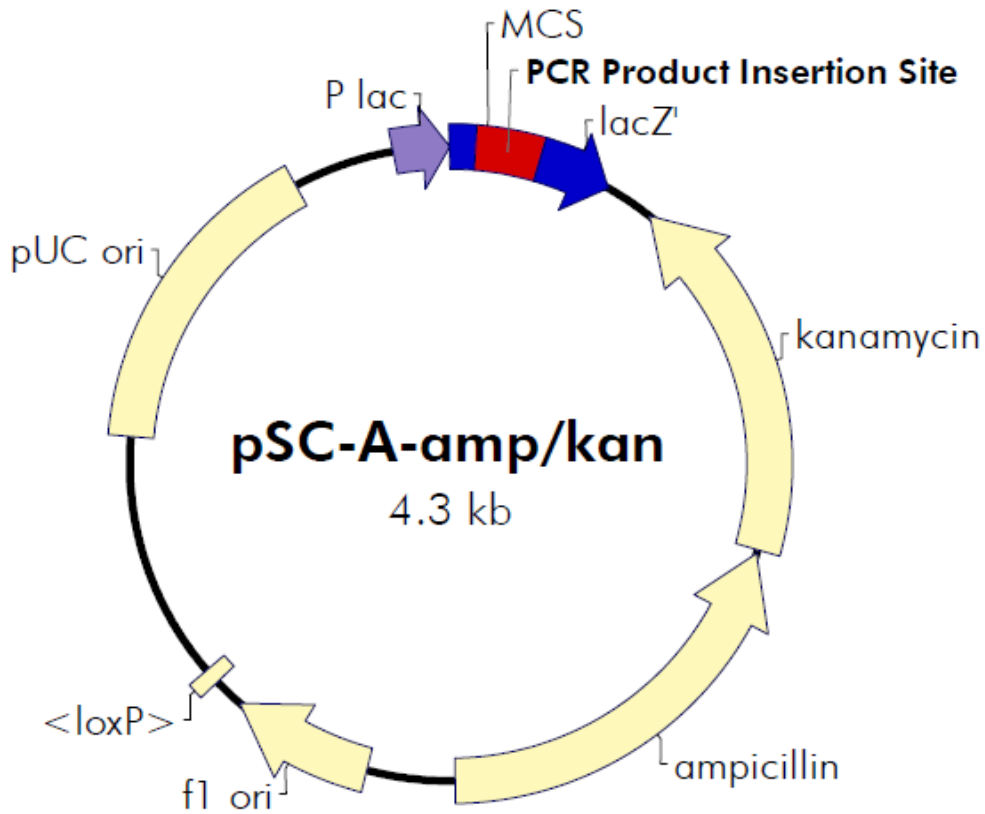
<https://www.addgene.org/48138/>

<https://www.addgene.org/8454/>



<https://www.addgene.org/71237/>

<https://www.addgene.org/12260/>



<https://www.agilent.com/cs/library/usermanuals/public/240205.pdf>

[https://systembio.com/wp-content/uploads/Manual\\_Cumate\\_system-1.pdf](https://systembio.com/wp-content/uploads/Manual_Cumate_system-1.pdf)

## 2.2 Methods

### 2.2.1 Cell culture

#### 2.2.1.1 Isolation of primary human monocytes

Monocytes were isolated from buffy coats provided by donors in the Centre for Transfusion Medicine and Haemotherapy in Giessen, Germany. All donors consent to use their blood samples for scientific purposes. The buffy coats were diluted 1:1 with PBS and 20 ml were carefully transferred into a 50 ml falcon tubes containing 10 ml of Ficoll (Figure 2.2.1). The tubes were centrifuged for 30 min at 800 x g with the breaks off. The centrifugation resulted in a distinct leukocyte layer. Leukocytes were transferred in a new tube containing PBS and centrifuged at 250 x g for 10 min.

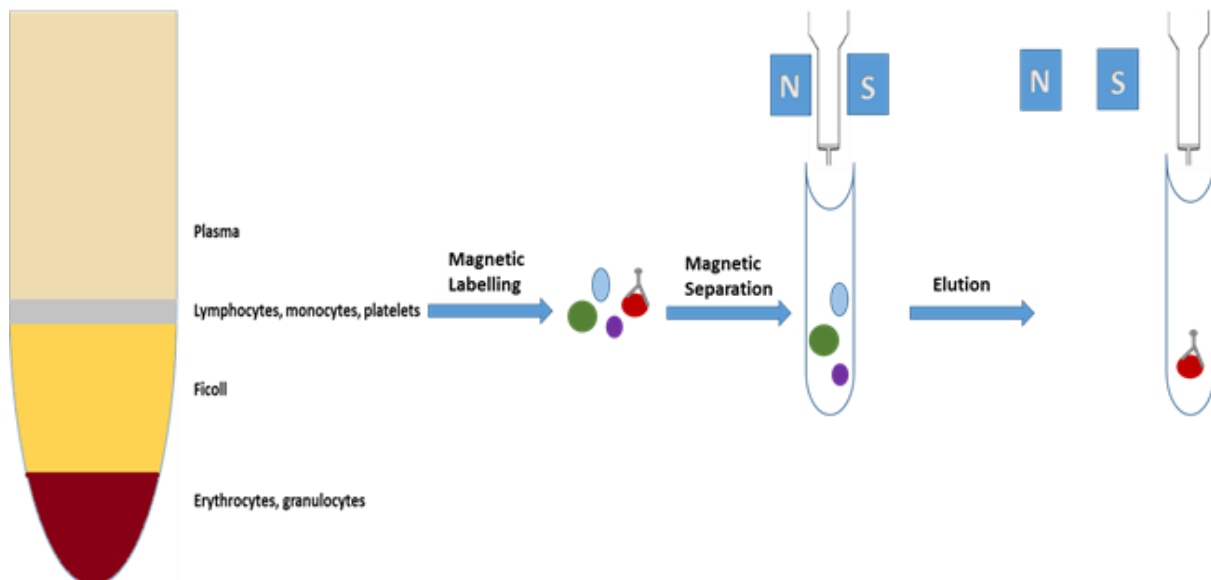


**Figure 2.2.1: Schematic representation of monocyte isolation by MACS protocol.** After centrifugation, four distinct layers were visible in the tube (top to the bottom): the plasma layer, the layer containing lymphocytes, monocytes and platelets, the Ficoll layer and at the bottom the layer of erythrocytes and granulocytes. The layer containing lymphocytes, monocytes and platelets was then transferred to a new tube and labelled magnetically with anti-CD14 beads. After the labelling, the cells were passed through a column that was placed in a magnet and the unlabelled cells were eluted in the flow-through. At the final step, the column was removed from the magnet and the labelled cells were eluted.

The PBS was removed and the pellet was again resuspended in PBS. The washing step was repeated until the supernatant was clear. For the isolation of monocytes, a magnetic-activated cell sorting (MACS) protocol was used (Miltenyi Biotec #130-050-201). In the final washing step the cells were counted and resuspended in an appropriate amount of MACS buffer (400  $\mu$ l for  $2 \times 10^8$  cells). Anti-CD14 beads were added accordingly (100  $\mu$ l for  $2 \times 10^8$  cells) and the

mixture was incubated for 20 min at 4°C. Labelled cells were magnetically separated in a MACS LS column. The column was washed 3 times with 3 ml of MACS buffer. The cells were eluted with 5 ml MACS buffer and the number of monocytes was measured. The purity of the population was verified by Flow cytometry, using an anti-CD14 antibody.

### **2.2.1.2 Macrophage differentiation and culture**

Monocytes isolated as described above were cultured in x-VIVO-15 medium (Lonza) containing 5% fetal calf serum (FCS), 25 µg/ml Gentamicin and 15 ng/ml or 100 ng/ml GM-CSF (Preprotech, #300-03) and cultured for 8 or 6 days, respectively, at 37°C and 5% CO<sub>2</sub>. When cultured for 8 days, on day 5 the cells were supplemented again with 15 ng/ml GM-CSF. After 6 or 8 days the morphology of the cells was macroscopically checked. After differentiation, the cells were used for further experiments.

### **2.2.1.3 Dendritic cell differentiation and culture**

Monocytes isolated as described above were cultured in x-VIVO-15 medium (Lonza) containing 5% fetal calf serum (FCS, Biochrom), 25 µg/ml Gentamicin and 15ng/ml or 50 ng/ml GM-CSF and 20 ng/ml IL-4 (Preprotech, #200-04) and cultured for 6 days at 37°C and 5% CO<sub>2</sub>. After 6 days the morphology of the cells was macroscopically checked.

### **2.2.1.4 Isolation of other immune cell populations**

For isolation of other immune cell populations MACS was employed again (Miltenyi Biotec). The different immune cells were incubated with different beads. For isolation of NK Cells and B-cells anti-CD56 (#130-050-401) and anti-CD19 beads (#130-050-301) were used respectively. For the T cell populations two rounds of selection were performed. First, the cells were incubated with either anti-CD4 (#130-045-101) or anti-CD8 beads (#130-045-201) and secondly the CD4<sup>+</sup> and CD8<sup>+</sup> populations were incubated with anti-CD45RO (#130-046-001) to distinguish between the memory and the naive T-cells. The granulocytes were isolated from whole blood sample (no Ficoll separation) with anti-CD66 Beads (#130-111-552).

### **2.2.1.5 Liver and Brain RNA**

For liver reference tissue collection, cirrhosis was an exclusion criterion. Non-diseased tissue from tumour resections was processed. All patients had provided oral and written informed consent and the local ethics committee approved the study (Marburg FB20 Ethikkommission Az.: Studie 14/17). Professor Dr. Pagenstecher provided the brain RNA samples.

### **2.2.1.6 THP1 and U937 cell culture and differentiation**

THP-1 cells are immortalized isolates of a one year old infant male with leukemia and used as a model for human monocytes (Tsuchiya, al., 1980) and U937 cells have been isolated from the histiocytic lymphoma of a 37-year-old male patient (Sundström et al., 1976) for the same purpose. The cell lines were purchased from the American Type Culture Collection (ATCC). The human monocytic suspension cell lines were cultured in RPMI medium (Thermo Fisher), supplemented with 10% (v/v) FCS in T75 tissue culture flasks at 37°C and 5% CO<sub>2</sub> at a density of  $2.5 \times 10^5$  cells/mL. Cells were splitted regularly to maintain the appropriate density. To obtain adherent macrophage-like cells, THP-1 and U937 monocytes were stimulated with 20 nM Phorbol-12-myristate-13-acetate (PMA) for 24 h. The morphology of the cells was microscopically checked before use for further experiments.

### **2.2.1.7 HEK-293T cell culture**

Human embryonic kidney cells 293T (HEK-293T) display an adherent epithelial morphology. The cell line was cultured in RPMI, supplemented with 10% (v/v) FCS in T75 tissue culture flasks at 37°C and 5% CO<sub>2</sub> and splitted regularly to maintain 70 - 90% confluency. For splitting, the supernatant of the adherent cells was discarded and the cells were detached from the flask by adding 5 ml of new medium directly on top of the cells and vigorous pipetting. The HEK-293T cells were used for the Lentiviral production.

## **2.2.2 Transcriptome Analysis**

### **2.2.2.1 RNA extraction by TRIZOL®**

For RNA expression analysis, either by quantitative real time PCR (qRT-PCR) or by RNA sequencing, RNA isolation was performed. The supernatant of the cells was removed and 500 µl of TRIZOL® reagent were added. After 5 min incubation, the lysed cells were transferred to a 1.5 ml Eppendorf tube and 200 µl of chloroform was added, followed by vigorous mixing. The mixture was centrifuged at 13000 rpm for 15 min at 4°C to separate into the aqueous and the organic layer. The aqueous phase, containing the RNA, was transferred into a new tube. RNA precipitation was achieved by the addition of 250 µl isopropanol to the aqueous phase. Additionally, 1 µl of GlycoBlue™ was added to conjugate and visualize precipitated RNA. The precipitation of the RNA was performed at -20°C either for 1 hour or overnight. Afterwards, the samples were centrifuged at 13000 rpm for 15 min at 4°C and the supernatant was removed. The RNA pellet was washed with 400 µl of 75% ethanol. After the ethanol was removed the

pellets were air-dried. To resuspend the pellet 43.5  $\mu$ l of H<sub>2</sub>O were added and the sample was incubated at 65°C for 5 min while shaking. The samples were either frozen or directly DNaseI digested.

### 2.2.2.2 RNA extraction by mirVana™ miRNA kit

To obtain high quality and purity of RNA for RNA sequencing, mirVANA™ miRNA kit was used. The supernatant of the cells was removed and the cells were washed with 1 ml of PBS and lysed with 600  $\mu$ l of Lysis/Binding Buffer. After vortexing vigorously, 60  $\mu$ l of miRNA Homogenate Additive was added and the samples were incubated for 10 min on ice. Next 600  $\mu$ l of Acid-Phenol:Chloroform was added and the samples were vortexed and centrifuged at 10000 x g for 5 min. The aqueous phase was then transferred to a new tube and filled with 700  $\mu$ l of 100% ethanol. Up to 700  $\mu$ l was placed into a Filter Cartridge, followed by centrifugation for 30 sec at 10000 x g. The flow-through was discarded and the step was repeated until all the cell lysate mixture was passed through the column. To wash the column, 700  $\mu$ l of miRNA Wash Solution 1 was applied and centrifuged for 30 sec at 10000 x g. This was followed by a second washing step with 500  $\mu$ l of Wash Solution 2/3 for 30 sec at 10000 x g (2 times). After the flow-through was discarded, the column was centrifuged once more at 1000 x g for 1 min. Finally, the Filter Cartridge was transferred into a new collection tube and 100  $\mu$ l of H<sub>2</sub>O (pre-warmed at 95°C) were added. The samples were centrifuged and the eluted RNA was either stored at -20°C or used for DNaseI Digestion.

### 2.2.2.3 DNaseI Digestion

To remove the DNA from the RNA samples, DNaseI digestion was performed. The reagents and the amounts of the reaction are indicated in the table below (Table 2.2.1).

**Table 2.2.1: DNase 1 mixture**

Component	Volume ( $\mu$ l)
RNA	43.5
RNase Inhibitor (Promega #N2511)	0.5
DNaseI Buffer 10x	5
DNaseI (Ambion #AM2222)	1

The mixture was incubated at 37°C for 30 min followed by incubation at 75°C for 5 min, to inactivate the DNase. After the inactivation 50  $\mu$ l of ultra-pure water and 100  $\mu$ l of PCI were



added on the top of the samples and mixed vigorously. The mixture was centrifuged at 13000 rpm for 15 min at 4°C. The upper layer was transferred into a new tube and 300 µl of a mixture of 30:1 ethanol / sodium acetate (EtOH/NaAcetate) was added for RNA precipitation. Additionally, 1 µl of GlycoBlue™ was added to conjugate and visualize precipitated RNA. The next steps are the same as the last steps of RNA extraction by TRIZOL® (see section 2.2.2.1).

#### 2.2.2.4 RNA quantification and quality check

The concentration of RNA was determined using a Nanodrop 2000 Spectrophotometer (Thermo Fisher Scientific). For samples that were sent for sequencing RNA integrity was verified on a Bioanalyzer 2100 (Agilent) according to the manufacturer's protocol. The ratio of intact 18s and 28s rRNA was used to calculate the RNA integrity number (RIN). The ratio should be 2:1, deviations from that indicate RNA degradation. A RIN of 10 reflects perfect RNA quality, while a RIN of 5 means partial degradation. Based on this guideline, samples with RINs > 8 were considered to have good-enough RNA quality for sequencing.

#### 2.2.2.5 cDNA synthesis

Total RNA was transcribed into cDNA via the High Capacity reverse transcription kit (Thermo Fisher). Depending on the RNA amount, 200 – 2,000 ng RNA were used for the transcription.

**Table 2.2.2: Mixture for cDNA synthesis**

Component	Volume (µl)
10X RT buffer	2
10X Random Primers	2
100 mM dNTPs	0.8
50 U/µl Multiscribe Reverse Transcriptase	1
RNA (250 – 2000 ng)	x
Ultrapure H <sub>2</sub> O	Up to 20

The cDNA reaction was performed according to the following program (Table 2.2.3)

**Table 2.2.3: Thermocycler program**

Cycle step	Temperature (°C)	Time (min)
Annealing	25	10
Elongation	37	120
Deactivation	85	5

Hold	8	$\infty$
------	---	----------

The cDNA was then diluted to a final concentration of 5 ng/ $\mu$ l and used for qRT-PCR.

### 2.2.2.6 Quantitative Real Time PCR (qRT-PCR)

For analysing the relative expression of different RNAs qRT-PCR with SYBR Green detection reagent was used. The following (Table 2.2.4) shows the reaction mixture.

**Table 2.2.4: QRT-PCR mixture**

Component	Volume ( $\mu$ l)
2X PowerUp™ SYBR™ Green Master mix	10
10 $\mu$ M forward primer	0.4
10 $\mu$ M reverse primer	0.4
cDNA	1.5
H <sub>2</sub> O	7.7

The reaction mix was pipetted into 96-wells and the plates were run on a ViiA7 Real-Time PCR System. The program is described on the following table (Table 2.2.5).

**Table 2.2.5: QRT-PCR program**

	Cycle step	Temperature (°C)	Time (sec)
	denaturation	95	20
40 cycles	denaturation	95	15
	primer binding/elongation	60	20
	end of the cycles	60	60
	melting curve	60-95	0.05 °C/s gradually
		95	15

In case of low abundant transcripts or low amount of RNA one-step qRT-PCR was used. In this case the reaction was performed directly after RNA isolation. The kit that was used in this case

was the Power SYBR® Green RNA-to-CT™ 1-Step Kit from Thermo Fisher. The reaction mixture is as described in the following table (Table 2.2.6).

**Table 2.2.6: Power SYBR® Green RNA-to-CT™ 1-Step mixture**

Component	Volume (µl)
2X SYBR® Green Master Mix	10
10 µM forward primer	0.2
10 µM reverse primer	0.2
Reverse transcriptase	0.16
RNA	variable
H <sub>2</sub> O	20 µl final volume

The reaction was performed in 96-wells and the plates were run on a ViiA7 Real-Time PCR System. The program is described on the following table (Table 2.2.7).

**Table 2.2.7: Power SYBR® Green RNA-to-CT™ 1-Step cyler program**

	Cycle step	Temperature (°C)	Time
	reverse transcription	48	30 min
	denaturation	95	10 min
40 cycles	denaturation	95	15 sec
	primer binding/elongation	60	1 min
	melting curve	95	15 sec
		60	1 min
		95	15 sec

### 2.2.3 Subcellular fractionation

To investigate the cellular localisation of different lncRNAs subcellular fractionation was performed. In this protocol the cells were separated into nucleus and the cytosol fractions. For this purpose,  $4 \times 10^6$  cells were spinned down at 250 x g and washed two times with PBS. Afterwards, the cells were resuspended in 200 µl of lysis buffer (see table 2.2.8) and incubated on ice for 5 min, while gently pipetting up and down.

**Table 2.2.8 Lysis Buffer**

Name	Concentration	Company	Ordering number
Tris-HCl pH 8	10 mM	Life Technologies	1567-027
NaCl	140 mM	Carl Roth GmbH & Co	9265.1
MgCl <sub>2</sub>	1.5 mM	Life Technologies	AM9530G
Vanadyl ribonucleoside (VRC)	2 mM	Sigma-Aldrich	R3380
IGEPAL®	0.5%	Sigma-Aldrich	I8896

From the lysate 30 µl were kept aside and 500 µl of Trizol® were added on the top for total RNA isolation. The rest of the lysate was centrifuged at 1000 x g for 3 min at 4 °C to pellet the nuclei and the supernatant was the cytosol. To succeed a pure cytosolic fraction the supernatant was centrifuged again at 13.000 rpm for 10 min at 4 °C and transferred into a new tube. Subsequently, 500 µl of Trizol® were added on top. To obtain pure nuclear RNA, the nuclear pellets underwent three additional washes with 160 µl of lysis buffer. Finally, the purified nuclei were resuspended in 100 µl of lysis buffer and 500 µl of Trizol® were added on top. The procedure was completed by RNA isolation and DNaseI digestion. For determining the subcellular localization of specific RNAs, qPCR was performed. The quantification was done by comparing the C(t) values of the respective RNA in the cytosol and in the nucleus. For validation of the method, RNAs with a known localisation pattern were used.

### **2.2.4 Rapid Amplification of cDNA Ends (RACE)**

To identify the exact cDNA sequence of the novel lncRNAs (MaIL1, LINC00211) Rapid Amplification of cDNA Ends (RACE) was employed, using the SMARTer® RACE 5'/3'kit (Clontech) protocol. First, high quality RNA was extracted and then 5'-RACE-Ready cDNA and 3'-RACE-Ready cDNA were prepared (Table 2.2.9).

**Table 2.2.9: RACE cDNA mixtures**

Reagent	Volume-5'-RACE-cDNA	Volume-3'-RACE-cDNA
RNA	7.5 $\mu$ l	7.5 $\mu$ l
5'-CDS-Primer A/3'-CDS-Primer A	1 $\mu$ l	1 $\mu$ l
H2O	2.5 $\mu$ l	3.5 $\mu$ l

The mixtures were then incubated at 72°C for 3 min and then at 42°C 2 min. After spinning down, for the 5'-RACE cDNA synthesis reaction 1  $\mu$ l of the SMARTer II A Oligonucleotide was added. In the next step another mixture was prepared and added to the two cDNA libraries (Table 2.2.10).

**Table 2.2.10: Reverse transcriptase mixture**

Reagent	Volume ( $\mu$ l)	
5X First-Strand Buffer	4	Pre-mix
DTT (100 mM)	0.5	
dNTPs (20 mM)	1	
RNase Inhibitor	0.5	
SMARTScribe™ Reverse Transcriptase (100U)	2	

The mixtures were first incubated at 42°C for 90 min, and then at 72°C for 10 min. The cDNA reactions were diluted with Tris-EDTA Buffer depending on the RNA concentration. After the cDNA library was prepared, a PCR was performed. For this purpose, a master mix was prepared according to Table 2.2.11

**Table 2.2.11: Mastermix of PCR**

Reagent	Volume ( $\mu$ l)
dd H <sub>2</sub> O	34.5
10X Advantage 2 PCR Buffer	5
dNTPs (10mM)	1
50X Advantage 2 Polymerase Mix	1

The mixture was then added to the PCR reaction, which is described on Table 2.2.12 and then run in a thermocycler (Table 2.2.13)

**Table 2.2.12: PCR reaction**

Component	Volume-5' or 3'- RACE sample (µl)	Volume-UPM only (µl)	Volume-GSP only (µl)
5' or 3'- RACE cDNA	2.5	2.5	2.5
10X UPM	5	5	-
5' or 3' GSP (10 µl)	1	-	1
H2O	-	1	5
Master mix Table 2.2.11	41.5	41.5	41.5

**Table 2.2.13: PCR program**

Cycles	Temperature (°C)	Time
5 cycles	94	30 sec
	72	3 min
5 cycles	94	30 sec
	70	30 sec
	72	3 min
25 cycles	94	30 sec
	68	30 sec
	72	3 min

After the PCRs were finished, the samples were run on 1% agarose gels. The DNA bands were then excised and purified using the Gene JET gel extraction kit (Thermo Fisher) according to the manufacturer's protocol. When the concentration was appropriate, the PCR fragments were cloned into a TOPO vector (Strataclone UA PCR cloning kit, Agilent) and send for Sanger Sequencing (Mycrosynth Seqlab). Below the full-length sequences, as inferred by RACE PCR, of LINC00211 and MaIL1 are shown.

**Full length LINC00211:**

GAGGAACAGTCTTACTCTGTCACCCAGGCTGCAGTGTAGTGGTGTGATCACAGCT  
 CACTGCAGCCTTGACCTCCTGGGCTTAGGTGATCCTCCCACCCTAGCCTCCCATGT  
 AGCTGGGACTAGAGGTATGTGCCACCTCACCTCCTTTTTTTCTTTTCTTTTCTTTT  
 TTGGAGAGACAGATTCTTCTTATGTTGCTATTTTAAACTCCTGAACTCAAGTGATC  
 CTCCTGCCTTGGCCTCCCAAAGTGCTGGGATTACAGGTGTGAGACACTGCACCCT  
 GCCAAGCACCTCTGCTCCGTGCCATGCTCTTGGCTAATTGGAGTTGTGAAAGGC  
 ATGAGGATTCTGGTCATGGACTCAGCTCTCCCATAGGGTTCTGACACCAAAGCAA  
 TGGTCACAACAGTGAAAGGAAGAATCCATCTGGCCAGGCTCAGGTGGTTCAAGG  
 CCTTCAGAATCTGCCTTGAGACTCTCACTGGCTTTAGACTGAAAACCATCTTGGCC  
 CCGTCCATCCGTGTAAGCAATTTAACGACAGCTTGCAAAGCACCGAGCTTTAACA  
 GAAAGAAGAGATGAGCACAGCGCAAGAACTTGGACTCCAGAAGAGCTGCCTAAC  
 AGATTATTTTTCTGTGGCATTTCATGAGAACAAACGAAGTAGGAATTTTCTTTTG  
 TTTGTCTGGCCTTTGGCATCGTTTACTTTCTTTTTATTCTTCTGAAATGTACTTCGA  
 GCCCTGGCAGCATTCTGTCCATAAATCTTATTGTCAGAGGTTTATTTTTCAGCTT  
 TTCAAATCATATCTGATAGAGTGAGTGTACTGCCTGGACTCATCACTTTACTTCAG  
 AAGAAATACAGCTCACCTTTAAATGACAATGGTGACTGTCCACATCTTTATGTTT  
 TCTACACTGAAGTGGCAGGCTTCATTTAAAATAATGTTTTCCCTCATCAAAGA  
 GAGCTAGGGTAGAACCGTCAACTCTGCTGTTGTCTGGGTAGTGACCTAACACCCA  
 CGTTTTGGACAATCACTCACTGTCTTATATTGGGTTTTTCATTGCATGTAGGATAAT  
 TCTTTGTCAATGGTAGTTTTGTCAACCGTGATCTGAGGTAATGAGGTTTTCTACTT  
 TTGCTTGAAATTTTGAAAATATGCAAGCTTTAAACATTT

**Full length MaIL1:**

AAAGGAGAACAATTCATCACGTCAGAGAAAAGATGCTCTCTCCATGTCGTAAGTT  
 ACACAAGAAGTATTCACGATAGACAAGATATGGAATCAATCTGTAACCATCAAC  
 AAATGAATAAAGACGCTGTGATGTATACACAAAATGGAATACTCTACAGCAGTC  
 CATTGTGAAAGAGAAGGAATTCCTGTCATTTATCACAACATGGGTGAATCTATAG  
 GACACGAAAAAAGGCTGGGCGTGGTGGATCACTTCTGTAATCCTAGCACTTTGGG  
 AGGCTGAGAAGCTCTGAGGAGTGAATCCACAATACAGTTCAAAGAGAGATTTAA  
 ATTGCTAATTTCCCGGCACTGGAATGTGGGGAAAGATTGTCACAGATTTAGCATG  
 AAAGCCATGTATTTAACATTCCATATGTAATAACCCTCTCTTAAATTGCATTTTGGT  
 TTGAGAAACAGCAAGAACAATTCAGCATTAGGGGGAAACTTTGCTGTTGATCTC  
 AAAGGGAATGAGAATTTAGGGAGCACCTCTGCCCACCAGGAAGGAGCTTTCTCTT  
 GAGTCTCCCACATGACTGTGTACTATGGATCACATTGGAAGAACTTCTCTTTTTCC  
 TAATGCTGTCTGAGTTTTGCATTTTGGTGCCAGAACAGGGGAAGTGAAGGGATACA  
 TAAGAGACACACATAATAGAAATGTAAAAGACAAGCAATACCACCAGACGATAG  
 ATGTAATTTGGAACAAAGATATTTTTATTTGCCTAAGGCTCAGAAAGTCGTGCCA  
 GGCAATGCTGGAAGGAATTGGTTGGCTTCCTCTCCCAAACCACTTCCTCAGTGCT  
 CATCTCTTTCAGGTGGACAAGATATGGCATTTTGACTGCTAGCAAATGTCACTGT  
 GACATTTCAATGGCACAATTGGTGACAATTCAGCCAATTTTTGTTGGGCACCCTCC  
 ACATGCCCCAGGGTCTGGGCTCAGCCCTTACGTACGTGGGCTCATTGATTTCTCC  
 ATGTTTTCTAGAATGTGATTTTACCCTGGCTGGCACAGAGTAAATGCCCAAAGAA  
 TGGTAGCTATTGTTTTTAATCATCATTATTAATTTTATAAATAACTTCCATATCAG  
 GTGATGGGAAAATTTACAGACTTTGATTTGGGCCTTGGAACACAGGTTCAAGTTTCA  
 GTAGATGGAGGTAAAAGGAGGCAAAGAGCGACCTTACGTAAATCCAAGGCTGAA  
 GGAAGGAGGCTCTAAGGGGTGTGTGGGTGATTAGGAGTAAAGTATCTTGTCTGA  
 AATGAAGAGTTTCTATACAGCATGCTTATTTGGAGTCATGCCTAACAAGATTACT  
 TTGGGTCTAATTTTGGAAGCTTGGTACTCCAGGGAGCTTGGACATGAATTTAAAG

ACAATGGGAACTCACATTTAAGTTTCTGAAACAGCCAGGCGTGGTGGCTCATGCC  
 TGTAATCCCAGCACTTCGGGAGGCTGAGGCAGGTGGATCACCTGAGATCAGGAG  
 TTTGAGACCAGTCTAACCAACATGGAGAAACCCCATCTCTACTTAAAAGAAAAA  
 AAAA

## 2.2.5 PCR amplification of the full length MaIL1

To amplify the MaIL1 transcript, poly A RNA was used. For this purpose, 74 µg (in 100 µl of H<sub>2</sub>O) of total RNA isolated from macrophages pre-treated with LPS (100 ng/ml) and IFN $\gamma$  (100ng/ml) were used. The RNA was heated at 65°C for 2 min to disrupt secondary structures. In the meantime, 200 µl of Dynabeads® were prepared. The beads were washed with 100 µl of Binding buffer and then diluted in another 100 µl of binding buffer. The RNA was mixed with the Dynabeads® and incubated for 5 min at room temperature. The beads were placed in a magnet and washed with 200 µl of Washing buffer B. The elution of the poly A RNA was performed with 10 µl of 10 mM Tris-HCl pH 7.5 at 80°C for 2 min. The poly A RNA was then reverse transcribed to cDNA (Table 2.2.14).

**Table 2.2.14: Reverse transcription mixture**

Name	Amount (µl)	concentration	Temperature- Time
H <sub>2</sub> O	11		65°C for 5 min
PolyA RNA	1		
dNTPs	1	10 mM	
Oligo dT	1		
SSIV buffer 5x	4		55°C for 10 min 80°C for 10 min
DTT	1	100 nM	
RNase inhibitor	1		
Reverse transcriptase	1		

**Table 2.2.15: PCR mixture for full-length MaIL1 amplification**

Component	Amount (µl)
5x HF buffer	10
Phusion Polymerase	0.5



Forward primer (OBS-1191)	0.5
Reverse primer (OBS-1182)	0.5
dNTPs 10mM	1
DMSO	1
cDNA	2
H <sub>2</sub> O	Up to 50

After the cDNA was transcribed, a PCR was performed with primers that bind to the two ends of MaIL1. The PCR mixture and the conditions are described in table 2.2.15 and 2.2.16, respectively.

**Table 2.2.16: PCR program for full-length MaIL1 amplification**

	Cycle step	Temperature (°C)	Time
	denaturation	95	3 min
30 cycles	denaturation	95	30 sec
	annealing	54	30 sec
	extension	72	1.5 min
	final extension	72	3 min

## 2.2.6 Lentiviral Transduction

### 2.2.6.1 Lentiviral production- small scale

To transduce cells lines in order to overexpress a specific gene (LINC00211 and MaIL1) lentiviral particles were produced in a small scale. For this purpose, HEK-293T cells were cultured as described in section 2.2.1.3. One day prior to transfection, the cells were counted and  $5 \times 10^5$  cells/well were plated in a 6 well plate. The next day the confluency of the cells was checked under microscope. If the cell confluency was between 70-85% then the cells were used for transfection. The amount of the plasmids used is described in the table below (Table 2.2.17).

**Table 2.2.17: Lentiviral production plasmids for small scale protocol**

Plasmid	Amount (µg)
pCMV-VSVG	1.5
Pspax2	3
SparQ with gene of interest	5

For the transfection, 7  $\mu$ l of Lipofectamine 2000 were added into 100  $\mu$ l of OPTIMEM medium and the plasmids were added into another tube with 100  $\mu$ l of OPTIMEM. The two tubes were mixed and incubated for 15 min at room temperature and then added drop-wise on top of the cells. On the next day, if the transfection was successful the cells were expressing the Green Fluorescence Protein (GFP). The supernatant of the cells was then removed and filtered through a 0.45  $\mu$ M filter and placed on top of  $2.5 \times 10^5$  THP-1 cells. The HEK-293T cells were supplemented with 2 ml of fresh medium. The THP-1 cells were then centrifuged for 10 min and plated into a 6-well plate. The next day the cells were checked under the microscope. The presence of GFP positive cell was an indicator of a successful transduction. If there were no or few GFP positive cells then the procedure was repeated with the 48 hours virus. Depending on the plasmid (or the cell line) the cells started to express GFP at different time-points or different levels. The GFP positive cells were then sorted by fluorescent activated cell sorting (FACS).

### 2.2.6.2 Lentiviral production- large scale

For primary cells or cell lines that are difficult to transduce, large-scale lentiviral production was performed. For this purpose,  $10^7$  cells were plated into a T175 flask and the confluency was checked the next day. If the cell confluency was between 70-85% then the cells were used for transfection. For the transfection, 50  $\mu$ l of Lipofectamine 2000 were added into 450  $\mu$ l of OPTIMEM media and the plasmids were added into a separate tube with another 450  $\mu$ l of OPTIMEM (Table 2.2.18).

**Table 2.2.18: Lentiviral production plasmids for large scale protocol**

Plasmid	Amount ( $\mu$ g)
pCMV-VSVG	7
psPAX2	20
SparQ with gene of interest	15

The content of the two tubes was mixed together and incubated for 15 min at room temperature and then added on top of the cells, drop-wise. On the next day, if the transfection was successful the cells were expressing GFP. The supernatant of the cells was then removed and filtered through a 0.45  $\mu$ M filter and placed into tubes for ultracentrifugation. The supernatants were centrifuged either for 3 hours or for overnight at 25000 rpm at 4°C. The pellet was then resuspended in 200  $\mu$ l of PBS and the viral particles were then flash frozen and stored at -80°C.

This was repeated also at 48 and 72 hours post transfection. For primary human macrophages, on day 4 of differentiation, the medium was removed and 100  $\mu$ l of the viral particles were added on the top. The cells were then centrifuged at 2200 rpm for 10 min. After 10 min 2 ml of medium (for a 6 well plated) were added on top of the cells. Normally, after few hours the cells were expressing GFP. On Day 6, the GFP positive cells were FACS sorted. For transduction of cell lines, the same protocol was used.

### 2.2.7 Genome editing by CRISPR/Cas9

In order to create lncRNA knock out THP1 cell lines, the CRISPR/Cas9 genome editing method was used (Ran et al., 2013). The method adapted to specifically target lncRNAs, because a point mutation may not alter the expression or the function of lncRNAs. To knock out lncRNA genes, the PX458 vector (Addgene) was modified in order to express two guide RNAs (gRNAs) targeting two distinct positions in proximity to the lncRNA promoter (Figure 2.2.3) (Janga et al., 2018). This way a fragment around the transcriptional start site was removed from the genomic sequence.

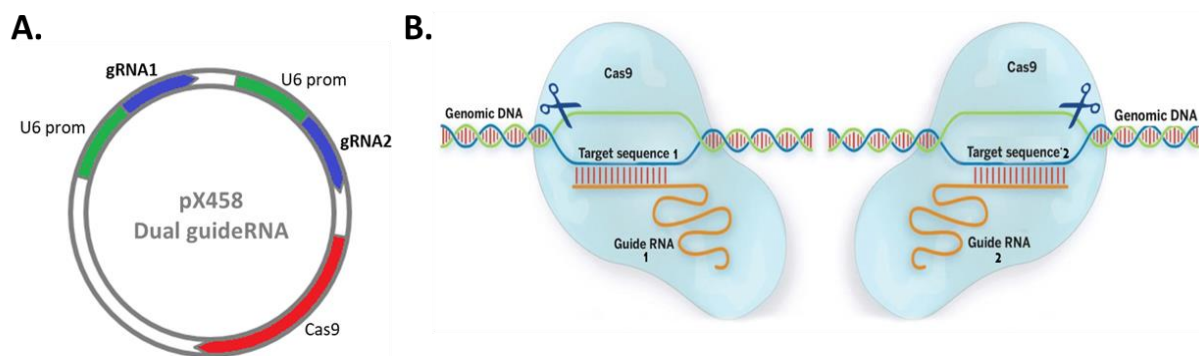


**Figure 2.2.2: CRISPR/Cas9 strategy to target lncRNA genes.** **A.** Simplified scheme of the modified plasmid used for the knock out strategy (Janga et al., 2018). The two gRNAs were transcribed from independent U6 promoters. **B.** Schematic representation of the dual gRNA mode of action. The two gRNAs were targeting two distinct regions on the genomic sequence of the lncRNA locus. The Cas9 enzyme was thereby able to cut out the desired sequence around the transcriptional start site. DNA ends are joined again by non-homologous end joining (NHEJ) repair (modified from: <https://www.manlitphil.ac.uk/events/molecular-surgery-crispr-cas9> ).

Sequence blocks containing the guide RNA pairs separated by a U6 promoter were ordered from IDT, with Bbs1 digestion sites at the two ends. For both the LINC00211 and the MaLL1 locus, two independent guide RNA pairs were designed, to rule out off-target effects. The gRNA pairs are listed below.

**Guide RNAs for LINC00211:**1<sup>st</sup> pair: CTCTGGACTCATGAGAACGC

TTACATGAATAGACAGCTAG

2<sup>nd</sup> pair: ACACGGTTCACCTCAATGAGT

GAGAGTTATAACATAATGGT

Sequence of the dual gRNA cloning cassette (yellow sequence) with the U6 promoter and the Bbs1 digestion sites (bold sequence):

GATCGAG**AAGAC**CTCACCG**CTCTGGACTCATGAGAACGC**gttttagagctaGAAAtagcaag  
 taaaataaggctagtcggtatcaactgaaaaagtggcaccgagtcggtgcTTTTTACTGATAGACTGGATCT  
GTTAGAATGAGCCTAGAGGGCCTATTTCCCATGATTCCTTCATATTTGCATATACG  
ATACAAGGCTGTTAGAGAGATAATTGGAATTAATTTGACTGTAAACACAAAGATA  
TTAGTACAAAATACGTGACGTAGAAAGTAATAATTTCTTGGGTAGTTTGCAGTTT  
TAAATTATGTTTTAAAATGGACTATCATATGCTTACCGTAACTTGAAAGTATTC  
GATTTCTTGGCTTTATATATCTTGTGGAAAGGACGAAACACCG**TTACATGAATAG**  
**ACAGCTAG**GTTTGGG**TCTTC**GATAGG

**Guide RNAs for MaLL1:**

1st pair: TTCTTGTGTAACCTTACGACA

GTGCAGTGGCCAATCATTAG

2nd pair: ATGAAACAACAAGAGTCATT

GGAAGTGAACATATGTGCAG

GATCGAG**AAGAC**CTCACCG**TTCTTGTGTAACCTTACGACA**gttttagagctaGAAAtagcaagt  
 taaaataaggctagtcggtatcaactgaaaaagtggcaccgagtcggtgcTTTTTACTGATAGACTGGATCTG  
TTAGAATGAGCCTAGAGGGCCTATTTCCCATGATTCCTTCATATTTGCATATACGA  
TACAAGGCTGTTAGAGAGATAATTGGAATTAATTTGACTGTAAACACAAAGATAT  
TAGTACAAAATACGTGACGTAGAAAGTAATAATTTCTTGGGTAGTTTGCAGTTT  
AAAATTATGTTTTAAAATGGACTATCATATGCTTACCGTAACTTGAAAGTATTTTCG  
ATTTCTTGGCTTTATATATCTTGTGGAAAGGACGAAACACCG**GTGCAGTGGCCAA**  
**TCATTAG**GTTTGGG**TCTTC**GATAGG

The guide RNA cassette was first cloned into a TOPO vector (Strataclone UA PCR cloning kit, Agilent), according to the manufacturer's instructions, and then amplified. The TOPO and the pX458 vector were then digested with Bbs1 (Thermo Fisher #ER1011) restriction enzyme (Table 2.2.19).

**Table 2.2.19: Restriction digestion reaction**

Compound	Amount
pX458 vector	5 µg
Insert (TOPO vector)	5 µg
10x FD Buffer (NEB)	3 µl
Bbs1	1 µl
H2O	Up to 30 µl

The reactions were then incubated for 2 hours or overnight at 37°C. After the digestion, the reactions were run on a 1% agarose gel and bands were purified, by gel extraction. The appropriate amounts of the insert (500 ng) and pX458 vector (25 ng) were then ligated (Table 2.2.20)

**Table 2.2.20: Ligation reaction**

Compound	Amount
PX458	25 ng
Insert	500 ng
10x T4 Ligase Buffer	2 µl
T4 Ligase	1 µl
H2O	Up to 20 µl

The mixture was incubated for 10 min at room temperature and then transformed into competent *E. coli* bacteria (custom-made). For the transformation, 5 µl of the ligation mixture and 50 µl of the competent cells were mixed and incubated on ice for 30 min. Afterwards the cells were heat-shocked at 42°C for 45 sec, followed by addition of 100 of LB medium and incubation for 30 min at 37°C. The mixture was plated on Agar plates with ampicillin and incubated overnight at 37°C. After the bacteria were amplified, the plasmids were isolated using the Macherey-Nagel plasmid isolation kit according to manufacturer's protocol. The successful insertion was tested by Sanger sequencing. Transfection of the plasmid was performed by Lipofectamine 3000 (2 µl for  $5 \times 10^5$  cells and 4 µl for  $10^6$  cells), with 15 µl of P3000 Reagent in Opti-MEM (100 µl for  $5 \times 10^5$  cells and 200 µl for  $10^6$  cells) and 5 µg of pX458 plasmid. After incubation for 15 min at room temperature, the mixture was placed on the cells, which were subsequently centrifuged for 2 h at 37°C at 500 g to achieve maximal transfection efficiency. The next day the GFP positive cells were single cell sorted, by FACS (Aria III, BD), into a 96 well plate containing RPMI with 10% FCS, 1% pen strep and 1:500 Normocin. The single cells were then

grown and cell clones were tested for successful knock out by both genomic PCR and qRT-PCR. (Table 2.2.21 and Table 2.2.22). Genomic DNA isolation was performed according to the manufacturer's instructions (Nucleospin Tissue kit, Macherey-Nagel).

**Table 2.2.21: Genomic PCR reaction**

Component	Amount ( $\mu$ l)
10x Taq buffer	5
Taq polymerase	0.5
Forward primer	1
Reverse primer	1
dNTPs 10 mM	0.2
DNA template	50-100 ng
H <sub>2</sub> O	Up to 50

**Table 2.2.22: Genomic PCR conditions**

	Cycle step	Temperature ( $^{\circ}$ C)	Time
	denaturation	95	3 sec
30 cycles	denaturation	95	30 sec
	annealing	65	30 sec
	extension	68	1 min
	final extension	68	5 min

For knock down of PU.1, the dCas9-KRAB repressor system (Gilbert et al., 2013) was employed. The cloning of the gRNAs was performed by digesting pLV hU6-sgRNA hUbc-dCas9-KRAB-T2a-GFP vector with BsmBI (Thermo Fisher #ER0451). Insert strands containing cloning overhangs were melted together and ligated as described above. Upon lentiviral production, cells were transduced dCas9-KRAB vectors. After the successful transduction, the GFP<sup>+</sup> cells were sorted and successful knockdown was verified by qRT-PCR. The gRNA oligo strands used for PU.1 knock down are listed below.

PU.1\_fw\_guide\_1: CACCGTACAGGCGTGCAAAATGGAA

PU.1\_rv\_guide\_1: AAACCTCCATTTTGCACGCCTGTAC

## 2.2.8 RNA antisense purification coupled with mass spectrometry (RAP-MS)

### 2.2.8.1 Cell preparation

For identification of MaIL1 protein binding partners an adjusted protocol from McHugh et al. was used (McHugh et. al., 2015) (Figure 2.2.2). Primary human macrophages were cultured as described before in 15 cm tissue culture plates ( $2 \times 10^8$  cells per experiment). On day 8 of differentiation cells were treated with LPS for 8 h and then the medium was removed and 10 ml of PBS was added. The PBS was removed and another 10 ml of PBS was added. The plates were then UV-crosslinked at  $8000 \times 100 \mu\text{J} / \text{cm}^2$  on ice. The cells were scraped off, transferred into 50 ml falcons and centrifuged at 1200 rpm for 5 min at  $4^\circ\text{C}$ . The pellets were flash-frozed in liquid nitrogen and stored at  $-80^\circ\text{C}$ .

### 2.2.8.2 Probe preparation

The probes were 80-nucleotide long oligos that covered the MaIL1 sequence without overlap. Control probes were 80-nucleotide random sequences. To avoid off-target-hybridization, BLAST was used to remove sequences with perfect 30 base pair matches or imperfect (90% identity) 60 base pair matches within other transcripts or genomic regions. The oligos were ordered and then diluted into ultrapure water. Oligo 3' biotinylation was performed by following the oligonucleotide 3' mono-biotinylation protocol, using the NEB Terminal Transferase reagents (# M0315S) and biotin-ddUTP (Jena Bioscience). The reaction is described in the following table (Table 2.2.23).

**Table 2.2.23: Biotinylation mixture**

Name	Amount
Oligo	40 pmol
10x Terminal Transferase Buffer	5 $\mu\text{l}$
ddUTP (1mM stock)	0.5 $\mu\text{l}$
CoCl <sub>2</sub>	5 $\mu\text{l}$
Terminal Transferase	2 $\mu\text{l}$
H <sub>2</sub> O	Up to 50 $\mu\text{l}$

To determine the appropriate amount of oligos a conversion of pmol to ng was performed. The formula is:  $\text{ng}/\text{pmol} = 0.66 \times \text{bp}$ . So, for an 80 nucleotide long oligo:  $0.66 \times 80\text{bp} = 52.8 \text{ ng}/\text{pmol}$ .

For 40 pmol approximately 2 µg of oligo are needed. Because the amount for the RAP-MS protocol is 10 µg per replicate the labelling reaction was performed 5 times in parallel. The labeling mix was incubated in a PCR machine at 37°C for 1.5 hours. Then, 50 µl of H<sub>2</sub>O and 100 µl of PCI for nucleic acid isolation were added on the mixture. The samples were vortexed and centrifuged a max speed for 15 min at 15°C. To remove free nucleotides Illustra G-25 microspin columns (#27532501, GE Healthcare Life Sciences) were used. The caps of the columns were removed and the bottom closures were snapped off. Columns were then transferred to collection tubes. The columns were then centrifuged at 730 x g for 1 min at room temperature and then transferred to 1.5 ml tube and the aqueous phase from the PCI-sample mixtures were placed in the centre of the columns. The columns were centrifuged at 730 x g for 2 min at room temperature. Three volumes of 30:1 Ethanol: NaAcetate and 1 µl of GlycoBlue™ were added to the flow-through. The next steps were the same as after DNaseI digestion (see section 2.2.2.3). The amount of the probe was quantified and to check the incorporation rate the oligoes were incubated with streptavidin coated magnetic capture beads and incubated and the bound and flow-through fraction was run on an agarose gel. The higher the incorporation rate the less strong the flow-through band appeared on the gel. The incorporation rate was usually more than 90%.

### 2.2.8.3 Cell lysis

Frozen pellets with  $1.8-2 \cdot 10^8$  cells were lysed with 900 µl of Total Cell Lysis Buffer (Table 2.2.24).

**Table 2.2.24: Total Cell Lysis buffer**

Name	Concentration	Company	Ordering number
Tris-HCl pH 7.5	10 mM	Life Technologies	1567-027
LiCl	500 mM	Sigma	L7026
Dodecyl maltoside (DDM)	0.5%	Sigma	D4641
Sodium dodecyl sulfate (SDS)	0.2%	Ambion	AM9820
Sodium Deoxycholate	0.1%	Sigma	06750



After the lysis 4.6  $\mu$ l and 23  $\mu$ l of 1x proteinase inhibitor (Thermo Fisher) and RNase inhibitor (Promega), respectively, were added. The cells were incubated for 10 min on ice while they were passed through a 26-gauge needle attached to a 1 ml syringe. For further lysis the cells were sonicated for 10 sec at 5 watts. After the sonication 4.8 1X DNase salt stock (Table 2.2.25) and 20 U (15  $\mu$ l) of TurboDNase (Ambion) were added and incubated for 10 min at 37°C. The samples were returned onto ice and 19.6  $\mu$ l of 500 mM EDTA, 9.8  $\mu$ l of 500 mM EGTA and 4.9  $\mu$ l of 500 mM TCEP were added. At this step the cell lysate was split into two tubes and 490  $\mu$ l of 1.5X hybridization buffer (Table 2.2.26) was added and incubated on ice for 10 min. The mixture was centrifuged at 16.000 x g for 10 min at 4°C.

**Table 2.2.25: 200x DNase salt stock**

Name	Concentration	Company	Ordering number
MgCl <sub>2</sub>	500 mM	Life Technologies	AM9530G
CaCl <sub>2</sub>	100 mM	Sigma	21115

**Table 2.2.26: Hybridization Buffer (2X)**

Name	Concentration	Company	Ordering number
Tris-HCl pH 7.5	20 mM	Life Technologies	1567-027
LiCl	1 M	Sigma	L7026
Dodecyl maltoside (DDM)	1%	Sigma	D4641
Sodium dodecyl sulfate (SDS)	0.4%	Ambion	AM9820
Sodium Deoxycholate	0.2%	Sigma	06750
Urea	8 M		
TCEP	5 mM		
EDTA	10 mM		

#### 2.2.8.4 Pre-clearing of lysates

To remove the proteins that have no specific binding to the beads the lysate was incubated with streptavidin-coated magnetic beads. An appropriate amount of beads (200  $\mu$ l per 10<sup>8</sup> cells) was

transferred into a tube and placed on a magnet. The storage liquid was removed and the beads were washed 4 times with 1 ml 10 mM Tris-HCL pH 7.5 and 2 times with 1 ml of 1x hybridization buffer. The lysate was mixed with the beads and incubated for 30 min at 37°C with intermittent mixing at 1100 rpm on a thermomixer (30 sec shaking, 30 sec off). Afterwards the beads were magnetically separated and the lysate was transferred into a new tube. A sample of 100000 cells worth of lysate was transferred to a PCR tube (RNA input sample).

### 2.2.8.5 Hybridization, capture and protein elution

To hybridize the proteins and MaIL1 with the biotinylated probes, 10 µg of control and anti-MaIL1 probes were heated at 85°C for 3 min. The probes were mixed with the Lysate and incubated for 2 hours at 67°C with intermittent mixing at 1100 rpm on a thermomixer (30 sec shaking, 30 sec off). During the 2 hours incubation 600 µl of beads (300 µl per 10<sup>8</sup> cells) were washed as described in the section 2.2.5.3. At the end of the 2 hours incubation 100000 cells worth of lysate was transferred to PCR tube (RNA input plus probe sample). The beads were mixed with the lysate and incubated for 30 min at 67°C with intermittent mixing at 1100 rpm on a thermomixer (30 sec shaking, 30 sec off). This was followed by magnetic separation of beads and from the flow-through again 100000 cells worth of lysate was transferred to a PCR tube (RNA flow-through sample). Afterwards the beads were washed 3 times with 1x Hybridization buffer. After each wash the samples were incubated for 5 min at 67°C. A sample of beads (around 1% of the total volume) was removed and transferred into a PCR tube (RNA elution sample). At this step, the beads with the captured proteins were stored at -80°C in order to be send later for Mass Spectrometry analysis. The RNA samples collected were used for the validation of MaIL1 pull down. More specifically the RNA elution samples were magnetically separated and the buffer was removed. The beads were resuspended into 20 µl of NLS Elution buffer (Table 2.2.22) and heated for 2 min at 95°C. The supernatant was then magnetically separated and transferred into a new tube. All other RNA samples were also filled up to 20 µl with NLS Elution buffer and incubated at 55°C for 1 hour with 1mg/ml proteinase K.

**Table 2.2.27: NLS Elution Buffer**

Name	Concentration	Company	Ordering number
Tris-HCl pH 8	20 mM	Life Technologies	1567-027
EDTA	10 mM		
NLS	2%		
TCEP	2.5 mM		

After the proteinase K treatment an RNA extraction with PCI was performed (see section 2.2.2.3). After RNA isolation and DNaseI digestion qRT-PCR was performed to validate the MaIL1 pull-down by the biotinylated antisense DNA oligo pools.

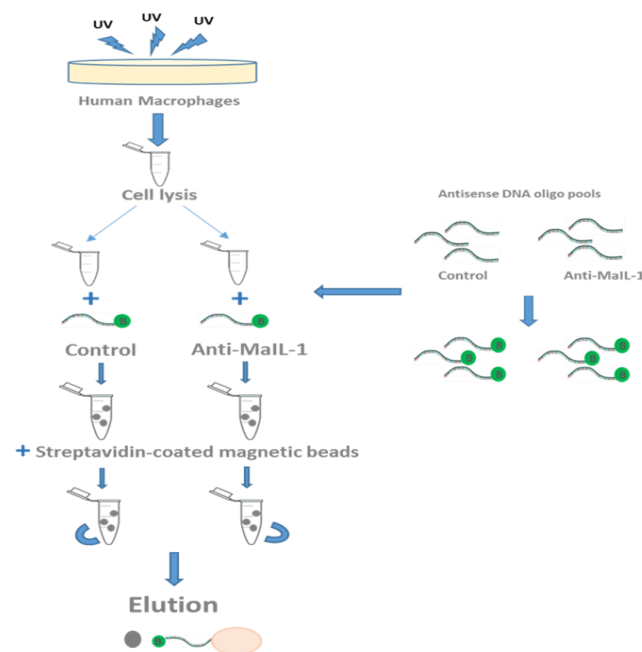


**Figure 2.2.3: Simplified scheme of the RAP-MS procedure.** UV-cross-linked primary human macrophages that were stimulated with 100 ng/ml LPS for 8 h, were lysed and incubated with biotinylated anti-sense DNA oligo pools against MaIL1 or random DNA oligo pools. Later the mixtures were further incubated with streptavidin-coated magnetic beads and separated via magnet. The MaIL1-protein complexes were eluted from the beads and the samples were sent for mass-spectrometry.

## 2.2.9 RNA Immunoprecipitation (RIP)

RNA immunoprecipitation (RIP) was used as a method to validate protein binding partners of lncRNAs after the mass spectrometry analysis of RAP-MS samples.

### 2.2.9.1 Preparation of cell lysate

The cells were cultured in 150 cm<sup>2</sup> cell culture plates, approximately 20\*10<sup>6</sup> cells/plate. After washing with PBS, the cells were UV crosslinked at 300mJ/cm<sup>2</sup> on ice. The cells were scraped off and frozen in liquid nitrogen and stored at -80 °C. On the day of the experiment the cell pellets were lysed in 1 ml of NP40 lysis buffer (Table 2.2.28), plus 1 µl of RNase inhibitor, protease inhibitor and 0.5 mM DTT. Then the mixtures were incubated on ice for 15 min. To completely lyse the cells 5 cycles of sonication with 10 sec on and 30 sec off sonication steps

were performed. In order to clear the lysate, the samples were centrifuged at 13000 x g for 15 min at 4°C.

**Table 2.2.28: NP40 lysis buffer (pH 7.5)**

Name	Concentration
HEPES pH 7.5	50 mM
KCL	150 mM
EDTA	2 mM
NaF	1 mM
IGEPAL®	0.5%

### 2.2.9.2 Preparation of Magnetic Beads

For RIP 60 µl of Dynabeads were used (Dynabeads coated with Protein G from Invitrogen for antibodies produced in mouse or goat and Dynabeads coated with Protein A for rabbit antibodies were used). The beads were washed 2 times with 1 ml of citrate-phosphate buffer (Table 2.2.29) using the magnetic separator and resuspended in 120 µl of citrate-phosphate buffer. The appropriate amount of antibody (2.5-10 µg) was added to the beads followed by 60 min incubation with shaking at room temperature. To remove the unbound antibody the beads were washed again 2 times with 1 ml of citrate-phosphate buffer. Finally, the beads were resuspended in 120 µl of lysis buffer.

**Table 2.2.29: Citrate-phosphate buffer**

Name	Concentration
Citric acid	4.7 g/L
Na <sub>2</sub> HPO <sub>4</sub>	9.2 g/L

### 2.2.9.3 Immunoprecipitation

Before the immunoprecipitation 60 µl for protein analysis and 60 µl for RNA extraction were kept aside from the total cell lysate. The clear lysate of the cells was resuspended with 2 ml of NP40 lysis buffer and the beads, and incubated for 4 hours at 4°C while rotating. After the incubation the lysate was removed and kept and the beads were washed with 3 ml of IP wash buffer (Table 2.2.30) for 15 min while rotating.

**Table 2.2.30: IP wash buffer**

Name	Concentration
HEPES-KOH pH 7.5	50 mM
KCL	300 mM
NP40	0.05%
DTT	0.5 mM
Protease Inhibitors	0.5%

After the wash the beads were diluted in 300  $\mu$ l of IP wash buffer and from this dilution 50  $\mu$ l were kept aside for protein analysis. From the rest of the beads, the IP wash buffer was removed and replaced with 250  $\mu$ l of RIP elution buffer (Table 2.2.31) containing 1  $\mu$ l of RNAse inhibitor and 2.5  $\mu$ l of 20 mg/ml Proteinase K. The mixture was incubated for 40 min at 60°C. Finally, 250  $\mu$ l of PCI were added and RNA extraction was performed.

**Table 2.2.31: RIP elution buffer**

Name	Concentration
Tris-HCl pH 8	100 mM
EDTA	10 mM
SDS	1%

## 2.2.10 Glycerol Gradient

For analysis of co-sedimentation of proteins and RNA molecules a 10%-60% glycerol gradient centrifugation was performed. The original method was described first by Dignam et al. in 1983. In this study it was performed with some modifications. To prepare the glycerol gradient a buffer was prepared according to the table 2.2.32.

**Table 2.2.32: Glycerol Lysis buffer solution**

Solution	Concentration
Tris pH 8	10mM
NaCl	150mM
KCl	10mM
MgCl <sub>2</sub>	1.5mM
Triton	0.5%

EDTA	0.5mM
DTT	1mM

The different glycerol concentrations were prepared according to the Table 2.2.33 from a buffered stock solution of 60% glycerol.

**Table 2.2.33: Glycerol gradient preparation**

<b>Final concentration</b>	<b>60 % Glycerol buffer (µl)</b>	<b>Buffer (µl)</b>
<b>55%</b>	4.58	0.42
<b>50%</b>	4.17	0.83
<b>45%</b>	3.75	1.25
<b>40%</b>	3.33	1.67
<b>35%</b>	2.92	2.08
<b>30%</b>	2.50	2.50
<b>25%</b>	2.08	2.92
<b>20%</b>	1.67	3.33
<b>15%</b>	1.25	3.75
<b>10%</b>	0.83	4.17

The different gradient solutions were layered into an ultracentrifuge tube with a cup. To this end, the tube was placed inside an ethanol / dry-ice slurry and 3.6 ml of the different glycerol solutions were added in decreasing concentration. Each concentration was added after the previous was frozen. The tubes were stored at -80°C and transferred at 4°C the day prior the experiment, to allow the formation of a continuous gradient. For the experiment, 10<sup>8</sup> BDMs were harvested and washed once with PBS. The cell pellet was then lysed in lysis buffer (Table 2.2.32) and incubated on ice for 10 min. During this incubation the lysate was passed through a 26 Gauge needle 5 times and the nuclei were broken by Dounce homogenizer with 8-10 strokes. Next, 2 µl of RNase inhibitor was added and samples were centrifuged briefly to remove the cellular debris. The supernatants were carefully layered onto the glycerol gradients, which were centrifuged at 50.200 x g (Sorvall S-34 rotor), acceleration 1, brakes off, for 20 hours at 4°C. After the centrifugation, 900 µl fractions were transferred into 2 ml tubes. From this 900 µl, 100 µl were kept for SDS-Page and silver staining. The rest was used for protein and RNA isolation via PCI. The RNA was extracted from the aqueous phase as described before. The protein (lower phase) was diluted with 800 µl of H<sub>2</sub>O, to remove the glycerol and allow the protein to precipitate. The sample was then centrifuged for 30 min at 15 °C and 17000 x g and

the aqueous phase was discarded. To the lower phase, 1.2 ml ice cold acetone were added and incubated, overnight at -20°C. The next day, the samples were centrifuged for 30 min at 17000 x g at 4°C. The pellets were dried and resuspended in 0.5-1 ml mass-spec grade 8 M urea. RNA samples were then sent for RNA sequencing and the protein samples for Mass Spectrometry.

## **2.2.11 Protein Analysis**

### **2.2.11.1 Western blot**

To analyse the expression levels of several proteins the Western blot method was used. For this purpose, cells were washed with PBS and lysed in RIPA buffer (without SDS). Lysed cells were centrifuged at maximum speed for 15 min at 4°C to remove cell debris. Protein concentration was measured by bicinchoninic acid assay (BCA assay) using the Pierce™ BCA Protein Assay Kit. Samples were diluted 1:10 and all steps were performed according to manufacturer's protocol. Optical density was measured at the Tecan Infinite M200 PRO plate reader (Thermo Fisher) at a wavelength of 595 nm, and protein concentration was calculated. Samples were prepared by adding 5X Laemmli-buffer and denatured for 5 min at 95°C. For protein separation, 10% SDS gels were used, and 20 to 30 µg of protein were loaded. A marker was included as a size reference. To run the proteins through the stacking gel, 80 V was applied, which then was increased to 120 V to run the proteins through the separation gel. Proteins were transferred to a nitrocellulose membrane by wet blot transfer for 1 h at 90 V. Afterwards, the membrane was blocked for 1 h at room temperature with 10% milk-powder and 3% Bovine serum albumin (BSA) in TBS-T solution. Primary antibody was added at a 1:1,000 dilution in TBS-T and incubated overnight at 4°C under rotation. Unbound protein was removed by several washing steps in TBS-T. HRP-conjugated secondary antibody was then added for 1 h at room temperature under rotation. After removal of excess antibody by washing, protein signal was detected on the Bioluminescence and Chemoluminescence Imager (INTAS). When required, quantification of signal was performed by densitometric analysis, using the LabImage 1D software (Kapelan Bio-Imaging GmbH).

### **2.2.11.2 Enzyme Linked Immunosorbent Assay (ELISA)**

For analysing proteins that are secreted into the supernatant of cells, enzyme-linked immunosorbent assay (ELISA) was used (Engvall and Perlmann, 1971). ELISAs were performed to determine secreted IFNA protein in supernatants of control and *L. pneumophila* infected samples with or without MaIL1 knock-down. Supernatants were used undiluted

because the secretion levels of IFN $\alpha$  proteins are relatively low. The plates were coated with 50  $\mu$ l/well 1:1000 dilution of anti-human IFN $\alpha$  antibody (PBL, Cat-no.21100-2-10, 100  $\mu$ g/ml), overnight at 4°C. The antibody was discarded and the plate was blocked with 250  $\mu$ l/well block-buffer (1x PBSdef., 0,05% Tween20, 1% BSA) for 1 h at room temperature. Logarithmic dilution series 1:1 (1 Std. 4  $\mu$ g/ml) of standard protein in block-buffer were prepared and 50  $\mu$ l/well were added (human-IFN $\alpha$ , Peprotech, cat-no.300-02A, 20  $\mu$ g/ml). 50  $\mu$ l of samples were added too and incubated for 1,5 hours at room temperature. After washing for 3 times, 50  $\mu$ l/well of detection antibody at a dilution of 1:1000 was added and incubated at room temperature for 1.5 hours (anti-human-IFN $\alpha$  HRP-conjugate, eBioscience, Cat-no.: BMS216MSTK). After washing three times, 50  $\mu$ l/well substrate-solution (1 OPD-tablet (20mg)(Sigma, Cat-no: P7288) in 20 ml substrate-buffer (35mM Citric acid x H<sub>2</sub>O, 67mM Na<sub>2</sub>HPO<sub>4</sub> x 2H<sub>2</sub>O in d.H<sub>2</sub>O) + 20  $\mu$ l 30% H<sub>2</sub>O<sub>2</sub> (AppliChem, A0626, 2500) were added. After colour development, the reaction was stopped by adding 25 $\mu$ /well 2M H<sub>2</sub>SO<sub>4</sub>. Plate measurements were carried out using the photometer Emax SofMaxPro5 at 650 nm wavelength and the analysis was performed according to manufacturer's instructions.

### **2.2.11.3 Quantification of expression levels by flow cytometry**

To measure the expression levels of receptors on the surface of cells flow cytometry was used. The stainings were performed in 50  $\mu$ l of PBS containing 0.1% FCS for 1 h on ice in the dark. The antibodies that were used are indicated in the respective experiment. After the staining, the cells were washed with PBS, resuspended in 400  $\mu$ l of PBS and measured on the Guava® easyCyte flow cytometer (Merck Millipore). The data were analysed using FlowJo v. 7.6.5.

### **2.2.12 Transfection of BDMs with siRNAs**

On day 7 of differentiation, primary human macrophages were transfected with siRNAs against MaIL1 or with control siRNA (see Table 2.1.8). The siRNAs were designed using a web tool (Naito et al., 2004). Transfection was performed using Lipofectamine 2000 (2  $\mu$ l for 5\*10<sup>5</sup> cells and 4  $\mu$ l for 10<sup>6</sup> cells) in Opti-MEM (100  $\mu$ l for 5\*10<sup>5</sup> cells and 200  $\mu$ l for 10<sup>6</sup> cells) and 50-200 nM siRNA again in Opti-MEM (100  $\mu$ l for 5\*10<sup>5</sup> cells and 200  $\mu$ l for 10<sup>6</sup> cells). The two mixtures were added together and incubated for 15 min at room temperature and added to the cells. Afterwards, cells were centrifuged for 2 h at 37°C for 2,000 rpm to achieve maximal transfection efficiency. Knockdowns mediated by the siRNAs were validated by qRT-PCR.



## 2.2.13 Stimulation of BDMs

### 2.2.13.1 Treatments with pro-inflammatory stimuli

For stimulation of human macrophages, several compounds were used. Lipopolysaccharide (LPS) (Sigma, # L6143-1MG) was used at concentrations of 1, 10, 100 and 1000 ng/ml and the simulations were performed for different time-points depending on the experiment. Poly I:C (Invivogen, # tlr1-pic) was used at a concentration of 20 µg/ml for different time-points depending on the experiments). IFN $\gamma$  (Peprotech #300-02, 20µg) was used at a concentration of 100 ng/ml for 8 and 16 hours. Stimulations with Pam3csK4 (Invivogen, #tlrl-pms, 100 ng/ml), M-TriDAP (Invivogen, #tlrl-mtd, 1 µg/ml) and Resiquimod (Invivogen, # tlr1-r848, 1 µg/ml) were performed for 8 h. All reagents were resuspended according to the manufacturer's instructions.

### 2.2.13.2 Treatments with inhibitors

Different inhibitors were used to investigate the pathway dependency of MaIL1. For NF-kB inhibition, NF-kB activation inhibitor was used (NF-AI, 6-Amino-4-(4-phenoxyphenylethylamino)quinazoline, Calbiochem #481406) at concentrations of 10 nM or 50 µM. For the inhibition of MEK1/2 and p38, U0126 and SB 203580 were used respectively. Both inhibitors were purchased from Calbiochem MerckMillipore (#66205 and #559389) and were used at concentrations of 10 µM or 50 µM. For TBK1 inhibition, Amlexanox was used at a concentration of 10 or 50 µM (Abcam #ab142825).

## 2.2.14 Infection of BDMs with *Legionella pneumophila*

Primary human macrophages were infected with *Legionella pneumophila*. Three days prior to infection, GFP positive *Legionella pneumophila* were plated onto a charcoal agar plate and incubated at 37°C. On the day of infection, bacteria were scraped from the prepared plate and resuspended in PBS (1:1) to an OD=0.5 which equals  $2 \times 10^9$  bacteria or colony forming units (CFUs) per ml. The ratio of bacteria to cells is defined as the multiplicity of infection (MOI). From the OD=1 suspension a dilution 1 to 10 was prepared and then 2.5 ml of this dilution were added into 7.5 ml of RPMI to achieve an MOI of 10, to infect  $5 \times 10^5$  cells. From this dilution 100 µl were used to reach an MOI=10. For MOI 1, this solution was further diluted 1 to 10. From this dilution 10 µl were used to infect the cells to achieve an MOI of 0.1. For determination of the exact MOI, 50 µl of the  $10^{-4}$  and  $10^{-5}$  dilutions from the infection solution were streaked on BCYE agar plates and incubated for 3 days at 37°C. After incubation, colony forming units

(CFUs) were counted and the precise MOI was calculated (CFU/ml = counted colonies x dilution factor).

### **2.2.15 Determination of infection efficiency by flow cytometry**

In order to identify infection efficiencies of human macrophages incubated with *Legionella pneumophila*, flow cytometry was used. Primary human macrophages were infected with a GFP-expressing strain of *Legionella pneumophila* at MOI 0.1 according to section 2.2.14. After 24 hours of infection, cells were washed once with PBS and scraped off and transferred to a tube. Subsequently, cells were centrifuged for 5 min at room temperature at 300 x g. The pellet was resuspended in PBS with 0.1% FCS and cells were measured on a Guava® easyCyte flow cytometer (Merck Millipore). The data were analysed using FlowJo v. 7.6.5.

### **2.2.16 MTT assay**

To assess cell proliferation of LINC00211 knock out and overexpression cells MTT assays were performed. To this end, cells were cultured in 96 wells in triplicates. Because the THP1 cells are non-adherent, and this can be a problem for the measurement, two hours prior to the measurement 20 nM of PMA were added on top of the cells. After the two hours 10 µl MTT solution was added into the wells. The cells were incubated for 3 hours and then the medium was removed and replaced with 200 µl of 1:1 DMSO: Ethanol. After 15 min, the absorbance was measured at 570 nm on the Tecan Infinite M200 PRO plate reader (Thermo Fisher).

### **2.2.17 RNA sequencing**

High quality RNA, isolated by mirVana™ miRNA isolation kit (total RNA isolation procedure), was sent to the in-house transcriptomics core facility of the medical faculty of the Philipps-University Marburg for generation of Illumina stranded mRNA libraries or to Vertis Biotech (Freising, Germany) for total RNA library generation. Barcoded libraries were generated using the TruSeq Stranded mRNA Kit (Illumina) or Vertis Biotech in-house kits. Libraries were sequenced (single-ends) on a HiSeq1500 machine in rapid mode with 50 bp read-length or a NextSeq500 device with 75 bp read-length. Prof. Dr. Leon Schulte performed the RNA sequencing data analysis. Briefly, demultiplexed reads (fastq-files) were imported into the CLC genomics workbench (Qiagen), and following TruSeq adapter- and quality-trimming mapped to the GRCh38 human reference genome annotation with standard settings (mismatch cost = 2; insertion cost = 3; deletion cost = 3; length fraction = 0.8; similarity fraction = 0.8). Differential gene expression analysis was done using DeSeq2, based on uniquely mapped reads.

Cluster (Eisen lab) was used for Hierarchical clustering and JAVA TreeView for generating the Heatmaps. To analyse the subcellular localization data, a correction was applied to the RPKM values taking into account the different RNA content of nucleus and cytosol. The percentage of Gapdh mRNA subcellular distribution was determined by qRT-PCR and applied to the following equation in order to calculate the correction factor (CF), which was then applied to all cytosolic RPKMs.

$$CF_{RPKM_{cytosol}} = \frac{\left( \frac{RPKM_{nucleus} \times \%_{cytosol}}{1 - \%_{cytosol}} \right)}{RPKM_{cytosol}} = \frac{\left( \frac{715.03 \times 0.8876}{1 - 0.8876} \right)}{625.46} = \underline{9.02}$$

The percent subcellular distribution was calculated by division of the corrected cytosolic RPKM and the sum of corrected cytosolic and the nuclear RPKM of a given gene. The results were validated by qRT-PCR. For the analysis of the RNA profiles of different human tissues the Human BodyMap 2.0 data sets were used (<http://www.ensembl.info/2011/05/24/human-bodymap-2-0-data-from-illumina/>). The RNA sequencing data of different leucocyte populations were obtained from the NCBI GEO source (GEO series GSE62408 and GSE60424). These data were obtained as fastq-files and treated as described above.

## 2.2.18 Proteomics

Prof. Dr. Linne Uwe and his research group performed Proteomics analysis. Samples bound to (magnetic) beads were washed three times with 100 µl 0.1 M ammoniumbicarbonate solution. They were digested "on-bead" by the addition of Sequencing Grade Modified Trypsin (Serva) and incubated at 37 °C for 45 min. Subsequently, the supernatant was transferred to fresh tubes. Peptides were desalted and concentrated using Chromabond C18WP spin columns (Macherey-Nagel, Part No. 730522). Finally, Peptides were dissolved in 25 µl of water with 5% acetonitrile and 0.1% formic acid. The mass spectrometric analysis of the samples was performed using an Orbitrap Velos Pro mass spectrometer (ThermoScientific). An Ultimate nanoRSLC-HPLC system (Dionex), equipped with a custom end-fritted 50cm x 75µm C18 RP column filled with 2.4 µm beads (Dr. Maisch GmbH) was connected online to the mass spectrometer through a Proxeon nanospray source. 1-15 µl (depending on peptide concentration and sample complexity) of the tryptic digest were injected onto a 300µm ID x 1cm C18 PepMap pre-concentration column (Thermo Scientific). Automated trapping and desalting of the sample was performed at a flowrate of 6 µl / min using water / 0.05% formic acid as solvent. Separation of the tryptic peptides was achieved with the following gradient of water / 0.05% formic acid

(solvent A) and 80% acetonitrile / 0.045% formic acid (solvent B) at a flow rate of 300 nl / min: holding 4% B for five min, followed by a linear gradient to 45% B within 30 min and linear increase to 95% solvent B in additional 5 min. The column was connected to a stainless steel nanoemitter (Proxeon, Denmark) and the eluent was sprayed directly towards the heated capillary of the mass spectrometer using a potential of 2300 V. A survey scan with a resolution of 60000 within the Orbitrap mass analyzer was combined with at least three data-dependent MS/MS scans with dynamic exclusion for 30 s either using CID with the linear ion-trap or using HCD combined with orbitrap detection at a resolution of 7500. Data analysis was performed using Proteome Discoverer 2.2 (Thermo Scientific) with SEQUEST search engine. Uniprot databases were used. For gradient samples, abundance values were normalized to the relative protein content in each fraction (determined using the BCA-method and silver-gel quantification).

### **2.1.19 Conservation analysis**

Sequence conservation was determined using NCBI BLASTN. The sequence of interest was compared to the Reference Genomic Sequence of selected species. BLASTN hits located within a genomic range of max. 100 kb were considered. All matching nucleotides were counted as 1 and all mismatches were considered as 0. The missing nucleotides from the reference sequence were also count as 0, whereas missing nucleotides from the input sequence were neglected.

### **2.2.20 Bronchoalveolar lavage (BAL) and patient selection**

Bronchoalveolar lavage fluid (BALF) samples were obtained from patients (Table 2.2.34) at the Department of Infectious Diseases and Respiratory Medicine of Charité University Hospital Berlin, through Prof. Dr. Leif E Sander. All patients underwent bronchoscopy including bronchoalveolar lavage (BAL) on clinical indication and had provided oral and written informed consent. The study was approved by the local Ethics Committee (EA2/086/16). BAL fluids from healthy donors as controls for the IPF study were obtained by means of an American Thoracic Society consensus procedure and in accordance with local ethics regulations (Marburg: 87/12). The lung fluids from resected IPF tissue (tissue provided by DZL biobank Giessen) were obtained by flushing the tissue with pre-warmed PBS. Obtained fluids were immediately stained and analysed by flow cytometry.

**Table 2.2.34: Patient information**

<b>No</b>	<b>Gender</b>	<b>Age</b>	<b>Infection</b>
1	m	53	control
2	m	49	control
3	m	38	control
4	w	71	control
5	w	49	control
6	m	62	control
7	m	28	control
8	m	29	control
9	w	27	control
10	m	64	control
11	w	25	bacterial
12	m	45	bacterial
13	w	64	bacterial
14	w	19	fungal
15	w	64	fungal
16	w	42	fungal
17	w	68	nd
18	w	59	nd
19	w	52	nd
20	w	58	nd
21	w	73	nd
22	w	61	polymicrobial

### **2.2.21 Statistical Analysis**

Statistical analysis was carried out with GraphPad Prism (Version 7). For data with multiple comparison variables One-way ANOVA (Analysis of variance) was performed followed by either Dunnett or Bonferroni comparison test. For comparison of two data columns, the unpaired t-test was used. For all tests, a Gaussian distribution was assumed, and the confidence interval was set to 95%. P-values  $\leq 0.05$  were considered as indication for significance. All performed statistical tests are specified in each figure legend.

## 3. Results

### 3.1 Results - LncRNAs in myeloid cell differentiation

#### 3.1.1 Identification of lncRNAs differentially expressed in distinct immune cell subsets

Due to limited research advances on the involvement of lncRNAs in haematopoiesis and leukocyte differentiation, a central aim of this study was to investigate cell-type specific lncRNA expression patterns in distinct leukocyte populations and investigate the functions of individual of these lncRNAs. For identification of lncRNAs that are specifically expressed in leukocytes, external high throughput RNA sequencing data from different organ systems were analysed. mRNA and lncRNA expression levels in leukocytes were compared to the expression levels in lymph nodes, adrenal, lung, adipose, prostate, ovaries, testes, breast, kidney, liver, brain, thyroid, colon, heart and skeletal muscle tissue, using publicly available Illumina Human Bodymap 2.0 data (Figure 3.1.1.A). Interestingly, leukocytes displayed a unique lncRNA and mRNA transcriptome signature. Most of these Leukocyte-expressed transcripts were also highly expressed in lymph nodes, which are rich in immune cells. Skeletal muscle tissue displayed the lowest expression of the leukocyte lncRNA and mRNA cluster. When the leukocyte specific mRNAs were analysed by KEGG (Kyoto Encyclopaedia of Genes and Genomes) pathway analysis, the results suggested that most of these genes are involved in immune related functions, such as hematopoietic lineage determination, NK cell mediated cytotoxicity, cytokine-cytokine receptor interaction, osteoclast differentiation, chemokine signalling pathway, T-cell receptor signalling pathway, platelet activation and cell adhesion. Furthermore, leukocyte specific mRNAs have been implicated in infections, like infections by tuberculosis, measles, trypanosoma cruzi (chagas disease) and influenza A (Figure 3.1.1.B). Thus, Human Bodymap 2.0 data analysis accurately detects transcripts implicated in leukocyte biology. In order to infer, which leukocyte subpopulations express the identified leukocyte marker transcripts, three replicates of independent, publically available monocyte, granulocyte, NK-, B- and T-cell high throughput RNA sequencing data (NCBI GEO series GSE62408 and GSE60424) were analysed. Principal component analysis with the RPKMs of leukocyte-specific mRNAs or lncRNAs in these cells revealed that all datasets segregated according to the underlying cell types (Figure 3.1.1.C). In line with this result, hierarchical clustering of leukocyte-specific transcript Z-scores revealed distinct clusters of mRNAs and lncRNAs,

specific to CD66+ granulocytes, CD14+ monocytes, CD19+ B-cells, CD56+ NK cells, CD4+ T-cells and CD8+ T-cells (Figure 3.1.1.D). Thus, besides mRNA markers, leukocytes express distinct clusters of lincRNAs, which may serve as novel non-coding markers of the major immune cell sub-populations.

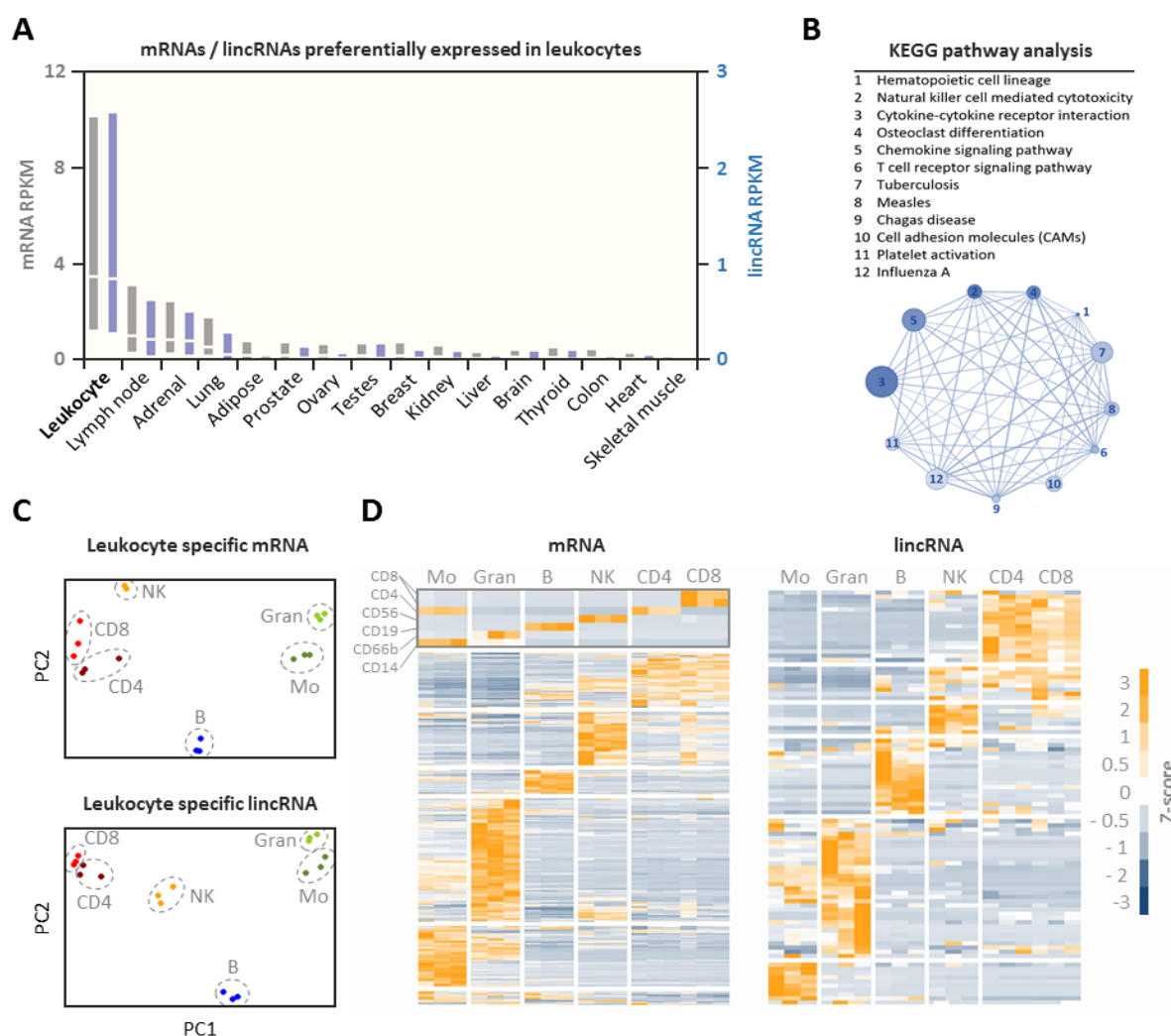


**Figure 3.1.1. Transcriptome analysis of leukocytes.** **A.** RPKM values of leukocyte specific mRNAs and lincRNAs in different tissues. **B.** KEGG pathway analysis of leukocyte specific mRNAs. **C.** PCA of the leukocyte specific mRNAs and lincRNAs expressed in granulocytes, monocytes, B-cells, NK cells, CD4+ T-cells and CD8+ T-cells. **D.** Heat maps of Z-scores of leukocyte specific mRNAs and lincRNAs in granulocytes, monocytes, B-cells, NK cells, CD4+ T-cells and CD8+ T-cells (3 highest expressed, -3 lowest expressed).

### 3.1.2 Validation of the expression levels of leukocyte specific lincRNAs

The top 10 myeloid- and lymphoid-cell specific lincRNAs were selected for further validations (Table 3.1.1). To this end, immune cell populations were enriched from buffy coats of human donors (Figure 3.1.2.A). CD4+ and CD8+ T cells were further subdivided into naïve (CD45RO-



negative) and memory (CD45RO-positive) cells. Furthermore, monocytes were differentiated into macrophages and dendritic cells, based on classical differentiation protocols with GM-CSF and IL-4.

**Table 3.1.1: Top 10 differentially expressed myeloid and lymphoid markers.** The numbers represent fold changes compared to brain tissue expression and standard deviations.

Alias	Monocytes	Granulocytes	B cells	NK cells	CD4 T cells	CD8 T cells
AC064805.1	<b>4.58</b> ± 1.19	0.23 ± 0.20	0.02 ± 0.03	0.09 ± 0.13	0.01 ± 0.01	0.00 ± 0.00
AP001257.1	<b>4.03</b> ± 1.73	0.01 ± 0.02	0.02 ± 0.04	0.02 ± 0.03	0.01 ± 0.02	0.03 ± 0.03
AP003774.3	<b>3.92</b> ± 1.83	0.06 ± 0.10	0.02 ± 0.04	0.04 ± 0.07	0.01 ± 0.01	0.01 ± 0.01
LINC02285	<b>3.69</b> ± 0.65	<b>2.11</b> ± 1.06	1.20 ± 0.44	1.62 ± 0.56	0.92 ± 0.18	1.25 ± 0.19
AC097504.2	<b>3.53</b> ± 0.45	0.00 ± 0.00	0.00 ± 0.00	0.00 ± 0.00	0.00 ± 0.00	0.00 ± 0.00
LUCAT1	2.49 ± 1.62	<b>23.97</b> ± 15.61	0.02 ± 0.01	0.03 ± 0.02	0.02 ± 0.02	0.03 ± 0.03
LINC01506	0.57 ± 0.09	<b>9.27</b> ± 2.93	0.03 ± 0.01	0.00 ± 0.00	0.00 ± 0.00	0.00 ± 0.00
AC007342.5	0.04 ± 0.05	<b>8.38</b> ± 1.80	0.01 ± 0.02	0.00 ± 0.00	1.18 ± 0.67	1.27 ± 0.66
LINC00211	0.71 ± 0.47	<b>4.63</b> ± 1.46	0.00 ± 0.00	0.04 ± 0.04	0.02 ± 0.03	0.02 ± 0.03
LINC00921	0.52 ± 0.24	<b>3.96</b> ± 1.01	0.14 ± 0.15	1.24 ± 1.30	0.33 ± 0.26	0.30 ± 0.29
AC104971.4	0.06 ± 0.11	0.00 ± 0.00	<b>7.52</b> ± 0.22	0.04 ± 0.04	0.50 ± 0.20	0.23 ± 0.20
AC009686.2	0.00 ± 0.00	0.00 ± 0.00	<b>5.18</b> ± 1.64	0.16 ± 0.28	0.16 ± 0.15	0.37 ± 0.30
AC006033.2	1.17 ± 0.11	0.10 ± 0.01	0.02 ± 0.04	<b>9.40</b> ± 1.20	0.02 ± 0.02	0.63 ± 0.22
AC093323.2	0.16 ± 0.25	0.17 ± 0.10	0.06 ± 0.04	<b>6.48</b> ± 1.97	1.35 ± 0.81	2.60 ± 1.17
LINC00861	0.21 ± 0.34	0.08 ± 0.13	0.05 ± 0.07	<b>10.34</b> ± 5.29	<b>10.49</b> ± 3.64	<b>9.21</b> ± 2.00
LINC01550	0.03 ± 0.05	0.01 ± 0.02	0.00 ± 0.00	0.02 ± 0.01	<b>2.20</b> ± 0.52	<b>1.97</b> ± 0.21
LINC02295	0.00 ± 0.00	0.00 ± 0.00	0.00 ± 0.00	0.00 ± 0.00	<b>0.81</b> ± 0.90	<b>0.46</b> ± 0.28
LINC02361	0.72 ± 0.25	0.48 ± 0.28	0.61 ± 0.43	2.30 ± 0.29	<b>9.96</b> ± 3.44	5.83 ± 1.50
LINC02273	0.03 ± 0.05	0.01 ± 0.02	0.06 ± 0.02	0.27 ± 0.05	<b>5.50</b> ± 0.67	3.01 ± 1.35
LINC02446	0.15 ± 0.26	0.02 ± 0.02	0.01 ± 0.01	0.40 ± 0.36	0.04 ± 0.05	<b>15.72</b> ± 7.31

The top 3 myeloid and lymphoid cell specific lncRNAs (Z-score shown in Figure 3.1.2.B) were selected for qRT-PCR validations (Figure 3.1.2.C). LINC00211, LUCAT1 and AC064805.1 were more highly expressed in the myeloid cell lineage and LINC02295, LINC02446, LINC00861 more in the lymphoid cell lineage. Interestingly, LINC02295 was present only in the T-cell population and low or absent from B-cells or NK-cells, which indicates that the expression is induced very late in hematopoietic development, when small lymphocytes give rise to B-cells and T-cells (see Figure 1.2). Other interesting expression patterns were observed. For example, the expression of LINC02446 seems to vanish from memory CD4<sup>+</sup> T-cells (CD4<sup>+</sup>/CD45RO<sup>+</sup> T-cells), while it is present in all the other T-cell populations, including the naïve CD4<sup>+</sup> T-cells. Furthermore, expression levels of this lincRNA seem to be higher in CD8<sup>+</sup> T-cells than in CD4<sup>+</sup> T-cells. These findings indicate that the expression of leukocyte lncRNAs is highly cell-type specific. LINC00211 had a clear myeloid-specific expression pattern, and thus was selected for further functional investigation.

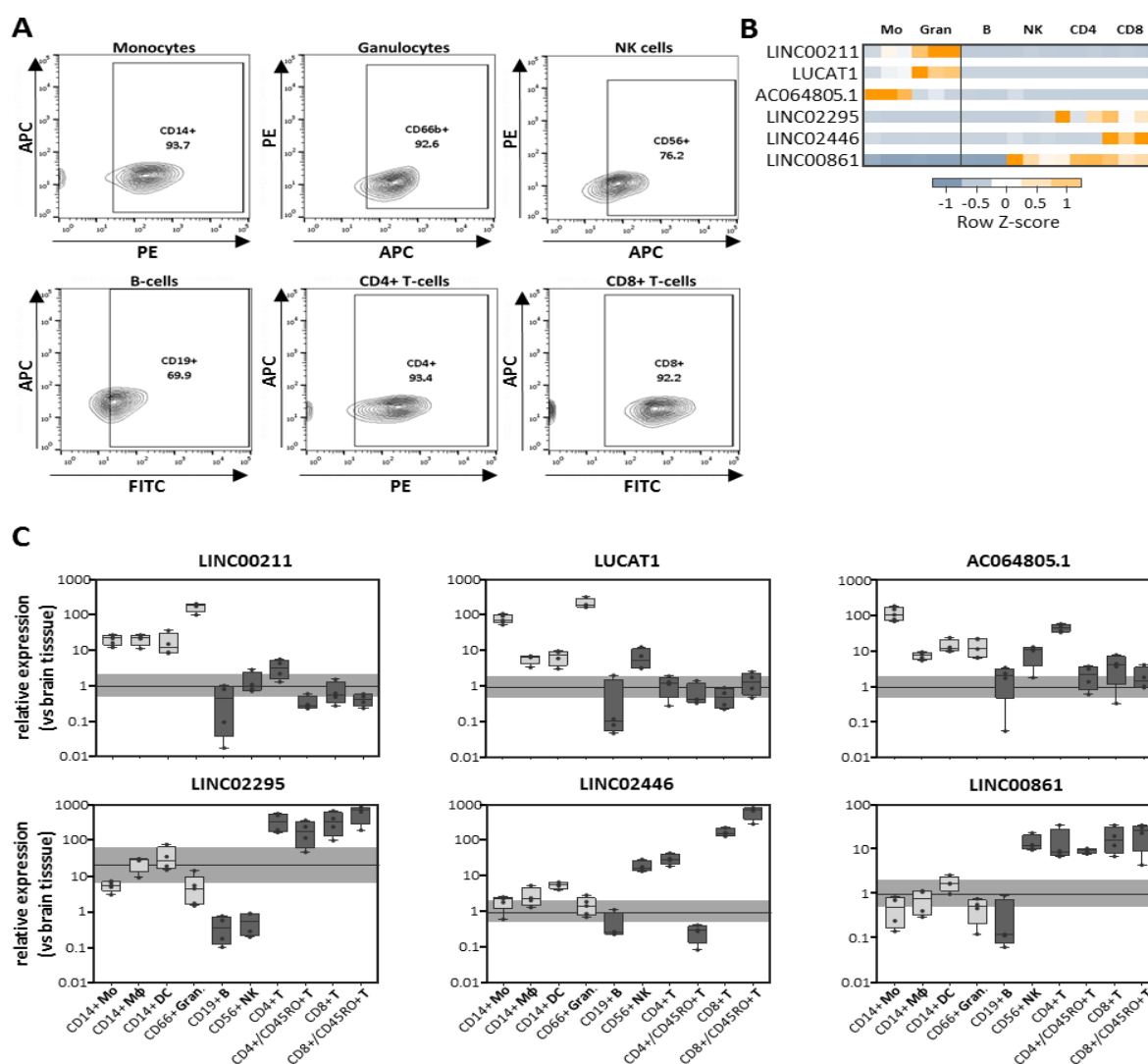


**Figure 3.1.2: Differential expression of lncRNAs in immune cells.** **A.** FACS plots of immune cell populations isolated from peripheral human blood. Anti-CD14, anti-CD66, anti-CD56, anti-CD19, anti-CD4 and anti-CD8 antibodies were used for staining of monocytes, granulocytes, NK cells, B-cells, CD4+ T-cells and CD8+ T-cells, respectively. The percentages were calculated after gating according to the unstained control for each population. **B.** Heat map of Z-scores of the top differentially expressed lncRNAs. **C.** qRT-PCR validations of the expression of the top differentially expressed lncRNAs. The expression levels were normalised to the expression levels of the lncRNAs in brain tissue.

### 3.1.3 Characterisation of LINC00211

LINC00211 is an uncharacterized intergenic lncRNA (lincRNA), located on chromosome 2. Due to the preliminary nature of present GENCODE lncRNA annotations, RACE-PCR and Sanger sequencing was performed to map the exact 5' and 3' ends and the exon structure of the transcript. The results characterized LINC00211 in BDMs as a 1879 bp long RNA with two exons, differing from the existing GENCODE prediction (1923 bp and three exons, Figure 3.1.3.A). Furthermore, using Ensembl (BLAST) evolutionary conservation LINC00211 was determined (Figure 3.1.3.B). To this end, the RACE-PCR refined human sequence was

compared against the genomes of chimpanzee, macaque, lemur, tree shrew, rabbit, mouse, dog, cow and pig. Whereas the lincRNA sequence was found to be highly conserved in primates, conservation dropped to approximately 20% in rodents. However, in other mammals, with greater evolutionary distance from primates, (cows and pigs), sequence similarity increased back to 60%-70%. These results indicate that the LINC00211 locus constitutes an ancient RNA-gene of unknown function within the mammalian lineage.

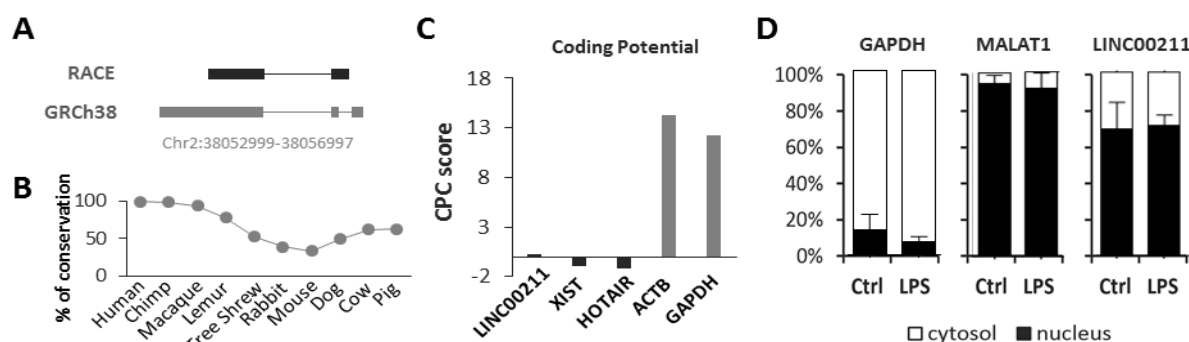


**Figure 3.1.3: Characterisation of LINC00211.** **A.** Schematic representation of full length LINC00211 structure, based on RACE results obtained from RNA of BDMs, in comparison to ENCODE annotation. **B.** Species-conservation analysis. The graph show the percentage of LINC00211 conservation in the NCBI reference genomes of indicated species compared to the human sequence (100%). **C.** Coding potential of LINC00211, as expressed by the CPC score. **D.** qRT-PCR based cellular localisation pattern of LINC00211. RNA from cytosolic and nuclear fractions of BDMs mock-treated or stimulated with LPS (100ng/ml) for 8 hours was used (n=3).

To verify the non-coding nature of the LINC00211 RNA, the coding potential was calculated using the online coding potential calculator (CPC) (<http://cpc2.cbi.pku.edu.cn/>) (Kang et al., 2017). As controls, two well-characterised lncRNAs, XIST and HOTAIR, and two known protein-coding genes, ACTB and GAPDH, were used. The CPC analysis of the RACE-PCR refined cDNA sequence revealed no relevant coding potential for LINC00211 (CPC score~+1), similar to XIST and HOTAIR (CPC scores~-1 and~-1.5 respectively), and different from ACTB and GAPDH, (CPC scores~+14 and~+12 respectively), (Figure 3.1.3.C). Next, subcellular localisation of the lncRNA was determined by cytoplasm / nucleus fractionation. Real-time PCR revealed that LINC00211 locates mostly, but not entirely to the nucleus (~70%), both in resting and LPS-activated BDMs (Figure 3.1.3.D).

### 3.1.4 Functional characterisation of LINC00211

In order to reveal its cellular function, LINC00211 loss- and gain of function experiments were performed. Due to the technically difficult manipulation of primary human myeloid cells, a monocytic cell line model, THP1, was employed. Using lentiviral transduction LINC00211 was ectopically expressed in THP1 cells (Figure 3.1.4.A) from a GFP-co-expressing backbone. The

GFP<sup>+</sup> cells were flow-sorted and qRT-PCR was used to confirm successful overexpression (OE) of the lincRNA in THP1 cells (Figure 3.1.4.B&D). As a control, cells were transduced with a lentivirus containing a scrambled transgene sequence.

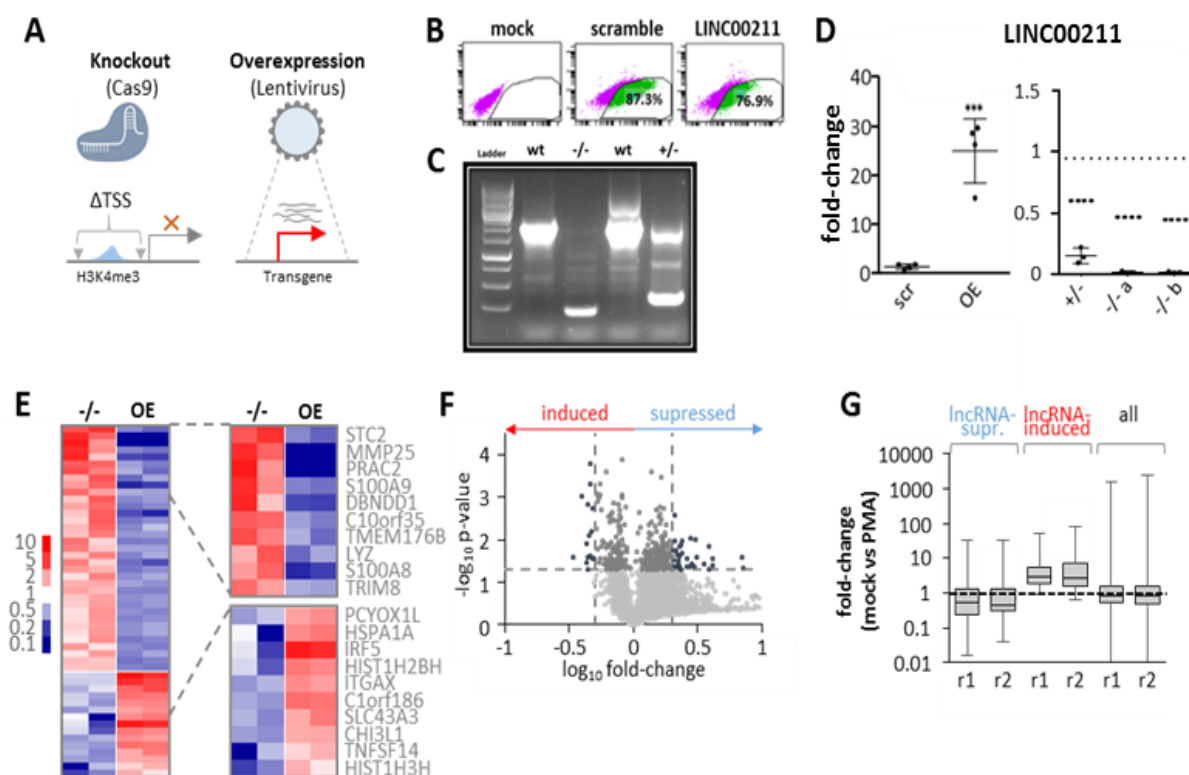


**Figure 3.1.4: LINC00211 gain and loss of function experiments.** **A.** Schematic representation of CRISPR/Cas9 knock out strategy and lentiviral overexpression strategy. **B.** Flow cytometry panels showing GFP<sup>+</sup> cell gates used for cell sorting to enrich cells transduced either with a scrambled or the LINC00211 sequence. **C.** Agarose gel analysis of genomic PCR products from the control and knock out clones generated by CRISPR/Cas9. The band at ~200bp represents the product after the deletion was introduced by CRISPR/Cas9 and the band ~2000 bp represents the wild type band. **D.** qRT-PCR analysis of the expression levels of LINC00211 in the overexpressing and knock down (+/-) and knock out (-/-) cell lines. The expression levels were compared to THP1 cells transduced with scrambled control for the overexpression cells and to the empty CRISPR/CAS9 vector (wt) transfection for the +/- and -/- cells. Black circles represent independent replicates. For statistical analysis an unpaired t-test was performed for the overexpression and a one-way ANOVA for the knock down and knock out experiments (\*\*p < 0.001, \*\*\*\*p < 0.0001). **E.** Heatmap of the RPKMs of the top differentially regulated genes upon overexpression and knock out of LINC00211. **F.** Volcano plot fold changes in association with the p-value of the differentially regulated genes. “Supressed” relates to genes elevated upon LINC00211 knockout and reduced upon LINC00211 over-expression (the latter values were transformed from down to up-regulations for this plot). Vice versa for “induced” genes. **G.** Fold changes of LINC00211-controlled genes from F) in PMA-versus mock-treated THP-1 cells, determined by RNA-Seq. Genes under negative control by LINC00211 are down-regulated upon PMA-treatment, while genes under positive control by the lincRNA are induced by PMA. No regulation trend is seen, when all RNA-Seq detected transcripts are plotted.

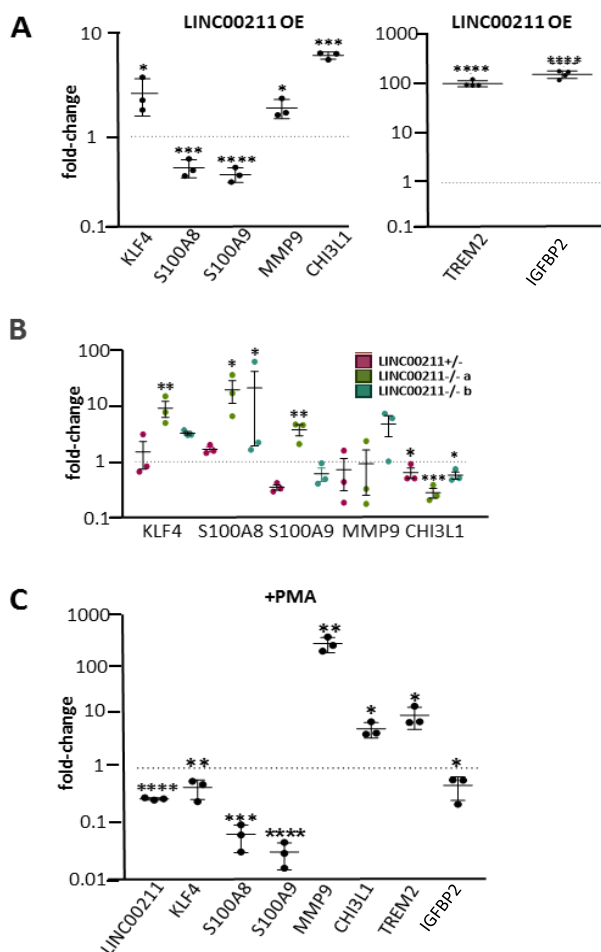


**Figure 3.1.5: Gene expression profiling. A.** Validation of differentially expressed genes upon overexpression of LINC00211 in THP1 cells by qRT-PCR. The graphs show the fold enrichment of genes compared to THP1 cells transduced with scramble control. **B.** qRT-PCR analysis of differentially expressed genes upon LINC00211 knock down (+/-) and knock out in THP1 cell lines (-/-). The expression levels were compared to cells transfected with empty CRISPR/CAS9 vector. **C.** Analysis of differentially expressed genes upon THP1 differentiation for 72 hours with PMA (20nM). The data are displayed as fold changes in comparison to undifferentiated THP1 cells. Circles represent independent replicates. For statistical analysis, one-way ANOVA was performed (\* $p \leq 0.05$ , \*\* $p \leq 0.01$ , \*\*\* $p \leq 0.001$ , \*\*\*\* $p \leq 0.0001$ ).

To generate LINC00211 loss-of-function THP1 cells, a CRISPR/Cas9 approach previously published by our group was used (Janga et al., 2018). Briefly, the pX458 CRISPR vector, expressing two gRNAs cleaving before and behind the LINC00211 transcriptional start-site (TSS) was transfected into THP1 cells. Using a first set of gRNAs a heterozygous (+/-) clone for LINC00211 TSS deletion was generated and with a second independent set of gRNAs two homozygous (-/-) clones was generated. For control, an empty pX458 vector (without gRNAs), expressing Cas9 was transfected into THP1 cells and the cells were treated the same way as the genetically modified clones (for more details see the methods section). Genomic PCR and Sanger sequencing (Figure 3.1.4.C) validated the successful TSS deletions and the clones were used for further experiments. Upon lentiviral transduction the expression levels of LINC00211 increased approximately 30-fold compared to the scramble control and in +/- and -/- TSS knockout clones expression levels sharply decreased (~10 fold less for the +/- clone and ~100 fold less for the -/- clones). RNA-Seq analysis revealed genes with altered expression levels in overexpression and knock out cells compared to the control cells. Interestingly, expression of several genes

changed into opposite directions upon LINC00211 overexpression and knock out, respectively (Figure 3.1.4.E), thus illustrating genes under positive or negative control by LINC00211 (Figure 3.1.4.F).

The specific expression of LINC00211 in myeloid cells suggests that this lincRNA plays a role in myeloid cell identity or terminal differentiation. Therefore genes were narrowed down, which are regulated during terminal differentiation by comparative RNA-Seq analysis of monocytic and PMA-differentiated macrophage-like THP1 cells. Interestingly, genes which are under negative control by the lincRNA were mostly suppressed during terminal differentiation and vice versa, genes under positive control by LINC00211 were mostly up-regulated during differentiation (Figure 3.1.4.G). This suggests that LINC00211 functions to facilitate the expression of genes involved in myeloid cell terminal differentiation. To further follow up this hypothesis, validation of the sequencing results was performed. Real-time PCR analysis revealed that in the overexpression cell line S100A8 and S100A9 were downregulated and KLF4, MMP9, CHI3L1, TREM2 and IGBP2 were upregulated as expected from the sequencing results (Figure 3.1.5.A). For the partial and full knock out cell lines only S100A8 and CHI3L1 were up and downregulated respectively as expected from the sequencing results. One of the two knock out cell lines also exhibited an upregulation of S100A9, but the result was not replicated in the partial knockout or the second full knockout cell line. The clonal nature of the knock out cells may be a possible explanation for the phenotypic differences that were observed. Next, the expression levels of the same genes were measured after PMA stimulation and differentiation of THP1 from monocytes to macrophage-like cells. Interestingly, LINC00211 was downregulated upon differentiation. S100A8, S100A9, MMP9, CHI3L1 and TREM2 showed the same pattern of expression compared to the overexpression cell line. Thus, the results validated that genes that are suppressed upon differentiation are also suppressed by the lincRNA and genes that are induced upon differentiation are induced by the lincRNA, too.

### **3.1.5 LINC00211 is involved in monocyte terminal differentiation**

Since differential gene expression results from knock out and overexpression cells indicated that LINC00211 may play role in monocyte to macrophage differentiation LINC00211 OE cells were analysed for morphological changes as well. To this end, cells were treated with PMA, stained with DAPI for nuclear visualization and analysed at the fluorescent microscope. Interestingly, LINC00211 OE cells showed a different morphology compared to control THP1 cells overexpressing a scrambled RNA, following PMA-differentiation (Figure 3.1.6.A). The OE cells appeared to be smaller, with reduced cytoplasm and no spindle-like morphology,

which is commonly observed after differentiation into macrophages. The morphological changes observed in the LINC00211 OE cells, were also inspected at the protein level. b-actin expression levels were much higher in the OE cells compared to the control cells, which suggests that cytoskeletal changes occur in these cells (Figure 3.1.6.B).

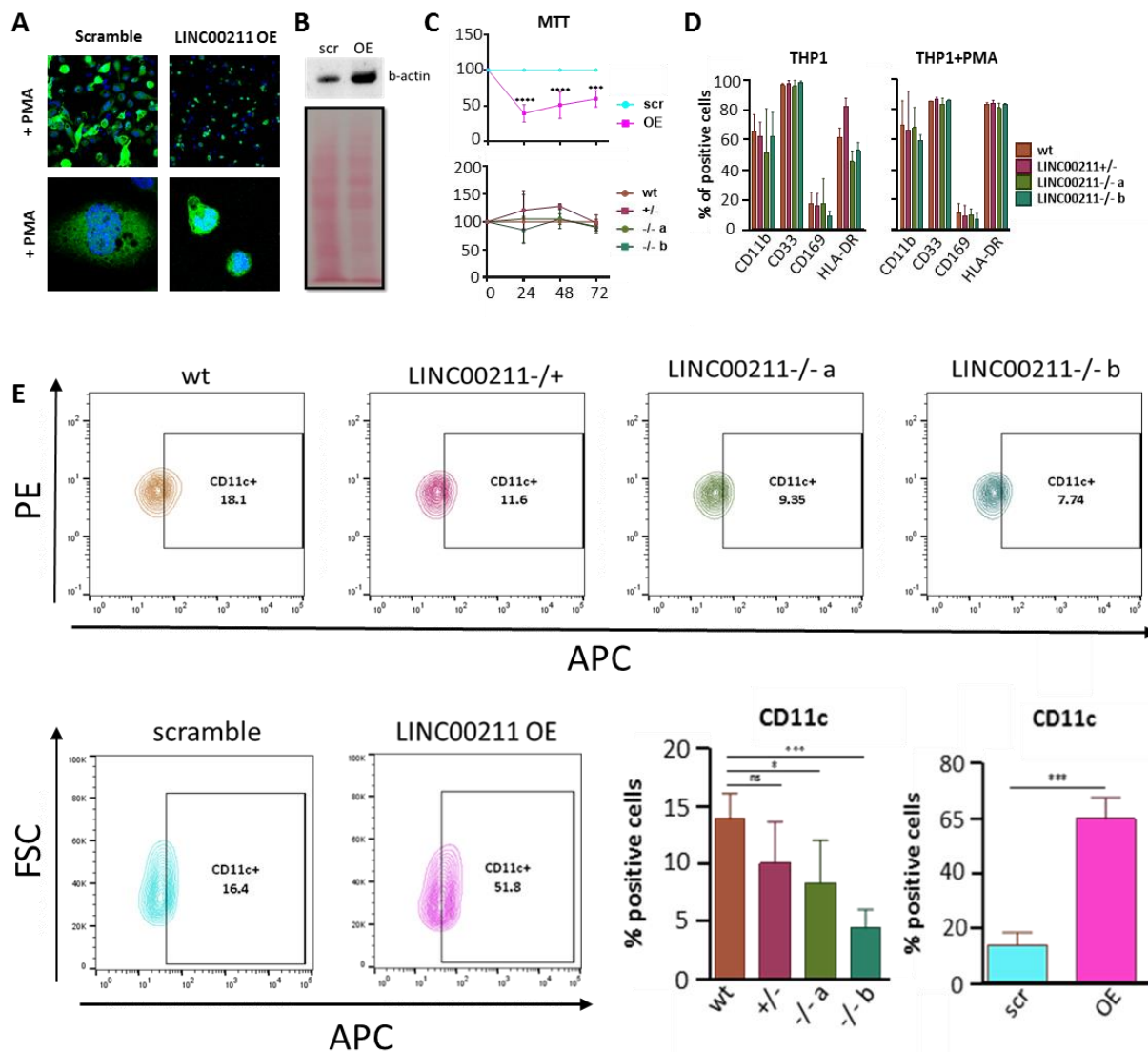


**Figure 3.1.6: LINC00211 is involved in monocyte to macrophage differentiation. A.** Fluorescent microscopy analysis of THP1 cells either overexpressing the scrambled RNA sequence or LINC00211. Prior to the analysis, the cells were differentiated with PMA (20nM) for 72 hours. **B.** Top: western blot and bottom: Ponceau staining of protein samples obtained from THP1 cells over-expressing either the scramble RNA or LINC00211. The blot was stained with anti-b-actin antibody. **C.** MTT assay of scramble, LINC00211, wt, +/-, -/- a) and -/- b) cells for 24, 48 and 72 hours. For statistical analysis two-way ANOVA was performed: \*\*\* $p \leq 0.001$ , \*\*\*\* $p \leq 0.0001$ . **D.** FACS data presented as percentage of positive cells. Different cell clones (wt, +/- and -/- a) and -/- b) were stained for CD11b, CD33, CD169 and HLA-DR both in THP1 cells and in differentiated THP1 cells (PMA for 72 hours) (n=3). **E.** FACS plots and quantification of scramble, LINC00211, wt, +/- and -/- a) and -/- b) cells stained with anti-CD11c antibody (n=3-4). One-way ANOVA and unpaired t-test were performed for the first and the second graph respectively: \* $p \leq 0.05$ , \*\*\* $p \leq 0.001$ .

Next, the proliferation rate of the OE and partial and full knock out cells was inspected using an MTT assay. The assay showed that OE cells proliferate much slower than the control cells. On the other hand, there were no significant differences in proliferation rates of knock out cells, compared to the wild type control cells (Figure 3.1.6.C). To further investigate differentiation-associated changes, LINC00211 knock out and overexpression cells were stained with a panel of fluorescent antibodies against myeloid surface markers. Because the overexpressing cells also express GFP from the lentiviral backbone, these cells could not be stained with all available antibodies. Surface expression of proteins CD11b, CD33, CD169 and HLA-DR showed no difference between the control, LINC00211 +/- and LINC00211 -/- cells (Figure 3.1.6.D). Differentiation marker CD11c was significantly reduced in undifferentiated LINC00211 knock out cells compared to control cells. On the other hand, when the LINC00211 was overexpressed the levels of CD11c were increased. Since CD11c is a known myeloid marker, increasing during terminal differentiation there is evidence for LINC00211 to be involved in the monocyte to macrophage differentiation process, by priming monocytes for this final differentiation step.

### **3.1.6 LINC00211 is regulated by the PU.1 transcription factor**

Co-expression network analysis showed that LINC00211 is co-expressed with genes that are regulated by the PU.1 transcription factor (Figure 3.1.7.A), which plays a major role in haematopoiesis and myeloid cell differentiation (McKercher et al., 1996, Scott et al., 1994, Colucci et al., 2001). To investigate the relationship between PU.1 and LINC00211, PU.1 knock down THP1 cells were generated using the dCas9-KRAB repressor system (Gilbert et al., 2013). The PU.1 knock down cells were not able to expand, in line with previous observations (Antony-Debré et al., 2017, Zhou et al., 2015). To overcome this limitation, RNA was isolated immediately after sorting of cells transduced with a PU.1 repressor lentivirus, co-expressing GFP. Importantly, besides PU.1 mRNA, expression levels of LINC00211 were significantly reduced in PU.1 knock down THP1 cells compared to control cells transduced with a control repressor virus not expressing any gRNAs (Figure 3.1.7.B). Furthermore, the expression levels of S100A9 and CHI3L1 were tested upon PU.1 knock down. Interestingly, similar to the expression trend seen upon LINC00211 overexpression (Figure 3.1.7.B), CHI3L1 was upregulated whereas S100A9 was downregulated upon PU.1 knock down. Thus, PU.1 is not only required for monocytic cell expansion but also promotes the expression of LINC00211 and S100A9, whereas it reduces CHI3L1 levels. Given the negative regulation of S100A9 and the positive control of CHI3L1 expression by LINC00211 these results suggest the following model: after induction of LINC00211, late during myeloid cell differentiation, the lincRNA acts



as a negative feedback regulator of PU.1, inhibiting proliferation (see Figure 3.1.6.C) and lifting expression of PU.1-suppressed terminal differentiation markers such as CHI3L1 (Figure 3.1.7.C).

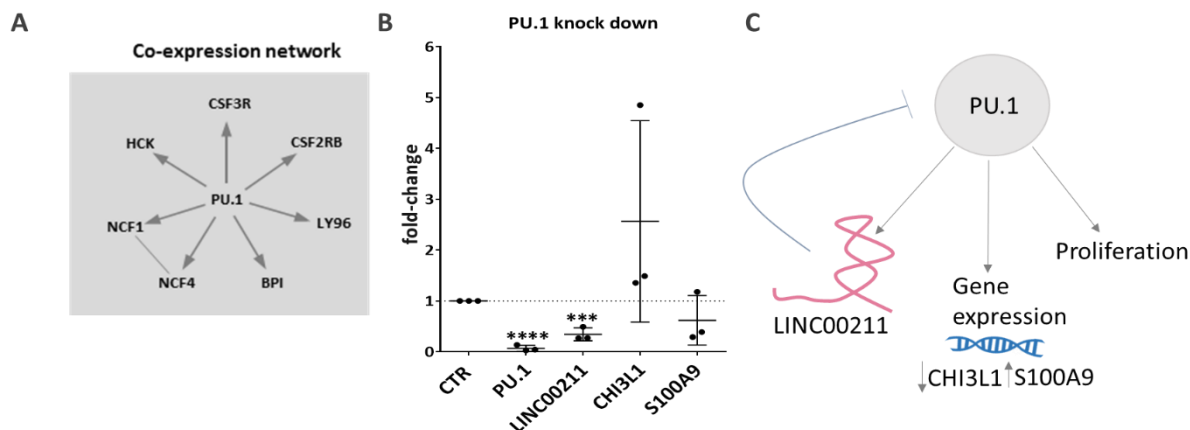


**Figure 3.1.7: Regulation of LINC00211 by PU.1.** **A.** Co-expression network analysis of LINC00211. **B.** qRT-PCR analysis of the expression levels of PU.1, LINC00211, CHI3L1 and S100A9 upon PU.1 knock down compared to control cells and normalised to U6 snRNA levels. For statistical analysis one-way ANOVA was performed ( $***p \leq 0.001$ ,  $****p \leq 0.0001$ ). **C.** Schematic representation of LINC00211 regulatory network.

### 3.1.7 LINC00211 is a biomarker of the inflamed lung

Since lung inflammation is characterised by high myeloid cell infiltration, bronchoalveolar lavage fluids (BAL) from infected and control-group patients were tested for LINC00211 expression. Healthy controls (n=10) and patients with different lung infections (n=12) were tested (see Table 2.2.34). The expression levels of LINC00211 in the infected individuals were much higher than in the control group (Figure 3.1.8.A) and correlated with the numbers of infiltrating neutrophils found in the BALs ( $R^2 = 0.8204$ ) (Figure 3.1.8.B). Furthermore, to test if the expression levels of the lincRNA are altered not only during acute inflammation but also in a chronic inflammatory setting, fluid flushed from lung tissue obtained from Idiopathic pulmonary fibrosis (IPF) patients was investigated. Idiopathic pulmonary fibrosis (IPF) is the most common form of the idiopathic interstitial pneumonias and it is age-related, chronic, irreversible and lethal (King et al., 2011). The disease is characterised by extracellular matrix deposition and inflammatory responses play critical role in the disease formation and progression (Piguel et al., 1993, Kolb et al., 2001, Richter et al., 2011, Kinder et al., 2008). As control, fluids from healthy tissue were also incorporated in the analysis. The samples were tested for cellular composition by flow cytometry and the results revealed that the levels of granulocytes were higher in the IPF lung tissue compared to healthy tissue (Figure 3.1.8.C),

consistent with previous studies (Richter et al., 2011). In line with the results from BALs, LINC00211 in IPF tissue fluid was linearly correlated with the percentage of granulocytes ( $R^2=0.8327$ ) (Figure 3.1.8.D). This suggests, that LINC00211 may serve as a diagnostic biomarker of both acute and chronic inflammatory lung conditions and myeloid cell infiltration. This finding also underpins the high specificity of LINC00211 expression towards myeloid cells.

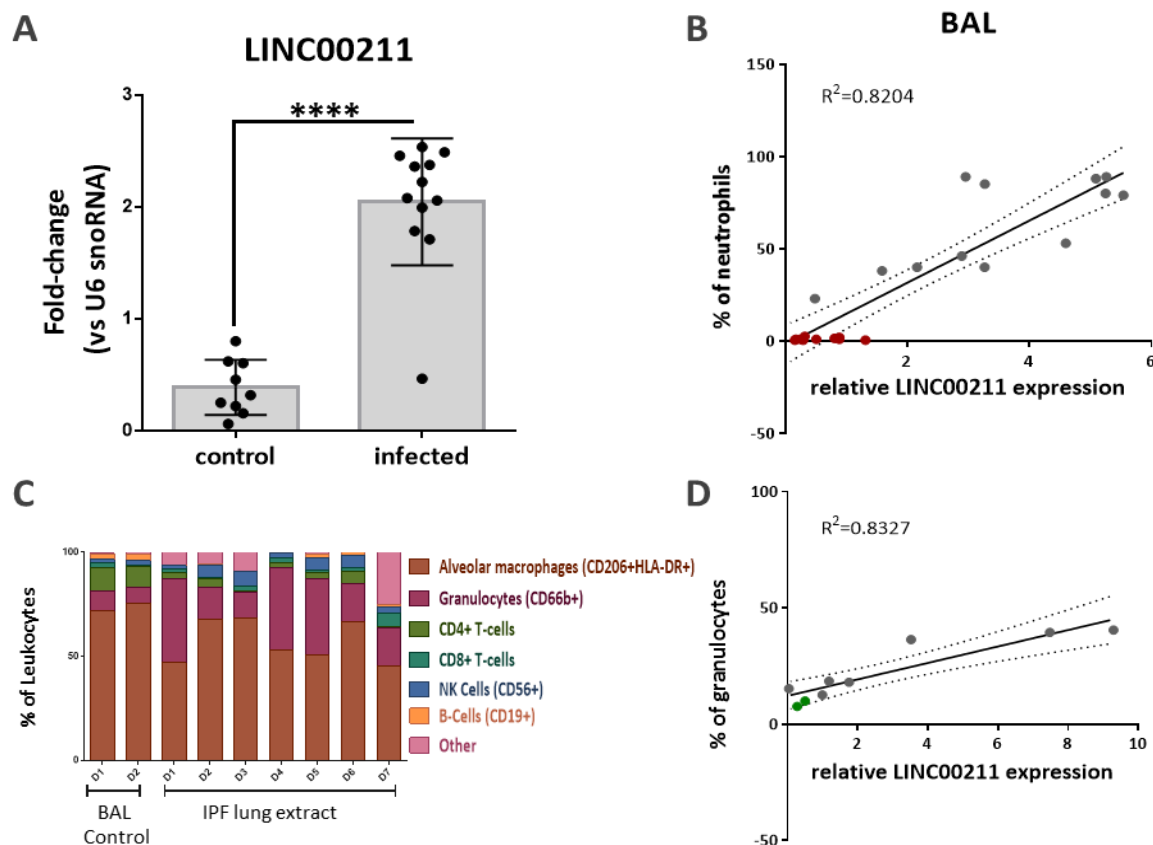


**Figure 3.1.8: LINC00211 is elevated in BALs from infected patients and correlates with granulocyte numbers in IPF patients.** **A.** qRT-PCR analysis of LINC00211 expression, relative to U6 snRNA and compared to median CT value in BALF pellets of 10 control individuals compared to 12 patients with bacterial or fungal infection (unpaired t-test, \*\*\*\* $p \leq 0.0001$ ). **B.** Correlation of LINC00211 expression with the percentage of neutrophils in BALF samples of healthy and infected individuals (controls= red dots, infected= grey dots). **C.** FACS data from fluid flushed from non-diseased or IPF tissue. Stainings: alveolar macrophages: anti-HLA-DR and CD206; granulocytes: anti-CD66b; T-cells: anti-CD4 anti-CD8; NK cells: anti-CD56; B-cells: anti-CD19. **D.** Correlation of LINC00211 expression with the percentage of granulocytes in fluid flushed from non-diseased or IPF tissue (controls= green dots, IPF= grey dots).

## 3.2 Results - LncRNAs in macrophage activation

### 3.2.1 Resting and activated BDMs differentially express lncRNAs

To identify novel functions of lncRNAs in human macrophage immunity multiple approaches including RNA-Seq, RNA antisense purification coupled with mass spectrometry (RAP-MS) and subcellular fractionation techniques were employed (Figure 3.2.1.A). Firstly, lncRNA profiles of resting and immune-activated macrophages were recorded followed by analysis of lncRNA abundances in macrophage subcellular fractions in order to discriminate between nuclear and cytoplasmic riboregulators and finally glycerol-gradient centrifugation was used to chart lncRNA co-sedimentation with cellular protein machineries. These approaches generate a macrophage map of lncRNAs with subcellular resolution, which may guide detailed mechanistic investigations. To record immune-responsive lncRNAs, human blood-derived macrophages were challenged with LPS from *Salmonella* Typhimurium and successful immune-activation was verified by qRT-PCR analysis of IL1 $\beta$  and CD80 mRNA induction (Figure 3.2.1.B). The samples were then used for RNA-Seq analysis of poly(A)-enriched RNA. This analysis confirmed that mRNAs (~94 %) and lncRNAs (~4 %) are the predominant classes of poly(A)-RNA (Figure 3.2.1.C). Differential gene-expression analysis using DeSeq2 revealed that 773 mRNAs were up- and 460 were down-regulated with a fold-change  $\geq 2$  and adjusted P-value  $\leq 0.05$  (Figure 3.2.1.D). Notably, using the same strict cut-offs, 43 lncRNAs were up- and 14 were down-regulated, suggesting an essential involvement of this RNA-class in macrophage immunity (Figure 3.2.1.D and E). These lncRNAs were further investigated. Inhibition of MAPK and NF- $\kappa$ B using chemical inhibitors, such as U0126 (MEK1/2/ERK1/2 inhibitor), SB203580 (p38 inhibitor) and NF-AI (NF- $\kappa$ B inhibitor), diminished the up-regulation of LPS-induced lncRNAs (Figure 3.2.1.G), confirming their dependence on TLR4 activation. AP003354.2 (henceforth MaIL1, for Macrophage Interferon-regulatory LincRNA 1), LINC01215, NRIR and LUCAT1 were highly upregulated upon LPS simulation (Figure 3.2.1.G). LncRNA MaIL1 and LINC01215 induction was also observed upon macrophage infection with the gram-negative bacterial pathogen *Legionella pneumophila* (Figure 3.2.1.G). Notably, NRIR expression was not regulated during *L. pneumophila* infection, which mainly induces inflammatory responses downstream the TLR2 receptor, suggesting a strict and highly specific regulation of lncRNAs during microbial infection.

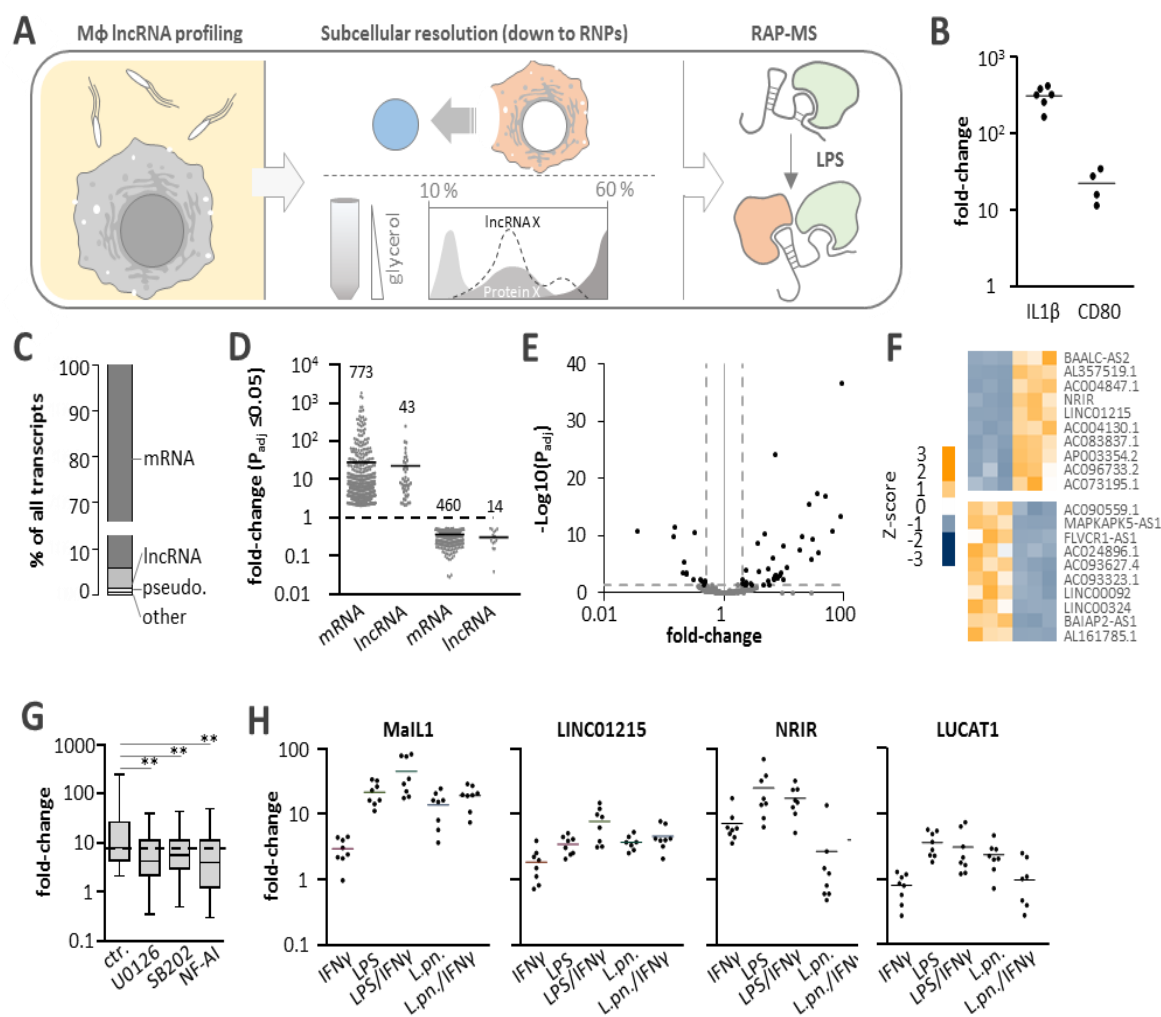


**Figure 3.2.1: Analysis of the primary human macrophage lncRNA landscape uncovers uncharacterized immune genes.** **A.** Outline of the experimental approach. lncRNA expression profiling in resting and immune-challenged blood-derived human macrophages is followed by investigation of lncRNA distribution in cytosol and nucleus and co-sedimentation on glycerol gradients with protein machineries. Additionally, RAP-MS was employed to investigate the mechanism of function of selected lncRNAs. **B.** Fold-change of IL1 $\beta$  and CD80 mRNA expression upon 8 h LPS (100 ng/ml) compared to mock-treatment, determined by qPCR. **C.** RNA-class distribution in LPS-treated macrophages from B, determined by RNA-Seq and averaged over 3 replicates. **D.** DeSeq2 reported fold-changes and number of regulated mRNAs and lncRNAs in samples from B. ( $P_{adj} \leq 0.05$ , fold-change  $\geq 2$  or  $\leq 0.5$ ). 6 independent experiments were performed and pooled RNA from of each two experiments was analysed in 3 RNA-Seq runs. **E.** Volcano plot with lncRNA fold-changes and adjusted P-values from RNA-Seq datasets described in D. **F.** Top 10 up- and down-regulated lncRNAs from D) (row Z-score heatmap; columns 1-3: mock-treatment; columns 4-6: LPS-treatment). **G.** Fold-changes of lncRNAs as obtained from RNA-seq data of BDMs treated with 50nM of U0126, SB203580 and NF-AI for 2h and then stimulated with 100 ng/ml LPS for another 2 hours **H.** Macrophages were stimulated with IFN $\gamma$  (100 ng/ml), LPS (100 ng/ml) and *Legionella pneumophila* (L.pn.; MOI 10) for 8 h. Mean fold-change compared to mock-treatment and individual data-points from 8 independent experiments are shown.

### 3.2.2 Macrophage lncRNAs predominantly localize to the cytosol.

In order to determine the subcellular localisation of lncRNAs, nuclear and cytosolic fractions of BDMs were submitted for RNA-seq. The results revealed that most lncRNAs, similar to mRNAs, are found in the cytosol (Figure 3.2.2.A and B). Importantly, the data recapitulate the known subcellular distribution of well-characterized lncRNAs such as NEAT1, MALAT1 (both nuclear) (Bhatt et al., 2012) and ZFAS1 (cytosolic) (Hansji et al., 2016) (Figure 3.2.2.A). Only few LPS-induced changes in subcellular lncRNA distribution were recorded. Potential shifts in lncRNA Hotairm1 and BIC subcellular distribution however did not reach significance at the  $P \leq 0.05$  level. qRT-PCR validated the localisation results obtained from RNA-seq analysis. Controls like GAPDH, MALAT1 and Hotairam1 were found in nucleus and cytosol respectively, as expected (Figure 3.2.2.C).

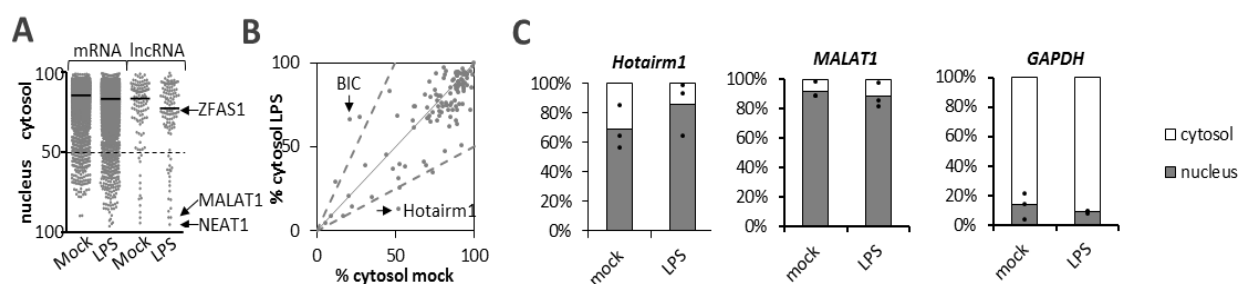


**Figure 3.2.2: Cellular localisation of immune responsive lncRNAs.** **A.** RNA-Seq analysis (two averaged replicates) of mRNA and lncRNA localization to nucleus and cytosol (in percent) in 8 h mock- or LPS-treated (100 ng/ml) macrophages. **B.** lncRNA cytosolic localization (in percent) in mock- compared against LPS-datasets from A. qRT-PCR of Hotairm1, MALAT1 and GAPDH in cytosolic and nuclear fractions. Individual data-points from three independent experiments are shown

### 3.2.3 Gradient profiling reveals distinct sedimentation-profiles of RNA classes and protein machineries

To increase subcellular resolution and narrow down potential interactors of the predominantly cytosolic and LPS-responsive macrophage lncRNAs, cellular fractionation by 10-60 % glycerol gradient ultracentrifugation was performed. Gradients were loaded with lysates of LPS-stimulated macrophages and, upon centrifugation, divided into consecutive fractions, which were analysed for their respective RNA and protein content by RNA-Seq and mass-spectrometry. A260 analysis showed the expected pattern of RNA-distribution with a sharp

increase towards the last fractions (Figure 3.2.3.A), which contain the heavy ribosomal complexes. For transcriptome and proteome analysis, the 44 obtained gradient fractions were reduced to 22 fractions. qPCR analysis confirmed the expected peak of U6 snRNA in the early gradient fractions (light-weight spliceosome complexes), while Gapdh mRNA spiked in the late (ribosomal) fractions (Figure 3.2.3.B). Furthermore, RNA-Seq confirmed the differential RNA class distribution along the gradient. mRNA and rRNA spiked in the last fraction while snRNA and miscRNA were predominantly found in the first fractions (Figure 3.2.3.C). Pseudogenes primarily occupied later fractions than snRNAs and miscRNAs and different from mRNA and were found in very low levels in the last gradient fraction (Figures 3.2.3.C), which verifies their non-coding nature. Previously, lncRNAs had been sub-categorized into intergenic lncRNAs (lincRNAs) and lncRNAs transcribed from coding gene loci (coding gene-associated lncRNAs; here galncRNAs). Both lincRNAs and galncRNAs, however, displayed a very similar gradient profile, similar to pseudogenes (Figure 3.2.3.C). Interestingly, lncRNA abundance in the last, ribosomal fraction was reduced but not completely absent when compared to mRNA, implying coding potential of some lncRNAs.

At the protein level, successful separation of cellular complexes was initially confirmed by silver-staining (Figure 3.2.3.D). To enable global co-sedimentation analysis of lncRNAs with protein machineries, proteome profiles of all gradient fractions were recorded. Ribosomal proteins mainly occupied the last gradient fraction (fraction 22), with a secondary peak in fraction 15 (Figure 3.2.3.E). This pattern could be explained by the localization of EIF3 proteins, which are involved in ribosomal recycling, in fraction 15 (Figure 3.2.3.E). Taking into account the RNA-Seq profiles, ribosomes co-localised with rRNAs and mRNAs in the last fraction. Spliceosomal proteins were more spread across the gradient, but predominantly occupied the first fractions, matching the pattern observed for snRNA. hnRNP proteins, which are involved in mRNA processing, were primarily found in the first fractions (Figure 3.2.3.E). The proteasome proteins peaked between fractions four and eight (Figure 3.2.3.E). In summary, the approach accurately portrays the distinct migration patterns of functional protein and RNA-classes, a requirement for global co-sedimentation analysis of macrophage lncRNAs and protein machineries.

In order to identify functional subgroups of lncRNAs the co-sedimentation patterns with cellular protein machineries were further investigated. Hierarchical clustering of mRNAs revealed a uniform co-sedimentation pattern with the expected peak in the last (ribosomal) fraction. On the other hand, lncRNA clustering revealed several subgroups with markedly

different gradient profiles (Figure 3.2.3.F): a group of low abundance in the ribosome-containing fraction 22 (group I) accounted for 76.6 % of all macrophage lncRNAs, while 23.4 % of lncRNAs (group II) displayed a pattern similar to mRNA (Figure 3.2.3.G, upper panel), in line with their largely cytosolic localization (Figure 3.2.2.A). Both the percentage of lncRNAs characterised as “coding” by the CPC2 algorithm and the average CPC2 coding score were elevated in group II in comparison to group I lncRNAs (Figure 3.2.3.H). When restricting the analysis to LPS-responsive lncRNAs, the percentages changed, with group II even rising to 49 % (Figure 3.2.3.G lower panel). These results are in line with other recent reports, claiming that several lncRNAs are actually ribosome-associated (Carlevaro-Fita et al., 2016, van Heesch et al., 2017). For the remainder of the present work the focus was then on LPS-responsive group I lncRNAs, which are absent from the ribosomal fraction and therefore likely to constitute true non-coding RNAs. LncRNAs of group I were highly heterogeneous, implying diverse associations with cellular machineries. Among group I, a subgroup (group Ia) of lncRNAs with similar migration behaviour was identified. (Figure 3.2.3.F). LncRNAs of group Ia mostly co-sedimented with proteins involved in proteasomal function. Furthermore, the well-characterized lncRNA NEAT1, which is a known innate immune regulator of type I interferon expression (Morchikh et al., 2017), belonged to group Ia. Additionally, group Ia contained other lncRNAs that were upregulated upon pro-inflammatory stimulation of human macrophages, like MaIL1 and LUCAT1. Due to the reduced likelihood of coding potential, the study was further focused on these lncRNAs.

### **3.2.4 MaIL1 lincRNA is a novel TLR-responsive gene**

One of the lncRNAs found in group Ia was MaIL1, which was identified as one of the most highly induced transcripts in response to LPS (Figure 3.2.1.H). MaIL1 was not only expressed in macrophages but also in monocytes, dendritic cells, B cells and naïve T cells (Figure 3.2.4.A), suggesting a broader function in the immune system. RACE-PCR largely verified the predicted 4-exon transcript architecture, however revealed extended 5' and 3' terminal exons (Figure 3.2.4.B) and a total cDNA length of 1543nt (Figure 3.2.4.C).

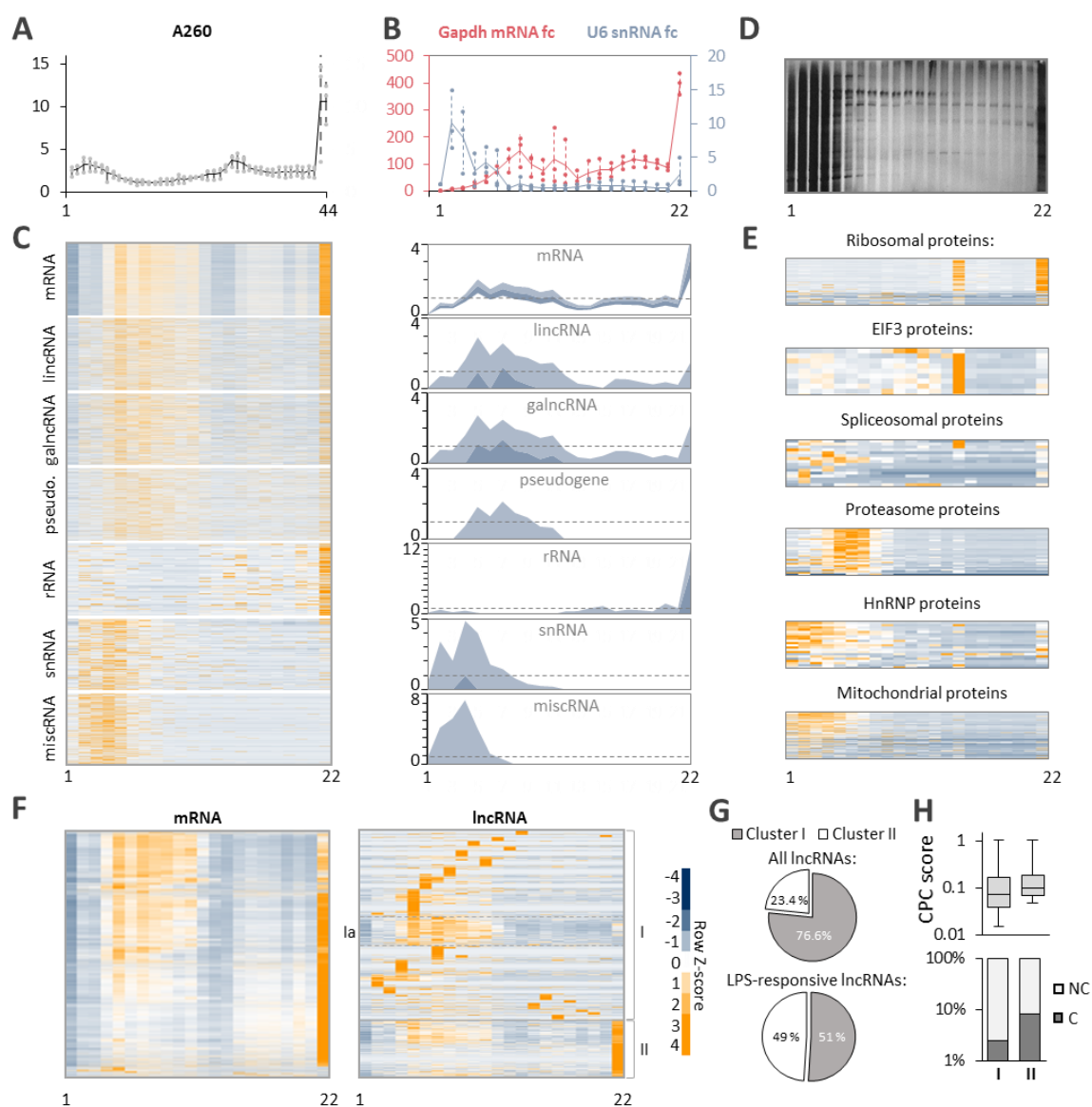


**Figure 3.2.3: Glycerol gradient analysis reveals co-sedimentation of macrophage lncRNAs with major cellular machineries.** **A.** A260 absorbance measurement in 44 successive 10-60 % glycerol gradient fractions (2 h LPS-stimulated macrophage lysates). **B.** *Gapdh* mRNA and U6 snRNA fold-change compared to fraction # 1 in samples from A, reduced to 22 successive gradient fractions, quantified by qPCR. **C.** Row Z-score heatmap (left) and fold-change plots (right, inner two quartiles shown, relative to fraction 1) depicting the sedimentation pattern of major RNA-classes, determined by RNA-Seq using samples from B. **D.** Representative silver-stained SDS gel illustrating protein content and differential protein sedimentation, using samples from B. **E.** Top: same as C but displaying major protein classes based on proteomics measurements. Bottom: Representative Western Blot confirming the differential sedimentation of major macrophage protein components. **F.** Hierarchical clustering of mRNA and lncRNA data from C). Major lncRNA clusters (I, Ia and II) are indicated. **G.** Percentages of lncRNAs in cluster I and II, identified in panel F). Top: percentages calculated based on all detected lncRNAs; bottom: percentages calculated based on LPS-responsive lncRNAs. **H.** Top: box-plot representation of CPC2 coding-scores of cluster I and II lncRNAs. Bottom: Percentages of lncRNAs deemed “protein-coding” in CPC2 analysis for cluster I and II. Where applicable, standard deviations and individual measurement points derived from three independent experiments are shown.



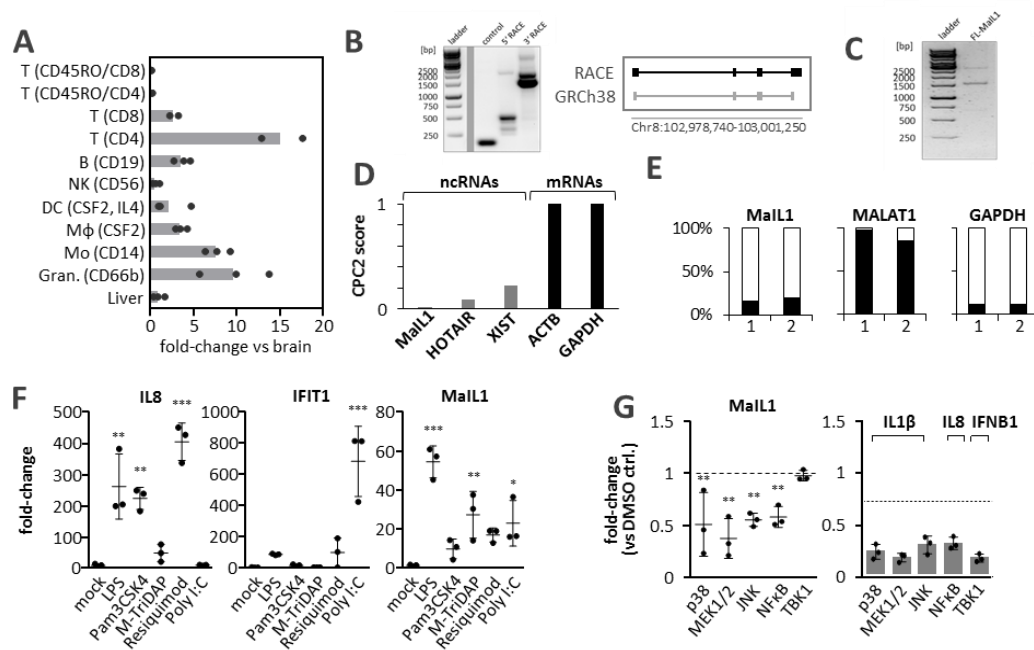


**Figure 3.2.4: Characterisation of MaIL1 as a TLR-responsive ncRNA.** **A.** qPCR analysis of MaIL1 lncRNA abundance in different immune-cell subsets and liver tissue relative to brain tissue. **B.** RACE PCR-determined MaIL1 exon architecture. **C.** Full length MaIL1 PCR. **D.** CPC2 coding-score of RACE-PCR refined MaIL1 RNA and indicated GRCh38 reference RNAs. **E.** Percent-localization of indicated RNAs to cytosol (white) and nucleus (black) in both RNA-Seq replicates from Fig. 3.1.2. **F.** qPCR-determined fold-changes of indicated control RNAs and MaIL1 upon macrophage stimulation with the indicated immune-agonists for 8 h, compared to mock-treatment (LPS, 100 ng/ml, Pam3CSK4 100 ng/ml, M-TriDAP1  $\mu$ g/ml, Resiquimod 1  $\mu$ g/ml, poly I:C 20  $\mu$ g/ml). **G.** MaIL1 inhibition in 8 h LPS-stimulated macrophages pre-treated with indicated pathway inhibitors (50  $\mu$ M) (fold-change compared to LPS + DMSO). Where applicable, standard deviations and individual measurement points derived from at least three independent experiments are shown. P values (\*\*\*)  $\leq$  0.0001, \*\*  $\leq$  0.01, \*  $\leq$  0.05) were calculated using a one-way ANOVA test.

Re-analysis of the RACE-refined RNA sequence by the CPC2 algorithm confirmed a low coding score, similar to well-characterized non-coding RNAs and different from mRNA (Figure 3.2.4.D). RNA-Seq analysis of subcellular fractions suggests that the majority of these copies are exported to the cytosol (Figure 3.2.4.E). Besides with LPS, MaIL1 was also induced upon stimulation with agonists of TLR2 (Pam3csk4) and TLR7/8 (Resiquimod) (Figure 3.2.4.F), which sense microbial lipoprotein and RNA, respectively. Interestingly, MaIL1 induction was also triggered by poly I:C, (Figure 3.2.4.F), an agonist of the TBK1-IRF3 pathway, involved in type I interferon activation. Overall, however, LPS caused the strongest MaIL1 induction (Figure 3.2.4.F). Since the macrophage response to LPS is controlled by transcription factors such as NF- $\kappa$ B, AP-1 and IRF3, inhibition of these may reveal the dependence of MaIL1 on the distinct TLR signalling cascades. Successful inhibition of MEK/ERK, p38 and JNK, kinases upstream of AP-1 and NF- $\kappa$ B (Figure 3.2.4.G right panel),

significantly attenuated MaIL1 induction by LPS (Figure 3.2.4.G). TBK1 kinase inhibition upstream of IRF3 on the other hand did not affect MaIL1 expression (Figure 3.2.4.G). Thus, MaIL1 is a novel immune-responsive, cytoplasmic non-coding RNA, triggered by NF $\kappa$ B and MAPK but not TBK1 signalling downstream of TLR activation.

### 3.2.5 Functional characterisation of MaIL1 by CRISPR/Cas 9

In order to mechanistically characterise MaIL1, CRISPR/Cas9 was employed. Two pairs of gRNAs were designed and introduced into the pX458 vector (See section 2.2.7). The plasmids were transfected into THP1 cells and single cell sorted. The successful knock out was tested by genomic PCR and qRT-PCR both in resting and LPS stimulated macrophages (Figure 3.2.5.A). A monoallelic knock out from one gRNA pair (MaIL1<sup>+/-</sup>) and a biallelic knock out from the second gRNA pair (MaIL1<sup>-/-</sup>) were used for further experiments. Two replicates (each representing a pool of four independent replicates) of PMA differentiated wild type (wt) (transfected with empty pX458 vector), MaIL1<sup>+/-</sup> and MaIL1<sup>-/-</sup> cells, were sent for RNA sequencing. The results verified the successful inhibition of MaIL1 expression in the MaIL1<sup>+/-</sup> and MaIL1<sup>-/-</sup> cells in a dose dependant manner (Figure 3.2.5.B). In PCA analysis, the generated cells lines clustered together and were far from the control cells under mock and LPS conditions (Figure 3.2.5.C). Interestingly, the sequencing results revealed that most of the LPS regulated genes were dysregulated in the MaIL1<sup>+/-</sup> and MaIL1<sup>-/-</sup> cells compared to the control cells in a dose dependent manner (Figure 3.2.5.D). Deeper investigation of the regulated genes unveiled that most of the genes are targets of two major inflammatory response transcription factors, p65 and the AP-1 (Figure 3.2.5.E). The majority of the genes that are upregulated by these two transcription factors are reduced in MaIL1<sup>+/-</sup> and MaIL1<sup>-/-</sup> cells in a MaIL1-dose depended manner. Further analysis of the MaIL1<sup>+/-</sup> and MaIL1<sup>-/-</sup> cells showed an impaired p65 activation. P65 phosphorylation was lower in knock out cells upon LPS stimulation compared to the wt cells (Figure 3.2.6.A). Surprisingly, phosphorylation of ERK1/2, a major kinase downstream the TLR4 pathway, was higher in the knock out cells compared to the wild type, both in resting and LPS activated differentiated THP1 cells (Figure 3.2.6.A). P65 phosphorylation was also tested by flow cytometry and the results verified the low levels of p65 phosphorylation in MaIL1<sup>+/-</sup> and MaIL1<sup>-/-</sup> cells compared to wt cells (Figure 3.2.6.B).

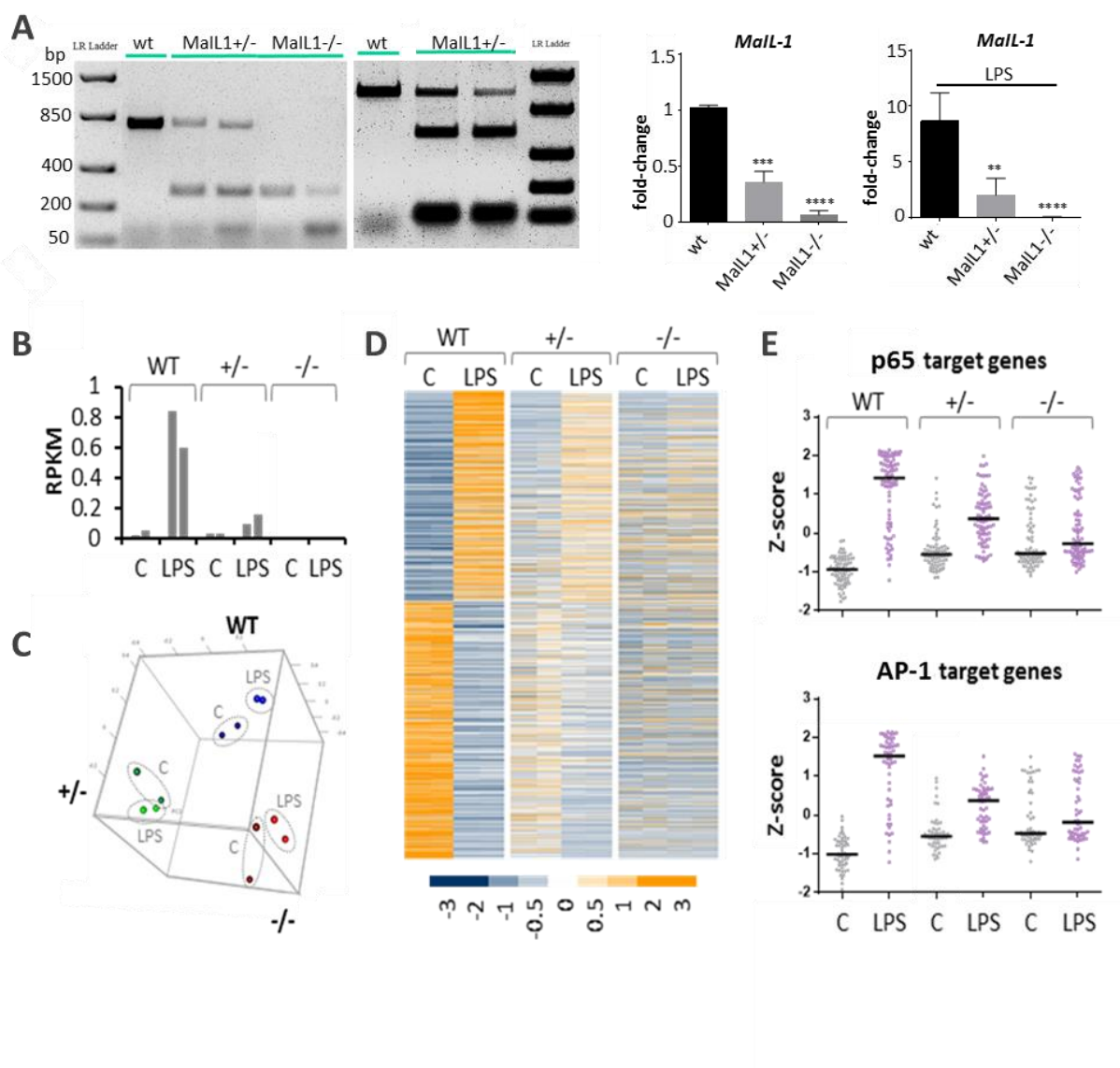


**Figure 3.2.5: Functional characterisation of MaIL1 by CRISR/Cas 9.** **A.** Left: agarose gel of genomic PCR products. On the left gel, bands are obtained after transfection with the first gRNA pair. On the right gel bands are obtained from the second gRNA pair. Right: qRT-PCR for MaIL1 in the wt and knock out cell lines in resting and LPS (100 ng/ml for 16h) activated differentiated THP1 cells (PMA 20nM for 24h). **B.** RPKMs of MaIL1 obtained from RNA sequencing analysis. **C.** PCA analysis of the different cell types under resting or LPS-stimulation conditions. **D.** Z-score heat map of the inflammatory genes up or downregulated upon LPS stimulation. **E.** Z- scores of the p65 and AP-1 inducible genes in the wt and knock out cells. For statistical analysis one-way ANOVA was performed (\*\*p-value  $\leq 0.01$ , \*\*\*p-value  $\leq 0.001$ , \*\*\*\*p-value  $\leq 0.0001$ ).

Major cytokines released upon TLR4 activation were also tested. The expression levels of IL-8, IL-6 and IL-1 $\beta$  were significantly reduced in MaIL1<sup>+/-</sup> and MaIL1<sup>-/-</sup> compared to wt cells (Figure 3.2.6.C). Furthermore, IL6 protein levels were significantly lower in the supernatants of the knock out cells (Figure 3.2.6.D). Taken together, MaIL1 lincRNA has a major influence on the inflammatory responses of THP1 cells.

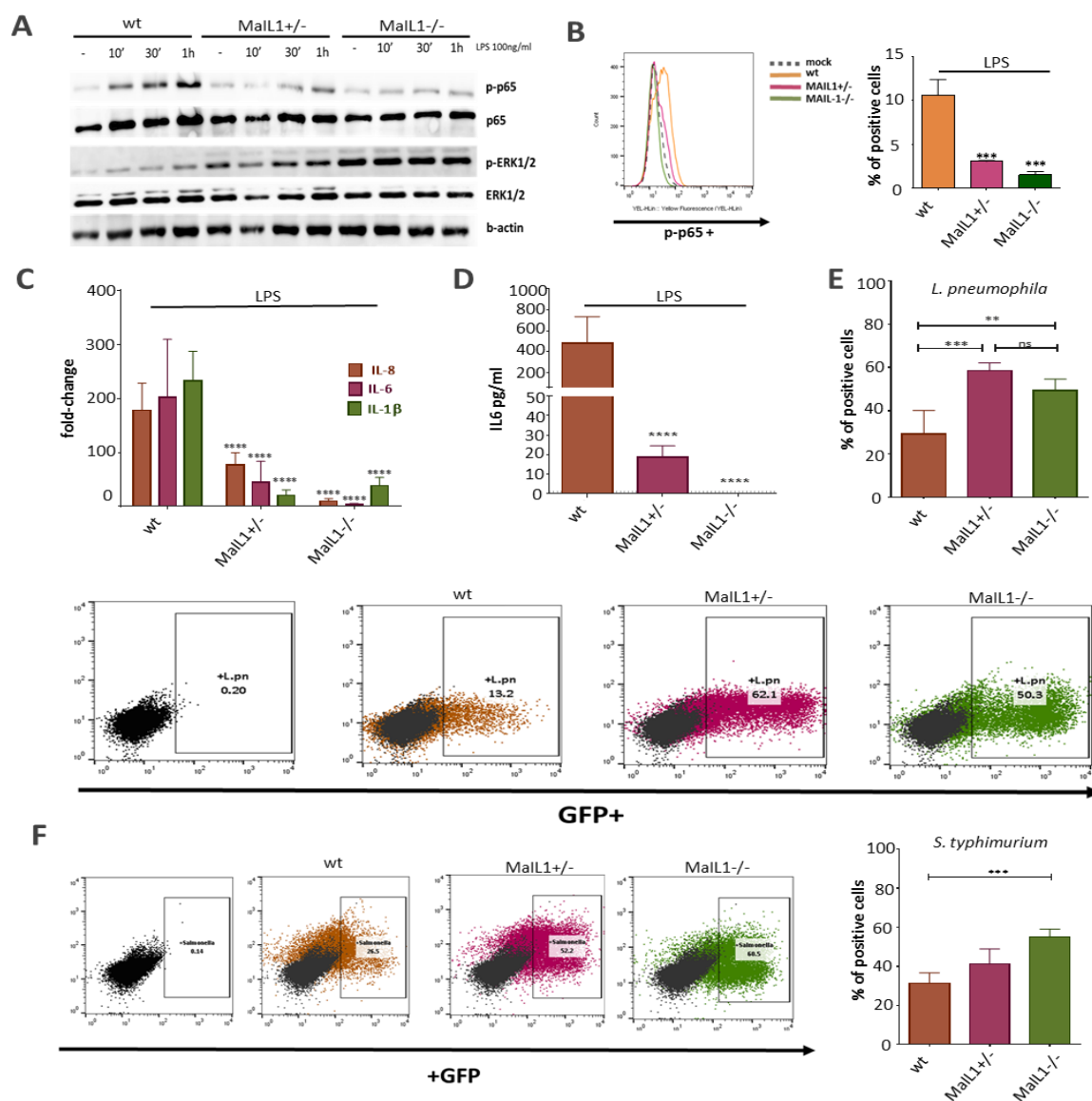


**Figure 3.2.6: Characterisation of MaIL1  $-/-$  cells.** **A.** Western blot analysis of p-p65, p65, p-ERK1/2, ERK1/2 and b-actin in wt and MaIL1 $+/-$  and MaIL1 $-/-$  cells after LPS (100 ng/ml) treatment for 10 min, 30 min and 1 hour. **B.** FACS analysis of p-p65 upon LPS (100 ng/ml) stimulation for 1 hour. **C.** qRT-PCR of IL-8, IL-6 and IL-1 $\beta$  after LPS (100 ng/ml) stimulation for 16 hours. **D.** IL6 release after 16 hours of LPS stimulation in wt and MaIL1 $+/-$  and MaIL1 $-/-$  cells. **E.** FACS analysis of *L. pneumophila* infected cells (GFP $+$  cells) (MOI=10 for 24 hours). **F.** FACS analysis of *S. Typhimurium* infected cells (GFP $+$  cells) (MOI=10 for 24 hours). For statistical analysis one-way ANOVA was performed (\*\*p-value  $\leq$  0.01, \*\*\*p-value  $\leq$  0.001, \*\*\*\*p-value  $\leq$  0.0001).

Finally, functional assays were performed in order to check the role of the lincRNA during the course of infection. Infection of differentiated THP1 cells with GFP $+$  *L. pneumophila* revealed that the MaIL1 $+/-$  and MaIL1 $-/-$  cells were more susceptible to infection compared to the wt cells (Figure 3.2.6.E). These results are in line with the impaired pro-inflammatory responses of these cells. Moreover, to exclude bacteria-specific phenotypes, the same experiments were

performed with GFP+ *Salmonella* Typhimurium (*S. Typhimurium*) (Figure 3.2.6.F). The results were similar to what was observed for *L. pneumophila* infections.

The strong phenotype observed after CRISPR/Cas9-mediated knock out of MaIL1, raised the question whether it might represent a cell-line artefact. Therefore, functional investigation of MaIL1 was extended to primary human macrophages, using siRNAs.

### **3.2.6 MaIL1 lincRNA controls TLR-induced type I interferon production**

To investigate the role of MaIL1 during LPS stimulation, RNAi was performed in primary human BDMs, followed by RNA-Seq analysis (Figure 3.2.7.A). Inhibition of LPS-induction of MaIL1, but not IL6 was observed with two different siRNA designs, with si#1 having stronger silencing capacity (Figure 3.2.7.A). Intriguingly, RNA-Seq analysis revealed a  $\geq 2$ -fold reduction of type I interferon expression upon MaIL1 knockdown in LPS-stimulated macrophages (Figure 3.2.7.B and C). When relaxing the regulation cut-off below 2-fold this effect extended to LPS-responsive genes in general (Figure 3.2.7.D) and vice versa genes sensitive to MaIL1 knockdown were mostly LPS-inducible (Figure 3.2.7.E). Reactome analysis of MaIL1-controlled genes revealed an enrichment of type I IFN and TP53-related pathways (Figure 3.2.7.F). Furthermore, network analysis predicted an underlying IRF and TP53 transcription factor network (Figure 3.2.7.G). Moreover, genes belonging to the IRF3 or TP53 but not the MAPK pathway, were down-regulated upon MaIL1 knockdown (Figure 3.2.7.H), in line with the known activation of TP53 genes by type I interferon (Rivas et al., 2010). Analysis of IFNA1, IFNB1, IFNA8, IFNA2, IFNA13, IFNA14 and IFNL1 expression by qPCR verified a pronounced suppression of type I interferon induction upon MaIL1 knockdown, but did not significantly alter the expression of other TLR-response genes such as IL23 or CD70 (Figure 3.2.7.I). In order to investigate the role of MaIL1 during activation of other TLR pathways, poly(I:C) was used to stimulate TLR3 in BDMs after MaIL1 knock down. Similar to LPS treatment, type I interferon responses were reduced compared to the control, but the effect was milder (Figure 3.2.7.J). To summarise, MaIL1 lincRNA constitutes a TLR-induced positive regulator of type I interferon gene expression. Importantly, MaIL1 knockdown in primary cells did not recapitulate the effect of MaIL1 on the NFkB pathway, seen in THP1 cells (see above).

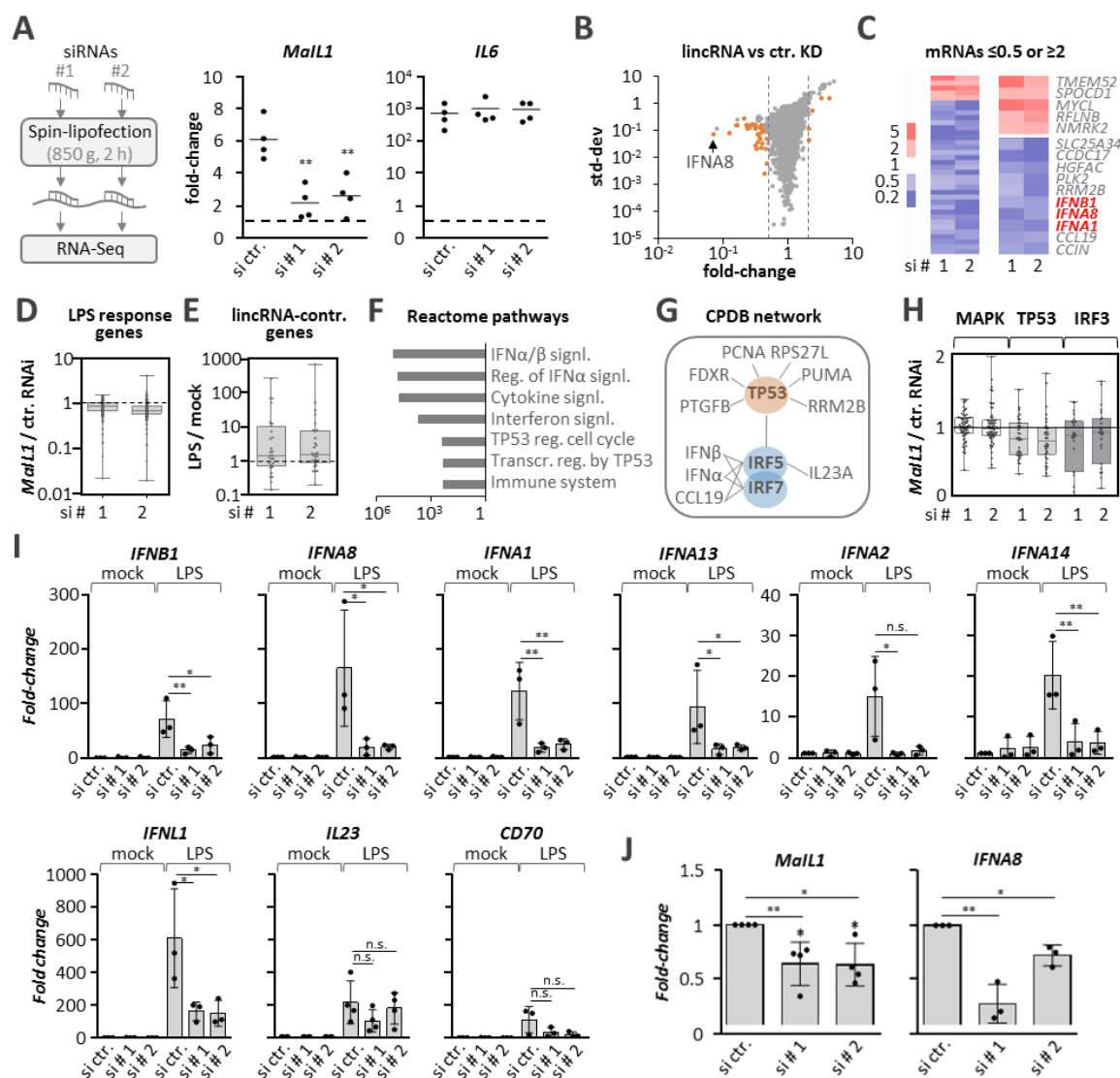


**Figure 3.2.7: Identification of *Mall1* lincRNA as a novel type I IFN regulator.** **A.** Left: *Mall1* knockdown-strategy using two independent siRNA designs. Right: qRT-PCR validation of *Mall1* knockdown and *IL6* expression after 8 h LPS stimulation (100 ng/ml) of BDMs. **B.** RNA-Seq plot showing mean fold-changes and standard deviation (*Mall1* siRNA 1 or 2 vs control siRNA knockdown). Genes with fold-changes  $\geq 2$  or  $\leq 0.5$  in both RNA-Seq runs are highlighted (orange colour). **C.** Fold-change heatmap for orange labelled genes from B. The resulting top 5 up and top 10 down-regulated genes are shown to the right. Type I IFN genes are highlighted. **D.** Box-plot showing expression changes of LPS-response genes (RNA-Seq-determined, fold-change  $\geq 2$ , LPS vs. mock) upon *Mall1* compared to control knockdown. **E.** Box-plot showing RNA-Seq-determined regulation of *Mall1* controlled genes from C in response to LPS. **F.** Reactome pathway analysis using down-regulated genes from C. **G.** ConsensusPathDB network analysis using down-regulated genes from C, revealing potential transcription factors driving the indicated gene subsets. **H.** Regulation of known MAPK, TP53 and IRF3 dependent genes upon *Mall1* compared to control knockdown (data from B). **I.** qRT-PCR validation of diminished type I IFN mRNA induction upon *Mall1* knockdown (values compared to control siRNA and mock stimulation). **J.** Left panel: *Mall1* knock down upon poly I:C stimulation, right panel: *IFNA8* expression upon poly I:C stimulation after *Mall1* knockdown. Standard deviations and individual data points from three independent experiments are shown. \* =  $P$ -value  $\leq 0.05$ , \*\* =  $P$ -value  $\leq 0.01$  (one-way ANOVA).

Therefore, the effect of MaIL1 on the TLR-NF $\kappa$ B axis was considered to represent a potential long-term effect resulting from MaIL1 deficiency over several cell passages, which does not explain the role of elevated MaIL1 expression during acute macrophage immune-activation. While the cell-line effect of MaIL1 on the NF $\kappa$ B pathway was not further followed up, the effect on the type I IFN pathway, observed in primary cells was investigated mechanistically.

### **3.2.7 MaIL1 promotes TLR4 induced IRF3 phosphorylation through interaction with Optineurin**

Type I interferon induction downstream of TLR4 relies on signal transduction through the intracellular adapter TRIF and subsequently on TBK1 and IRF3 phosphorylation (Kawai and Akira, 2011). In order to investigate the involvement of MaIL1 in the activation of this pathway the gradient results were further investigated to screen for potential interaction partners. One of the lncRNAs co-sedimenting with MaIL1 on glycerol gradients was NEAT1 (Figure 3.2.8.A), which has been implicated in type I IFN signalling through association with splice-regulatory protein SFPQ. RNA-immunoprecipitation confirmed the interaction of NEAT1 with SFPQ and revealed an additional interaction with MaIL1 (Figure 3.2.8.F). Western blot confirmed a co-localization of SFPQ with the first glycerol-gradient peak of MaIL1, but not with the second, and major peak (Figure 3.2.8.A), suggesting that SFPQ does not represent the main interactor of MaIL1. In order to find specific MaIL1 interactors RNA affinity chromatography was performed. Recently, RAP-MS was introduced as a sensitive approach to co-purify endogenous RNAs and bound proteins using UV-crosslinking and biotinylated antisense oligo pools, complementary to the RNA of interest (McHugh et al., 2015) (Figure 3.2.8.B). This approach was used to purify MaIL1 RNA and potential interactors from crosslinked primary macrophage lysates, followed by RNA-Seq (RAP-Seq) and mass-spectrometry (RAP-MS) analysis. To confirm the specificity of the approach, eluates from chromatographies with MaIL1 antisense oligonucleotide probes and random oligonucleotides were sent for RNA-seq. The results revealed that MaIL1 was highly enriched in MaIL1-1 eluates, but not other RNA molecules, suggesting that MaIL1 is not an RNA-binding lncRNA (Figure 3.2.8.C). Proteomics (RAP-MS) analysis revealed multiple MaIL1 co-purified proteins ( $P_{adj} \leq 0.05$ , fold-change  $\geq 2$ , Fig. 3.2.8.C). Intriguingly, the essential TLR4-TRIF signal transduction component Optineurin (OPTN) ranked highest. Ubiquitinated Optineurin (Ubi-OPTN) forms a platform mediating the progression of the TLR4-TRIF signalling arm via phospho-TBK1 to phospho-IRF3, which activates the type I interferon genes (Gleason et al., 2011, Munitic et al., 2013).

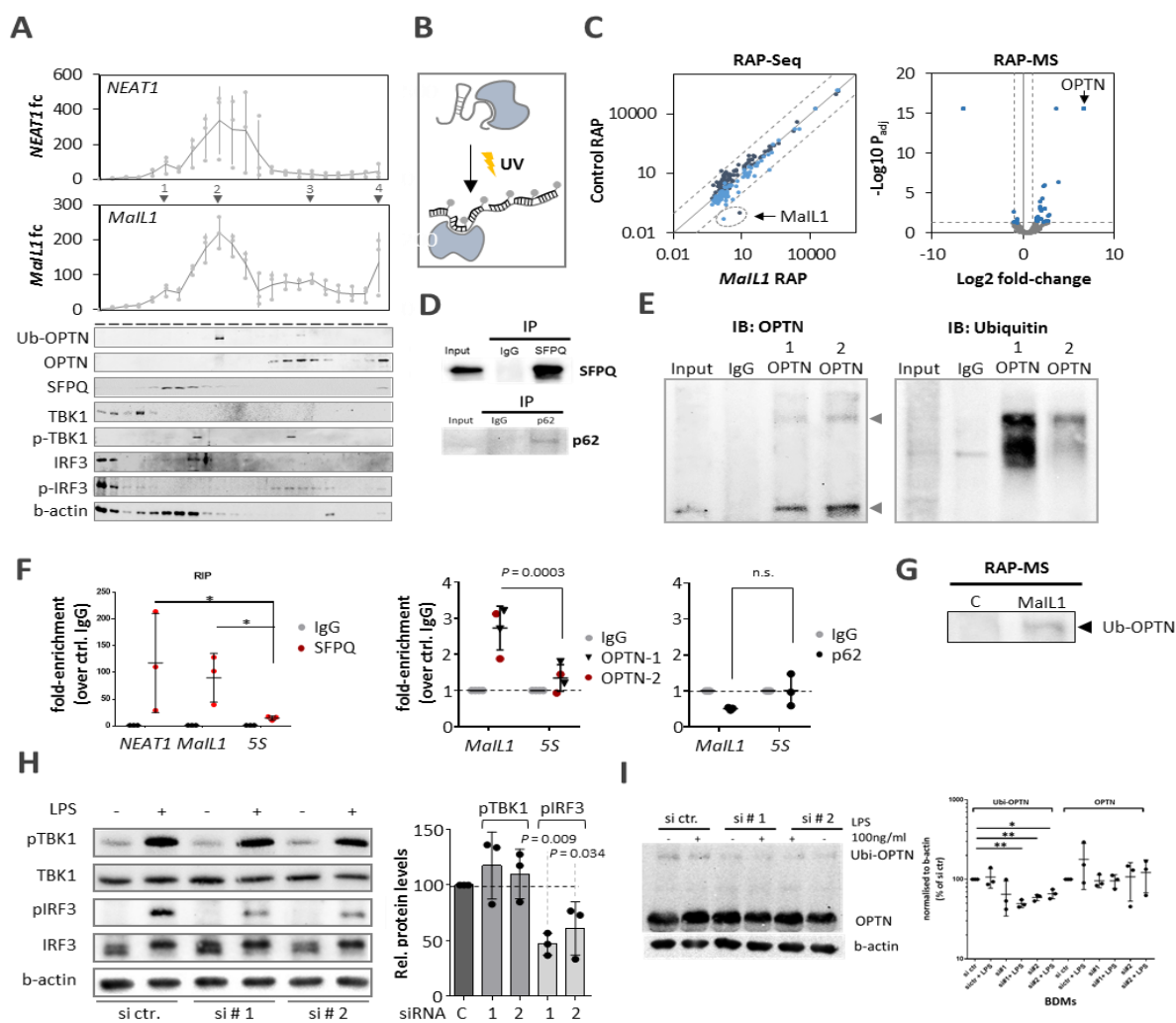


**Figure 3.2.8: MaIL1 lncRNA interacts with OPTN and controls TLR-triggered IRF3 phosphorylation and OPTN ubiquitination.** **A.** Top: qRT-PCR validation of NEAT1 and MaIL1 lncRNA profiles on 10-60 % glycerol gradients (2 h LPS-stimulated macrophage lysates, relative to fraction 1). Bottom: representative Western blots (Ubi = ubiquitinated protein form). Proteins detected on independent blots, with the same protein samples. **B** RNA affinity purification (RAP) procedure: UV-crosslinking of RNA-protein contacts is followed by hybridization of biotinylated DNA oligos to the target RNA and streptavidin-based purification. **C.** Left: RNA-Seq analysis of eluate fractions from control and MaIL1 RAP (RPKM values, two colour-coded replicates). Enriched MaIL1 lncRNA is highlighted. Dashed lines indicate 10-fold-enrichment over perfect-correlation line. Right: volcano-plot showing results from protein mass-spectrometry analysis of eluate fractions from three independent control and MaIL1 RAPs. Dashed lines indicate 2-fold cutoff (MaIL1 vs control RAP comparison) and  $P_{adj} \leq 0.05$  cutoff, respectively. OPTN is highlighted as the top hit. **D.** Pull down blots of SFPQ and p62. **E.** Left: pull down blot of OPTN stained with anti-OPTN antibody. Right: pull down blot of OPTN stained with anti-Ubi antibody. **F.** qRT-PCR analysis of MaIL1, NEAT1 and 5S rRNA levels in SFPQ, OPTN (two different antibodies) and p62 (control protein) CoIP eluates compared to control (IgG) CoIPs. **G.** Western blot from RAP-MS control and MaIL1 eluates. **H.** Quantification of phospho-TBK1 and -IRF3 signals (three independent Western blots, relative to actin). **I.** Quantification of OPTN and OPTN-Ubi levels after MaIL1 knock down (three independent replicates, relative to actin). Statistical significances were evaluated using a one-way ANOVA test (\*p-value  $\leq 0.05$ , \*\*p-value  $\leq 0.01$ ).



In agreement with these results, selective enrichment of Ubi-OPTN in MaIL1 RAP-MS eluates was observed in Western blot analysis (Figure 3.1.8.G). Furthermore, glycerol gradient analysis by Western blot revealed Ubi-OPTN to peak at fraction 10, which is the same fraction as the highest peak of MaIL1 (Figure 3.2.8.A). In contrast, the non-Ubi-OPTN form peaked in later gradient fractions and coincided with the MaIL1 smaller peaks, between fractions 14 and 18 and fraction 22. The interaction of MaIL1 with OPTN could be confirmed by RNA-immunoprecipitation (RIP) experiments (Figure 3.2.8.E and F). Both OPTN and Ubi-OPTN were successfully pulled down (Figure 3.2.8.E) and q-PCR analysis revealed that MaIL1 was specifically enriched in the OPTN pull down compared to a control RNA, 5S.

Furthermore, when RNA immuno-purification was performed for p62, a known regulator of OPTN, MaIL1 was not enriched, underpinning once again the specificity of the binding between OPTN and MaIL1 (Figure 3.2.8.F). pTBK1 and pIRF3, which are downstream of the signalling cascade were also found in the same fractions as the second peak for MaIL1 and OPTN on glycerol gradients (Figure 3.2.8.A). More specifically, pTBK1 was found in fraction 9 and 15 and IRF3 between fractions 1-3 and 14-18. Since OPTN promotes TBK1-to-IRF3 phosphorylation in the TLR4-TRIF cascade, MaIL1 lncRNA deficiency was expected to impact at the same step. Indeed, Western blot analysis confirmed a significant reduction of IRF3 but not TBK1 phosphorylation in MaIL1 silenced LPS-challenged macrophages (Figure 3.2.8.H). Intriguingly, MaIL1 silencing coincided with reduced OPTN ubiquitination (Figure 3.2.8.I), suggesting that interaction with MaIL1 lncRNA serves to maintain the ubiquitinated state required for TLR4-TRIF signal transduction. Interestingly, the levels of the total OPTN did not significantly change upon MaIL1 knock down.

### **3.2.8 MaIL1 is an infection biomarker promoting antimicrobial defence**

To determine the contribution of MaIL1 to cell-autonomous innate defence bacterial infections of human macrophage cultures were performed. Classically regarded to act predominantly in antiviral defence, type I interferons are increasingly recognized as regulators of antimicrobial immunity as well (Boxx and Cheng, 2016). *Legionella pneumophila* for instance is a human-pathogenic bacterium, which preferentially replicates inside human macrophages and is sensitive to type I interferon (Lippmann et al., 2011). To test whether silencing of type I interferon positive-regulator MaIL1 influences antimicrobial defence, macrophages were infected with GFP-expressing *L. pneumophila* at a low MOI, comparable to the one used in a previous study (Lippmann et al., 2011). MaIL1 knockdown resulted in a ~2-3 fold increase in the number of infected (GFP-positive) macrophages (Figure 3.2.9.A), and the effect was

stronger with siRNA design #1, which is in agreement with the previous observation that the design #1 had better MaIL1 silencing capacity (Figure 3.2.9.A). Importantly, this effect was rescued by exogenous supplementation of the infection cultures with recombinant IFN $\beta$  (Figure 3.2.9.A). ELISA confirmed the expected induction of type I interferon IFN $\alpha$  upon challenge of control-siRNA treated macrophages with the pathogen (Figure 3.2.9.B). In contrast, in MaIL1 knockdown cultures IFN $\alpha$  levels were blunted with siRNA design # 1 and highly reduced with siRNA design # 2 (Figure 3.2.9.B).

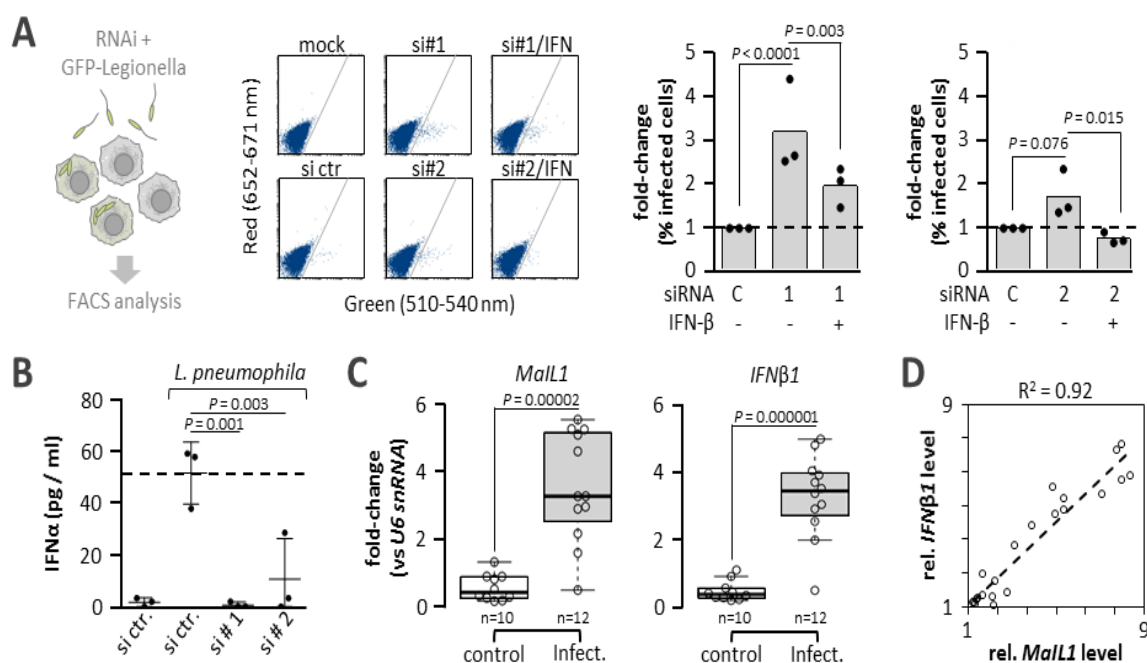


**Figure 3.2.9: MaIL1 affects bacterial replication and is elevated in BALs from infected patients.** **A.** Left: experimental layout: primary macrophages are transfected with siRNAs, followed by GFP-*Legionella* infection and FACS quantification of GFP-positive and -negative cells. Middle: representative FACS plots, showing GFP-positive *L. pneumophila* infected (high green-fluorescence) and uninfected (background-green-fluorescence) macrophages upon control-siRNA, MaIL1 siRNA (si#1 and si#2) and IFN $\beta$  (IFN) treatment. Right: FACS-quantification of *Legionella* infection rates in percent (MOI 0.1, 24 h), upon control- or MaIL1 knockdown with or without recombinant IFN treatment. Left: experiment with MaIL1 siRNA 1; right: experiment with MaIL1 siRNA 2. Three independent replicates and one-way ANOVA test. **B.** IFN $\alpha$  ELISA with supernatants from mock- or *L. pneumophila* treated macrophages (MOI 0.1, 24 h), transfected with control siRNA or MaIL1 siRNA 1 or 2. Three independent replicates and one-way ANOVA test. **C.** qRT-PCR analysis of MaIL1 (left) and IFN $\beta$ 1 (right) expression, relative to U6 snRNA and compared against median CT value in BALF pellets of 10 control individuals compared to 12 patients with bacterial or fungal infection (two-tailed students t-test, assuming equal variances). **D.** Correlation of MaIL1 and IFN $\beta$ 1 mRNA expression in the same BALF samples.

In order to test whether MaIL1 plays a role in human disease, the expression of MaIL1 was measured in bronchoalveolar lavage (BAL) fluids of patients with bacterial or fungal broncho-

pulmonary infection and in samples from healthy controls. Expression of MaIL1 was significantly increased in the infection group, as compared to healthy non-infected controls, suggesting that MaIL1 is specifically induced upon infection in vivo (Figure 3.2.9.C). The same was observed for IFN $\beta$  and in line with the critical role of MaIL1 in IRF3 activation, qRT-PCR analysis revealed a linear relationship between IFN $\beta$  and MaIL1 expression in BAL samples ( $R^2 = 0.92$ ) (Figure 3.1.7.D).

In summary, MaIL1 lncRNA is induced upon activation of the TLR-MyD88 axis and functions as a critical riboregulator of TBK1-IRF3-IFN signalling, by fostering ubiquitination of OPTN and promoting downstream IRF3 phosphorylation (Figure 3.2.10).

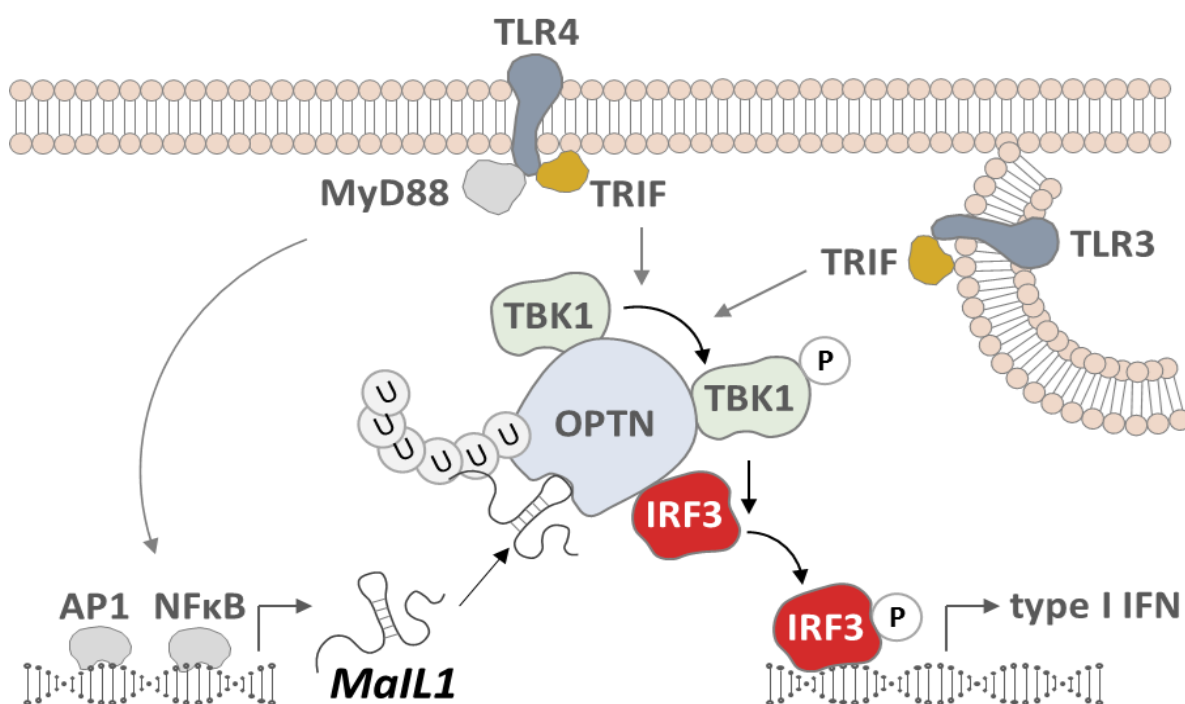


**Figure 3.1.10: Summarizing model of MaIL1 regulation and function.** Upon activation by TLR-Myd88 signalling MaIL1 expression is induced. The induction facilitates the activation of TLR-TRIF pathway via interaction with Optineurin. The interaction leads to Optineurin Ubiquitination and subsequently to IRF3-phosphorylation and type I IFN production.

## 4. Discussion

### 4.1 Discussion - LncRNAs in myeloid cell differentiation

Regulation of haematopoiesis and leukocyte differentiation is a strictly controlled process that is regulated by many cellular components. It is now evident that several lncRNAs are also involved in the regulation of haematopoiesis and immune cell differentiation (Venkatraman et al., 2013, Whang et al., 2014, Luo et al., 2015). As there are relatively few examples of functional long noncoding RNAs acting in the development of immune cells (Ranzani et al., 2015, Spurlock et al., 2015, Kotzin et al., 2016), in this study the lncRNA landscape of six subsets of human primary leukocytes was investigated. LncRNAs have been reported to have higher tissue specificity than mRNAs (Derrien et al., 2012). In line with this observation specific clusters of lncRNAs expressed in the different primary human leukocyte subsets, respectively were identified. In this analysis, LINC00211 was identified as a novel lincRNA involved in differentiation of monocytes to macrophages, by influencing PU.1 dependent gene expression. Besides LINC00211, other signature lncRNAs were identified, which might be exploited to distinguish leukocyte populations at the molecular level.

Other studies have addressed the roles of lncRNAs in the differentiation of hematopoietic cell lineages as well (Guttman et al., 2011). In the mouse immune system, during differentiation of naïve into memory CD8<sup>+</sup> T-cells the expression of several lncRNAs changes (Pang et al., 2009). In the present study a similar observation was made in human naïve and memory CD4<sup>+</sup> T-cells, where LINC02446 is absent from memory CD4<sup>+</sup> T-cells, while it is expressed in naïve CD4<sup>+</sup> T-cells. In another study in mouse, lnc-DC was highly upregulated during the differentiation of monocytes into dendritic cells (Wang et al., 2015). Lnc-DC regulates the expression of several genes that are key players in dendritic cell differentiation, maturation and function, by binding to STAT3. Another study identified Lnc-MC as a PU.1-regulated lncRNA that competes with miR-199a-5p and alleviates repression of the mRNA of activin A receptor type 1B (ACVR1B), an important regulator of monocyte to macrophage differentiation (Chen et al., 2015). Similarly, in the present study, PU.1 dependent lncRNA LINC00211 was found to be downregulated upon differentiation of monocytes to macrophages and it regulates several genes that have been associated with the differentiation process. For example, S100A8 and S100A9, two proteins that were dysregulated upon LINC00211 overexpression or knock out, are myeloid related proteins that have been involved in several aspects in myeloid cell differentiation and function (Ingersoll et al., 2010, Edgeworth et al., 1991). Notably, expression of the two proteins seems to be higher in classical CD14<sup>++</sup>CD16<sup>-</sup> monocytes compared to

nonclassical CD14<sup>+</sup>CD16<sup>++</sup> monocytes (Ingersoll et al., 2010). This suggests that these proteins may be involved in controlling cell lineage fate. Furthermore, S100A8 and S100A9 are more abundant in neutrophils and constitute ~45% of all cytosolic proteins, compared to only about 1% in monocytes (Edgeworth et al., 1991), which again correlates with the expression levels of LINC00211 that is higher in granulocytes compared to monocytes. Additionally, another protein, CHI3L1, was upregulated upon overexpression of LINC00211. This gene is expressed in a variety of cells, including neutrophils and macrophages (Nordenbaek et al., 1998, Rahli et al., 2003). It has been reported to be upregulated during monocyte to macrophage differentiation and during polarisation into an 'M1'-like phenotype of macrophages (Di Rosa et al., 2013). Together, these data suggest that LINC00211 is essential for the physiological development and differentiation of immune cells. Moreover, LINC00211 may serve as a novel biomarker for myeloid immune cell infiltration, as it is upregulated in lung fluid from patients with acute infection or IPF as a chronic inflammatory disease (see above). Interestingly LINC00211 controlled gene S100A9 has been suggested as a biomarker for IPF. Hara et al., demonstrated that patients with IPF have higher levels of S100A9 in their BAL fluids compared to healthy controls (Hara et al., 2011). The present study shows that, LINC00211, expression of which is also elevated in IPF lungs, negatively regulates the expression of S100A9, probably in a feedback-manner through PU.1.

Myeloid cell development critically depends on the PU.1 transcription factor. PU.1 knock out mice die during the late stage of embryonic development or immediately after birth and show impaired granulocyte, monocyte, B-cell and NK cell, but not megakaryocyte and erythrocyte development (McKercher et al., 1996, Scott et al., 1994, Colucci et al., 2001). The regulation of LINC00211 by PU.1 suggests an involvement of this lincRNA in the development and differentiation of myeloid cells. Furthermore, genes that are downregulated or upregulated upon LINC00211 overexpression are also downregulated and upregulated in the same manner upon PU.1 knock down, respectively. This suggests a negative feedback regulation of PU.1 by LINC00211. Negative feedback loops are very common in nature, and other non-coding RNAs function through this regulation mode. For example, miR-146a is upregulated by the TLR-NF- $\kappa$ B pathway but inhibits the same signalling axis by targeting TRAF6 and IRAK1 (Taganov et al., 2006). Recently, lincRNA p-21 has been shown to be part of a double negative feedback loop involving p53, the miR-181 family and PKC- $\delta$  during microglia activation (Ye et al., 2018). Another lincRNA, Lethe, feed-back regulates NF $\kappa$ B, by directly binding to this protein (Rapicavoli et al., 2013). It remains to be tested, whether LINC00211 adopts a similar regular

mode of negative feed-back control by interacting with its upstream transcription factor PU.1 directly.

The limited knowledge about the roles of lncRNAs in leukocyte differentiation and the mechanistic nature of lncRNAs in general, suggests that this topic will be of high interest to the community in the years to come. In the current project, previously unknown lncRNAs were characterised as specific leukocyte markers and LINC00211 was revealed as an important regulator of monocyte to macrophage differentiation. The presented data and previous reports suggest that more lncRNAs might be involved in the regulation of haematopoiesis than currently known. This prediction is also in line with the notion that the number of lncRNA but not mRNA genes increases with the cellular complexity of an organism (Mattick et al., 2018, Liu et al., 2013, Taft et al., 2007). The immune systems of higher vertebrates represent a good example of such cellular complexity, requiring precise control mechanisms to prevent from defects in the formation of the different lineages. PU.1 for instance primes cells to enter a specific hematopoietic differentiation program, but the exact PU.1 dose determines the eventual terminal cell fate (Mak et al., 2011). Thus, precise stabilization of the levels of transcription factors generating cellular heterogeneity, such as PU.1, is required, for instance through negative feedback control by lncRNAs such as LINC00211. Understanding the involvement of further lncRNAs in this process may not only refine our knowledge about immune cell development, but also aid the fight against pathologies, were this process is impaired or dysregulated.

## **4.2 Discussion - LncRNAs in macrophage activation**

During the past few years, it has become evident that lncRNAs play major roles in a variety of cellular processes. The recent methodological advantages made it possible to unveil the functions of several lncRNAs and acknowledge their importance as cellular biomolecules, similar to mRNAs and other well-characterised RNA classes. This study was focused on lncRNAs that are involved in macrophage activation by inflammatory stimuli. Probably due to the heterogeneity in lncRNA function, and the lack of methodological consensus regarding their characterization, most of the robustly LPS-induced lncRNAs that were identified in this study have remained largely uncharacterised (Figure 3.2.1.F). Previously, lncRNAs were sub-classified as cis- or trans-acting or genic and intergenic depending on their mode of action and their site of origin in the genome, respectively (Spurlock et al., 2016, Rinn and Chang, 2012). In agreement with previous published findings, this study suggests that lncRNAs can be further subcategorized according to their association and co-sedimentation with ribosomes, and thus

their coding potential. In macrophages, 23.4 % of all lncRNAs co-sedimented with ribosomes and among the LPS-inducible lncRNAs the percentage found in the ribosomal fraction was increased to 49%. In line with this observation, lncRNAs were found to be located predominantly in the cytoplasm (Figure 3.1.2.A). While the classic narrative assumes lncRNAs to function mostly in the nucleus, recent literature supports the notion that lncRNAs may locate to and act in the cytoplasm (Bouvrette et al., 2018, Carlevaro-Fita et al., 2019). Furthermore, large numbers of lncRNAs are found to be associated with ribosomal mono- and polysome fractions in sucrose gradient studies (Carlevaro-Fita et al., 2016, Van Heesch et al., 2014). Recently, > 35 % of lncRNAs in bacterially challenged murine macrophages were reported to associate with ribosomes (Jackson et al., 2018). The authors also found non-canonical open reading frames in a number of ribosome-associated lncRNAs, questioning their non-coding nature. On the other hand, cytoplasmic lncRNAs might associate with ribosomes to regulate translation rather than being translated. lncRNAs, which do not co-sediment with ribosomes, exhibit highly heterogeneous glycerol-gradient sedimentation profiles, which indicates association with distinct protein complexes and thus suggests their involvement in various cellular processes. In contrast to sucrose gradients, glycerol gradients can resolve molecular complexes lighter than the heavy ribosomal complexes, and they have been used to investigate other lncRNAs. NEAT1 lincRNA was found to co-sedimentate with paraspeckle and immune-regulatory proteins after glycerol gradient sedimentation (Morchikh et al., 2017). Recently, glycerol gradient profiling was also applied to illustrate the differential association of bacterial regulatory RNA with RNA-binding proteins (Smirnov et al., 2016) and in this study, a similar strategy was adopted to extend lncRNA subcellular resolution from the presently available polysome profiles to light-weight molecular machineries. The distinct migration profiles of ribosome-independent lncRNAs match the expected diversity of lncRNA functions and subcellular localization patterns. The datasets of this study provide a rich resource to investigate the functional properties of many uncharacterized macrophage lncRNAs based on their subcellular localization and co-migration with cellular machineries.

The subcellular profiling approach was used in this study to select ribosome-independent, previously uncharacterized lncRNAs for further mechanistic investigation. From the datasets, MaIL1 was chosen, due to several criteria like high upregulation upon LPS stimulation, ribosome-independence and cytosolic localisation. MaIL1 was identified as a novel positive regulator of TLR4-triggered type I IFN induction and antimicrobial defence. Very recently, lncRNA Lnczc3h7a was described as a positive regulator of type I IFN induction in antiviral immunity downstream of RIG-I (Lin et al., 2019). Interestingly, Lnczc3h7a interacts with the

TRIM25 ubiquitin-ligase and induces RIG-I ubiquitination, similar to the control of OPTN ubiquitination by MaIL1. Thus, several lncRNAs may be involved in the control of ubiquitination-dependent immune signal transduction. Another very recent report characterizes NRIR, a top-induced transcript in the datasets generated during the present study, as a positive regulator of the autocrine response to type I IFNs in human monocytes (Mariotti et al., 2019). These findings suggest that TLR4-TIRF or RIG-I activation involves different lncRNAs such as Lnczc3h7a or MaIL1 to promote type I IFN production and later other lncRNAs, such as NRIR, to promote the autocrine response. Other lncRNAs, such as Lnc-Lsmb3, lnc-ITPRIP-1 and NEAT1, have previously been implicated in type I IFN responses as well. Lnc-Lsmb3 for instance negatively regulates type I IFN, by antagonising the binding of exogenous RNAs to RIG-I. The binding prevents the conformational changes of RIG-I and thus the downstream signalling (Jiang et al., 2018). Lnc-ITPRIP-1 on the other hand positively regulates type I IFN production through binding to the viral RNA sensor MDA5 and boosting its oligomerisation and thus promoting IRF3 phosphorylation (Xie et al., 2018). LncRNA NEAT, which was also found to co-sedimentate with MaIL1 on the glycerol gradient, binds to SFPQ and HEXIM1 and mediates the formation of a protein complex that facilitates the production of type I IFNs (Morchikh et al., 2017). MaIL1 though, is the first lncRNA shown to be required for TLR-signalling in primary human cells to promote IFN expression and antimicrobial immunity. Type I IFN genes, which are activated by IRF transcription factors, are also co-regulated by the NF- $\kappa$ B transcription factor. It has been reported that NF- $\kappa$ B activity is also controlled by several non-coding RNAs in myeloid and non-myeloid cells. Micro RNAs, such as miR-146 and miR-155, are known to be involved in the regulation of the NF- $\kappa$ B signal transduction by targeting several components of the signal cascade (Taganov et al., 2006, Schulte et al., 2012, Janga et al., 2018). Besides miRNAs, several lncRNAs have also been implicated in the NF- $\kappa$ B signalling pathway. For example, PACER directly interacts with NF- $\kappa$ B repressive subunit p50 and prevents it from binding to the Cox-2 promoter (Krawczyk et al., 2014). Lethe on the other hand acts as a negative feedback regulator of the NF- $\kappa$ B pathway. The NF- $\kappa$ B signalling pathway induces Lethe, which subsequently interacts with the p65 NF- $\kappa$ B subunit and inhibits its activity (Rapicavoli et al., 2013). Another example is the cytoplasmic lncRNA Carlr, which promotes NF- $\kappa$ B dependent immune gene expression and has been associated with Celiac disease (Castellanos-Rubio et al., 2017). Taken together these different studies suggest a complex lncRNA network regulating the innate immune signalling pathways in order to balance the immune-response outcome. Surprisingly, despite several existing examples of immune-



associated lncRNAs, the RNA-Seq profiles of this study suggest that only a small fraction of immune-responsive lncRNAs in human macrophages has been characterized to date.

The present work fosters an improved understanding of lncRNAs involved in inflammatory responses in general and human macrophages specifically. The recorded RNA sequencing data provide a comprehensive catalogue of mostly uncharacterised lncRNAs with potential implications in the pathophysiological responses of macrophages. Furthermore, the gradient co-seidimentation data are a valuable resource for further functional characterisation of these novel lncRNAs. The characterisation of MAIL1 as an important regulator of the type I interferon production may serve as a blueprint for further studies. In the light of emerging antisense drug chemistry, riboregulators, like MAIL1, might also constitute superior target-candidates to prevent from or control malfunctions of the immune system due to their strict spatiotemporal expression patterns.

## 5. References

Aiuti A, Webb IJ, Bleul C, Springer T, Gutierrez-Ramos JC (1997) The chemokine SDF-1 is a chemoattractant for human CD34+ hematopoietic progenitor cells and provides a new mechanism to explain the mobilization of CD34+ progenitors to peripheral blood. *The Journal of experimental medicine* **185**: 111-120

Akashi K, Traver D, Miyamoto T, Weissman IL (2000) A clonogenic common myeloid progenitor that gives rise to all myeloid lineages. *Nature* **404**: 193-197

Akira S, Uematsu S, Takeuchi O (2006) Pathogen recognition and innate immunity. *Cell* **124**: 783-801

Anderson DM, Anderson KM, Chang CL, Makarewich CA, Nelson BR, McAnally JR, Kasaragod P, Shelton JM, Liou J, Bassel-Duby R, Olson EN (2015) A micropeptide encoded by a putative long noncoding RNA regulates muscle performance. *Cell* **160**: 595-606

Antony-Debré I, Paul A, Leite J, Mitchell K, Kim HM, Carvajal LA, Todorova TI, Huang K, Kumar A, Farahat AA, Bartholdy B, Narayanagari S-R, Chen J, Ambesi-Impiombato A, Ferrando AA, Mantzaris I, Gavathiotis E, Verma A, Will B, Boykin DW, Wilson WD, Poon GMK, Steidl U (2017) Pharmacological inhibition of the transcription factor PU.1 in leukemia. *The Journal of Clinical Investigation* **127**: 4297-4313

Aravin A, Gaidatzis D, Pfeffer S, Lagos-Quintana M, Landgraf P, Iovino N, Morris P, Brownstein MJ, Kuramochi-Miyagawa S, Nakano T, Chien M, Russo JJ, Ju J, Sheridan R, Sander C, Zavolan M, Tuschl T (2006) A novel class of small RNAs bind to MILI protein in mouse testes. *Nature* **442**: 203-207

Aravin AA, Naumova NM, Tulin AV, Vagin VV, Rozovsky YM, Gvozdev VA (2001) Double-stranded RNA-mediated silencing of genomic tandem repeats and transposable elements in the *D. melanogaster* germline. *Current Biology* **11**: 1017-1027

- Aravin AA, Sachidanandam R, Bourc'his D, Schaefer C, Pezic D, Toth KF, Bestor T, Hannon GJ (2008) A piRNA pathway primed by individual transposons is linked to de novo DNA methylation in mice. *Molecular cell* **31**: 785-799
- Atianand MK, Hu W, Satpathy AT, Shen Y, Ricci EP, Alvarez-Dominguez JR, Bhatta A, Schattgen SA, McGowan JD, Blin J, Braun JE, Gandhi P, Moore MJ, Chang HY, Lodish HF, Caffrey DR, Fitzgerald KA (2016) A Long Noncoding RNA lincRNA-EPS Acts as a Transcriptional Brake to Restrain Inflammation. *Cell* **165**: 1672-1685
- Baldrige MT, King KY, Goodell MA (2011) Inflammatory signals regulate hematopoietic stem cells. *Trends in immunology* **32**: 57-65
- Barbagallo D, Vittone G, Romani M, Purrello M (2018) Noncoding RNAs in Health and Disease. *International journal of genomics* **2018**: 9135073
- Bazzini AA, Johnstone TG, Christiano R, Mackowiak SD, Obermayer B, Fleming ES, Vejnar CE, Lee MT, Rajewsky N, Walther TC, Giraldez AJ (2014) Identification of small ORFs in vertebrates using ribosome footprinting and evolutionary conservation. *The EMBO journal* **33**: 981-993
- Benoit Bouvrette LP, Cody NAL, Bergalet J, Lefebvre FA, Diot C, Wang X, Blanchette M, Lécuyer E (2018) CeFra-seq reveals broad asymmetric mRNA and noncoding RNA distribution profiles in Drosophila and human cells. *Rna* **24**: 98-113
- Berger KH, Isberg RR (1993) Two distinct defects in intracellular growth complemented by a single genetic locus in *Legionella pneumophila*. *Molecular Microbiology* **7**: 7-19
- Bertin J, Nir W-J, Fischer CM, Tayber OV, Errada PR, Grant JR, Keilty JJ, Gosselin ML, Robison KE, Wong GHW, Glucksmann MA, DiStefano PS (1999) Human CARD4 Protein Is a Novel CED-4/Apaf-1 Cell Death Family Member That Activates NF- $\kappa$ B. *Journal of Biological Chemistry* **274**: 12955-12958

- Bertrand JY, Kim AD, Violette EP, Stachura DL, Cisson JL, Traver D (2007) Definitive hematopoiesis initiates through a committed erythromyeloid progenitor in the zebrafish embryo. *Development* **134**: 4147-4156
- Beutler B (2004) Innate immunity: an overview. *Molecular Immunology* **40**: 845-859
- Bhatt DM, Pandya-Jones A, Tong AJ, Barozzi I, Lissner MM, Natoli G, Black DL, Smale ST (2012) Transcript dynamics of proinflammatory genes revealed by sequence analysis of subcellular RNA fractions. *Cell* **150**: 279-290
- Bhatt Dev M, Pandya-Jones A, Tong A-J, Barozzi I, Lissner Michelle M, Natoli G, Black Douglas L, Smale Stephen T (2012) Transcript Dynamics of Proinflammatory Genes Revealed by Sequence Analysis of Subcellular RNA Fractions. *Cell* **150**: 279-290
- Bleul CC, Fuhlbrigge RC, Casasnovas JM, Aiuti A, Springer TA (1996) A highly efficacious lymphocyte chemoattractant, stromal cell-derived factor 1 (SDF-1). *The Journal of experimental medicine* **184**: 1101-1109
- Bleul CC, Wu L, Hoxie JA, Springer TA, Mackay CR (1997) The HIV coreceptors CXCR4 and CCR5 are differentially expressed and regulated on human T lymphocytes. *Proceedings of the National Academy of Sciences* **94**: 1925-1930
- Borchert GM, Lanier W, Davidson BL (2006) RNA polymerase III transcribes human microRNAs. *Nature structural & molecular biology* **13**: 1097-1101
- Boxx GM, Cheng G (2016) The Roles of Type I Interferon in Bacterial Infection. *Cell host & microbe* **19**: 760-769
- Brack C, Hirama M, Lenhard-Schuller R, Tonegawa S (1978) A complete immunoglobulin gene is created by somatic recombination. *Cell* **15**: 1-14
- Brand BC, Sadosky AB, Shuman HA (1994) The Legionella pneumophila icm locus: a set of genes required for intracellular multiplication in human macrophages. *Molecular Microbiology* **14**: 797-808

Brannan CI, Dees EC, Ingram RS, Tilghman SM (1990) The product of the H19 gene may function as an RNA. *Molecular and cellular biology* **10**: 28-36

Brinkmann V, Reichard U, Goosmann C, Fauler B, Uhlemann Y, Weiss DS, Weinrauch Y, Zychlinsky A (2004) Neutrophil Extracellular Traps Kill Bacteria. *Science* **303**: 1532-1535

Brown CJ, Hendrich BD, Rupert JL, Lafrenière RG, Xing Y, Lawrence J, Willard HF (1992) The human XIST gene: Analysis of a 17 kb inactive X-specific RNA that contains conserved repeats and is highly localized within the nucleus. *Cell* **71**: 527-542

Broz P, Ohlson MB, Monack DM (2012) Innate immune response to *Salmonella typhimurium*, a model enteric pathogen. *Gut Microbes* **3**: 62-70

Cabili MN, Trapnell C, Goff L, Koziol M, Tazon-Vega B, Regev A, Rinn JL (2011) Integrative annotation of human large intergenic noncoding RNAs reveals global properties and specific subclasses. *Genes & development* **25**: 1915-1927

Cai X, Hagedorn CH, Cullen BR (2004) Human microRNAs are processed from capped, polyadenylated transcripts that can also function as mRNAs. *Rna* **10**: 1957-1966

Carlevaro-Fita J, Rahim A, Guigo R, Vardy LA, Johnson R (2016) Cytoplasmic long noncoding RNAs are frequently bound to and degraded at ribosomes in human cells. *Rna* **22**: 867-882

Carpenter S, Aiello D, Atianand MK, Ricci EP, Gandhi P, Hall LL, Byron M, Monks B, Henry-Bezy M, Lawrence JB, O'Neill LAJ, Moore MJ, Caffrey DR, Fitzgerald KA (2013) A Long Noncoding RNA Mediates Both Activation and Repression of Immune Response Genes. *Science* **341**: 789-792

Carrieri C, Cimatti L, Biagioli M, Beugnet A, Zucchelli S, Fedele S, Pesce E, Ferrer I, Collavin L, Santoro C, Forrest AR, Carninci P, Biffo S, Stupka E, Gustincich S (2012) Long non-coding antisense RNA controls Uchl1 translation through an embedded SINEB2 repeat. *Nature* **491**: 454-457

- Carthew RW, Sontheimer EJ (2009) Origins and Mechanisms of miRNAs and siRNAs. *Cell* **136**: 642-655
- Caruso R, Warner N, Inohara N, Nunez G (2014) NOD1 and NOD2: signaling, host defense, and inflammatory disease. *Immunity* **41**: 898-908
- Castellanos-Rubio A, Fernandez-Jimenez N, Kratchmarov R, Luo X, Bhagat G, Green PHR, Schneider R, Kiledjian M, Bilbao JR, Ghosh S (2016) A long noncoding RNA associated with susceptibility to celiac disease. *Science* **352**: 91-95
- Cazalet C, Rusniok C, Bruggemann H, Zidane N, Magnier A, Ma L, Tichit M, Jarraud S, Bouchier C, Vandenesch F, Kunst F, Etienne J, Glaser P, Buchrieser C (2004) Evidence in the *Legionella pneumophila* genome for exploitation of host cell functions and high genome plasticity. *Nature genetics* **36**: 1165-1173
- Chamaillard M, Hashimoto M, Horie Y, Masumoto J, Qiu S, Saab L, Ogura Y, Kawasaki A, Fukase K, Kusumoto S, Valvano MA, Foster SJ, Mak TW, Nuñez G, Inohara N (2003) An essential role for NOD1 in host recognition of bacterial peptidoglycan containing diaminopimelic acid. *Nature immunology* **4**: 702-707
- Chen MT, Lin HS, Shen C, Ma YN, Wang F, Zhao HL, Yu J, Zhang JW (2015) PU.1-Regulated Long Noncoding RNA Inc-MC Controls Human Monocyte/Macrophage Differentiation through Interaction with MicroRNA 199a-5p. *Molecular and cellular biology* **35**: 3212-3224
- Chen W, Jin W, Hardegen N, Lei KJ, Li L, Marinos N, McGrady G, Wahl SM (2003) Conversion of peripheral CD4<sup>+</sup>CD25<sup>-</sup> naive T cells to CD4<sup>+</sup>CD25<sup>+</sup> regulatory T cells by TGF-β induction of transcription factor Foxp3. *The Journal of experimental medicine* **198**: 1875-1886
- Chen YG, Satpathy AT, Chang HY (2017) Gene regulation in the immune system by long noncoding RNAs. *Nature immunology* **18**: 962-972

- Chistiakov DA, Orekhov AN, Sobenin IA, Bobryshev YV (2014) Plasmacytoid dendritic cells: development, functions, and role in atherosclerotic inflammation. *Frontiers in physiology* **5**: 279
- Choi YJ, Im E, Chung HK, Pothoulakis C, Rhee SH (2010) TRIF mediates Toll-like receptor 5-induced signaling in intestinal epithelial cells. *The Journal of biological chemistry* **285**: 37570-37578
- Chua F, Dunsmore SE, Clingen PH, Mutsaers SE, Shapiro SD, Segal AW, Roes J, Laurent GJ (2007) Mice lacking neutrophil elastase are resistant to bleomycin-induced pulmonary fibrosis. *Am J Pathol* **170**: 65-74
- Cianciotto NP, Fields BS (1992) Legionella pneumophila mip gene potentiates intracellular infection of protozoa and human macrophages. *Proceedings of the National Academy of Sciences* **89**: 5188-5191
- Clemens DL, Lee B-Y, Horwitz MA (2000) Deviant Expression of Rab5 on Phagosomes Containing the Intracellular Pathogens *Mycobacterium tuberculosis* and *Legionella pneumophila* Is Associated with Altered Phagosomal Fate. *Infection and immunity* **68**: 2671-2684
- Clemson CM, Hutchinson JN, Sara SA, Ensminger AW, Fox AH, Chess A, Lawrence JB (2009) An architectural role for a nuclear noncoding RNA: NEAT1 RNA is essential for the structure of paraspeckles. *Molecular cell* **33**: 717-726
- Cobaleda C, Schebesta A, Delogu A, Busslinger M (2007) Pax5: the guardian of B cell identity and function. *Nature immunology* **8**: 463-470
- Collin M, Bigley V (2018) Human dendritic cell subsets: an update. *Immunology* **154**: 3-20
- Colonna M, Nakajima H, Navarro F, López-Botet M (1999) A novel family of Ig-like receptors for HLA class I molecules that modulate function of lymphoid and myeloid cells. *Journal of leukocyte biology* **66**: 375-381

- Colucci F, Samson SI, DeKoter RP, Lantz O, Singh H, Di Santo JP (2001) Differential requirement for the transcription factor PU.1 in the generation of natural killer cells versus B and T cells. *Blood* **97**: 2625-2632
- Cuff AO, Robertson FP, Stegmann KA, Pallett LJ, Maini MK, Davidson BR, Male V (2016) Eomeshi NK Cells in Human Liver Are Long-Lived and Do Not Recirculate but Can Be Replenished from the Circulation. *Journal of immunology* **197**: 4283-4291
- Cumano A, Godin I (2007) Ontogeny of the hematopoietic system. *Annual review of immunology* **25**: 745-785
- Curtale G, Mirolo M, Renzi TA, Rossato M, Bazzoni F, Locati M (2013) Negative regulation of Toll-like receptor 4 signaling by IL-10-dependent microRNA-146b. *Proceedings of the National Academy of Sciences of the United States of America* **110**: 11499-11504
- Czech B, Malone CD, Zhou R, Stark A, Schlingehayde C, Dus M, Perrimon N, Kellis M, Wohlschlegel JA, Sachidanandam R, Hannon GJ, Brennecke J (2008) An endogenous small interfering RNA pathway in Drosophila. *Nature* **453**: 798-802
- Czernielewski JM, Demarchez M (1987) Further Evidence for the Self-Reproducing Capacity of Langerhans Cells in Human Skin. *Journal of Investigative Dermatology* **88**: 17-20
- Dahl R, Walsh JC, Lancki D, Laslo P, Iyer SR, Singh H, Simon MC (2003) Regulation of macrophage and neutrophil cell fates by the PU.1:C/EBPalpha ratio and granulocyte colony-stimulating factor. *Nature immunology* **4**: 1029-1036
- D'Apuzzo M, Rolink A, Loetscher M, Hoxie JA, Clark-Lewis I, Melchers F, Baggiolini M, Moser B (1997) The chemokine SDF-1, stromal cell-derived factor 1, attracts early stage B cell precursors via the chemokine receptor CXCR4. *European Journal of Immunology* **27**: 1788-1793
- Davies LC, Jenkins SJ, Allen JE, Taylor PR (2013) Tissue-resident macrophages. *Nature immunology* **14**: 986-995



- Davis MP, Carrieri C, Saini HK, van Dongen S, Leonardi T, Bussotti G, Monahan JM, Auchynnikava T, Bitetti A, Rappsilber J, Allshire RC, Shkumatava A, O'Carroll D, Enright AJ (2017) Transposon-driven transcription is a conserved feature of vertebrate spermatogenesis and transcript evolution. *EMBO reports* **18**: 1231-1247
- DebRoy S, Dao J, Soderberg M, Rossier O, Cianciotto NP (2006) Legionella pneumophila type II secretome reveals unique exoproteins and a chitinase that promotes bacterial persistence in the lung. *Proceedings of the National Academy of Sciences of the United States of America* **103**: 19146-19151
- Deiwick J, Salcedo SP, Boucrot E, Gilliland SM, Henry T, Petermann N, Waterman SR, Gorvel J-P, Holden DW, Méresse S (2006) The Translocated *Salmonella* Effector Proteins SseF and SseG Interact and Are Required To Establish an Intracellular Replication Niche. *Infection and immunity* **74**: 6965-6972
- Derrien T, Johnson R, Bussotti G, Tanzer A, Djebali S, Tilgner H, Guernec G, Martin D, Merkel A, Knowles DG, Lagarde J, Veeravalli L, Ruan X, Ruan Y, Lassmann T, Carninci P, Brown JB, Lipovich L, Gonzalez JM, Thomas M, Davis CA, Shiekhhattar R, Gingeras TR, Hubbard TJ, Notredame C, Harrow J, Guigo R (2012) The GENCODE v7 catalog of human long noncoding RNAs: analysis of their gene structure, evolution, and expression. *Genome research* **22**: 1775-1789
- Desai O, Winkler J, Minasyan M, Herzog EL (2018) The Role of Immune and Inflammatory Cells in Idiopathic Pulmonary Fibrosis. *Front Med (Lausanne)* **5**: 43-43
- Desterro JMP, Keegan LP, Lafarga M, Berciano MT, O'Connell M, Carmo-Fonseca M (2003) Dynamic association of RNA-editing enzymes with the nucleolus. *Journal of Cell Science* **116**: 1805-1818
- Di Rosa M, Malaguarnera G, De Gregorio C, Drago F, Malaguarnera L (2013) Evaluation of CHI3L-1 and CHIT-1 expression in differentiated and polarized macrophages. *Inflammation* **36**: 482-492

- Didichenko SA, Spiegl N, Brunner T, Dahinden CA (2008) IL-3 induces a Pim1-dependent antiapoptotic pathway in primary human basophils. *Blood* **112**: 3949-3958
- Dignam JD, Lebovitz RM, Roeder RG (1983) Accurate transcription initiation by RNA polymerase II in a soluble extract from isolated mammalian nuclei. *Nucleic acids research* **11**: 1475-1489
- Dominissini D, Moshitch-Moshkovitz S, Schwartz S, Salmon-Divon M, Ungar L, Osenberg S, Cesarkas K, Jacob-Hirsch J, Amariglio N, Kupiec M, Sorek R, Rechavi G (2012) Topology of the human and mouse m6A RNA methylomes revealed by m6A-seq. *Nature* **485**: 201-206
- Donskoy E, Goldschneider I (1992) Thymocytopoiesis is maintained by blood-borne precursors throughout postnatal life. A study in parabiotic mice. *The Journal of Immunology* **148**: 1604-1612
- Drickamer K (1999) C-type lectin-like domains. *Current Opinion in Structural Biology* **9**: 585-590
- Dubos RJ (1939) STUDIES ON A BACTERICIDAL AGENT EXTRACTED FROM A SOIL BACILLUS : I. PREPARATION OF THE AGENT. ITS ACTIVITY IN VITRO. *The Journal of experimental medicine* **70**: 1-10
- Ebert RH, Florey HW (1939) The Extravascular Development of the Monocyte Observed In vivo. *Br J Exp Pathol* **20**: 342-356
- Edgeworth J, Gorman M, Bennett R, Freemont P, Hogg N (1991) Identification of p8,14 as a highly abundant heterodimeric calcium binding protein complex of myeloid cells. *Journal of Biological Chemistry* **266**: 7706-7713
- Engvall E, Perlmann P (1971) Enzyme-linked immunosorbent assay (ELISA) quantitative assay of immunoglobulin G. *Immunochemistry* **8**: 871-874

- Ensminger AW (2016) Legionella pneumophila, armed to the hilt: justifying the largest arsenal of effectors in the bacterial world. *Current opinion in microbiology* **29**: 74-80
- Ewald SE, Engel A, Lee J, Wang M, Bogyo M, Barton GM (2011) Nucleic acid recognition by Toll-like receptors is coupled to stepwise processing by cathepsins and asparagine endopeptidase. *The Journal of experimental medicine* **208**: 643-651
- Fàbrega A, Vila J (2013) >Salmonella enterica</span> Serovar Typhimurium Skills To Succeed in the Host: Virulence and Regulation. *Clinical Microbiology Reviews* **26**: 308-341
- Fairbairn LJ, Cowling GJ, Reipert BM, Dexter TM (1993) Suppression of apoptosis allows differentiation and development of a multipotent hemopoietic cell line in the absence of added growth factors. *Cell* **74**: 823-832
- Finlay BB, Ruschkowski S, Dedhar S (1991) Cytoskeletal rearrangements accompanying salmonella entry into epithelial cells. *Journal of Cell Science* **99**: 283-296
- Fire A, Xu S, Montgomery MK, Kostas SA, Driver SE, Mello CC (1998) Potent and specific genetic interference by double-stranded RNA in *Caenorhabditis elegans*. *Nature* **391**: 806-811
- Forstemann K, Tomari Y, Du T, Vagin VV, Denli AM, Bratu DP, Klattenhoff C, Theurkauf WE, Zamore PD (2005) Normal microRNA maturation and germ-line stem cell maintenance requires Loquacious, a double-stranded RNA-binding domain protein. *PLoS biology* **3**: e236
- Foster JW, Hall HK (1991) Inducible pH homeostasis and the acid tolerance response of *Salmonella typhimurium*. *Journal of Bacteriology* **173**: 5129-5135
- Franchi L (2011) Role of inflammasomes in salmonella infection. *Frontiers in microbiology* **2**: 8-8
- Francis CL, Ryan TA, Jones BD, Smith SJ, Falkow S (1993) Ruffles induced by *Salmonella* and other stimuli direct macropinocytosis of bacteria. *Nature* **364**: 639-642

- Franco IS, Shuman HA, Charpentier X (2009) The perplexing functions and surprising origins of *Legionella pneumophila* type IV secretion effectors. *Cellular microbiology* **11**: 1435-1443
- Frankenberger M, Hofer TPJ, Marei A, Dayyani F, Schewe S, Strasser C, Aldraihim A, Stanzel F, Lang R, Hoffmann R, Costa OPd, Buch T, Ziegler-Heitbrock L (2012) Transcript profiling of CD16-positive monocytes reveals a unique molecular fingerprint. *European Journal of Immunology* **42**: 957-974
- Freud AG, Mundy-Bosse BL, Yu J, Caligiuri MA (2017) The Broad Spectrum of Human Natural Killer Cell Diversity. *Immunity* **47**: 820-833
- Friedman RC, Farh KK, Burge CB, Bartel DP (2009) Most mammalian mRNAs are conserved targets of microRNAs. *Genome research* **19**: 92-105
- Frutuoso MS, Hori JI, Pereira MS, Junior DS, Sonogo F, Kobayashi KS, Flavell RA, Cunha FQ, Zamboni DS (2010) The pattern recognition receptors Nod1 and Nod2 account for neutrophil recruitment to the lungs of mice infected with *Legionella pneumophila*. *Microbes and infection* **12**: 819-827
- Galloway JL, Zon LI (2003) 3 Ontogeny of hematopoiesis: Examining the emergence of hematopoietic cells in the vertebrate embryo. In *Current Topics in Developmental Biology* Vol. 53, pp 139-158. Academic Press
- Garcia-del Portillo F, Finlay BB (1994) Salmonella invasion of nonphagocytic cells induces formation of macropinosomes in the host cell. *Infection and immunity* **62**: 4641-4645
- Garcia-del Portillo F, Finlay BB (1995) Targeting of *Salmonella typhimurium* to vesicles containing lysosomal membrane glycoproteins bypasses compartments with mannose 6-phosphate receptors. *The Journal of cell biology* **129**: 81-97
- Garduno RA, Garduno E, Hiltz M, Hoffman PS (2002) Intracellular growth of *Legionella pneumophila* gives rise to a differentiated form dissimilar to stationary-phase forms. *Infection and immunity* **70**: 6273-6283

Gasteiger G, D'Oswaldo A, Schubert DA, Weber A, Bruscia EM, Hartl D (2017) Cellular Innate Immunity: An Old Game with New Players. *Journal of innate immunity* **9**: 111-125

Geering B, Stoeckle C, Conus S, Simon HU (2013) Living and dying for inflammation: neutrophils, eosinophils, basophils. *Trends in immunology* **34**: 398-409

Gilbert LA, Larson MH, Morsut L, Liu Z, Brar GA, Torres SE, Stern-Ginossar N, Brandman O, Whitehead EH, Doudna JA, Lim WA, Weissman JS, Qi LS (2013) CRISPR-mediated modular RNA-guided regulation of transcription in eukaryotes. *Cell* **154**: 442-451

Girard A, Sachidanandam R, Hannon GJ, Carmell MA (2006) A germline-specific class of small RNAs binds mammalian Piwi proteins. *Nature* **442**: 199-202

Girardin SE, Boneca IG, Carneiro LAM, Antignac A, Jéhanno M, Viala J, Tedin K, Taha M-K, Labigne A, Zähringer U, Coyle AJ, DiStefano PS, Bertin J, Sansonetti PJ, Philpott DJ (2003) Nod1 Detects a Unique Muropeptide from Gram-Negative Bacterial Peptidoglycan. *Science* **300**: 1584-1587

Gleason CE, Ordureau A, Gourlay R, Arthur JS, Cohen P (2011) Polyubiquitin binding to optineurin is required for optimal activation of TANK-binding kinase 1 and production of interferon beta. *The Journal of biological chemistry* **286**: 35663-35674

Gleason CE, Ordureau A, Gourlay R, Arthur JSC, Cohen P (2011) Polyubiquitin binding to optineurin is required for optimal activation of TANK-binding kinase 1 and the production of interferon  $\beta$ . *Journal of Biological Chemistry*

Goldstein B, Agranat-Tamir L, Light D, Ben-Naim Zgayer O, Fishman A, Lamm AT (2017) A-to-I RNA editing promotes developmental stage-specific gene and lncRNA expression. *Genome research* **27**: 462-470

- Gomez JA, Wapinski OL, Yang YW, Bureau JF, Gopinath S, Monack DM, Chang HY, Brahic M, Kirkegaard K (2013) The NeST long ncRNA controls microbial susceptibility and epigenetic activation of the interferon-gamma locus. *Cell* **152**: 743-754
- Gordon S, Taylor PR (2005) Monocyte and macrophage heterogeneity. *Nature reviews Immunology* **5**: 953-964
- Gu W, Lee HC, Chaves D, Youngman EM, Pazour GJ, Conte D, Jr., Mello CC (2012) CapSeq and CIP-TAP identify Pol II start sites and reveal capped small RNAs as *C. elegans* piRNA precursors. *Cell* **151**: 1488-1500
- Guo S, Lu J, Schlanger R, Zhang H, Wang JY, Fox MC, Purton LE, Fleming HH, Cobb B, Merkenschlager M, Golub TR, Scadden DT (2010) MicroRNA miR-125a controls hematopoietic stem cell number. *Proceedings of the National Academy of Sciences of the United States of America* **107**: 14229-14234
- Guttman M, Amit I, Garber M, French C, Lin MF, Feldser D, Huarte M, Zuk O, Carey BW, Cassady JP, Cabili MN, Jaenisch R, Mikkelsen TS, Jacks T, Hacohen N, Bernstein BE, Kellis M, Regev A, Rinn JL, Lander ES (2009) Chromatin signature reveals over a thousand highly conserved large non-coding RNAs in mammals. *Nature* **458**: 223-227
- Guttman M, Donaghey J, Carey BW, Garber M, Grenier JK, Munson G, Young G, Lucas AB, Ach R, Bruhn L, Yang X, Amit I, Meissner A, Regev A, Rinn JL, Root DE, Lander ES (2011) lincRNAs act in the circuitry controlling pluripotency and differentiation. *Nature* **477**: 295-300
- Haas T, Metzger J, Schmitz F, Heit A, Muller T, Latz E, Wagner H (2008) The DNA sugar backbone 2' deoxyribose determines toll-like receptor 9 activation. *Immunity* **28**: 315-323
- Halle S, Halle O, Forster R (2017) Mechanisms and Dynamics of T Cell-Mediated Cytotoxicity In Vivo. *Trends in immunology* **38**: 432-443
- Hansji H, Leung EY, Baguley BC, Finlay GJ, Cameron-Smith D, Figueiredo VC, Askarian-Amiri ME (2016) ZFAS1: a long noncoding RNA associated with ribosomes in breast cancer cells. *Biology direct* **11**: 62

Hansji H, Leung EY, Baguley BC, Finlay GJ, Cameron-Smith D, Figueiredo VC, Askarian-Amiri ME (2016) ZFAS1: a long noncoding RNA associated with ribosomes in breast cancer cells. *Biology direct* **11**: 62

Hara A, Sakamoto N, Ishimatsu Y, Kakugawa T, Nakashima S, Hara S, Adachi M, Fujita H, Mukae H, Kohno S (2012) S100A9 in BALF is a candidate biomarker of idiopathic pulmonary fibrosis. *Respiratory medicine* **106**: 571-580

Harris TH, Banigan EJ, Christian DA, Konradt C, Tait Wojno ED, Norose K, Wilson EH, John B, Weninger W, Luster AD, Liu AJ, Hunter CA (2012) Generalized Levy walks and the role of chemokines in migration of effector CD8+ T cells. *Nature* **486**: 545-548

Hawn TR, Smith KD, Aderem A, Skerrett SJ (2006) Myeloid Differentiation Primary Response Gene (88)— and Toll-Like Receptor 2—Deficient Mice Are Susceptible to Infection with Aerosolized *Legionella pneumophila*. *The Journal of Infectious Diseases* **193**: 1693-1702

Hickman HD, Reynoso GV, Ngudiankama BF, Cush SS, Gibbs J, Bennink JR, Yewdell JW (2015) CXCR3 chemokine receptor enables local CD8(+) T cell migration for the destruction of virus-infected cells. *Immunity* **42**: 524-537

Hirai H, Zhang P, Dayaram T, Hetherington CJ, Mizuno S, Imanishi J, Akashi K, Tenen DG (2006) C/EBPbeta is required for 'emergency' granulopoiesis. *Nature immunology* **7**: 732-739

Hoffman W, Lakkis FG, Chalasani G (2016) B Cells, Antibodies, and More. *Clinical journal of the American Society of Nephrology : CJASN* **11**: 137-154

Hornung V, Ellegast J, Kim S, Brzózka K, Jung A, Kato H, Poeck H, Akira S, Conzelmann K-K, Schlee M, Endres S, Hartmann G (2006) 5'-Triphosphate RNA Is the Ligand for RIG-I. *Science* **314**: 994-997

Horwitz MA (1984) Phagocytosis of the legionnaires' disease bacterium (*legionella pneumophila*) occurs by a novel mechanism: Engulfment within a Pseudopod coil. *Cell* **36**: 27-33

Horwitz MA, Maxfield FR (1984) Legionella pneumophila inhibits acidification of its phagosome in human monocytes. *The Journal of cell biology* **99**: 1936-1943

Horwitz MA, Maxfield FR (1984) Legionella pneumophila inhibits acidification of its phagosome in human monocytes. *The Journal of cell biology* **99**: 1936-1943

Hou W, Gibbs JS, Lu X, Brooke CB, Roy D, Modlin RL, Bennink JR, Yewdell JW (2012) Viral infection triggers rapid differentiation of human blood monocytes into dendritic cells. *Blood* **119**: 3128-3131

Hu G, Gong A-Y, Wang Y, Ma S, Chen X, Chen J, Su C-J, Shibata A, Strauss-Soukup JK, Drescher KM, Chen X-M (2016) LincRNA-Cox2 Promotes Late Inflammatory Gene Transcription in Macrophages through Modulating SWI/SNF-Mediated Chromatin Remodeling. *Journal of immunology (Baltimore, Md : 1950)* **196**: 2799-2808

Hu G, Tang Q, Sharma S, Yu F, Escobar TM, Muljo SA, Zhu J, Zhao K (2013) Expression and regulation of intergenic long noncoding RNAs during T cell development and differentiation. *Nature immunology* **14**: 1190-1198

Hubber A, Roy CR (2010) Modulation of host cell function by Legionella pneumophila type IV effectors. *Annual review of cell and developmental biology* **26**: 261-283

Husebye H, Aune MH, Stenvik J, Samstad E, Skjeldal F, Halaas O, Nilsen NJ, Stenmark H, Latz E, Lien E, Mollnes TE, Bakke O, Espevik T (2010) The Rab11a GTPase controls Toll-like receptor 4-induced activation of interferon regulatory factor-3 on phagosomes. *Immunity* **33**: 583-596

Hutvagner G, McLachlan J, Pasquinelli AE, Bálint É, Tuschl T, Zamore PD (2001) A Cellular Function for the RNA-Interference Enzyme Dicer in the Maturation of the *let-7* Small Temporal RNA. *Science* **293**: 834-838



Huynh H, Zheng J, Umikawa M, Zhang C, Silvany R, Iizuka S, Holzenberger M, Zhang W, Zhang CC (2011) IGF binding protein 2 supports the survival and cycling of hematopoietic stem cells. *Blood* **118**: 3236-3243

Ilott NE, Heward JA, Roux B, Tsitsiou E, Fenwick PS, Lenzi L, Goodhead I, Hertz-Fowler C, Heger A, Hall N, Donnelly LE, Sims D, Lindsay MA (2014) Long non-coding RNAs and enhancer RNAs regulate the lipopolysaccharide-induced inflammatory response in human monocytes. *Nature communications* **5**: 3979

Imamura K, Takaya A, Ishida Y-i, Fukuoka Y, Taya T, Nakaki R, Kakeda M, Imamachi N, Sato A, Yamada T, Onoguchi-Mizutani R, Akizuki G, Tanu T, Tao K, Miyao S, Suzuki Y, Nagahama M, Yamamoto T, Jensen TH, Akimitsu N (2018) Diminished nuclear RNA decay upon Salmonella infection upregulates antibacterial noncoding RNAs. *The EMBO journal* **37**: e97723

Ingersoll MA, Spanbroek R, Lottaz C, Gautier EL, Frankenberger M, Hoffmann R, Lang R, Haniffa M, Collin M, Tacke F, Habenicht AJR, Ziegler-Heitbrock L, Randolph GJ (2010) Comparison of gene expression profiles between human and mouse monocyte subsets. *Blood* **115**: e10-e19

Inohara N, Koseki T, del Peso L, Hu Y, Yee C, Chen S, Carrio R, Merino J, Liu D, Ni J, Núñez G (1999) Nod1, an Apaf-1-like Activator of Caspase-9 and Nuclear Factor- $\kappa$ B. *Journal of Biological Chemistry* **274**: 14560-14567

Inohara N, Ogura Y, Fontalba A, Gutierrez O, Pons F, Crespo J, Fukase K, Inamura S, Kusumoto S, Hashimoto M, Foster SJ, Moran AP, Fernandez-Luna JL, Nunez G (2003) Host recognition of bacterial muramyl dipeptide mediated through NOD2. Implications for Crohn's disease. *The Journal of biological chemistry* **278**: 5509-5512

Ivanovs A, Rybtsov S, Welch L, Anderson RA, Turner ML, Medvinsky A (2011) Highly potent human hematopoietic stem cells first emerge in the intraembryonic aorta-gonad-mesonephros region. *The Journal of experimental medicine* **208**: 2417-2427

Iwasaki H, Akashi K (2007) Myeloid lineage commitment from the hematopoietic stem cell. *Immunity* **26**: 726-740

Iwasaki H, Somoza C, Shigematsu H, Duprez EA, Iwasaki-Arai J, Mizuno S, Arinobu Y, Geary K, Zhang P, Dayaram T, Fenyus ML, Elf S, Chan S, Kastner P, Huettner CS, Murray R, Tenen DG, Akashi K (2005) Distinctive and indispensable roles of PU.1 in maintenance of hematopoietic stem cells and their differentiation. *Blood* **106**: 1590-1600

Jackson R, Kroehling L, Khitun A, Bailis W, Jarret A, York AG, Khan OM, Brewer JR, Skadow MH, Duizer C, Harman CCD, Chang L, Bielecki P, Solis AG, Steach HR, Slavoff S, Flavell RA (2018) The translation of non-canonical open reading frames controls mucosal immunity. *Nature* **564**: 434-438

Jackson R, Kroehling L, Khitun A, Bailis W, Jarret A, York AG, Khan OM, Brewer JR, Skadow MH, Duizer C, Harman CCD, Chang L, Bielecki P, Solis AG, Steach HR, Slavoff S, Flavell RA (2018) The translation of non-canonical open reading frames controls mucosal immunity. *Nature* **564**: 434-438

Jakubzick C, Tacke F, Ginhoux F, Wagers AJ, van Rooijen N, Mack M, Merad M, Randolph GJ (2008) Blood monocyte subsets differentially give rise to CD103<sup>+</sup> and CD103<sup>-</sup> pulmonary dendritic cell populations. *Journal of immunology* **180**: 3019-3027

James KD, Jenkinson WE, Anderson G (2018) T-cell egress from the thymus: Should I stay or should I go? *Journal of leukocyte biology* **104**: 275-284

Janeway CA, Jr., Medzhitov R (2002) Innate immune recognition. *Annual review of immunology* **20**: 197-216

Janga H, Aznaourova M, Boldt F, Damm K, Grunweller A, Schulte LN (2018) Cas9-mediated excision of proximal DNaseI/H3K4me3 signatures confers robust silencing of microRNA and long non-coding RNA genes. *PloS one* **13**: e0193066

- Jiang M, Zhang S, Yang Z, Lin H, Zhu J, Liu L, Wang W, Liu S, Liu W, Ma Y, Zhang L, Cao X (2018) Self-Recognition of an Inducible Host lncRNA by RIG-I Feedback Restricts Innate Immune Response. *Cell* **173**: 906-919.e913
- Johansson C, Ingman M, Jo Wick M (2006) Elevated neutrophil, macrophage and dendritic cell numbers characterize immune cell populations in mice chronically infected with Salmonella. *Microbial Pathogenesis* **41**: 49-58
- Johns JL, Macnamara KC, Walker NJ, Winslow GM, Borjesson DL (2009) Infection with *Anaplasma phagocytophilum* induces multilineage alterations in hematopoietic progenitor cells and peripheral blood cells. *Infection and immunity* **77**: 4070-4080
- Jones LC, Lin M-L, Chen S-S, Krug U, Hofmann W-K, Lee S, Lee Y-H, Koeffler HP (2002) Expression of C/EBP $\beta$  from the *C/ebp $\alpha$*  gene locus is sufficient for normal hematopoiesis in vivo. *Blood* **99**: 2032-2036
- Jung AL, Herkt CE, Schulz C, Bolte K, Seidel K, Scheller N, Sittka-Stark A, Bertrams W, Schmeck B (2017) Legionella pneumophila infection activates bystander cells differentially by bacterial and host cell vesicles. *Scientific reports* **7**: 6301
- Kambara H, Niazi F, Kostadinova L, Moonka DK, Siegel CT, Post AB, Carnero E, Barriocanal M, Fortes P, Anthony DD, Valadkhan S (2014) Negative regulation of the interferon response by an interferon-induced long non-coding RNA. *Nucleic acids research* **42**: 10668-10680
- Kang YJ, Yang DC, Kong L, Hou M, Meng YQ, Wei L, Gao G (2017) CPC2: a fast and accurate coding potential calculator based on sequence intrinsic features. *Nucleic acids research* **45**: W12-W16
- Kariuki S, Revathi G, Kariuki N, Kiiru J, Mwituria J, Hart CA (2006) Characterisation of community acquired non-typhoidal Salmonella from bacteraemia and diarrhoeal infections in children admitted to hospital in Nairobi, Kenya. *BMC Microbiology* **6**: 101
- Kato H, Takeuchi O, Sato S, Yoneyama M, Yamamoto M, Matsui K, Uematsu S, Jung A, Kawai T, Ishii KJ, Yamaguchi O, Otsu K, Tsujimura T, Koh CS, Reis e Sousa C, Matsuura Y,

Fujita T, Akira S (2006) Differential roles of MDA5 and RIG-I helicases in the recognition of RNA viruses. *Nature* **441**: 101-105

Kawai T, Akira S (2011) Toll-like receptors and their crosstalk with other innate receptors in infection and immunity. *Immunity* **34**: 637-650

Keller G, Snodgrass R (1990) Life span of multipotential hematopoietic stem cells in vivo. *The Journal of experimental medicine* **171**: 1407-1418

Kim JM, Oh YK, Kim YJ, Youn J, Ahn MJ (2004) Escherichia coli up-regulates proinflammatory cytokine expression in granulocyte/macrophage lineages of CD34 stem cells via p50 homodimeric NF-kappaB. *Clinical and experimental immunology* **137**: 341-350

Kinder BW, Brown KK, Schwarz MI, Ix JH, Kervitsky A, King TE (2008) Baseline BAL Neutrophilia Predicts Early Mortality in Idiopathic Pulmonary Fibrosis. *Chest* **133**: 226-232

King TE, Pardo A, Selman M (2011) Idiopathic pulmonary fibrosis. *The Lancet* **378**: 1949-1961

Kino T, Hurt DE, Ichijo T, Nader N, Chrousos GP (2010) Noncoding RNA Gas5 Is a Growth Arrest- and Starvation-Associated Repressor of the Glucocorticoid Receptor. *Science Signaling* **3**: ra8-ra8

Kolb M, Margetts PJ, Anthony DC, Pitossi F, Gauldie J (2001) Transient expression of IL-1 $\beta$  induces acute lung injury and chronic repair leading to pulmonary fibrosis. *The Journal of Clinical Investigation* **107**: 1529-1536

Kondo M, Scherer DC, Miyamoto T, King AG, Akashi K, Sugamura K, Weissman IL (2000) Cell-fate conversion of lymphoid-committed progenitors by instructive actions of cytokines. *Nature* **407**: 383-386

Kondo M, Weissman IL, Akashi K (1997) Identification of Clonogenic Common Lymphoid Progenitors in Mouse Bone Marrow. *Cell* **91**: 661-672

- Kong L, Zhang Y, Ye ZQ, Liu XQ, Zhao SQ, Wei L, Gao G (2007) CPC: assess the protein-coding potential of transcripts using sequence features and support vector machine. *Nucleic acids research* **35**: W345-349
- Kotzin JJ, Spencer SP, McCright SJ, Kumar DBU, Collet MA, Mowel WK, Elliott EN, Uyar A, Makiya MA, Dunagin MC, Harman CCD, Virtue AT, Zhu S, Bailis W, Stein J, Hughes C, Raj A, Wherry EJ, Goff LA, Klion AD, Rinn JL, Williams A, Flavell RA, Henao-Mejia J (2016) The long non-coding RNA Morrbid regulates Bim and short-lived myeloid cell lifespan. *Nature* **537**: 239-243
- KOZAK GK, MacDONALD D, LANDRY L, FARBER JM (2013) Foodborne Outbreaks in Canada Linked to Produce: 2001 through 2009. *Journal of Food Protection* **76**: 173-183
- Krawczyk M, Emerson BM (2014) p50-associated COX-2 extragenic RNA (PACER) activates COX-2 gene expression by occluding repressive NF-kappaB complexes. *eLife* **3**: e01776
- Krawczyk M, Emerson BM (2014) p50-associated COX-2 extragenic RNA (PACER) activates COX-2 gene expression by occluding repressive NF-κB complexes. *eLife* **3**: e01776
- Krek A, Grun D, Poy MN, Wolf R, Rosenberg L, Epstein EJ, MacMenamin P, da Piedade I, Gunsalus KC, Stoffel M, Rajewsky N (2005) Combinatorial microRNA target predictions. *Nature genetics* **37**: 495-500
- Krol J, Loedige I, Filipowicz W (2010) The widespread regulation of microRNA biogenesis, function and decay. *Nature reviews Genetics* **11**: 597-610
- Kubori T, Nagai H (2016) The Type IVB secretion system: an enigmatic chimera. *Current opinion in microbiology* **29**: 22-29
- Kung JT, Colognori D, Lee JT (2013) Long noncoding RNAs: past, present, and future. *Genetics* **193**: 651-669

- Lanier LL, Le AM, Civin CI, Loken MR, Phillips JH (1986) The relationship of CD16 (Leu-11) and Leu-19 (NKH-1) antigen expression on human peripheral blood NK cells and cytotoxic T lymphocytes. *The Journal of Immunology* **136**: 4480-4486
- Lanier LL, Le AM, Phillips JH, Warner NL, Babcock GF (1983) Subpopulations of human natural killer cells defined by expression of the Leu-7 (HNK-1) and Leu-11 (NK-15) antigens. *The Journal of Immunology* **131**: 1789-1796
- Laslo P, Spooner CJ, Warmflash A, Lancki DW, Lee HJ, Sciammas R, Gantner BN, Dinner AR, Singh H (2006) Multilineage transcriptional priming and determination of alternate hematopoietic cell fates. *Cell* **126**: 755-766
- LeBien TW, Tedder TF (2008) B lymphocytes: how they develop and function. *Blood* **112**: 1570-1580
- Lee RC, Feinbaum RL, Ambros V (1993) The *C. elegans* heterochronic gene *lin-4* encodes small RNAs with antisense complementarity to *lin-14*. *Cell* **75**: 843-854
- Lee Y, Ahn C, Han J, Choi H, Kim J, Yim J, Lee J, Provost P, Rådmark O, Kim S, Kim VN (2003) The nuclear RNase III Drosha initiates microRNA processing. *Nature* **425**: 415-419
- Lee Y, Kim M, Han J, Yeom K-H, Lee S, Baek SH, Kim VN (2004) MicroRNA genes are transcribed by RNA polymerase II. *The EMBO journal* **23**: 4051-4060
- Lemaitre B, Nicolas E, Michaut L, Reichhart J-M, Hoffmann JA (1996) The Dorsoventral Regulatory Gene *Cassette* *spätzle/Toll/cactus* Controls the Potent Antifungal Response in *Drosophila* Adults. *Cell* **86**: 973-983
- Levanon EY, Eisenberg E, Yelin R, Nemzer S, Hallegger M, Shemesh R, Fligelman ZY, Shoshan A, Pollock SR, Sztybel D, Olshansky M, Rechavi G, Jantsch MF (2004) Systematic identification of abundant A-to-I editing sites in the human transcriptome. *Nature biotechnology* **22**: 1001-1005

- Lewis BP, Shih Ih, Jones-Rhoades MW, Bartel DP, Burge CB (2003) Prediction of Mammalian MicroRNA Targets. *Cell* **115**: 787-798
- Lewis SH, Quarles KA, Yang Y, Tanguy M, Frezal L, Smith SA, Sharma PP, Cordaux R, Gilbert C, Giraud I, Collins DH, Zamore PD, Miska EA, Sarkies P, Jiggins FM (2018) Panarthropod analysis reveals somatic piRNAs as an ancestral defence against transposable elements. *Nature ecology & evolution* **2**: 174-181
- Li Z, Chao T-C, Chang K-Y, Lin N, Patil VS, Shimizu C, Head SR, Burns JC, Rana TM (2014) The long noncoding RNA *THRIL* regulates TNF $\alpha$  expression through its interaction with hnRNPL. *Proceedings of the National Academy of Sciences* **111**: 1002-1007
- Liddicoat BJ, Piskol R, Chalk AM, Ramaswami G, Higuchi M, Hartner JC, Li JB, Seeburg PH, Walkley CR (2015) RNA editing by ADAR1 prevents MDA5 sensing of endogenous dsRNA as nonself. *Science* **349**: 1115-1120
- Lin CC, Liu LZ, Addison JB, Wonderlin WF, Ivanov AV, Ruppert JM (2011) A KLF4-miRNA-206 autoregulatory feedback loop can promote or inhibit protein translation depending upon cell context. *Molecular and cellular biology* **31**: 2513-2527
- Lin H, Jiang M, Liu L, Yang Z, Ma Z, Liu S, Ma Y, Zhang L, Cao X (2019) The long noncoding RNA *Lnczc3h7a* promotes a TRIM25-mediated RIG-I antiviral innate immune response. *Nature immunology*
- Lippmann J, Muller HC, Naujoks J, Tabeling C, Shin S, Witzenrath M, Hellwig K, Kirschning CJ, Taylor GA, Barchet W, Bauer S, Suttorp N, Roy CR, Opitz B (2011) Dissection of a type I interferon pathway in controlling bacterial intracellular infection in mice. *Cellular microbiology* **13**: 1668-1682
- Liu B, Sun L, Liu Q, Gong C, Yao Y, Lv X, Lin L, Yao H, Su F, Li D, Zeng M, Song E (2015) A cytoplasmic NF-kappaB interacting long noncoding RNA blocks IkappaB phosphorylation and suppresses breast cancer metastasis. *Cancer cell* **27**: 370-381

- Liu G, Mattick J, Taft RJ (2013) A meta-analysis of the genomic and transcriptomic composition of complex life. *Cell Cycle* **12**: 2061-2072
- Livak KJ, Schmittgen TD (2001) Analysis of Relative Gene Expression Data Using Real-Time Quantitative PCR and the  $2^{-\Delta\Delta CT}$  Method. *Methods* **25**: 402-408
- Ljunggren H-G, Kärre K (1990) In search of the 'missing self': MHC molecules and NK cell recognition. *Immunology Today* **11**: 237-244
- Loo YM, Gale M, Jr. (2011) Immune signaling by RIG-I-like receptors. *Immunity* **34**: 680-692
- Love MI, Huber W, Anders S (2014) Moderated estimation of fold change and dispersion for RNA-seq data with DESeq2. *Genome biology* **15**: 550-550
- Lu J, Wu X, Hong M, Tobias P, Han J (2013) A Potential Suppressive Effect of Natural Antisense IL-1 $\beta$  RNA on Lipopolysaccharide-Induced IL-1 $\beta$  Expression. *The Journal of Immunology* **190**: 6570-6578
- Lugthart G, Melsen JE, Vervat C, van Ostaijen-Ten Dam MM, Corver WE, Roelen DL, van Bergen J, van Tol MJ, Lankester AC, Schilham MW (2016) Human Lymphoid Tissues Harbor a Distinct CD69+CXCR6+ NK Cell Population. *Journal of immunology* **197**: 78-84
- Lunemann A, Vanoaica LD, Azzi T, Nadal D, Munz C (2013) A distinct subpopulation of human NK cells restricts B cell transformation by EBV. *Journal of immunology* **191**: 4989-4995
- Luo M, Jeong M, Sun D, Park HJ, Rodriguez BA, Xia Z, Yang L, Zhang X, Sheng K, Darlington GJ, Li W, Goodell MA (2015) Long non-coding RNAs control hematopoietic stem cell function. *Cell stem cell* **16**: 426-438
- Lytle JR, Yario TA, Steitz JA (2007) Target mRNAs are repressed as efficiently by microRNA-binding sites in the 5' UTR as in the 3' UTR. *Proceedings of the National Academy of Sciences of the United States of America* **104**: 9667-9672



Ma H, Han P, Ye W, Chen H, Zheng X, Cheng L, Zhang L, Yu L, Wu Xa, Xu Z, Lei Y, Zhang F (2017) The Long Noncoding RNA NEAT1 Exerts Antihantaviral Effects by Acting as Positive Feedback for RIG-I Signaling. *J Virol* **91**: e02250-02216

Ma Q, Jones D, Borghesani PR, Segal RA, Nagasawa T, Kishimoto T, Bronson RT, Springer TA (1998) Impaired B-lymphopoiesis, myelopoiesis, and derailed cerebellar neuron migration in CXCR4- and SDF-1-deficient mice. *Proceedings of the National Academy of Sciences* **95**: 9448-9453

Ma Q, Jones D, Springer TA (1999) The Chemokine Receptor CXCR4 Is Required for the Retention of B Lineage and Granulocytic Precursors within the Bone Marrow Microenvironment. *Immunity* **10**: 463-471

MacNamara KC, Racine R, Chatterjee M, Borjesson D, Winslow GM (2009) Diminished hematopoietic activity associated with alterations in innate and adaptive immunity in a mouse model of human monocytic ehrlichiosis. *Infection and immunity* **77**: 4061-4069

Maenner S, Blaud M, Fouillen L, Savoye A, Marchand V, Dubois A, Sanglier-Cianferani S, Van Dorsselaer A, Clerc P, Avner P, Visvikis A, Branlant C (2010) 2-D structure of the A region of Xist RNA and its implication for PRC2 association. *PLoS biology* **8**: e1000276

Mak KS, Funnell APW, Pearson RCM, Crossley M (2011) PU.1 and Haematopoietic Cell Fate: Dosage Matters. *International journal of cell biology* **2011**: 808524-808524

Mancuso G, Gambuzza M, Midiri A, Biondo C, Papasergi S, Akira S, Teti G, Beninati C (2009) Bacterial recognition by TLR7 in the lysosomes of conventional dendritic cells. *Nature immunology* **10**: 587-594

Mariotti B, Servaas NH, Rossato M, Tamassia N, Cassatella MA, Cossu M, Beretta L, van der Kroef M, Radstake TRDJ, Bazzoni F (2019) The Long Non-coding RNA NRIR Drives IFN-Response in Monocytes: Implication for Systemic Sclerosis. *Frontiers in Immunology* **10**

Marquardt N, Beziat V, Nystrom S, Hengst J, Ivarsson MA, Kekalainen E, Johansson H, Mjosberg J, Westgren M, Lankisch TO, Wedemeyer H, Ellis EC, Ljunggren HG, Michaelsson J, Bjorkstrom NK (2015) Cutting edge: identification and characterization of human intrahepatic CD49a+ NK cells. *Journal of immunology* **194**: 2467-2471

Marquardt N, Kekalainen E, Chen P, Kvedaraite E, Wilson JN, Ivarsson MA, Mjosberg J, Berglin L, Safholm J, Manson ML, Adner M, Al-Ameri M, Bergman P, Orre AC, Svensson M, Dahlen B, Dahlen SE, Ljunggren HG, Michaelsson J (2017) Human lung natural killer cells are predominantly comprised of highly differentiated hypofunctional CD69(-)CD56(dim) cells. *The Journal of allergy and clinical immunology* **139**: 1321-1330 e1324

Massis LM, Zamboni DS (2011) Innate immunity to legionella pneumophila. *Frontiers in microbiology* **2**: 109

Mattick JS (2018) The State of Long Non-Coding RNA Biology. *Noncoding RNA* **4**: 17

Maudet C, Mano M, Sunkavalli U, Sharan M, Giacca M, Förstner KU, Eulalio A (2014) Functional high-throughput screening identifies the miR-15 microRNA family as cellular restriction factors for Salmonella infection. *Nature communications* **5**: 4718

McCoy CE, Sheedy FJ, Qualls JE, Doyle SL, Quinn SR, Murray PJ, O'Neill LA (2010) IL-10 inhibits miR-155 induction by toll-like receptors. *The Journal of biological chemistry* **285**: 20492-20498

McKercher SR, Torbett BE, Anderson KL, Henkel GW, Vestal DJ, Baribault H, Klemsz M, Feeney AJ, Wu GE, Paige CJ, Maki RA (1996) Targeted disruption of the PU.1 gene results in multiple hematopoietic abnormalities. *The EMBO journal* **15**: 5647-5658

Mele M, Mattioli K, Mallard W, Shechner DM, Gerhardinger C, Rinn JL (2017) Chromatin environment, transcriptional regulation, and splicing distinguish lincRNAs and mRNAs. *Genome research* **27**: 27-37

- Merad M, Manz MG, Karsunky H, Wagers A, Peters W, Charo I, Weissman IL, Cyster JG, Engleman EG (2002) Langerhans cells renew in the skin throughout life under steady-state conditions. *Nature immunology* **3**: 1135-1141
- Mercer TR, Mattick JS (2013) Structure and function of long noncoding RNAs in epigenetic regulation. *Nature Structural & Molecular Biology* **20**: 300
- Meyer KD, Saletore Y, Zumbo P, Elemento O, Mason CE, Jaffrey SR (2012) Comprehensive analysis of mRNA methylation reveals enrichment in 3' UTRs and near stop codons. *Cell* **149**: 1635-1646
- Miao EA, Leaf IA, Treuting PM, Mao DP, Dors M, Sarkar A, Warren SE, Wewers MD, Aderem A (2010) Caspase-1-induced pyroptosis is an innate immune effector mechanism against intracellular bacteria. *Nature immunology* **11**: 1136
- Miesen P, Girardi E, van Rij RP (2015) Distinct sets of PIWI proteins produce arbovirus and transposon-derived piRNAs in *Aedes aegypti* mosquito cells. *Nucleic acids research* **43**: 6545-6556
- Mikkola HK, Orkin SH (2006) The journey of developing hematopoietic stem cells. *Development* **133**: 3733-3744
- Morchikh M, Cribier A, Raffel R, Amraoui S, Cau J, Severac D, Dubois E, Schwartz O, Bennasser Y, Benkirane M (2017) HEXIM1 and NEAT1 Long Non-coding RNA Form a Multi-subunit Complex that Regulates DNA-Mediated Innate Immune Response. *Molecular cell* **67**: 387-399 e385
- Mosmann TR, Cherwinski H, Bond MW, Giedlin MA, Coffman RL (1986) Two types of murine helper T cell clone. I. Definition according to profiles of lymphokine activities and secreted proteins. *The Journal of Immunology* **136**: 2348-2357
- Mueller SN, Gebhardt T, Carbone FR, Heath WR (2013) Memory T cell subsets, migration patterns, and tissue residence. *Annual review of immunology* **31**: 137-161

- Munitic I, Giardino Torchia ML, Meena NP, Zhu G, Li CC, Ashwell JD (2013) Optineurin insufficiency impairs IRF3 but not NF-kappaB activation in immune cells. *Journal of immunology* **191**: 6231-6240
- Murali A, Li X, Ranjith-Kumar CT, Bhardwaj K, Holzenburg A, Li P, Kao CC (2008) Structure and function of LGP2, a DEX(D/H) helicase that regulates the innate immunity response. *The Journal of biological chemistry* **283**: 15825-15833
- Mylonas KJ, Jenkins SJ, Castellan RF, Ruckerl D, McGregor K, Phythian-Adams AT, Hewitson JP, Campbell SM, MacDonald AS, Allen JE, Gray GA (2015) The adult murine heart has a sparse, phagocytically active macrophage population that expands through monocyte recruitment and adopts an 'M2' phenotype in response to Th2 immunologic challenge. *Immunobiology* **220**: 924-933
- Nagano T, Mitchell JA, Sanz LA, Pauler FM, Ferguson-Smith AC, Feil R, Fraser P (2008) The *Air* Noncoding RNA Epigenetically Silences Transcription by Targeting G9a to Chromatin. *Science* **322**: 1717-1720
- Nagasawa T, Hirota S, Tachibana K, Takakura N, Nishikawa S-i, Kitamura Y, Yoshida N, Kikutani H, Kishimoto T (1996) Defects of B-cell lymphopoiesis and bone-marrow myelopoiesis in mice lacking the CXC chemokine PBSF/SDF-1. *Nature* **382**: 635-638
- Nahrendorf M, Pittet MJ, Swirski FK (2010) Monocytes: Protagonists of Infarct Inflammation and Repair After Myocardial Infarction. *Circulation* **121**: 2437-2445
- Naito Y, Yamada T, Ui-Tei K, Morishita S, Saigo K (2004) siDirect: highly effective, target-specific siRNA design software for mammalian RNA interference. *Nucleic acids research* **32**: W124-W129
- Naujoks J, Tabeling C, Dill BD, Hoffmann C, Brown AS, Kunze M, Kempa S, Peter A, Mollenkopf HJ, Dorhoi A, Kershaw O, Gruber AD, Sander LE, Witzernath M, Herold S, Nerlich A, Hocke AC, van Driel I, Suttorp N, Bedoui S, Hilbi H, Trost M, Opitz B (2016) IFNs Modify the Proteome of Legionella-Containing Vacuoles and Restrict Infection Via IRG1-Derived Itaconic Acid. *PLoS pathogens* **12**: e1005408

Newsome AL, Baker RL, Miller RD, Arnold RR (1985) Interactions between *Naegleria fowleri* and *Legionella pneumophila*. *Infection and immunity* **50**: 449-452

Nordenbaek C, Johansen JS, Junker P, Borregaard N, Sørensen O, Price PA (1999) YKL-40, a Matrix Protein of Specific Granules in Neutrophils, Is Elevated in Serum of Patients with Community-Acquired Pneumonia Requiring Hospitalization. *The Journal of Infectious Diseases* **180**: 1722-1726

Novikova IV, Hennelly SP, Sanbonmatsu KY (2012) Structural architecture of the human long non-coding RNA, steroid receptor RNA activator. *Nucleic acids research* **40**: 5034-5051

Obar JJ, Lefrancois L (2010) Memory CD8+ T cell differentiation. *Annals of the New York Academy of Sciences* **1183**: 251-266

O'Connell RM, Taganov KD, Boldin MP, Cheng G, Baltimore D (2007) MicroRNA-155 is induced during the macrophage inflammatory response. *Proceedings of the National Academy of Sciences of the United States of America* **104**: 1604-1609

Ogura Y, Inohara N, Benito A, Chen FF, Yamaoka S, Nunez G (2001) Nod2, a Nod1/Apaf-1 family member that is restricted to monocytes and activates NF-kappaB. *The Journal of biological chemistry* **276**: 4812-4818

Ohl M.E, Miller SI (2001) Salmonella: A Model for Bacterial Pathogenesis. *Annual Review of Medicine* **52**: 259-274

Ohyagi H, Onai N, Sato T, Yotsumoto S, Liu J, Akiba H, Yagita H, Atarashi K, Honda K, Roers A, Muller W, Kurabayashi K, Hosoi-Amaike M, Takahashi N, Hirokawa M, Matsushima K, Sawada K, Ohteki T (2013) Monocyte-derived dendritic cells perform hemophagocytosis to fine-tune excessive immune responses. *Immunity* **39**: 584-598

Opitz B, Vinzing M, van Laak V, Schmeck B, Heine G, Gunther S, Preissner R, Slevogt H, N'Guessan PD, Eitel J, Goldmann T, Flieger A, Suttorp N, Hippenstiel S (2006) *Legionella*

pneumophila induces IFN $\beta$  in lung epithelial cells via IPS-1 and IRF3, which also control bacterial replication. *The Journal of biological chemistry* **281**: 36173-36179

Orkin SH, Zon LI (2008) Hematopoiesis: an evolving paradigm for stem cell biology. *Cell* **132**: 631-644

Ozata DM, Gainetdinov I, Zoch A, O'Carroll D, Zamore PD (2019) PIWI-interacting RNAs: small RNAs with big functions. *Nature reviews Genetics* **20**: 89-108

Palazzo AF, Lee ES (2015) Non-coding RNA: what is functional and what is junk? *Frontiers in genetics* **6**: 2

Palis J, Yoder MC (2001) Yolk-sac hematopoiesis: The first blood cells of mouse and man. *Experimental Hematology* **29**: 927-936

Palmer E (2003) Negative selection--clearing out the bad apples from the T-cell repertoire. *Nature reviews Immunology* **3**: 383-391

Palsson-McDermott EM, Doyle SL, McGettrick AF, Hardy M, Husebye H, Banahan K, Gong M, Golenbock D, Espevik T, O'Neill LA (2009) TAG, a splice variant of the adaptor TRAM, negatively regulates the adaptor MyD88-independent TLR4 pathway. *Nature immunology* **10**: 579-586

Pang KC, Dinger ME, Mercer TR, Malquori L, Grimmond SM, Chen W, Mattick JS (2009) Genome-wide identification of long noncoding RNAs in CD8+ T cells. *Journal of immunology* **182**: 7738-7748

Paul F, Arkin Y, Giladi A, Jaitin DA, Kenigsberg E, Keren-Shaul H, Winter D, Lara-Astiaso D, Gury M, Weiner A, David E, Cohen N, Lauridsen FK, Haas S, Schlitzer A, Mildner A, Ginhoux F, Jung S, Trumpp A, Porse BT, Tanay A, Amit I (2015) Transcriptional Heterogeneity and Lineage Commitment in Myeloid Progenitors. *Cell* **163**: 1663-1677

Penny GD, Kay GF, Sheardown SA, Rastan S, Brockdorff N (1996) Requirement for Xist in X chromosome inactivation. *Nature* **379**: 131-137

- Penny GD, Kay GF, Sheardown SA, Rastan S, Brockdorff N (1996) Requirement for Xist in X chromosome inactivation. *Nature* **379**: 131-137
- Picardi E, D'Erchia AM, Gallo A, Montalvo A, Pesole G (2014) Uncovering RNA Editing Sites in Long Non-Coding RNAs. *Frontiers in bioengineering and biotechnology* **2**: 64
- Pichlmair A, Schulz O, Tan CP, Näslund TI, Liljeström P, Weber F, Reis e Sousa C (2006) RIG-I-Mediated Antiviral Responses to Single-Stranded RNA Bearing 5'-Phosphates. *Science* **314**: 997-1001
- Piguet PF, Ribaux C, Karpuz V, Grau GE, Kapanci Y (1993) Expression and localization of tumor necrosis factor-alpha and its mRNA in idiopathic pulmonary fibrosis. *Am J Pathol* **143**: 651-655
- Pippig DA, Hellmuth JC, Cui S, Kirchhofer A, Lammens K, Lammens A, Schmidt A, Rothenfusser S, Hopfner KP (2009) The regulatory domain of the RIG-I family ATPase LGP2 senses double-stranded RNA. *Nucleic acids research* **37**: 2014-2025
- Poulsen H, Nilsson J, Damgaard CK, Egebjerg J, Kjems J (2001) CRM1 mediates the export of ADAR1 through a nuclear export signal within the Z-DNA binding domain. *Molecular and cellular biology* **21**: 7862-7871
- Quinn JJ, Chang HY (2016) Unique features of long non-coding RNA biogenesis and function. *Nature reviews Genetics* **17**: 47-62
- Quinton LJ, Nelson S, Boé DM, Zhang P, Zhong Q, Kolls JK, Bagby GJ (2002) The Granulocyte Colony-Stimulating Factor Response after Intrapulmonary and Systemic Bacterial Challenges. *The Journal of Infectious Diseases* **185**: 1476-1482
- Ran FA, Hsu PD, Wright J, Agarwala V, Scott DA, Zhang F (2013) Genome engineering using the CRISPR-Cas9 system. *Nature protocols* **8**: 2281-2308

- Ranzani V, Rossetti G, Panzeri I, Arrigoni A, Bonnal RJ, Curti S, Guarini P, Provasi E, Sugliano E, Marconi M, De Francesco R, Geginat J, Bodega B, Abrignani S, Pagani M (2015) The long intergenic noncoding RNA landscape of human lymphocytes highlights the regulation of T cell differentiation by linc-MAF-4. *Nature immunology* **16**: 318-325
- Rapicavoli NA, Qu K, Zhang J, Mikhail M, Laberge RM, Chang HY (2013) A mammalian pseudogene lncRNA at the interface of inflammation and anti-inflammatory therapeutics. *eLife* **2**: e00762
- Rapicavoli NA, Qu K, Zhang J, Mikhail M, Laberge R-M, Chang HY (2013) A mammalian pseudogene lncRNA at the interface of inflammation and anti-inflammatory therapeutics. *eLife* **2**: e00762
- Rehli M, Niller HH, Ammon C, Langmann S, Schwarzfischer L, Andreesen R, Krause SW (2003) Transcriptional regulation of CHI3L1, a marker gene for late stages of macrophage differentiation. *The Journal of biological chemistry* **278**: 44058-44067
- Richter AG, Perkins GD, Chavda A, Sapey E, Harper L, Thickett DR (2011) Neutrophil chemotaxis in granulomatosis with polyangiitis (Wegener's) and idiopathic pulmonary fibrosis. *The European respiratory journal* **38**: 1081-1088
- Rinn JL, Chang HY (2012) Genome Regulation by Long Noncoding RNAs. *Annual Review of Biochemistry* **81**: 145-166
- Rinn JL, Kertesz M, Wang JK, Squazzo SL, Xu X, Bruggmann SA, Goodnough LH, Helms JA, Farnham PJ, Segal E, Chang HY (2007) Functional Demarcation of Active and Silent Chromatin Domains in Human HOX Loci by Noncoding RNAs. *Cell* **129**: 1311-1323
- Ritz J, Campen T, Schmidt R, Royer H, Hercend T, Hussey R, Reinherz E (1985) Analysis of T-cell receptor gene rearrangement and expression in human natural killer clones. *Science* **228**: 1540-1543
- Rivas C, Aaronson SA, Munoz-Fontela C (2010) Dual Role of p53 in Innate Antiviral Immunity. *Viruses* **2**: 298-313



Rivas C, Aaronson SA, Munoz-Fontela C (2010) Dual Role of p53 in Innate Antiviral Immunity. *Viruses* **2**: 298-313

Robinson MJ, Sancho D, Slack EC, LeibundGut-Landmann S, Reis e Sousa C (2006) Myeloid C-type lectins in innate immunity. *Nature immunology* **7**: 1258-1265

Rogers NC, Slack EC, Edwards AD, Nolte MA, Schulz O, Schweighoffer E, Williams DL, Gordon S, Tybulewicz VL, Brown GD, Reis e Sousa C (2005) Syk-dependent cytokine induction by Dectin-1 reveals a novel pattern recognition pathway for C type lectins. *Immunity* **22**: 507-517

Rowbotham TJ (1980) Preliminary report on the pathogenicity of *Legionella pneumophila* for freshwater and soil amoebae. *Journal of Clinical Pathology* **33**: 1179-1183

Rydström A, Wick MJ (2007) Monocyte Recruitment, Activation, and Function in the Gut-Associated Lymphoid Tissue during Oral *Salmonella* Infection. *The Journal of Immunology* **178**: 5789-5801

Saito K, Ishizuka A, Siomi H, Siomi MC (2005) Processing of pre-microRNAs by the Dicer-1-Loquacious complex in *Drosophila* cells. *PLoS biology* **3**: e235

Saito T, Hirai R, Loo YM, Owen D, Johnson CL, Sinha SC, Akira S, Fujita T, Gale M, Jr. (2007) Regulation of innate antiviral defenses through a shared repressor domain in RIG-I and LGP2. *Proceedings of the National Academy of Sciences of the United States of America* **104**: 582-587

Salameh A, Lee AK, Cardo-Vila M, Nunes DN, Efstathiou E, Staquicini FI, Dobroff AS, Marchio S, Navone NM, Hosoya H, Lauer RC, Wen S, Salmeron CC, Hoang A, Newsham I, Lima LA, Carraro DM, Oliviero S, Kolonin MG, Sidman RL, Do KA, Troncoso P, Logothetis CJ, Brentani RR, Calin GA, Cavenee WK, Dias-Neto E, Pasqualini R, Arap W (2015) PRUNE2 is a human prostate cancer suppressor regulated by the intronic long noncoding RNA PCA3. *Proceedings of the National Academy of Sciences of the United States of America* **112**: 8403-8408

Salcedo SP, Holden DW (2003) SseG, a virulence protein that targets Salmonella to the Golgi network. *The EMBO journal* **22**: 5003-5014

Saldanha AJ (2004) Java Treeview—extensible visualization of microarray data. *Bioinformatics* **20**: 3246-3248

Sancho D, Reis e Sousa C (2012) Signaling by myeloid C-type lectin receptors in immunity and homeostasis. *Annual review of immunology* **30**: 491-529

Sasai M, Linehan MM, Iwasaki A (2010) Bifurcation of Toll-Like Receptor 9 Signaling by Adaptor Protein 3. *Science* **329**: 1530-1534

Schamberger A, Sarkadi B, Orban TI (2012) Human mirtrons can express functional microRNAs simultaneously from both arms in a flanking exon-independent manner. *RNA biology* **9**: 1177-1185

Schlackow M, Nojima T, Gomes T, Dhir A, Carmo-Fonseca M, Proudfoot NJ (2017) Distinctive Patterns of Transcription and RNA Processing for Human lincRNAs. *Molecular cell* **65**: 25-38

Schulte LN, Eulalio A, Mollenkopf HJ, Reinhardt R, Vogel J (2011) Analysis of the host microRNA response to *Salmonella* uncovers the control of major cytokines by the *let-7* family. *The EMBO journal* **30**: 1977-1989

Schulte LN, Westermann AJ, Vogel J (2012) Differential activation and functional specialization of miR-146 and miR-155 in innate immune sensing. *Nucleic acids research* **41**: 542-553

Schulz O, Hammerschmidt SI, Moschovakis GL, Forster R (2016) Chemokines and Chemokine Receptors in Lymphoid Tissue Dynamics. *Annual review of immunology* **34**: 203-242

Schulz O, Hammerschmidt SI, Moschovakis GL, Förster R (2016) Chemokines and Chemokine Receptors in Lymphoid Tissue Dynamics. *Annual review of immunology* **34**: 203-242

- Scott E, Simon M, Anastasi J, Singh H (1994) Requirement of transcription factor PU.1 in the development of multiple hematopoietic lineages. *Science* **265**: 1573-1577
- Scott I (2010) The role of mitochondria in the mammalian antiviral defence system. *Mitochondrion* **10**: 316-320
- Seong S-Y, Matzinger P (2004) Hydrophobicity: an ancient damage-associated molecular pattern that initiates innate immune responses. *Nature Reviews Immunology* **4**: 469-478
- Serti E, Werner JM, Chattergoon M, Cox AL, Lohmann V, Rehermann B (2014) Monocytes activate natural killer cells via inflammasome-induced interleukin 18 in response to hepatitis C virus replication. *Gastroenterology* **147**: 209-220 e203
- Shahbazian LM, Quinton LJ, Bagby GJ, Nelson S, Wang G, Zhang P (2004) Escherichia coli pneumonia enhances granulopoiesis and the mobilization of myeloid progenitor cells into the systemic circulation. *Critical Care Medicine* **32**: 1740-1746
- Sharma S, Findlay GM, Bandukwala HS, Oberdoerffer S, Baust B, Li Z, Schmidt V, Hogan PG, Sacks DB, Rao A (2011) Dephosphorylation of the nuclear factor of activated T cells (NFAT) transcription factor is regulated by an RNA-protein scaffold complex. *Proceedings of the National Academy of Sciences of the United States of America* **108**: 11381-11386
- Shim HK, Kim JY, Kim MJ, Sim HS, Park DW, Sohn JW, Kim MJ (2009) Legionella lipoprotein activates toll-like receptor 2 and induces cytokine production and expression of costimulatory molecules in peritoneal macrophages. *Experimental & molecular medicine* **41**: 687-694
- Simon AK, Hollander GA, McMichael A (2015) Evolution of the immune system in humans from infancy to old age. *Proceedings Biological sciences* **282**: 20143085
- Simon H-U (2001) Regulation of eosinophil and neutrophil apoptosis – similarities and differences. *Immunological Reviews* **179**: 156-162

- Singh P, Yao Y, Weliver A, Broxmeyer HE, Hong SC, Chang CH (2008) Vaccinia virus infection modulates the hematopoietic cell compartments in the bone marrow. *Stem cells* **26**: 1009-1016
- Smirnov A, Förstner KU, Holmqvist E, Otto A, Günster R, Becher D, Reinhardt R, Vogel J (2016) Grad-seq guides the discovery of ProQ as a major small RNA-binding protein. *Proceedings of the National Academy of Sciences* **113**: 11591-11596
- Sprangers S, de Vries TJ, Everts V (2016) Monocyte Heterogeneity: Consequences for Monocyte-Derived Immune Cells. *Journal of immunology research* **2016**: 1475435
- Spurlock CF, 3rd, Tossberg JT, Guo Y, Collier SP, Crooke PS, 3rd, Aune TM (2015) Expression and functions of long noncoding RNAs during human T helper cell differentiation. *Nature communications* **6**: 6932
- Squires JE, Patel HR, Nousch M, Sibbritt T, Humphreys DT, Parker BJ, Suter CM, Preiss T (2012) Widespread occurrence of 5-methylcytosine in human coding and non-coding RNA. *Nucleic acids research* **40**: 5023-5033
- Stegmann KA, Robertson F, Hansi N, Gill U, Pallant C, Christophides T, Pallett LJ, Peppas D, Dunn C, Fusai G, Male V, Davidson BR, Kennedy P, Maini MK (2016) CXCR6 marks a novel subset of T-bet(lo)Eomes(hi) natural killer cells residing in human liver. *Scientific reports* **6**: 26157
- Struhl K (2007) Transcriptional noise and the fidelity of initiation by RNA polymerase II. *Nature Structural & Molecular Biology* **14**: 103
- Sun L, Wu J, Du F, Chen X, Chen ZJ (2013) Cyclic GMP-AMP Synthase Is a Cytosolic DNA Sensor That Activates the Type I Interferon Pathway. *Science* **339**: 786-791
- Suzuki K, Okawa Y, Hashimoto K, Suzuki S, Suzuki M (1984) Protecting Effect of Chitin and Chitosan on Experimentally Induced Murine Candidiasis. *Microbiology and Immunology* **28**: 903-912

- Swanson M.S, Hammer BK (2000) Legionella Pneumophila Pathogenesis: A Fateful Journey from Amoebae to Macrophages. *Annual Review of Microbiology* **54**: 567-613
- Taft RJ, Pheasant M, Mattick JS (2007) The relationship between non-protein-coding DNA and eukaryotic complexity. *BioEssays* **29**: 288-299
- Taganov KD, Boldin MP, Chang KJ, Baltimore D (2006) NF-kappaB-dependent induction of microRNA miR-146, an inhibitor targeted to signaling proteins of innate immune responses. *Proceedings of the National Academy of Sciences of the United States of America* **103**: 12481-12486
- Takahasi K, Kumeta H, Tsuduki N, Narita R, Shigemoto T, Hirai R, Yoneyama M, Horiuchi M, Ogura K, Fujita T, Inagaki F (2009) Solution structures of cytosolic RNA sensor MDA5 and LGP2 C-terminal domains: identification of the RNA recognition loop in RIG-I-like receptors. *The Journal of biological chemistry* **284**: 17465-17474
- Takeuchi A (1967) Electron microscope studies of experimental Salmonella infection. I. Penetration into the intestinal epithelium by Salmonella typhimurium. *Am J Pathol* **50**: 109-136
- Thannickal VJ, Toews GB, White ES, III JPL, Martinez FJ (2004) Mechanisms of Pulmonary Fibrosis. *Annual Review of Medicine* **55**: 395-417
- Tilney LG, Harb OS, Connelly PS, Robinson CG, Roy CR (2001) How the parasitic bacterium *Legionella pneumophila* modifies its phagosome and transforms it into rough ER: implications for conversion of plasma membrane to the ER membrane. *Journal of Cell Science* **114**: 4637-4650
- Tong Q, Gong A-Y, Zhang X-T, Lin C, Ma S, Chen J, Hu G, Chen X-M (2016) LincRNA-Cox2 modulates TNF- $\alpha$ -induced transcription of Il12b gene in intestinal epithelial cells through regulation of Mi-2/NuRD-mediated epigenetic histone modifications. *The FASEB Journal* **30**: 1187-1197

Tsai M-C, Manor O, Wan Y, Mosammaparast N, Wang JK, Lan F, Shi Y, Segal E, Chang HY (2010) Long Noncoding RNA as Modular Scaffold of Histone Modification Complexes. *Science* **329**: 689-693

Tsuchiya S, Yamabe M, Yamaguchi Y, Kobayashi Y, Konno T, Tada K (1980) Establishment and characterization of a human acute monocytic leukemia cell line (THP-1). *International Journal of Cancer* **26**: 171-176

Tuck AC, Tollervey D (2013) A transcriptome-wide atlas of RNP composition reveals diverse classes of mRNAs and lncRNAs. *Cell* **154**: 996-1009

Turvey SE, Broide DH (2010) Innate immunity. *The Journal of allergy and clinical immunology* **125**: S24-32

Tyson JY, Pearce MM, Vargas P, Bagchi S, Mulhern BJ, Cianciotto NP (2013) Multiple Legionella pneumophila Type II Secretion Substrates, Including a Novel Protein, Contribute to Differential Infection of the Amoebae Acanthamoeba castellanii, Hartmannella vermiformis, and Naegleria lovaniensis. *Infection and immunity* **81**: 1399-1410

Ulitsky I, Bartel DP (2013) lincRNAs: genomics, evolution, and mechanisms. *Cell* **154**: 26-46

Vagin VV, Sigova A, Li C, Seitz H, Gvozdev V, Zamore PD (2006) A Distinct Small RNA Pathway Silences Selfish Genetic Elements in the Germline. *Science* **313**: 320-324

van Furth R, Cohn ZA (1968) The origin and kinetics of mononuclear phagocytes. *The Journal of experimental medicine* **128**: 415-435

van Heesch S, van Iterson M, Jacobi J, Boymans S, Essers PB, de Bruijn E, Hao W, MacInnes AW, Cuppen E, Simonis M (2014) Extensive localization of long noncoding RNAs to the cytosol and mono- and polyribosomal complexes. *Genome Biology* **15**: R6

Vasudevan S, Tong Y, Steitz JA (2007) Switching from Repression to Activation: MicroRNAs Can Up-Regulate Translation. *Science* **318**: 1931-1934

Venkatraman A, He XC, Thorvaldsen JL, Sugimura R, Perry JM, Tao F, Zhao M, Christenson MK, Sanchez R, Yu JY, Peng L, Haug JS, Paulson A, Li H, Zhong XB, Clemens TL, Bartolomei MS, Li L (2013) Maternal imprinting at the H19-Igf2 locus maintains adult haematopoietic stem cell quiescence. *Nature* **500**: 345-349

Wan Y, Kertesz M, Spitale RC, Segal E, Chang HY (2011) Understanding the transcriptome through RNA structure. *Nature reviews Genetics* **12**: 641-655

Wang P, Hou J, Lin L, Wang C, Liu X, Li D, Ma F, Wang Z, Cao X (2010) Inducible microRNA-155 feedback promotes type I IFN signaling in antiviral innate immunity by targeting suppressor of cytokine signaling 1. *Journal of immunology* **185**: 6226-6233

Wang P, Xue Y, Han Y, Lin L, Wu C, Xu S, Jiang Z, Xu J, Liu Q, Cao X (2014) The STAT3-Binding Long Noncoding RNA Inc-DC Controls Human Dendritic Cell Differentiation. *Science* **344**: 310-313

Wang Y, Zhong H, Xie X, Chen CY, Huang D, Shen L, Zhang H, Chen ZW, Zeng G (2015) Long noncoding RNA derived from CD244 signaling epigenetically controls CD8<sup>+</sup> T-cell immune responses in tuberculosis infection. *Proceedings of the National Academy of Sciences of the United States of America* **112**: E3883-3892

Watarai M, Derre I, Kirby J, Growney JD, Dietrich WF, Isberg RR (2001) *Legionella pneumophila* is internalized by a macropinocytotic uptake pathway controlled by the Dot/Icm system and the mouse *Lgn1* locus. *The Journal of experimental medicine* **194**: 1081-1096

Watson RO, Bell SL, MacDuff DA, Kimmey JM, Diner EJ, Olivás J, Vance RE, Stallings CL, Virgin HW, Cox JS (2015) The Cytosolic Sensor cGAS Detects *Mycobacterium tuberculosis* DNA to Induce Type I Interferons and Activate Autophagy. *Cell host & microbe* **17**: 811-819

- Watts JM, Dang KK, Gorelick RJ, Leonard CW, Bess JW, Jr., Swanstrom R, Burch CL, Weeks KM (2009) Architecture and secondary structure of an entire HIV-1 RNA genome. *Nature* **460**: 711-716
- Weaver CT, Harrington LE, Mangan PR, Gavrieli M, Murphy KM (2006) Th17: an effector CD4 T cell lineage with regulatory T cell ties. *Immunity* **24**: 677-688
- Weisheit C, Zhang Y, Faron A, Kopke O, Weisheit G, Steinstrasser A, Frede S, Meyer R, Boehm O, Hoeft A, Kurts C, Baumgarten G (2014) Ly6C(low) and not Ly6C(high) macrophages accumulate first in the heart in a model of murine pressure-overload. *PloS one* **9**: e112710
- Willingham AT, Orth AP, Batalov S, Peters EC, Wen BG, Aza-Blanc P, Hogenesch JB, Schultz PG (2005) A Strategy for Probing the Function of Noncoding RNAs Finds a Repressor of NFAT. *Science* **309**: 1570-1573
- Wilusz JE, Freier SM, Spector DL (2008) 3' end processing of a long nuclear-retained noncoding RNA yields a tRNA-like cytoplasmic RNA. *Cell* **135**: 919-932
- Winter J, Jung S, Keller S, Gregory RI, Diederichs S (2009) Many roads to maturity: microRNA biogenesis pathways and their regulation. *Nature Cell Biology* **11**: 228
- Wong KL, Yeap WH, Tai JJ, Ong SM, Dang TM, Wong SC (2012) The three human monocyte subsets: implications for health and disease. *Immunologic research* **53**: 41-57
- Wu H, Yang L, Chen LL (2017) The Diversity of Long Noncoding RNAs and Their Generation. *Trends in genetics : TIG* **33**: 540-552
- Wu R, Su Y, Wu H, Dai Y, Zhao M, Lu Q (2016) Characters, functions and clinical perspectives of long non-coding RNAs. *Molecular genetics and genomics : MGG* **291**: 1013-1033
- Wynn TA (2011) Integrating mechanisms of pulmonary fibrosis. *The Journal of experimental medicine* **208**: 1339-1350



- Xie Q, Chen S, Tian R, Huang X, Deng R, Xue B, Qin Y, Xu Y, Wang J, Guo M, Chen J, Tang S, Li G, Zhu H (2018) Long Noncoding RNA ITPRIP-1 Positively Regulates the Innate Immune Response through Promotion of Oligomerization and Activation of MDA5. *J Virol* **92**: e00507-00518
- Yang VW, Lerner MR, Steitz JA, Flint SJ (1981) A small nuclear ribonucleoprotein is required for splicing of adenoviral early RNA sequences. *Proceedings of the National Academy of Sciences of the United States of America* **78**: 1371-1375
- Ye Y, He X, Lu F, Mao H, Zhu Z, Yao L, Luo W, Sun X, Wang B, Qian C, Zhang Y, Lu G, Zhang S (2018) A lincRNA-p21/miR-181 family feedback loop regulates microglial activation during systemic LPS- and MPTP- induced neuroinflammation. *Cell death & disease* **9**: 803
- Yoneyama M, Kikuchi M, Natsukawa T, Shinobu N, Imaizumi T, Miyagishi M, Taira K, Akira S, Fujita T (2004) The RNA helicase RIG-I has an essential function in double-stranded RNA-induced innate antiviral responses. *Nature immunology* **5**: 730-737
- Yousefi S, Gold JA, Andina N, Lee JJ, Kelly AM, Kozlowski E, Schmid I, Straumann A, Reichenbach J, Gleich GJ, Simon HU (2008) Catapult-like release of mitochondrial DNA by eosinophils contributes to antibacterial defense. *Nature medicine* **14**: 949-953
- Zelensky AN, Gready JE (2005) The C-type lectin-like domain superfamily. *The FEBS journal* **272**: 6179-6217
- Zelensky AN, Gready JE (2005) The C-type lectin-like domain superfamily. *The FEBS journal* **272**: 6179-6217
- Zhang D-E, Zhang P, Wang N-d, Hetherington CJ, Darlington GJ, Tenen DG (1997) Absence of granulocyte colony-stimulating factor signaling and neutrophil development in CCAAT enhancer binding protein  $\alpha$ -deficient mice. *Proceedings of the National Academy of Sciences* **94**: 569-574
- Zhang N, Bevan MJ (2011) CD8(+) T cells: foot soldiers of the immune system. *Immunity* **35**: 161-168

- Zhang P, Iwasaki-Arai J, Iwasaki H, Fenyus ML, Dayaram T, Owens BM, Shigematsu H, Levantini E, Huettner CS, Lekstrom-Himes JA, Akashi K, Tenen DG (2004) Enhancement of hematopoietic stem cell repopulating capacity and self-renewal in the absence of the transcription factor C/EBP alpha. *Immunity* **21**: 853-863
- Zhang P, Nelson S, Bagby GJ, Siggins R, 2nd, Shellito JE, Welsh DA (2008) The lineage-c-Kit+Sca-1+ cell response to Escherichia coli bacteremia in Balb/c mice. *Stem cells* **26**: 1778-1786
- Zhang Q, Chao TC, Patil VS, Qin Y, Tiwari SK, Chiou J, Dobin A, Tsai CM, Li Z, Dang J, Gupta S, Urdahl K, Nizet V, Gingeras TR, Gaulton KJ, Rana TM (2019) The long noncoding RNA *ROCK1* regulates inflammatory gene expression. *The EMBO journal* **38**: e100041
- Zhao E, Xu H, Wang L, Kryczek I, Wu K, Hu Y, Wang G, Zou W (2012) Bone marrow and the control of immunity. *Cellular & molecular immunology* **9**: 11-19
- Zhou, J., Zhang, X., Wang, Y., & Guan, Y. (2015). PU.1 affects proliferation of the human acute myeloid leukemia U937 cell line by directly regulating MEIS1. *Oncology Letters*, 10, 1912-1918. <https://doi.org/10.3892/ol.2015.3404>
- Zhu J, Paul WE (2008) CD4 T cells: fates, functions, and faults. *Blood* **112**: 1557-1569

# Curriculum Vitae

## Personal Data

Name	Aznaourova Marina
Date of birth	12.05.1988
Nationality	Greek

## Studies

July 2015- November 2019

PhD student at the Institute of Lung Research at Philipps University of Marburg under the supervision of Prof. Dr. Leon N. Schulte.

October 2012- November 2014

Master degree of Molecular Biology and Biomedicine at the University of Crete with grade 'Excellent' (9,55/10).

September 2006- March 2011

Bachelor degree of Molecular Biology and Genetics at the Democritus University of Thrace (Alexandroupoli, Greece) (General Grade 7.39/10).

June 2006

Graduated from 1<sup>st</sup> lyceum of Menemeni, Tessaloniki (General grade 'Excellent' 18.7/20).

## **Verzeichnis der akademischen Lehrer**

Meine akademischen Lehrer waren die Damen und Herren in Alexandroupolis and Heraklion:

Sandaltzopoulos, Galanis, Kourkoutas, Chlichlia, Glykos, Koffa, Agianian, Chatzaki, Boukouvala, Fadouloglou, Fakis, Fylaktakidou, Grigoriou, Pappa, Paschou, Skavdis, Tsatsanis, Garinis, Spilianakis, Tokatlidis, Athanasaki, Kalantidis, Delidakis, Iliopoulos D., Iliopoulos I., Sieden, Bretsias, Mayrothalassitis, Gravanis, Poirazi, Tzamarias, Vondas, Petratos, Tavernarakis, Oikonomou, Papamatheakis, Zachos, Kokkinidis

# Acknowledgments

At this point, I would like to thank all those who contributed to the success of this work, in professional and personal level. My special thanks go to Prof. Dr. Leon Schulte for accepting me as a member of his working group, for designing this study, for analysis of the RNA sequencing results and for the fruitful and constructive guidance and discussions. In addition, I would like to thank Prof. Dr. Bernd Schmeck for accepting me as a member of the Institute for Lung research and for financial support. I would also like to thank all my cooperation partners who helped me with this work. Prof. Dr. Stefan Bauer and Prof. Dr. Leif Sander for providing material, productive criticism and ideas to this project. Prof. Dr. Linne Uwe for analysis the mass spectrometry data, Dr. Andreas Kaufmann and Dorna Jens for facilitating with the infection experiments.

I would like also to acknowledge all the current and former members of the institute of lung research for the beautiful cooperation and the great working atmosphere. More specifically, my college and friend Harshavardhan Janga, who helped me throughout all the years of the doctorate thesis, not only in professional but also in personal level. My special thanks go also to Stephanie Sefried for helping me during the most stressful year of my doctoral thesis, not only with experiments but also with psychological support. I would like to express my gratitude to Nadine Siebert, Dr. Evelyn Vollmeister, Dr. Tina Herkt and Stephan Ringshandl for helping me adjust in Marburg, for providing a roof over my head and a bed to sleep, for scientific discussions, for helping me with the laboratory work and for the many fun days! Furthermore, I would like to thank Kerstin Hofmann for the support, advices and for performing experiments and Nils Schmerer for performing experiments and being a good company. Many thanks to Marlene von Schenck for the everlasting assistance and advice at organizational and administrative problems. At this point, I would like to thank all the former and current, Bachelor, Master, doctoral students, technicians and post docs, Björn Klabunde, Katrin Bedenbender, Vincent Franz, Nora Lindhauer, Philipp Burkhard, Sebastian Müller, Diana Boehm, Fabian Böldt, Rösser Lisa, Jeff Bierwagen, Jonas Wehrenberg, Isabell Weigand, Dr. Benedikter Birke, Dr. Bertrams Wigo, Dr. Anna Lena Jung and my students Tabea Tharra, Thevis Lara and Leonie Gather for the wonderful time together inside but also outside the laboratory. Moreover, many thanks to the MBML members, Stefan Hadzic, Christina Malainou and Francesco Palumbo for their friendship and scientific discussions and of course the great moments that we all shared.

My special thanks go to my friend Georgia Papadogianni for listening to all my PhD related problems and frustrations and for all the wonderful trips we made in order to discover Germany.

In addition, I would like to thank my lifetime long friends Souzana Saakian and Anastasia Kilikidou for all their support through everything, their encouragement and their belief in me and of course, for all the unforgettable moments we have experienced together. I would like also to thank my friend Theofanis Rafail for love, support, for trying to make my life easier and for making me smile and Panagiota Katsanou for all the nice advices, her love, the fun days and nights and the best food in the world. Special acknowledgments to my cat, Touvlo, for being just a cat and making me always laugh.

Finally yet importantly, I would like to thank my family, my mother Foteini Kritharidou, my father Dimokritos Aznaourov, my sister Katerina Aznaourova, my aunt Maria Kritharidou and my grandmother Mimoza Fotiadou for supporting all my crazy ideas, being always there for me and have faith in me. Without their love and support throughout my lifetime, none of these would have been possible.

# Ehrenwörtliche Erklärung

Ich erkläre ehrenwörtlich, dass ich die dem Fachbereich Medizin Marburg zur Promotionsprüfung eingereichte Arbeit mit dem Titel "Long non-coding RNAs involved in myeloid cell differentiation and macrophage activation" im Institut für Lungenforschung unter Leitung von Jun. Prof. Dr. Leon Nicolas Schulte ohne sonstige Hilfe selbst durchgeführt und bei der Abfassung der Arbeit keine anderen als die in der Dissertation aufgeführten Hilfsmittel benutzt habe. Ich habe bisher an keinem in- oder ausländischen Medizinischen Fachbereich ein Gesuch um Zulassung zur Promotion eingereicht, noch die vorliegende oder eine andere Arbeit als Dissertation vorgelegt.

Ich versichere, dass ich sämtliche wörtlichen oder sinngemäßen Übernahmen und Zitate kenntlich gemacht habe.

Mit dem Einsatz von Software zur Erkennung von Plagiaten bin ich einverstanden.

Vorliegende Arbeit wurde noch nicht veröffentlicht.

---

Ort, Datum, Unterschrift

Die Hinweise zur Erkennung von Plagiaten habe ich zur Kenntnis genommen, die Angebote der Philipps-Universität zur Plagiatserkennung (Plagiatssoftware zu beziehen über das Hochschulrechenzentrum) sind mir bekannt.

---

Ort, Datum, Unterschrift Betreuer